UNIVERSITÀ DEGLI STUDI DI SASSARI

---

DIPARTIMENTO DI SCIENZE CHIMICHE, FISICHE, MATEMATICHE E NATURALI
Scuola di Dottorato in Scienze e Tecnologie Chimiche
Ciclo XXXV

# Metalli e sistemi biologici: target, interazioni e implicazioni biomediche

Relatore:
Prof. Serenella Medici

Dottorando:
Dott. Alessio Pelucelli

Co-relatore:
Prof. Massimiliano Francesco Peana

Anno Accademico 2022-2023

# Indice

**Capitolo IV**

**Studio dell'interazione degli ioni metallici Cu²⁺ e Zn²⁺ con l'interfaccia di riconoscimento di ACE2 per la proteina Spike SARS-CoV-2**

**Articolo**

- **Zn²⁺ and Cu²⁺ Interaction with the Recognition Interface of ACE2 for SARS-CoV-2 Spike Protein**. *International Journal of Molecular Sciences* 2023, *24*

**Capitolo V**

**Effetto dei metalli tossici sulla salute umana**

**Review**

- **An updated overview on metal nanoparticles toxicity**. *Semin Cancer Biol* 2021, *76*, 17-26.
- **Biological Effects of Human Exposure to Environmental Cadmium**. *Biomolecules* 2022, *13*.
- **Metal Toxicity and Speciation: A Review**. *Curr Med Chem* 2021, *28*, 7190-7208.
- **Environmental barium: potential exposure and health-hazards**. *Arch Toxicol* 2021, *95*, 2605-2612.

# Capitolo I

## Introduzione

### 1.1 Prefazione

Le interazioni tra ioni metallici e proteine rappresentano una delle fondamenta della vita sulla Terra, governando una vasta gamma di processi biologici che vanno dalla catalisi enzimatica alla stabilizzazione delle strutture proteiche, dal trasporto di molecole e ioni attraverso le membrane cellulari alla regolazione dei processi metabolici [1,2]. La complessità e la diversità delle funzioni svolte dagli ioni metallici in sinergia con le proteine sono sorprendenti, ed è proprio questa interazione che rende possibile la vita così come la conosciamo.

Le proteine, infatti, sono le macchine molecolari che costituiscono la base della vita, il cui legame con gli ioni metallici è spesso cruciale per il loro corretto funzionamento. Le proteine metallo-dipendenti, o metalloproteine, sono infatti in grado di legare selettivamente ioni metallici specifici, grazie a specifici siti di coordinazione che permettono anche l'interazione tra il metallo e la catena laterale degli amminoacidi che costituiscono la proteina. Questa stretta relazione tra ioni metallici e proteine consente di stabilizzarne la struttura tridimensionale, migliorandone la stabilità e la funzionalità [1].

In natura gli ioni metallici svolgono quindi un ruolo cruciale nella stabilizzazione delle proteine, ma anche come cofattori enzimatici, attivando e modulando l'attività catalitica delle proteine (metalloproteasi). Ad esempio, il magnesio è coinvolto in oltre 300 reazioni enzimatiche, mentre il ferro è fondamentale per il trasporto dell'ossigeno nel sangue e per la regolazione della respirazione cellulare. Il manganese invece è essenziale per la dismutazione dei superossidi, un processo fondamentale per neutralizzare i dannosi radicali

liberi [3]. Questi sono solo alcuni esempi del ruolo delle proteasi e delle innumerevoli funzioni che gli ioni metallici svolgono in collaborazione con le proteine.

Tuttavia, non tutte le interazioni metallo-proteina sono benefiche. Alcuni cationi come quelli di piombo, mercurio e cadmio, possono essere altamente tossici per gli organismi viventi, in quanto possono competere con quelli di metalli essenziali per i siti di coordinazione delle proteine, causando disfunzioni e danni cellulari [4]. È quindi fondamentale comprendere le interazioni tra gli ioni metallici e le proteine, non solo per approfondire la nostra conoscenza dei meccanismi biochimici alla base della vita, ma anche per identificare e contrastare gli effetti negativi di questi processi.

La comprensione di queste interazioni si rivela inoltre essenziale per decifrare le complesse reti di regolazione che caratterizzano la fisiologia umana e per approfondire la nostra conoscenza dei meccanismi molecolari alla base di diverse patologie. In particolare, le interazioni tra ioni metallici e proteine possono avere un impatto diretto sulla funzione delle proteine coinvolte, influenzando la loro conformazione, stabilità e attività. Essa può avere inoltre importanti implicazioni nella ricerca e nello sviluppo di nuovi farmaci e terapie. Ad esempio, la terapia chelante, che prevede l'utilizzo di molecole in grado di legare selettivamente determinati cationi, è stata ampiamente utilizzata nel trattamento di avvelenamenti da metalli pesanti e di alcune malattie metaboliche [5]. Allo stesso modo, l'ingegneria di proteine in grado di legare selettivamente gli ioni metallici può aprire nuove frontiere nel campo della biotecnologia e della medicina personalizzata.

Un altro aspetto importante delle interazioni tra metalli e proteine riguarda il loro ruolo nella patogenesi di diverse malattie neurodegenerative, come l'Alzheimer, il Parkinson e la sclerosi laterale amiotrofica (SLA) [6-8]. In queste condizioni, gli squilibri nell'omeostasi di metalli come calcio, alluminio, magnesio, zinco, ferro e rame [8-10], possono portare all'accumulo di specie metallo-proteiche aberranti, in grado di causare stress ossidativo, disfunzioni

mitocondriali e aggregazione proteica, contribuendo così alla progressione della malattia. Approfondire la nostra conoscenza delle interazioni tra ioni metallici e proteine può quindi portare a nuovi approcci terapeutici per il trattamento di queste patologie devastanti.

Infine, le interazioni metallo-proteina possono avere un impatto significativo sulla resistenza ai farmaci e sulle strategie terapeutiche in ambito oncologico. Ad esempio, alcuni composti contenenti metalli, come il cisplatino e il carboplatino, sono stati ampiamente utilizzati nella chemioterapia per il trattamento di diversi tipi di tumori [11,12]. Tuttavia, la resistenza ai farmaci e la tossicità sistemica limitano l'efficacia di questi agenti chemioterapici. Una migliore comprensione delle interazioni tra gli ioni metallici e le proteine coinvolte nei meccanismi di resistenza e di azione dei farmaci potrebbe aprire nuove strade per lo sviluppo di terapie più efficaci e meno tossiche.

In sintesi, le interazioni metallo-proteina svolgono un ruolo cruciale in una vasta gamma di processi biologici e patologici. La comprensione delle basi molecolari di queste interazioni e delle loro implicazioni nella fisiologia e nella patologia umana è di fondamentale importanza per lo sviluppo di nuove strategie terapeutiche e per la prevenzione di malattie legate alla presenza e all'accumulo di metalli. Attraverso un'approfondita analisi delle interazioni tra ioni metallici e proteine, questa tesi mira a gettare nuova luce su tali fenomeni complessi e a contribuire alla nostra comprensione delle loro interazioni e delle implicazioni per la salute umana.

La ricerca qui presentata si propone di contribuire a colmare alcune delle lacune nella nostra conoscenza delle interazioni metallo-proteina, utilizzando una combinazione di tecniche sperimentali avanzate e modellistica molecolare per esaminare queste interazioni in diversi contesti biologici e patologici. In particolare, questa ricerca si concentra su:

- interazioni tra gli ioni metallici e molecole chelanti derivati dell'acido kojico;

- interazioni tra gli ioni metallici $Zn^{2+}$, $Mn^{2+}$, $Fe^{2+}$ e proteine batteriche trasportatrici del ferro, in particolare la proteina transmembrana FeoB;
- interazione tra il recettore umano Angiotensin Convertin Enzyme 2 (di seguito ACE2) e gli ioni metallici $Cu^{2+}$ e $Zn^{2+}$, con l'obiettivo di valutare se queste interazioni possano influenzare il normale funzionamento del recettore ACE2 e, in ultima analisi, avere un impatto sulla fisiologia umana nell'ambito delle patologie legate al covid-19.

Attraverso questo studio approfondito delle interazioni tra ioni metallo-proteina, la tesi punta a fornire nuove intuizioni sui meccanismi molecolari alla base di questi meccanismi e sulle loro implicazioni nella fisiologia e nella patologia umana. Di seguito una breve anticipazione dei temi trattati e dei risultati ottenuti, che verranno sviluppati più compiutamente nelle sezioni ad essi dedicate.

## 1.2 Derivati dell'acido kojico

In una prima parte della ricerca è stata analizzata la capacità di formare complessi da parte di una serie di derivati dell'acido kojico [Figura 1] con $Pb^{2+}$ e $Cd^{2+}$, utilizzando le tecniche di potenziometria e spettrofotometria, supportate da spettroscopia NMR $^1H$ e $^{13}C$ e calcoli DFT. Queste molecole combinano le proprietà chelanti dei pironi e delle poliammine. Abbiamo quindi dimostrato un diverso meccanismo di coordinazione tra $Pb^{2+}$ e $Cd^{2+}$. Nel caso del $Pb^{2+}$, la coordinazione avviene esclusivamente tramite gli atomi di ossigeno delle unità di acido kojico, mentre nel caso del $Cd^{2+}$, il contributo degli atomi di azoto nel legante appare rilevante. Inoltre, tutti i leganti studiati formano complessi di stabilità significativamente superiore con $Pb^{2+}$ rispetto a $Cd^{2+}$. La stabilità dei complessi formati con il legante tripodale SC [Figura 1.1], superiore di diversi ordini di grandezza rispetto a quella ottenuta con tutti gli altri leganti, è di sicuro interesse per le possibili applicazioni di questo legante nella eliminazione di ioni metallici tossici dall'acqua inquinata.
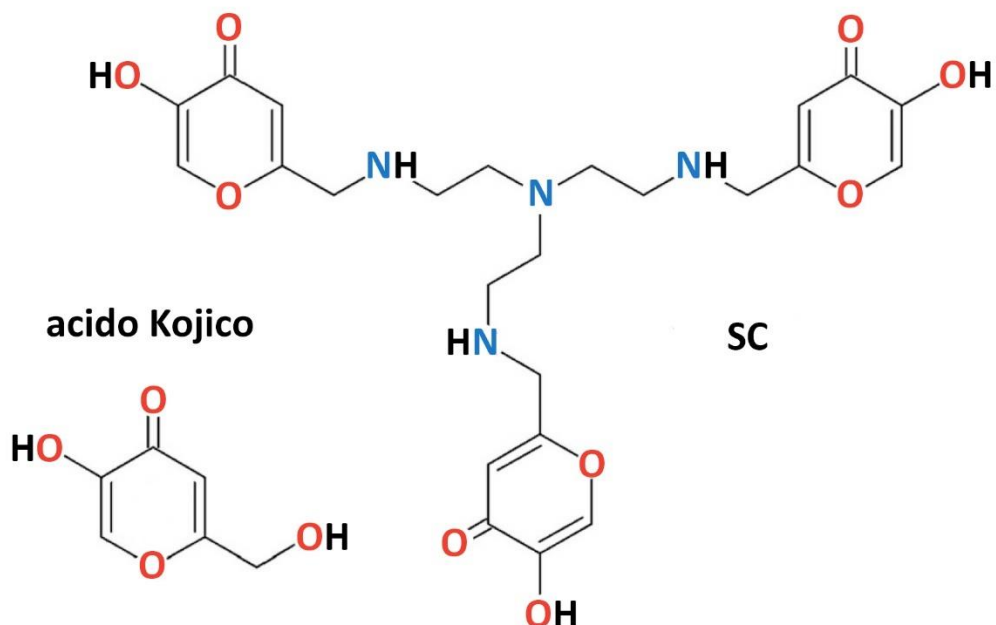
**Figura 1.1**. Struttura dell'acido Kojico e del legante tripodale SC.

L'inquinamento da metalli pesanti, come il piombo e il cadmio, è diventato un problema sempre più urgente a causa della loro persistenza nell'ambiente e della loro tossicità per gli esseri umani, gli animali e le piante [13]. Negli ultimi decenni, l'industrializzazione e l'urbanizzazione hanno avuto un impatto negativo sull'ambiente, portando all'introduzione di sostanze nocive e pericolose che hanno causato gravi problemi per lo sviluppo antropico. L'accumulo di metalli pesanti in natura è aumentato a causa di tali processi. I metalli pesanti in questione non hanno alcuna funzione biologica o meccanismi di omeostasi e si accumulano nell'aria, nell'acqua, nei suoli e nella catena alimentare [14,15]. Per la rimozione di tali metalli sono disponibili diversi metodi, tra cui assorbimento, precipitazione, scambio ionico, estrazione e rilevamento elettrochimico [16-18]. Tuttavia, è importante considerare che la forma in cui il metallo è presente potrebbe dipendere dalla sua concentrazione, solubilità, dal pH e dal mezzo ionico. Pertanto, gli studi di complessazione risultano cruciali per molte applicazioni, come la bonifica, la previsione del

trasporto e del destino dei metalli e la progettazione di metodi per sequestrare un metallo tossico dai sistemi naturali [19-22].

Tra i metalli più tossici per animali, piante ed esseri umani, senza alcuna funzione biologica e meccanismo di omeostasi, vi sono proprio il piombo e il cadmio. Sebbene essi abbiano avuto utilizzi storici diversi, rispettivamente risalenti all'età del bronzo e alla seconda metà del XIX secolo, il loro impiego attuale in ambito industriale, agricolo e domestico è estremamente variegato. Ad esempio, il piombo è utilizzato nella produzione di batterie, munizioni e dispositivi per schermare i raggi X, mentre il cadmio è impiegato in leghe e pigmenti [23,24]. Entrambi i metalli presentano caratteristiche chimico-fisiche e profili tossicologici diversi, con linee guida aggiornate rispettivamente al 2020 e 2012 secondo l'US Agency for Toxic Substances & Disease Registry [25]. Nonostante l'adozione di divieti sull'uso e l'emissione nell'ambiente di questi due cationi metallici da parte di molti governi nazionali e sovranazionali a causa della consapevolezza della loro tossicità, la loro rilevanza tossicologica rimane elevata.

## 1.3 Trasportatore batterico FeoB

La seconda parte della ricerca è stata incentrata sulla coordinazione dello ione $Fe^{2+}$ da parte della proteina trasportatrice batterica FeoB. L'*Escherichia coli* (*E. coli*) resistente ai farmaci sta diventando una preoccupazione globale, poiché i ceppi patogeni di questo batterio sono stati la principale causa di morte legata alla resistenza agli antimicrobici nel 2019 [26]. Si stima che l'*E. coli* resistente ai farmaci sarà responsabile di 3 milioni di morti all'anno entro il 2050 [27]. La multi-antibiotico-resistenza in questo batterio deriva dalla capacità di acquisire geni di resistenza attraverso il trasferimento genico orizzontale, ad esempio geni che codificano per le β-lattamasi e le carbapenemasi [28]. Nel 2017, l'*E. coli* resistente ai carbapenemi è stato riconosciuto dall'OMS in un elenco di batteri per i quali sono urgentemente

necessari nuovi antibiotici [29]. Un modo alternativo per trattare le infezioni batteriche potrebbe derivare dallo studio del processo naturale di immunità nutrizionale. Durante un'infezione batterica, infatti, l'organismo ospite limita la quantità di ioni metallici essenziali disponibili per i patogeni [30]. Per crescere e sostenere la propria patogenicità, i batteri devono acquisire diversi metalli dall'ospite, ad esempio ferro, manganese e zinco. Questi metalli sono coinvolti in processi metabolici batterici cruciali, come la respirazione cellulare, la sintesi e la riparazione del DNA, la disintossicazione dei radicali liberi o come cofattori strutturali essenziali delle proteine enzimatiche [31,32]. Per la maggior parte di questi processi il ferro è indispensabile, rendendo così la capacità di assorbire efficientemente il ferro dall'ambiente un fattore limitante per la sopravvivenza dei batteri patogeni [33,34]. In condizioni aerobiche, il ferro è presente principalmente sotto forma di ioni Fe(III), che i batteri assorbono utilizzando piccoli chelanti organici caratterizzati da un'affinità molto alta per gli ioni Fe(III), chiamati siderofori.

Tuttavia, in condizioni anaerobiche, e a basso pH, la forma di ferro più diffusa è il $Fe^{2+}$. Per i batteri che si trovano in ambienti simili, ad esempio nel tratto gastrointestinale anossico degli animali, l'assorbimento efficace di $Fe^{2+}$ diventa uno dei fattori di virulenza più importanti [35,36]. Nonostante il ruolo cruciale del $Fe^{2+}$ nella patogenicità, la descrizione dettagliata dei meccanismi di assorbimento batterico di questo catione è ancora relativamente scarsa, soprattutto a livello molecolare, rispetto al trasporto del Fe(III). Gli studi di chimica di coordinazione del $Fe^{2+}$ con i trasportatori batterici sono necessari per determinare i siti di legame del metallo nei trasportatori e quindi chiarire il meccanismo di trasporto del $Fe^{2+}$; tuttavia, tali studi sono significativamente carenti nella letteratura, molto probabilmente a causa delle difficoltà nel lavorare con lo ione $Fe^{2+}$, sensibile all'ossidazione, e nel mantenere le condizioni anaerobiche durante gli esperimenti.

## 1.4 Interazione di ioni metallici con il recettore ACE2

La terza ed ultima parte di studio e lavoro nell'ambito di questo dottorato è stata dedicata alla comprensione dei meccanismi alla base dell'interazione tra il recettore ACE2 e la proteina *spike* del SARS-CoV-2. La proteina *spike* (S) del SARS-CoV-2 ha infatti dimostrato un'affinità molto più elevata nel legarsi al recettore umano dell'enzima di conversione dell'angiotensina 2 (ACE2) rispetto ad altri coronavirus [37,38]. L'interfaccia di legame tra il recettore ACE2 e la *Spike* gioca un ruolo critico nel meccanismo di ingresso del virus SARS-CoV-2 nella cellula ospite, e specifici amminoacidi sono coinvolti nell'interazione tra la proteina S e il recettore ACE2. Questa specificità di legame è fondamentale affinché il virus possa instaurare un'infezione sistemica e causare la malattia COVID-19 [39-41]. Nel recettore ACE2, la maggior parte degli amminoacidi che svolgono un ruolo cruciale nel meccanismo di interazione e riconoscimento della proteina S si trovano nella parte C-terminale, che rappresenta proprio la principale regione di legame tra ACE2 e S. Questo frammento è ricco di residui con proprietà coordinanti, come aspartato, glutammato ed istidina, che potrebbero essere bersaglio di ioni metallici. A questo proposito, è dimostrato che lo ione $Zn^{2+}$ si lega al recettore ACE2 nel suo sito catalitico e ne modula l'attività, contribuendo inoltre alla stabilità strutturale dell'intera proteina [42,43]. La capacità del recettore ACE2 umano di coordinare cationi metallici come lo $Zn^{2+}$, nella stessa regione in cui avviene il legame con la proteina S, potrebbe quindi avere un impatto cruciale sul meccanismo di riconoscimento e interazione ACE2-S, con conseguenze sull'affinità di legame che meritano di essere indagate. Per testare questa possibilità, il nostro progetto si proponeva di caratterizzare la capacità di coordinazione dello $Zn^{2+}$ e, a titolo di confronto, anche del $Cu^{2+}$, utilizzando modelli peptidici selezionati che rappresentano l'interfaccia di legame ACE2. Questo studio è stato condotto mediante l'impiego di tecniche complementari spettroscopiche e potenziometriche, allo scopo di ottenere una dettagliata caratterizzazione delle interazioni metallo-legante [44].

# Capitolo II

## Studio delle interazioni tra gli ioni metallici e molecole chelanti derivati dell'acido kojico

### 2.1 Introduzione

Nel presente capitolo viene riassunta la prima parte della ricerca, rivolta allo studio della capacità di complessazione di una serie di leganti idrossipironici (HPO) derivati dall'acido kojico (KA), precedentemente sintetizzati, nei confronti degli ioni metallici $Pb^{2+}$ e $Cd^{2+}$ [45-47]. I leganti HPO sono caratterizzati da due o tre unità di acido kojico collegate tra loro tramite dei ponti amminici [Figura 2.1]. L'obiettivo principale dello studio è stato quello di indagare gli effetti dei potenziali gruppi coordinanti (amminici, carbonilici e idrossilici) sulla stabilità dei complessi formati con i due ioni metallici selezionati, di modo da approfondire la comprensione del comportamento di questi due cationi e della loro modalità di coordinazione.

Per condurre questo studio è stato utilizzato un approccio a tecnica multipla, che combina potenziometria e spettrofotometria, supportato da spettroscopia NMR multidimensionale ed eteronucleare, e calcoli DFT. Gli esperimenti potenziometrici sono stati eseguiti a 25 °C utilizzando una soluzione di forza ionica 0.1 M. Le soluzioni dei leganti sono state preparate pesando i composti solidi precedentemente sintetizzati secondo i metodi riportati in letteratura [45,46]. Come fonti di ioni metallici sono stati utilizzati i sali $CdCl_2$ e $Pb(NO_3)_2$.

Gli esperimenti potenziometrici e spettrofotometrici sono stati condotti tramite titolazioni computerizzate in atmosfera inerte (azoto o argon), per garantire una corretta valutazione delle costanti di stabilità. Questo approccio ha inoltre permesso di prevenire l'ossidazione dei leganti durante gli esperimenti. Gli

esperimenti NMR sono stati eseguiti utilizzando uno spettrometro Bruker Ascend™ 400 MHz. Le strutture dei complessi di $Pb^{2+}$ e $Cd^{2+}$ sono state ottimizzate mediante calcoli DFT.
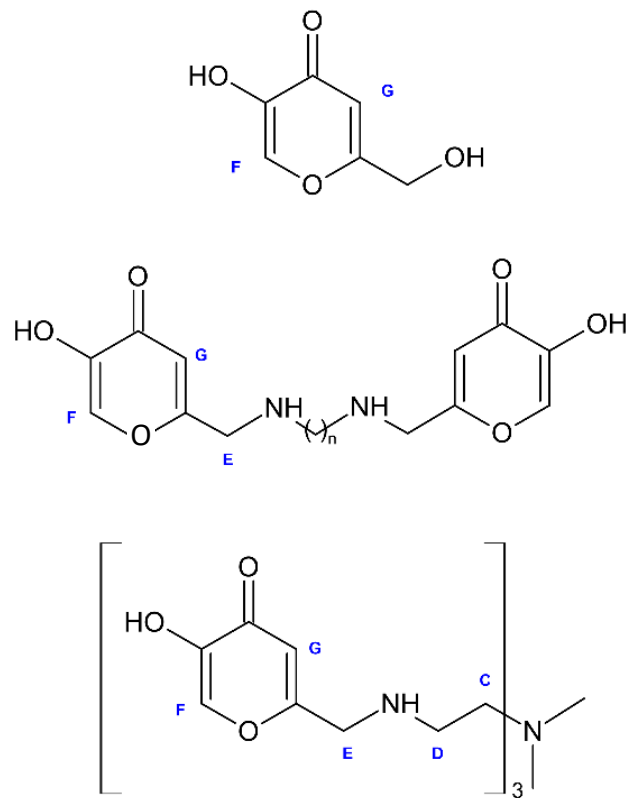


**Figura 2.1**. Dall'alto, struttura dell'acido kojico. Al centro, struttura generale dei leganti S(n). In basso, struttura del legante SC.

I risultati ottenuti hanno evidenziato che la capacità di complessazione dei leganti idrossipironici è influenzata dal numero di unità di acido kojico, dal tipo di ammina impiegata per unire tali unità e dalla presenza di gruppi donatori di azoto addizionali. In generale, si è osservato che i leganti contenenti tre unità di acido kojico e gruppi donatori di azoto addizionali presentano una maggiore capacità di complessazione rispetto a quelli con solamente due unità di acido kojico [48].

## 2.2 Caratterizzazione in soluzione dei leganti e dei complessi metallici

Le costanti di deprotonazione dei quattro leganti, KA, S2, S3, S4 e SC sono state derivate dai precedenti studi e sono disponibili in letteratura [45,47]. Le costanti di stabilità derivate in questo nostro studio per i complessi formati tra i cationi $Pb^{2+}$ e $Cd^{2+}$ e i leganti idrossipironici, si sono rivelate generalmente elevate, indicando che tali leganti potrebbero essere impiegati con successo nel sequestro di questi metalli pesanti in soluzione. Inoltre, le informazioni dettagliate sulla struttura dei complessi e sulle interazioni tra i leganti e gli ioni metallici ottenute attraverso gli esperimenti NMR e i calcoli DFT hanno sottolineato il ruolo cruciale dei gruppi coordinanti di ossigeno e azoto nel processo di stabilizzazione dei complessi. Gli equilibri di formazione dei complessi tra i cinque leganti e gli ioni $Pb^{2+}$ e $Cd^{2+}$ sono stati analizzati mediante titolazioni potenziometriche e spettrofotometriche congiunte. I dati potenziometrici sono stati elaborati utilizzando il software HyperQuad [49], mentre i dati spettrofotometrici sono stati processati con il programma HypSpec [50]. Le costanti di formazione dei complessi sono riportate nella Tabella 1. Inoltre, i dati spettrofotometrici hanno evidenziato l'inizio della precipitazione degli idrossidi metallici ad alti valori di pH. I modelli di complessazione sono stati sviluppati tenendo conto delle costanti di protonazione e con il supporto della spettroscopia NMR e dei calcoli DFT.

| Species | logβ | | | | |
|---|---|---|---|---|---|
| | KA | S2 | S3 | S4 | SC |
| | | | | | |
| $PbLH_4$ | | | | | 46.69(3) |
| $PbLH_3$ | | | 32.73(5) | | 39.52(1) |
| $PbLH_2$ | | | | | 31.07(3) |
| $PbLH$ | | | | | 22.62(1) |
| $PbL$ | 5.88(3) | | | | 12.98(2) |
| $PbL_2$ | 9.85(5) | | | | |
| $Pb_2L_2H_5$ | | | 63.58(3) | 64.86(6) | |
| $Pb_2L_2H_4$ | | 53.15(8) | 56.41(2) | 57.82(3) | |
| $Pb_2L_2H_3$ | | 45.8(1) | 47.92(2) | 48.28(8) | |
| $Pb_2L_2H_2$ | | 38.88(6) | 38.64(3) | 39.43(2) | |
| $Pb_2L_2H$ | | 29.9(1) | 29.43(2) | | |
| $Pb_2L_2$ | | 21.0(6) | | | |
| **pPb** | **6.57** | **6.49** | **6.43** | **6.73** | **10.88** |
| | | | | | |
| $CdLH_3$ | | | | | 35.63(5) |
| $CdLH_2$ | | | | | 28.82(5) |
| $CdLH$ | | | | | 21.55(5) |
| $CdL$ | 4.3(1) | | | | 13.89(2) |
| $CdLH_{-1}$ | | | | | 3.49(3) |
| $CdL_2$ | 8.1(1) | | | | |
| $Cd_2L_2H_5$ | | | 58.9(1) | 61.2(1) | |
| $Cd_2L_2H_4$ | | 50.61(7) | 51.1(1) | 53.6(1) | |
| $Cd_2L_2H_3$ | | | 42.85(7) | 44.43(7) | |
| $Cd_2L_2H_2$ | | 36.00(5) | 33.60(5) | 34.6(1) | |
| $Cd_2L_2H$ | | 28.15(5) | 23.86(4) | | |
| $Cd_2L_2$ | | 19.96(5) | | | |
| $Cd_2L_2H_{-1}$ | | 10.25(6) | | | |
| **pCd** | **6.03** | **6.02** | **6.00** | **6.00** | **7.89** |

**Tabella 2.1**. Costanti di formazione dei complessi di $Pb^{2+}$ e $Cd^{2+}$.

## 2.3 Complessi di Pb$^{2+}$

Una prima analisi riguarda i possibili composti di coordinazione tra le molecole in esame e lo ione metallico Pb$^{2+}$. Risulta evidente che l'acido kojico forma complessi con Pb$^{2+}$ di due diverse stechiometrie, con rapporto molare metallo-legante 1:1 e 1:2. La formazione del complesso [PbL]$^{+}$ inizia a pH 4 [Figura 2.2], raggiungendo l'80% di formazione a pH 6. A questo punto inizia la formazione del complesso PbL$_2$, che aumenta fino al 50% oltre pH 8. La precipitazione degli idrossidi metallici si verifica a pH $\approx$ 10. Dal valore di pM (6.57) si deduce che, a una concentrazione 1 µM di Pb$^{2+}$, è necessaria una quantità di legante 10 volte superiore per complessare il 70% del metallo.
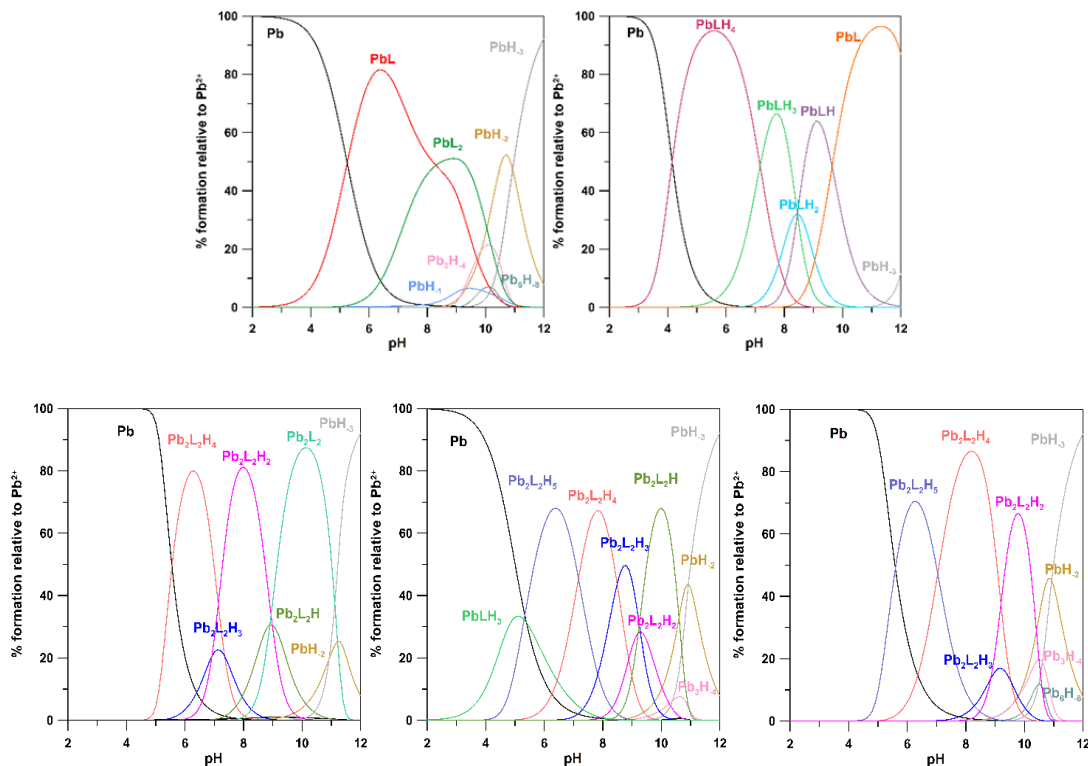


**Figura 2.2**. Grafici di speciazione per i sistemi Pb$^{2+}$-legante. In alto, da sinistra a destra i grafici relativi a KA e SC. In basso, da sinistra a destra, i grafici relativi a S2, S3 e S4.

I leganti bis-kojici invece formano solo complessi binucleari quando si trovano in soluzione con lo ione $Pb^{2+}$, in cui ciascuno dei due ioni metallici è coordinato dagli atomi di ossigeno delle porzioni di acido kojico dei due diversi leganti. In particolare, il primo spettro UV-Vis della titolazione del sistema $Pb^{2+}$-S2 a pH 6.18, relativo alla specie $[Pb_2L_2H_4]^{4+}$, mostra la banda dei gruppi OH protonati (276 nm) diminuita di circa il 70-80% di assorbanza (OH e tre gruppi amino ancora protonati), che scompare completamente a favore della banda dei gruppi $O^-$ deprotonati (308 nm) a causa della perdita di un protone (pK 7.3), formando la specie $[Pb_2L_2H_3]^{3+}$. Le successive deprotonazioni avvengono sui gruppi amino carichi e sono spettralmente silenti. Solo in eccesso di legante si formano anche i complessi mononucleari 1:2 $[PbL_2H_3]^+$ e $PbL_2H_2$.

Gli spettri NMR sono stati registrati a pH 7.68, aumentando progressivamente la concentrazione di $Pb^{2+}$ fino a raggiungere un rapporto molare metallo:legante di 1:1. Il sistema $Pb^{2+}$-S2 presenta una rapida velocità di scambio nei tempi NMR: l'aggiunta di quantità substechiometriche di $Pb^{2+}$ alla soluzione di legante provoca uno spostamento graduale dei segnali $^1H$ NMR, che appaiono come una media tra gli stati libero e legato [Figura 2.3].
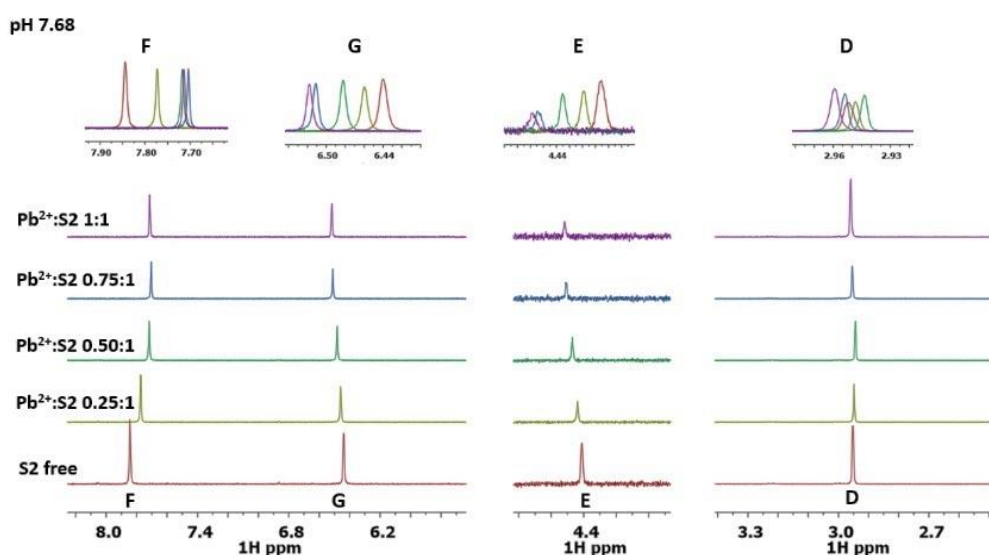


**Figura 2.3**. Spettri $^1H$ NMR del sistema $Pb^{2+}$-S2 a differenti rapporti metallo legante, a pH 7.68.

Analizzando l'intero intervallo di pH è possibile osservare che la maggiore perturbazione dei *chemical shift* riguarda i nuclei F, che si trovano più vicini ai gruppi O⁻ di coordinazione [Figura 2.4].
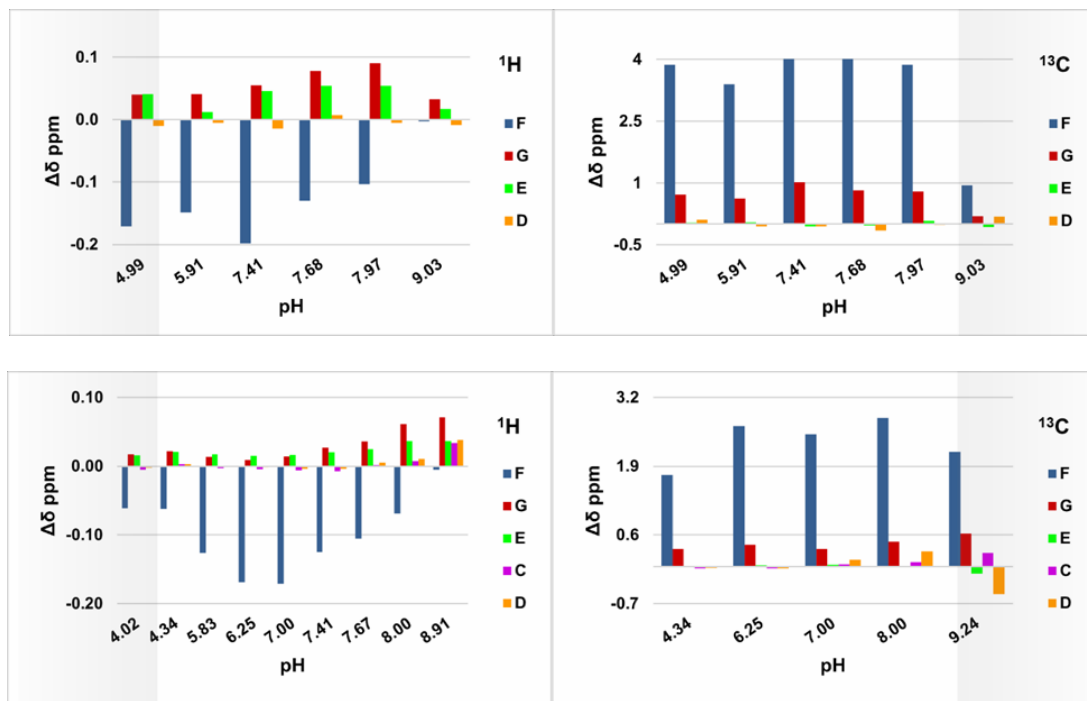


**Figura 2.4**. Variazione dei *chemical shift* ¹H e ¹³C nel sistema Pb²⁺-legante a diversi intervalli di pH. In alto la variazione relativa al sistema Pb²⁺-S2, in basso la variazione relativa al sistema Pb²⁺-SC.

Questi sono seguiti da G ≥ E >> D, il che conferma che la coordinazione avviene principalmente attraverso i donatori di ossigeno delle unità kojiche, mentre i donatori di azoto sono esclusi dalla formazione del complesso. Aumentando il valore di pH oltre 9, il legante non sembra essere influenzato dallo ione metallico, in quanto quest'ultimo è coinvolto nella formazione e precipitazione degli idrossidi metallici.

Per ottenere i modelli atomici dei complessi binucleari di Pb²⁺, sono stati effettuati calcoli DFT sulle strutture ipotizzate sperimentalmente. Gli stati di

protonazione considerati sono stati $[Pb_2(S2)_2H]^+$, $[Pb_2(S2)_2H_2]^{2+}$ e $[Pb_2(S2)_2H_3]^{3+}$. I risultati dei calcoli DFT mostrano che ciascuna delle due molecole di legante S2 si lega a entrambi gli ioni metallici attraverso le due unità fenoliche chelanti. Inoltre, solo un atomo di ossigeno per ciascun legante S2 agisce da ponte tra i due ioni metallici. La protonazione del legante coinvolge i quattro gruppi amminici presenti nelle due molecole di S2.

Si osserva invece un diverso schema di complessazione all'inizio dell'interazione tra il legante S3 e il $Pb^{2+}$, in quanto nel complesso $[PbLH_3]^{3+}$ lo ione $Pb^{2+}$ è legato a una sola unità kojica, mentre la seconda unità rimane protonata, così come i due atomi di azoto nel linker. La combinazione di due complessi $[PbLH_3]^{3+}$ porta alla formazione di un complesso binucleare $[Pb_2L_2H_5]^{5+}$ [Figura 2.3], strutturalmente simile al complesso $[Pb_2L_2H_4]^{4+}$ già visto con il legante S2, con protonazione su tutti e quattro i gruppi amminici. Analogamente a quanto osservato con il legante S2, si verifica la perdita di un protone dall'ultima unità di KA non coordinata, con pK 7.17, formando il complesso $[Pb_2L_2H_4]^{4+}$. Ulteriori protoni vengono persi nell'intervallo di pK 8.48-9.28, fino alla formazione del complesso $[Pb_2L_2H]^+$.

Il legante S4 presenta un modello di complessazione simile a quello del legante S3, completando la coordinazione di $Pb^{2+}$ con la perdita di un protone con pK 7.04 dal complesso $[Pb_2L_2H_5]^{5+}$ [Figura 2.2].

Lo studio NMR mostra un comportamento simile a quello osservato per il legante S2 sia per il legante S3 che per il legante S4. In tutti questi sistemi, infatti, l'interazione con il metallo inizia a circa pH 5, coinvolgendo gli atomi donatori di ossigeno delle unità di KA, e prosegue fino a circa pH 9.

Questi risultati forniscono ulteriori informazioni sulle interazioni tra gli ioni metallici tossici e i leganti idrossipironici, e possono contribuire allo sviluppo di nuovi leganti per la rimozione di metalli pesanti dall'ambiente e alla comprensione del loro comportamento chimico in sistemi naturali.

Per quanto riguarda il legante tris-kojico SC, lo studio potenziometrico indica la formazione di una specie mononucleare $[PbLH_4]^{3-}$ a partire da un pH inferiore a 4 [Figura 2.2], in cui il $Pb^{2+}$ è presumibilmente coordinato da due unità KA (mentre la terza unità e i tre atomi di azoto del linker sono ancora protonati). I dati spettrofotometrici mostrano che il primo protone viene perso dall'unità KA, poiché la deprotonazione avviene a un pK di 7.2, come nel legante libero. I successivi tre protoni amminici vengono persi nell'intervallo di pK 8.4-9.6, leggermente inferiore a quello del legante libero.

Le variazioni dei *chemical shift* [Figura 2.4] sono analoghe a quelle dei sistemi precedentemente descritti, e mostrano che il legame con lo ione metallico coinvolge gli atomi di ossigeno fenolici chelanti delle unità KA. La struttura dei complessi del legante SC con $Pb^{2+}$ è stata investigata mediante calcoli DFT [Figure 2.5 e 2.6], considerando gli stati di protonazione $[Pb(SC)]^-$, $[Pb(SC)H]$, $[Pb(SC)H_2]^+$, $[Pb(SC)H_3]^{2+}$ e $[Pb(SC)H_4]^{3+}$. Indipendentemente dalla carica complessiva del complesso, la coordinazione preferenziale del metallo avviene sempre attraverso gli atomi di ossigeno fenolici chelanti delle unità KA.



Pb(SC)⁻

0.0 kJ/mol

34.9 kJ/mol

183.6 kJ/mol

268.7 kJ/mol
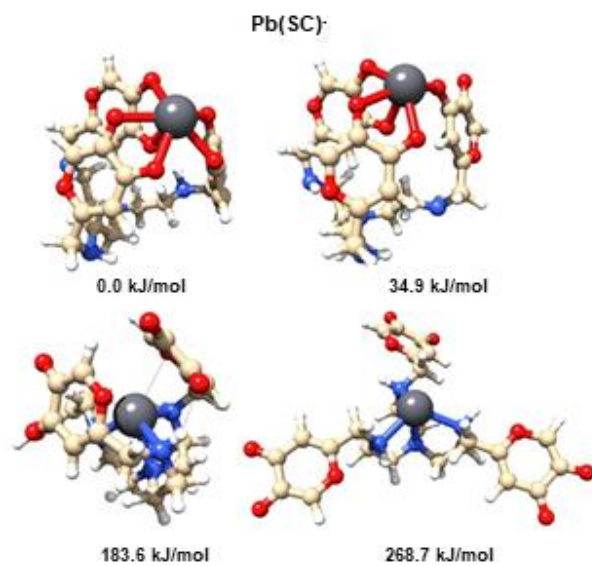
**Figura 2.5**. Sistema [Pb(SC)]. In soluzione acquosa, strutture più stabili calcolate mediante DFT e relativi valori di energia libera di Gibbs.
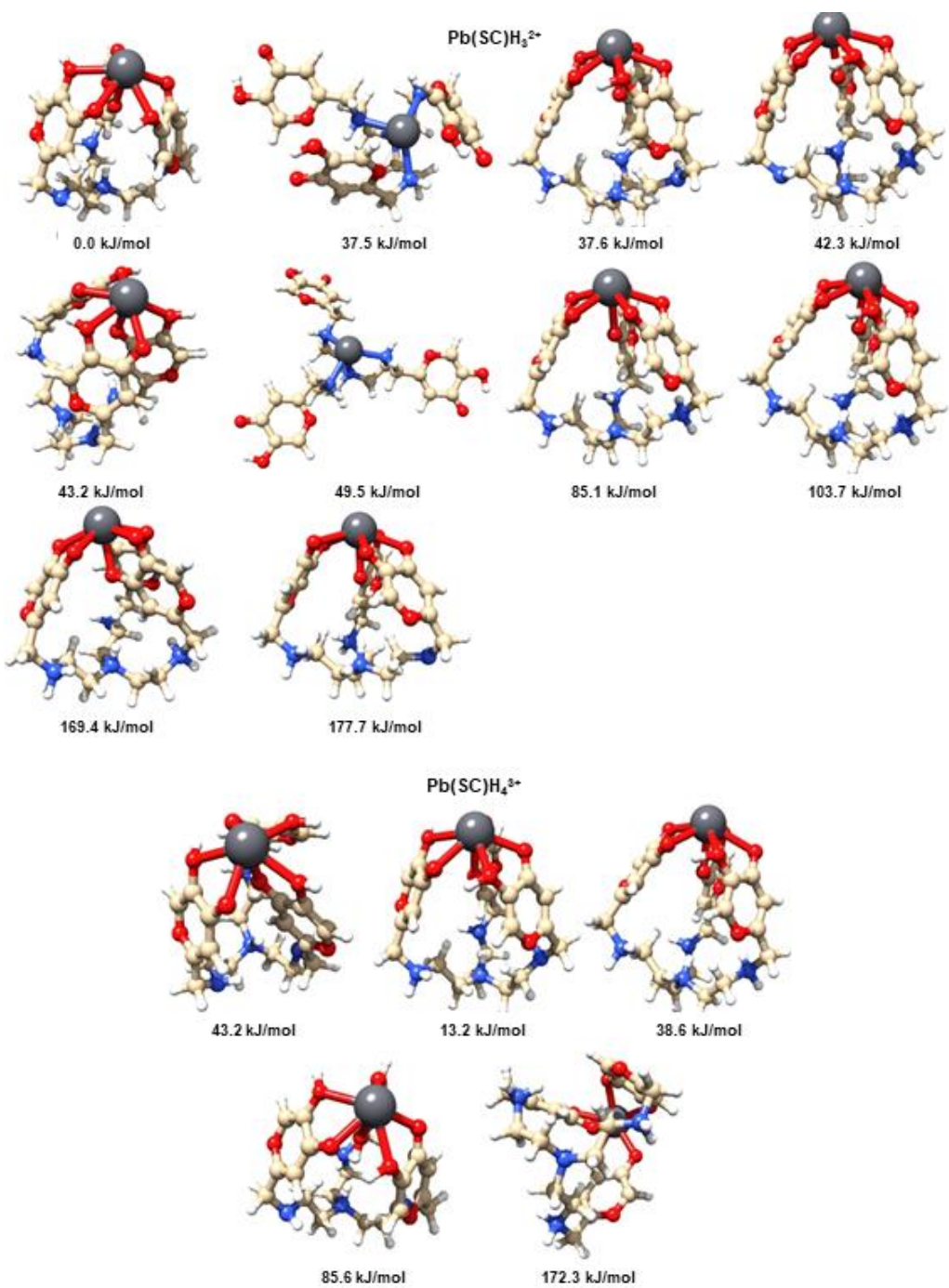
**Figura 2.6**. Sistemi $[Pb(SC)H_3]^{2+}$ (in alto) e $[Pb(SC)H_4]^{3+}$ (in basso) in soluzione acquosa, tautomeri più stabili calcolate mediante DFT e relativi valori di energia libera di Gibbs.

## 2.4 Complessi di Cd$^{2+}$

Per quanto riguarda le interazioni tra i leganti e lo ione Cd$^{2+}$, l'acido kojico mostra la formazione di un complesso 1:1 a pH > 5, [CdL]$^+$, e un complesso 1:2 dopo pH 6, [CdL$_2$] [Figura 2.7]. La loro stechiometria e le relative costanti di stabilità sono in accordo con quanto riportato in letteratura [51].
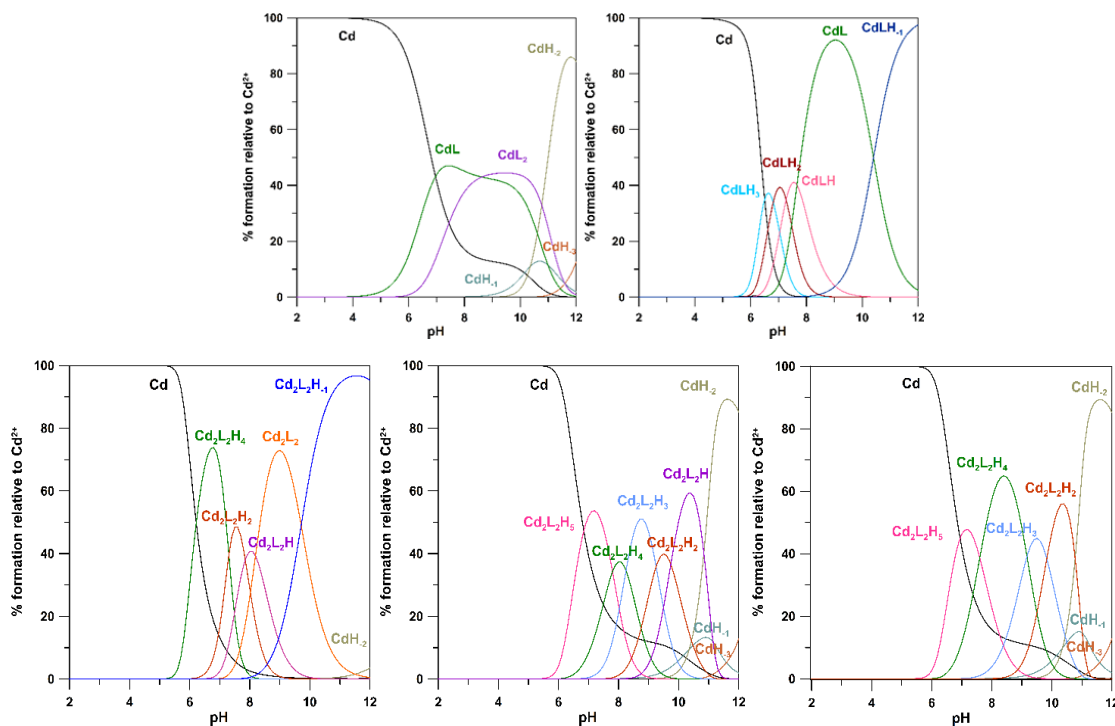


**Figura 2.7**. Grafici di speciazione per i sistemi Cd$^{2+}$-legante. In alto, da sinistra a destra i grafici relativi a KA e SC. In basso, da sinistra a destra, i grafici relativi a S2, S3 e S4.

Dall'andamento delle perturbazioni in funzione del pH identificate dagli spettri NMR, risulta che l'interazione del Cd$^{2+}$ con KA è più complicata rispetto a quanto studiato con lo ione Pb$^{2+}$ a causa della presenza di diverse specie in soluzione, ma sostanzialmente in accordo con i risultati potenziometrici. Tutte le specie coinvolgono donatori di ossigeno dell'unità KA. Si osserva una diminuzione delle perturbazioni di *chemical shift* a pH > 10, associata alla

formazione di specie idrossilate che causano la precipitazione del metallo e la riformazione di KA libero.

È interessante notare come i leganti bis-kojici formino complessi di $Cd^{2+}$ con la stessa stechiometria dei complessi di $Pb^{2+}$, ma bisogna ricordare che il comportamento spettrale dei sistemi studiati non implica necessariamente il coinvolgimento delle stesse unità KA nella coordinazione dello ione metallico.

Il legante S2 mostra il complesso $[Cd_2L_2H_4]^{4+}$ (similmente ai complessi con $Pb^{2+}$) come prima specie formata, che perde i suoi quattro protoni più un quinto da una molecola d'acqua coordinata (non può essere assegnato a una particolare fase di deprotonazione) nell'intervallo di pH 7.3-9.7 [Figura 2.7]. Diversamente da quanto osservato per i complessi di $Pb^{2+}$, i dati spettrofotometrici UV-Vis mostrano che la banda caratteristica dei gruppi $O^-$ deprotonati (316 nm) si forma in piccola misura, il che implica che il $Cd^{2+}$ sia coordinato solo parzialmente da KA.

Una ulteriore conferma arriva dagli spettri NMR registrati a pH 7.84 aumentando la concentrazione di $Cd^{2+}$ fino a un rapporto molare metallo:legante 1:1 e dalle variazioni dei *chemical shift* in un ampio intervallo di pH: l'andamento dei segnali $^1H$ segue l'ordine G >> F [Figura 2.8, e 2.9] (opposto alla complessazione di $Pb^{2+}$) e la perturbazione dei nuclei D ed E è più consistente di quella osservata nella complessazione di $Pb^{2+}$. Ciò potrebbe indicare che, almeno per alcune specie in soluzione, siano i donatori di azoto del linker ad essere coinvolti nell'interazione metallica.
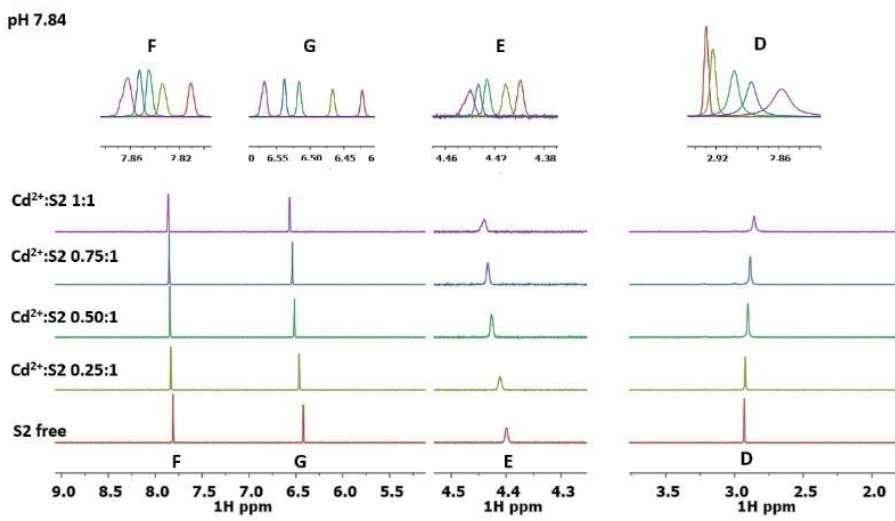
**Figura 2.8**. Spettri ^{1}H NMR del sistema Cd$^{2+}$-S2 a differenti rapporti metallo legante, a pH 7.84.
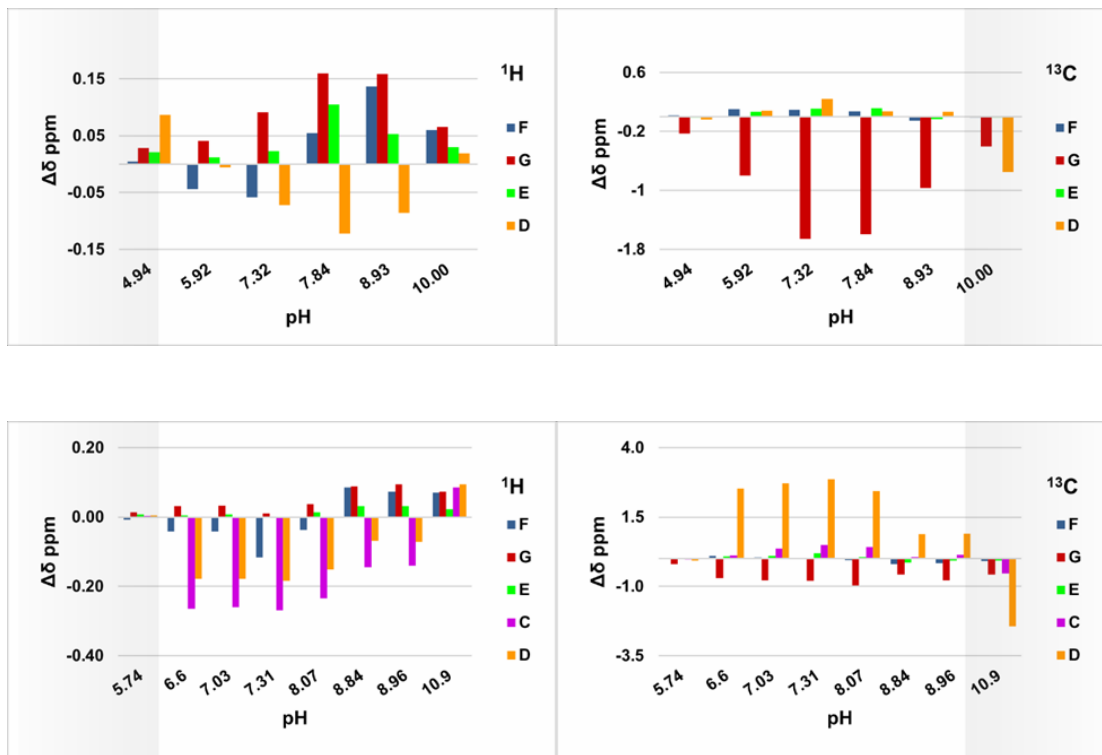


**Figura 2.9**. Variazione dei *chemical shift* [1]H e ^{13}C nel sistema Cd$^{2+}$-legante a diversi intervalli di pH. In alto la variazione relativa al sistema Cd$^{2+}$-S2, in basso la variazione relativa al sistema Cd$^{2+}$-SC.

I calcoli DFT sono stati eseguiti su $[Cd_2(S2)_2H]^+$, $[Cd_2(S2)_2H_2]^{2+}$ e $[Cd_2(S2)_2H_3]^{3+}$, utilizzando la stessa stechiometria e schema di coordinazione dei complessi di $Pb^{2+}$ con il legante S2 [Figura 2.10].
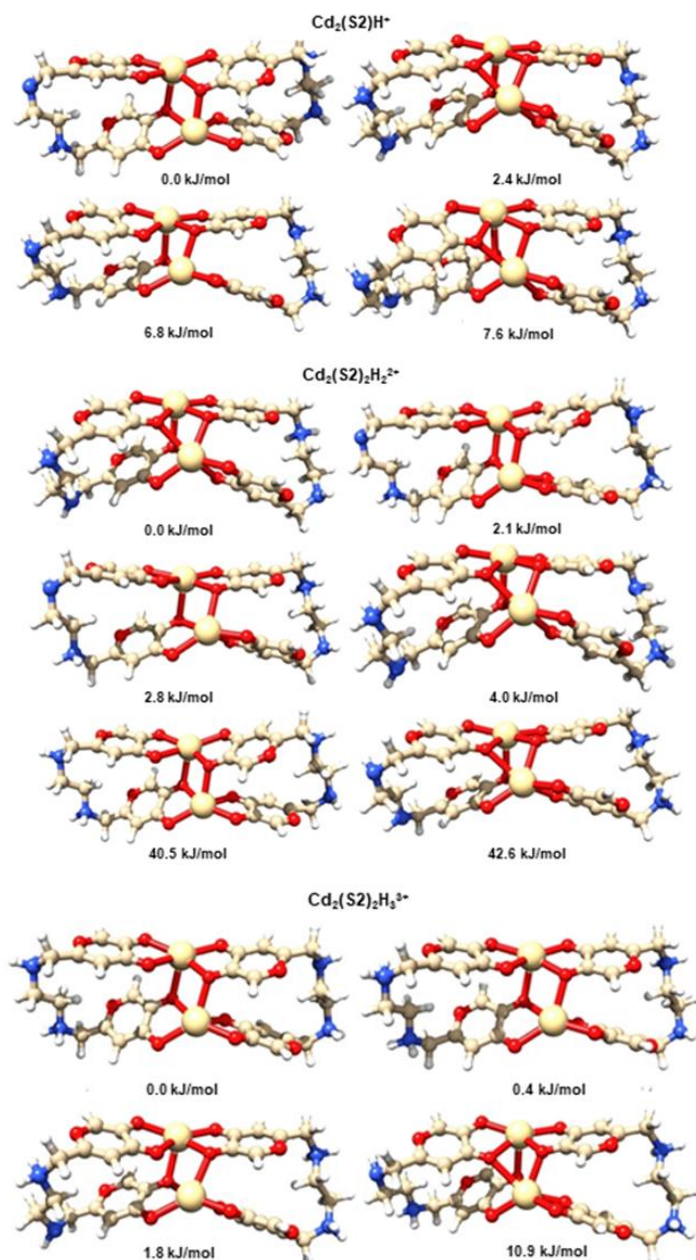


**Figura 2.10**. Sistemi $[Cd_2(S2)_2H]^+$ (in alto), $[Cd_2(S2)_2H_2]^{2+}$ (al centro) e $[Cd_2(S2)_2H_3]^{3+}$ (in basso) in soluzione acquosa, tautomeri più stabili calcolati mediante DFT e relativi valori di energia libera di Gibbs.

I leganti S3 e S4 presentano un comportamento simile tra loro [Figura 2.8]. La prima specie formata è $[Cd_2L_2H_5]^{5+}$ per entrambi, a cui segue una serie di deprotonazioni che portano alla formazione di $[Cd_2L_2H]^+$ per S3 e di $[Cd_2L_2H_2]^{2+}$ per S4. Al contrario dei complessi visti per il legante S2, per i leganti S3 e S4 le maggiori variazioni di *chemical shift* sono state rilevate per i nuclei G e F, mentre i nuclei D ed E sono blandamente influenzati. Di conseguenza, sembra che gli atomi donatori di azoto non partecipino alla coordinazione [Figura 2.9].

I complessi mononucleari di $Cd^{2+}$ si formano anche con il legante SC. Il complesso $[CdLH_3]^{2+}$ perde sequenzialmente quattro protoni fino alla formazione dell'idrosso-complesso $[CdLH_{-1}]^{2-}$, in cui le unità di KA non sono coinvolte nella coordinazione di $Cd^{2+}$, secondo i dati spettrofotometrici. Inoltre, come appare chiaramente dalla Figura 2.10, D e C sono i nuclei più influenzati a pH 6.6, prima del quale (pH 5.74) non si osserva alcuna interazione metallica (in accordo con i dati potenziometrici). La variazione dei *chemical shift* si mantiene abbastanza costante fino a pH 8, suggerendo la presenza di una specie predominante in soluzione. Da pH 8 in poi, si verifica una graduale variazione di tendenza che porta a una nuova specie ad alti valori di pH (pH 10.9) proponendo il coinvolgimento degli atomi donatori di azoto nei complessi $Cd^{2+}$-SC. La presenza di due picchi separati nella Figura 2.11, uno relativo alla conformazione libera di SC e il secondo relativo alla conformazione di $Cd^{2+}$-SC, suggerisce uno scambio lento nella scala temporale NMR e un elevato livello di affinità con $Cd^{2+}$. È interessante notare che i calcoli DFT evidenziano la presenza di una differenza fondamentale tra i complessi di cadmio del legante SC. Infatti, mentre per $[Cd(SC)]^-$ [Figura 2.12], la coordinazione metallica preferenziale avviene attraverso gli atomi di ossigeno fenolico delle tre unità KA, e per la forma protonata $[Cd(SC)H_3]^{2+}$ la specie più stabile mostra la coordinazione preferenziale attraverso i quattro atomi di azoto amminici del legante.
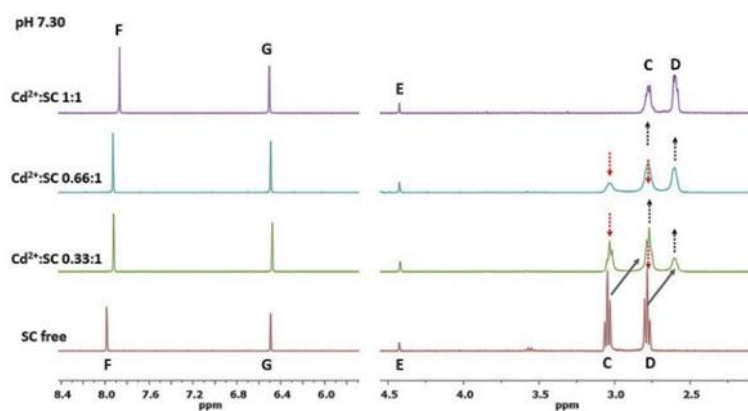
**Figura 2.11**. Spettri 1D 1H del sistema Cd$^{2+}$-SC a differenti rapporti molari.
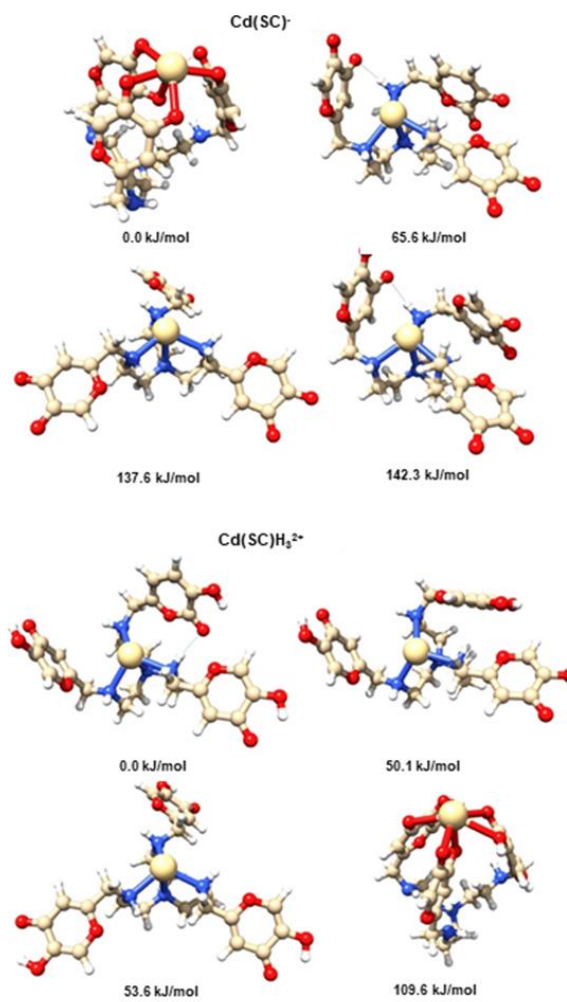


**Figura 2.12**. Sistemi [Cd(SC)]$^-$ (in alto) e [Cd(SC)H$_3$]$^{2+}$ (in basso) in soluzione acquosa, tautomeri più stabili calcolati mediante DFT e relativi valori di energia libera di Gibbs.

## 2.5 Conclusioni

Per riassumere e concludere la discussione sui dati esaminati in questa fase dello studio è possibile evidenziare alcuni punti di rilievo. Come primo punto, è apparso chiaro che tutti i leganti studiati formano complessi di stabilità notevolmente più elevata con lo ione $Pb^{2+}$ rispetto allo ione $Cd^{2+}$, e lo si può dedurre dai valori di pM ottenuti. È poi importante sottolineare il diverso meccanismo di coordinazione dei leganti nei confronti di $Pb^{2+}$ e $Cd^{2+}$. Nel caso di $Pb^{2+}$, la coordinazione avviene esclusivamente tramite gli atomi di ossigeno nelle unità KA, mentre nel caso di $Cd^{2+}$ il contributo degli atomi di azoto nel linker appare rilevante. Infine, è opportuno sottolineare come la stabilità dei complessi formati con il legante SC sia più elevata di diversi ordini di grandezza rispetto a quella ottenuta con tutti gli altri leganti. E' possibile confrontare l'affinità e la capacità di coordinazione dei leganti studiati nei confronti degli ioni metallici, attraverso i valori pM [Tabella 1]. Questi valori sono calcolati su soluzioni contenenti una concentrazione iniziale di 1 µM degli ioni metallici tossici, che corrisponde a 207 µg/L per $Pb^{2+}$ e 112 µg/L per $Cd^{2+}$. Tali concentrazioni sono estremamente più elevate rispetto ai limiti di soglia per l'acqua potabile di 5 µg/L per entrambi gli ioni metallici secondo la normativa statunitense [52,53], e di 10 µg/L per $Pb^{2+}$ e 3 µg/L per $Cd^{2+}$ secondo l'OMS [54]. I valori di pM calcolati corrispondono alla concentrazione dello ione metallico libero dopo l'aggiunta di un eccesso dieci volte superiore di legante. Nel caso del $Pb^{2+}$, il valore di pM 6.43 con S3 (il valore più basso) corrisponde a una diminuzione della concentrazione di $Pb^{2+}$ libero da 207 a 77 µg/L dopo l'aggiunta del legante, il valore di pM 6.73 con S4 da 207 a 39 µg/L, e il valore di pM 10.88 per SC corrisponde a una diminuzione da 207 a 0.003 µg/L (diminuzione del 99.999%). Quindi, anche se una grande quantità di ione metallico libero viene rimossa da KA, S2, S3 e S4, questi leganti non sono in grado di portare la concentrazione entro i limiti legali. Al contrario, SC è estremamente efficace nel produrre acqua pura da una soluzione altamente inquinata. Anche nel caso dello ione $Cd^{2+}$, solo il legante SC è in grado di ridurre in modo significativo la concentrazione dello ione metallico. Pertanto,

l'utilizzo del legante SC nella forma libera o bloccata su un supporto solido è sicuramente promettente, ma richiede ulteriori studi per determinare le migliori condizioni per un'applicazione pratica efficace.

I risultati di questo studio sono attualmente in fase di seconda revisione nella rivista scientifica Chemosphere:

Cappai, R.; Fantasia, A.; Barone, G.; Peana, M.F.; Pelucelli, A.; Medici, S.; Crisponi, G.; Nurchi, V.; Zoroddu, M.A. **A Family of Kojic Acid Derivatives Aimed to Remediation of Pb$^{2+}$ and Cd$^{2+}$** Chemosphere, (2023), *in revision*


L'articolo è disponibile in formato preprint al link:

https://papers.ssrn.com/sol3/papers.cfm?abstract_id=4402583

# Capitolo III

## Analisi delle interazioni tra gli ioni metallici e proteine batteriche trasportatrici del ferro

### 3.1 Introduzione

La seconda parte dello studio ha riguardato il trasporto dello ione $Fe^{2+}$ attraverso le membrane biologiche, con l'obiettivo ultimo di comprenderne meglio i dettagli e sfruttare questo punto cruciale del metabolismo batterico come leva per combattere l'antibiotico resistenza. Gli ioni metallici bivalenti di transizione vengono infatti acquisiti dai batteri Gram-negativi tramite proteine localizzate nella membrana interna, che facilitano il trasporto degli ioni dal periplasma al citoplasma [55]. Il trasporto attraverso la membrana esterna verso il periplasma si pensa sia basato principalmente sulla diffusione libera degli ioni metallici attraverso canali non selettivi chiamati porine; tuttavia, è stata proposta anche la presenza di canali più selettivi della membrana esterna, ad esempio per gli ioni $Mn^{2+}$ [56,57]. La maggior parte dei trasportatori della membrana interna non è specifica per lo ione metallico, e lo dimostra il fatto che ne può trasportarne più di uno, ad esempio $Fe^{2+}$, $Mn^{2+}$, $Zn^{2+}$, $Co^{2+}$, $Cu^{2+}$. Sistemi come *ZupT* e *YfeABCD* sono in grado di trasportare ioni $Fe^{2+}$, $Mn^{2+}$ e $Zn^{2+}$ [58,59]. Oltre a ciò, gli ioni $Mn^{2+}$ e $Fe^{2+}$ possono essere acquisiti anche dal trasportatore *MntH* [60].

Il sistema Feo è considerato il trasportatore di $Fe^{2+}$ più importante nei batteri, essenziale per l'acquisizione di ferro in condizioni acide e anaerobiche [61,62]. Mutazioni o delezioni nei geni che codificano le proteine del sistema Feo causano gravi compromissioni nell'acquisizione degli ioni $Fe^{2+}$ e quindi nella virulenza di alcune specie batteriche, come *Streptococcus suis*,

*Campylobacter jejuni* e *Helicobacter pylori* [63,64]. Il sistema Feo è composto dalle proteine citoplasmatiche FeoA e FeoC e dalla proteina transmembrana FeoB, che è direttamente coinvolta nel trasferimento degli ioni metallici attraverso la membrana interna [Figura 3.1].
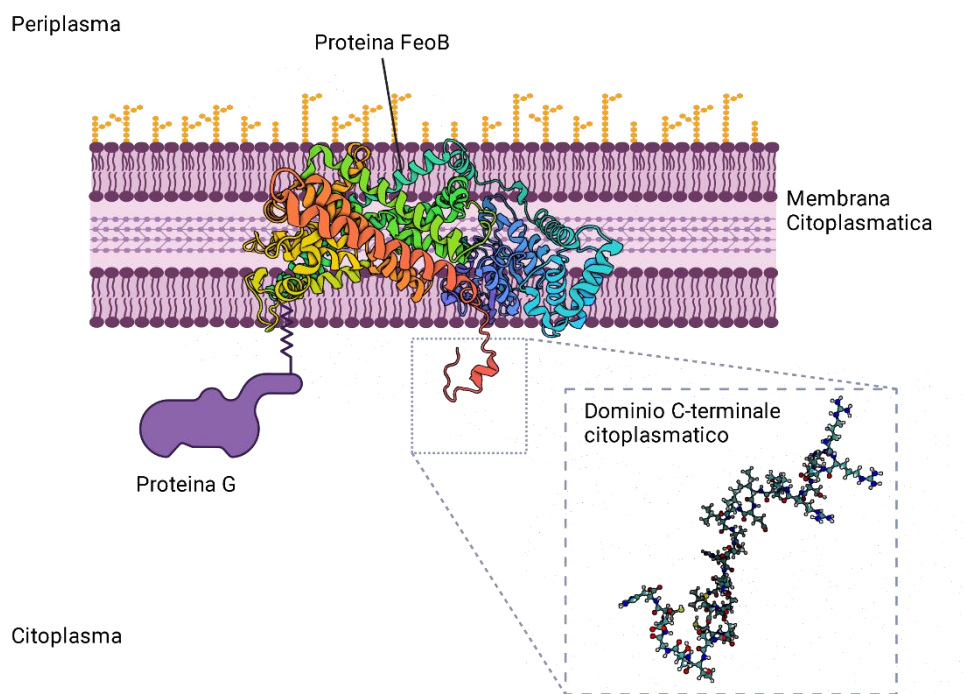


**Figura 3.1**. Sistema Feo, composto dalle tre subunità FeoA, FeoB e FeoC, Nel dettaglio, la sequenza peptidica presa in esame corrisponde al frammento C-terminale citosolico.

A oggi non c'è consenso sul meccanismo di trasporto del $Fe^{2+}$ da parte di FeoB; tuttavia, sono stati proposti alcuni siti di legame per il metallo nella sequenza proteica. Tali siti includono:

- i motivi Gate 1 e Gate 2, situati nella parte periplasmatica della proteina [Figura 3.2] e strutturalmente simili alla permeasi del ferro del lievito *Ftr1p*;

- la regione Core CFeoB, situata nel citoplasma tra la sesta e la settima elica transmembrana;

- il motivo EXXE, localizzato nel dominio G-proteico citoplasmatico [Figura 3.3] [65,66].
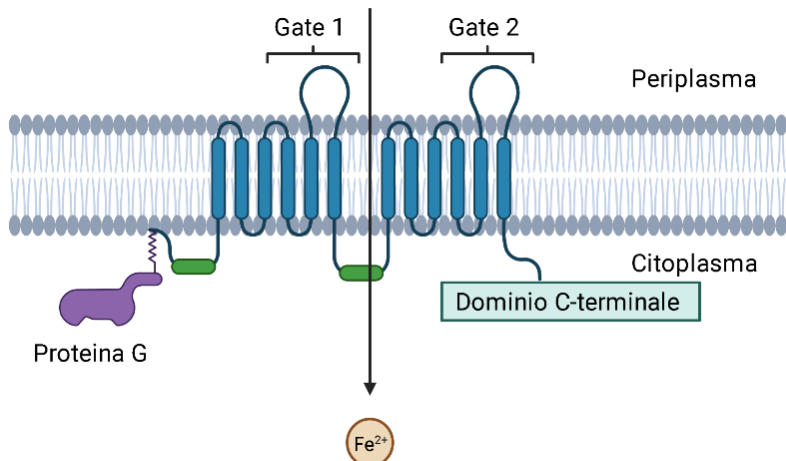


**Figura 3.2**. Le regioni Gate 1 e Gate 2 si trovano a livello del periplasma. Il dominio C-terminale di FeoB si trova nella parte citoplasmatica della cellula.

Tutti questi potenziali siti di legame contengono residui conservati che si ritiene siano in grado di legare il $Fe^{2+}$ con buona affinità. Un altro potenziale sito di legame per il $Fe^{2+}$, riconosciuto in letteratura, potrebbe essere il frammento C-terminale della proteina FeoA [65]. Nella classe dei gammaproteobatteri (ad esempio *E. coli*, *Y. pestis*, *S. typhimurium*), il frammento C-terminale citoplasmatico della proteina FeoB è ricco di residui di cisteina altamente conservati, oltre che residui di istidina, di acido glutammico e di acido aspartico che potrebbero agire come leganti del metallo nel citoplasma dopo il trasferimento dello ione metallico attraverso la membrana [Figura 3.2]. Sebbene Feo sia generalmente considerato specifico per il $Fe^{2+}$, molti sistemi di acquisizione batterica di questo catione possono trasportare anche ioni $Mn^{2+}$ e $Zn^{2+}$, come mostrato in precedenza. Secondo la teoria di Pearson degli acidi e delle basi *hard e soft*, la sequenza FeoB C-terminale possiede leganti che si legano in modo efficiente sia allo ione $Mn^{2+}$ *hard* (ad esempio, gli atomi

di ossigeno dei residui di Asp e Glu) che ai più *soft* $Fe^{2+}$ e $Zn^{2+}$ (ad esempio, gli atomi di zolfo dei residui di Cys) [67,68]. Inoltre, ci sono proteine in cui il manganese può essere coordinato anche dagli atomi di zolfo della cisteina e dagli atomi di azoto dell'istidina, ad esempio nel caso della calprotectina [69,70]. Pertanto, si è deciso di esaminare le proprietà di coordinazione dei metalli del frammento FeoB C-terminale. Per farlo, sono state scelte due sequenze peptidiche della proteina FeoB del ceppo *E. coli K12*, che differiscono per lunghezza: il peptide 2 è la parte citoplasmatica completa del dominio C-terminale di FeoB (Ac-R$_{743}$RARSRVDIELLATRKSVSSCCAASTTGDCH$_{773}$, P2), mentre il peptide 1 (Ac-C$_{763}$CAASTTGDCH$_{773}$, P1) è il frammento più corto che è stato esaminato per caratterizzare in dettaglio l'importanza dei residui di acido aspartico (D8) e acido glutammico (E10) per il legame con gli ioni metallici [Figura 3.3].
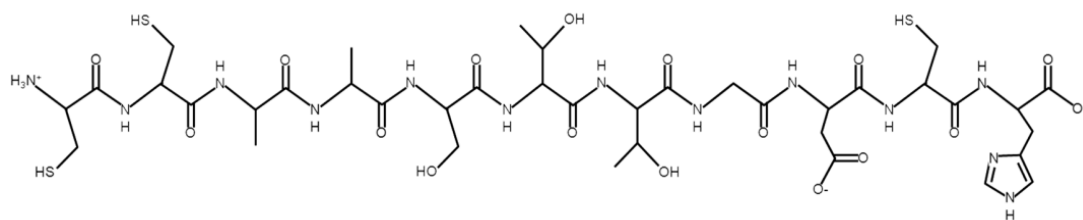


**Figura 3.3**. Struttura amminoacidica del peptide P1.

Gli amminoacidi N-terminali sono stati acetilati sull'azoto per rendere il modello peptidico più realistico della proteina nativa e per evitare il suo coinvolgimento nella complessazione. Nello specifico, tramite l'uso di tecniche complementari quali potenziometria, spettrometria di massa, spettroscopie NMR ed EPR è stata esaminata la termodinamica dei complessi di $Fe^{2+}$, $Zn^{2+}$ e $Mn^{2+}$ con i modelli sopra menzionati, determinando le costanti di protonazione dei peptidi, le costanti di stabilità dei complessi metallici, la loro stechiometria e le modalità di coordinazione.

I complessi di $Fe^{2+}$, $Zn^{2+}$ e $Mn^{2+}$ con Ac-$C_{763}$CAASTTGDCH$_{773}$ (P1) e Ac-$R_{743}$RARSRVDIELLATRKSVSSCCAASTTGDCH$_{773}$ (P2) sono stati studiati mediante una combinazione di tecniche potenziometriche, spettroscopiche (NMR, EPR) e spettrometriche (ESI-MS). Le titolazioni potenziometriche hanno permesso di calcolare le costanti di protonazione dei leganti e le costanti di stabilità dei complessi, oltre a fornire i diagrammi di speciazione e competizione nell'intervallo di pH 2-11. Le misure di spettrometria di massa hanno fornito indicazioni sulla stechiometria dei complessi formati, mentre le tecniche spettroscopiche hanno confermato i residui coinvolti nel legame con gli ioni metallici e fornito informazioni sulla geometria dei complessi.

A causa della sensibilità all'ossidazione dello ione ferroso, i campioni contenenti $Fe^{2+}$ sono stati preparati in atmosfera inerte di argon, utilizzando solventi deossigenati. A causa del carattere paramagnetico di $Mn^{2+}$ e $Fe^{2+}$, gli esperimenti NMR sono stati condotti eseguendo una titolazione dei leganti con quantità sub-stechiometriche di ione metallico, per evitare un eccessivo allargamento dei segnali che avrebbe precluso l'analisi e caratterizzazione di questi sistemi.

I leganti P1 e P2 contengono gruppi in grado di deprotonarsi nell'intervallo di pH compreso tra 2 e 11: il gruppo carbossilico del residuo laterale dell'acido aspartico e glutammico, l'azoto dell'anello imidazolico dell'istidina, i gruppi tiolici della cisteina e il gruppo carbossi-terminale. Il peptide P1 è costituito da 11 aminoacidi (Ac-$C_{763}$CAASTTGDCH$_{773}$), mentre P2 (Ac-$R_{743}$RARSRVDIELLATRKSVSSCCAASTTGDCH$_{773}$) da 31 aminoacidi, contenenti l'intero frammento carbossi-terminale citosolico di ECFeoB.

Nell'intervallo di pH compreso tra 2 e 11, P1 si comporta come un acido $H_6L$. La prima costante corrisponde alla deprotonazione del gruppo carbossilico terminale (pK = 3.37). La successiva deprotonazione avviene al residuo dell'acido aspartico, con pK = 4.19. La costante successiva deriva dalla deprotonazione dell'azoto imidazolico dell'istidina (pK = 6.96). Le ultime tre

costanti infine derivano dalla deprotonazione dei residui di cisteina (valori di pK compresi tra 8.15 e 9.81).

P2, più lungo di 20 aminoacidi rispetto a P1, ha però solo due ulteriori gruppi in grado di deprotonarsi nell'intervallo di pH testato. Questi sono i gruppi carbossilici di un ulteriore residuo di acido aspartico e di un residuo di acido glutammico. Quindi, P2 si comporta come un acido $H_8L$, con valori di pK corrispondenti simili a quelli di P1. La deprotonazione inizia dal gruppo C-terminale (pK = 2.15), con due acidi aspartici (valori di pK di 3.12 e 3.74), acido glutammico (pK = 4.38) e istidina (pK = 6.73) che si deprotonano successivamente. I valori di pK dei tre residui di cisteina in P2 sono compresi tra 8.15 e 10.11. Le costanti di protonazione dei leganti sono presentate nella Tabella 3.1.

| Peptide | Specie | Logβ | LogK | Deprotonazione |
|---------|--------|------|------|----------------|
| P1 | $[HL]^{4-}$ | 9.91(2) | | Cys |
| | $[H_2L]^{3-}$ | 18.73(2) | 8.92 | Cys |
| | $[H_3L]^{2-}$ | 26.88(3) | 8.15 | Cys |
| | $[H_4L]^{-}$ | 33.84(3) | 6.96 | His |
| | $[H_5L]$ | 38.03(4) | 4.19 | Asp |
| | $[H_6L]^{+}$ | 41.40(4) | 3.37 | $C_{term}$ |
| | | | | |
| P2 | $[HL]$ | 10.11(1) | | Cys |
| | $[H_2L]^{+}$ | 19.14(1) | 9.03 | Cys |
| | $[H_3L]^{2+}$ | 27.29(1) | 8.15 | Cys |
| | $[H_4L]^{3+}$ | 34.02(2) | 6.73 | His |
| | $[H_5L]^{4+}$ | 38.40(2) | 4.38 | Glu |
| | $[H_6L]^{5+}$ | 42.14(2) | 3.74 | Asp |
| | $[H_7L]^{6+}$ | 45.26(2) | 3.12 | Asp |
| | $[H_8L]^{7+}$ | 47.41(2) | 2.15 | $C_{term}$ |

**Tabella 3.1**. Costanti di protonazione dei due leganti esaminati.

## 3.2 Complessi di Fe$^{2+}$

La stechiometria dei complessi formati da P1 e P2 con Fe$^{2+}$ è stata confermata essere, dagli esperimenti ESI-MS, 1:1 (M:L). L'assegnazione corretta dei picchi è stata sempre confermata confrontando la loro distribuzione isotopica simulata e sperimentale. Lo spettro di massa per il sistema P1:Fe$^{2+}$ è mostrato, a titolo di esempio, in Figura 3.4.
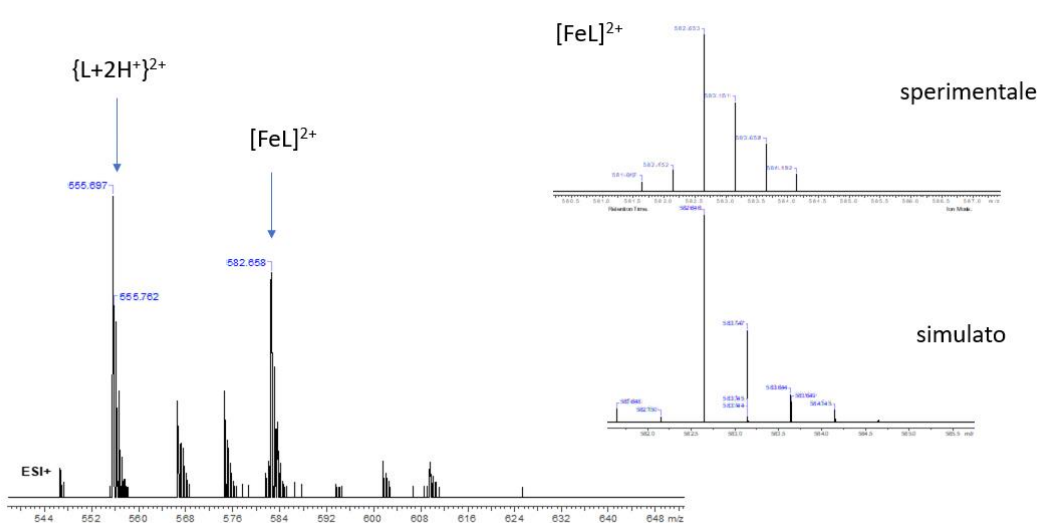


**Figura 3.4**. Spettro ESI-MS del Sistema P1-Fe$^{2+}$ a pH 7,4, rapporto metallo:legante 1:1. Lo spettro di distribuzione isotopica simulato e sperimentale del picco m/z=582,66 è mostrato in alto a destra.

Le costanti di protonazione dei complessi P1-Fe$^{2+}$ e P2-Fe$^{2+}$ sono presentate nella Tabella 3.1.

Per il sistema P1-Fe$^{2+}$, la prima forma osservata attraverso l'analisi potenziometrica è [FeH$_4$L]$^+$, presente nella soluzione dall'inizio della titolazione [Figura 3.5]. Questa forma contiene probabilmente il gruppo carbossilico terminale e l'acido aspartico in stato deprotonato. La forma successiva, [FeH$_3$L], è probabilmente legata alla deprotonazione del residuo istidina e domina nella soluzione in un ampio intervallo di pH, da circa 4.7 a 7.5.
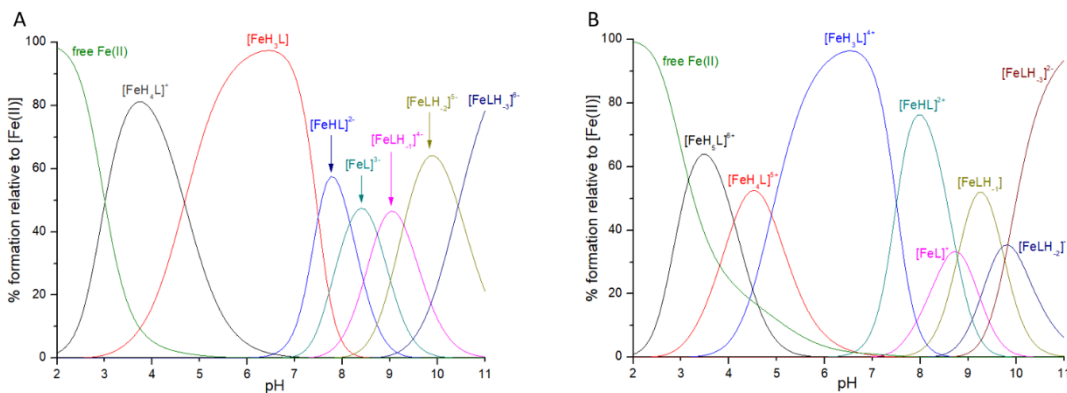
**Figura 3.5**. Grafici di speciazione per il sistema P1-$Fe^{2+}$ (a sinistra) e per il sistema P2-$Fe^{2+}$ (a destra).

| Peptide | Specie | Logβ | LogK | Deprotonazione |
|---------|--------|------|------|----------------|
| P1 | $[FeH_4L]^+$ | 38.76(2) | | |
| | $[FeH_3L]$ | 34.08(4) | 4.68 | His |
| | $[FeHL]^{2-}$ | 19.10(5) | - | Cys, Cys |
| | $[FeL]^{3-}$ | 10.94(5) | 8.16 | Cys |
| | $[FeLH_{-1}]^{4-}$ | 2.21(6) | 8.73 | $O_{water}$ / $N_{amide}$ |
| | $[FeLH_{-2}]^{5-}$ | -7.08(5) | 9.29 | $O_{water}$ / $N_{amide}$ |
| | $[FeLH_{-3}]^{6-}$ | -17.52(5) | 10.44 | $O_{water}$ / $N_{amide}$ |
| | | | | |
| P2 | $[FeH_5L]^{6+}$ | 42.75(2) | | |
| | $[FeH_4L]^{5+}$ | 38.65(4) | 4.13 | Glu |
| | $[FeH_3L]^{4+}$ | 33.75(4) | 4.90 | His |
| | $[FeHL]^{2+}$ | 18.76(5) | - | Cys, Cys |
| | $[FeL]^+$ | 10.01(7) | 8.75 | Cys |
| | $[FeLH_{-1}]$ | 1.21(6) | 8.80 | $O_{water}$ / $N_{amide}$ / Lys |
| | $[FeLH_{-2}]^-$ | -8.48(7) | 9.69 | $O_{water}$ / $N_{amide}$ / Lys |
| | $[FeLH_{-3}]^{2-}$ | -18.31(6) | 9.83 | $O_{water}$ / $N_{amide}$ / Lys |

**Tabella 3.2**. Costanti di protonazione dei complessi P1-$Fe^{2+}$ e P2-$Fe^{2+}$.

Questa forma contiene oltre il 90% del $Fe^{2+}$ nella soluzione a pH = 6.5. Il valore di pK di 4.68 è significativamente diminuito rispetto al valore di pK di 6.96 per questo residuo nel legante libero, suggerendo la partecipazione di una catena laterale di istidina nella coordinazione. Gli spettri NMR registrati al pH di 6.3 indicano il chiaro coinvolgimento dell'istidina H31. Anche il residuo D29 risulta perturbato dall'effetto paramagnetico dello ione $Fe^{2+}$ [Figura 3.6].
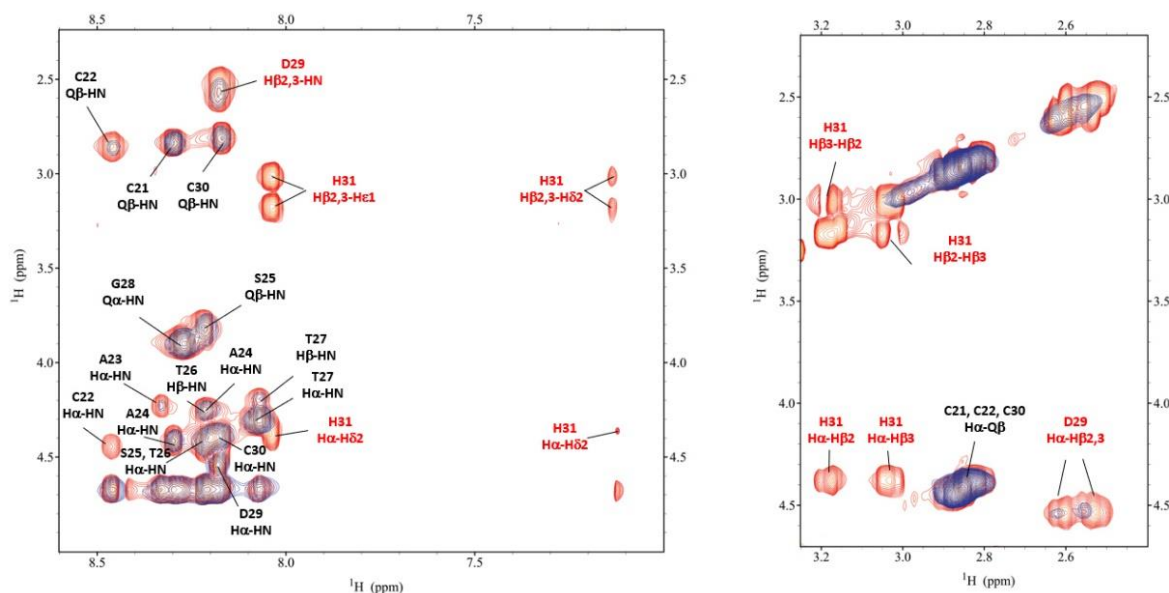


**Figura 3.6**. Selezione di spettri $^1$H-$^1$H TOCSY a pH 6.3. In rosso il peptide libero e in blu il sistema P1-$Fe^{2+}$ 1:0.3.

Molto probabilmente, la deprotonazione di due residui di cisteina porta alla formazione di $[FeHL]^{2-}$. La forma $[FeH_2L]^-$ non può essere rilevata dalla potenziometria, probabilmente essendo solo una forma transitoria, la cui concentrazione nella soluzione è bassa. L'ultima deprotonazione del residuo di cisteina corrisponde alla formazione di $[FeL]^{3-}$. Il valore ridotto di pK di questa cisteina nel complesso (pK = 8.16) rispetto al legante (pK = 9.81) suggerisce il suo coinvolgimento nella coordinazione del metallo. L'analisi NMR effettuata ai valori di pH di 8.16 mostra un forte effetto generalizzato paramagnetico dello ione $Fe^{2+}$ anche se è possibile notare un maggiore

allargamento dei segnali relativamente ai tre residui di cisteina C21, C22 e C30 oltre che dell'istidina H31 e aspartato D29. All'aumentare del pH fino a 9.45 i segnali dell'istidina H31 appaiono meno perturbati e la coordinazione dello ione $Fe^{2+}$ potrebbe coinvolgere principalmente i residui di cisteina.

Nel sistema P2:$Fe^{2+}$ osserviamo una varietà di forme nell'intervallo di pH studiato. La prima forma rilevata dalla potenziometria è $[FeH_5L]^{6+}$, in cui probabilmente il gruppo carbossilico terminale C e i due residui di acido aspartico sono già deprotonati. Questa forma è presente nella soluzione dall'inizio della titolazione [Figura 3.5].

La deprotonazione del residuo di acido glutammico porta probabilmente alla formazione di $[FeH_4L]^{5+}$ (il valore di pK di 4.13 è quasi lo stesso del legante libero). A partire da un pH di circa 4.90, la forma $[FeH_3L]^{4+}$ domina nella soluzione, fino a un pH di circa 7.5, assomigliando alla forma $[FeH_3L]$ osservata per P1. Entrambe sono probabilmente le prime forme nella soluzione a contenere l'istidina deprotonata, con il valore di pK di 4.90 significativamente più basso rispetto al legante libero, suggerendo il coinvolgimento dell'azoto dell'imidazolo nella coordinazione del metallo. La titolazione NMR effettuata con aggiunte successione di $Fe^{2+}$ a pH 6.2 indica il chiaro coinvolgimento dell'istidina H31 nella sfera di coordinazione dello ione metallico [Figura 3.7].
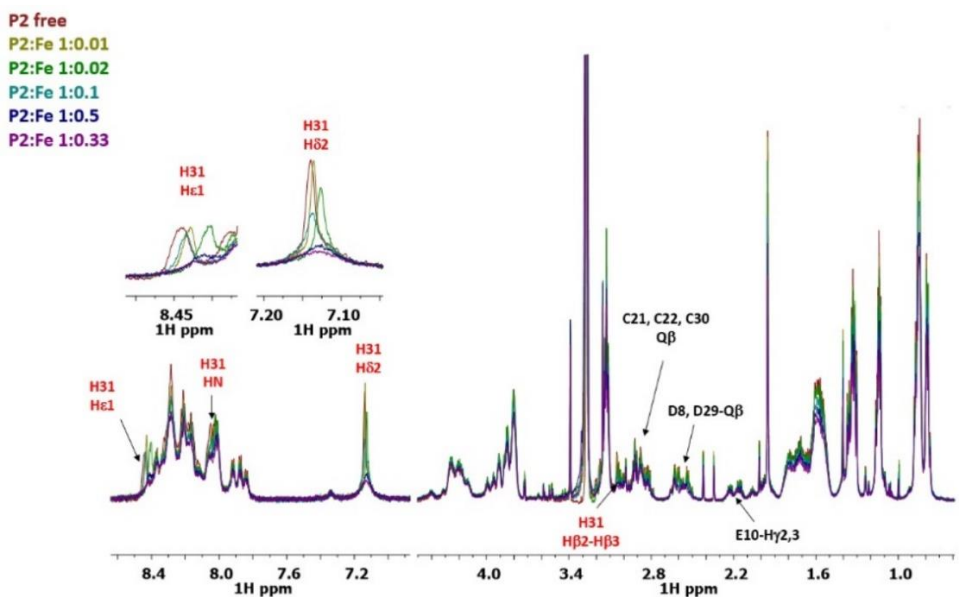
**Figura 3.7**. Titolazione $^1$H NMR del peptide P2 con aggiunte successive di $Fe^{2+}$ a pH 6.2

La forma successiva è $[FeHL]^{2+}$, molto probabilmente il risultato della deprotonazione di due residui di cisteina. Come per P1, la forma transitoria $[FeH_2L]^{3+}$ non può essere rilevata dalla potenziometria. La deprotonazione dell'ultimo residuo di cisteina porta poi alla formazione di $[FeL]^+$, con il valore di pK significativamente ridotto rispetto al legante libero (pK = 8.75 e 10.11 rispettivamente), suggerendo la presenza di questo residuo di cisteina nella sfera di coordinazione del metallo. L'analisi NMR effettuata al pH di 8.5 mostra una maggiore e selettiva perturbazione per i residui di H31, di cisteina C21, C22 e C30 e di D29. I residui di D8 e E10 invece non risultano perturbati. I valori di pK delle ultime tre forme ($[FeLH_{-1}]$, $[FeLH_{-2}]^-$ e $[FeLH_{-3}]^{2-}$) sono nell'intervallo di 8.80-9.83 e corrispondono molto probabilmente alla deprotonazione di tre molecole d'acqua, o al residuo di lisina e due molecole d'acqua. Anche a valori di pH superiori (pH 9.5) l'analisi NMR, seppur limitata da un generalizzato effetto paramagnetico dello ione ferroso, fornisce un risultato analogo a quello di pH 8.5.

### 3.3 Complessi di $Zn^{2+}$

Le costanti di stabilità dei sistemi peptidi: $Zn^{2+}$ sono raccolte nella Tabella 3.3 e i grafici di speciazione in Figura 3.8.
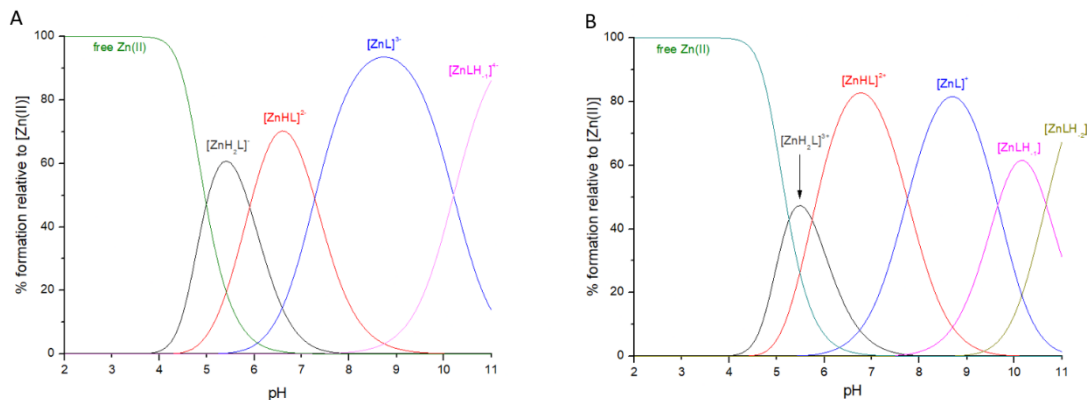


. **Figura 3.8**. Grafici di speciazione per il sistema P1-$Zn^{2+}$ (a sinistra) e per il sistema P2-$Zn^{2+}$ (a destra).

| Peptide | Specie | Logβ | LogK | Deprotonazione |
|---------|--------|------|------|----------------|
| P1 | $[ZnH_2L]^-$ | 26.97(2) | | |
| | $[ZnHL]^{2-}$ | 21.06(2) | 5.91 | His |
| | $[ZnL]^{3-}$ | 13.79(4) | 7.27 | Cys |
| | $[ZnLH_{-1}]^{4-}$ | 3.58(4) | 10.21 | $O_{water}$ |
| | | | | |
| P2 | $[ZnH_2L]^{3+}$ | 26.65(4) | | |
| | $[ZnHL]^{2+}$ | 20.91(2) | 5.74 | His |
| | $[ZnL]^+$ | 13.16(6) | 7.75 | Cys |
| | $[ZnLH_{-1}]$ | 3.51(6) | 9.65 | Lys |
| | $[ZnLH_{-2}]^-$ | -7.16(6) | 10.57 | $O_{water}$ |

**Tabella 3.3**. Costanti di protonazione dei complessi P1-$Zn^{2+}$ e P2-$Zn^{2+}$.

Il primo complesso $Zn^{2+}$ con P1 rilevato dalla potenziometria è $[ZnH_2L]^-$, che inizia a formarsi a un pH di circa 4. In questa specie, il gruppo C-terminale, l'Asp e due residui di Cys sono probabilmente deprotonati. La complessazione degli ioni $Zn^{2+}$ può portare a un diverso ordine di deprotonazione dei residui degli amminoacidi rispetto alla titolazione del legante libero: i residui di cisteina possono deprotonarsi prima dell'istidina, comportamento che è stato già osservato per diversi peptidi contenenti cisteina [71]. Gli spettri NMR registrati a pH 5.4 mostrano la scomparsa dei segnali C20 e C21, confermando la loro partecipazione alla coordinazione del metallo, nella modalità {$2S^-$}. Il segnale di H31 è perturbato negli spettri, il che potrebbe significare che inizia anche a partecipare al legame con lo $Zn^{2+}$ nella forma $[ZnHL]^{2-}$, che è già presente nella soluzione a questo pH. Gli spettri NMR registrati a pH = 6.1, dove $[ZnHL]^{2-}$ è la forma principale nella soluzione, confermano che effettivamente questa forma deriva dalla deprotonazione di H31 e che l'atomo di azoto dell'imidazolo di H31 è coinvolto nella coordinazione dello ione metallico, in accordo con il ridotto valore di pK del residuo di His nel complesso $Zn^{2+}$ (pK = 5.91) rispetto al legante (pK = 6.96). L'ultima deprotonazione del residuo di cisteina (C30) porta alla formazione del complesso $[ZnL]^{3-}$, che include oltre il 90% degli ioni $Zn^{2+}$ nella soluzione alla concentrazione massima della forma a pH circa 8.7 per P1. La scomparsa dei segnali di C30 può essere osservata negli spettri NMR registrati a pH 8.5, indicando che il residuo C30 completa la coordinazione tetraedrica attorno allo ione $Zn^{2+}$: {$3S^-$, $N_{im}$} [Figura 3.9]. La perturbazione del segnale D29 osservata a questo pH è probabilmente la conseguenza della vicinanza ai residui impegnati nel legame con il metallo. L'ultima forma del complesso, $[ZnLH_{-1}]^{4-}$, corrisponde probabilmente alla deprotonazione della molecola d'acqua. Gli spettri NMR registrati a pH 10.4 sono risultati analoghi a quelli a pH 8.5.
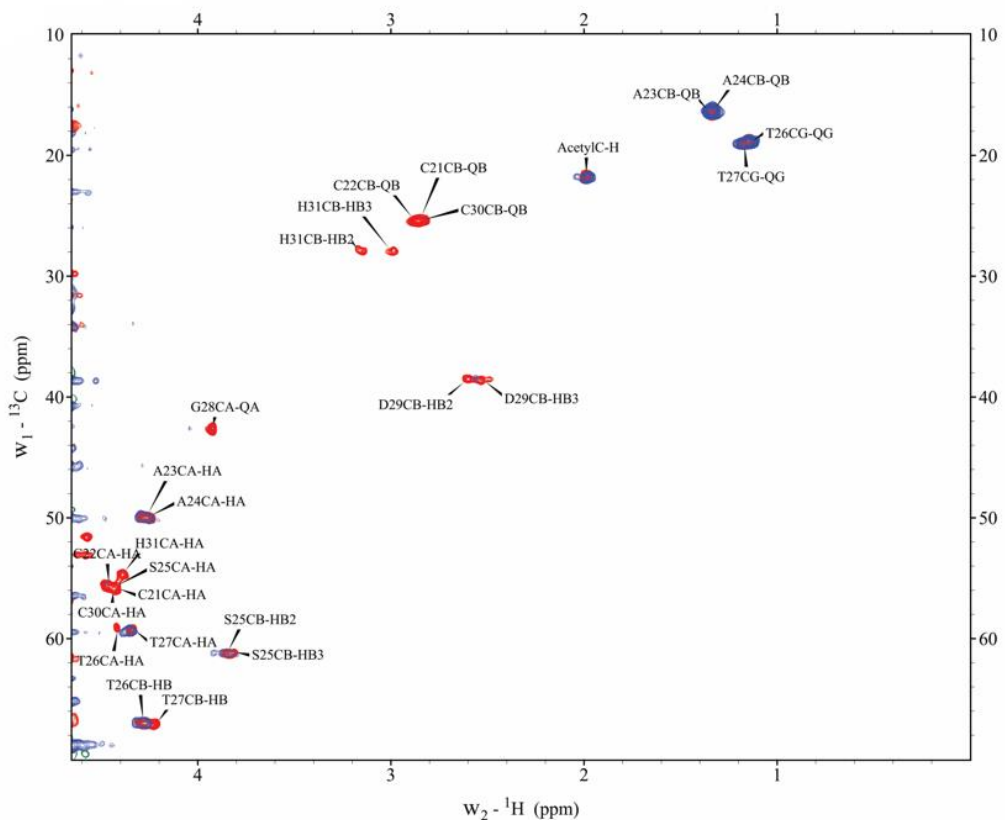
**Figura 3.9**. Paragone degli spettri $^1$H-$^{13}$C HSQC a pH 8.5. In rosso il peptide libero e in blu il sistema P1-Zn$^{2+}$ 1:1.

Nel caso di P2, i gruppi acidi aggiuntivi (D8 e E10) non portano alla formazione di ulteriori specie a pH acido rilevate dalla potenziometria. Allo stesso modo, come per P1, la prima specie è [ZnH$_2$L]$^{3+}$, che inizia a formarsi a pH di circa 4, con il gruppo C-terminale, due acidi aspartici, acido glutammico e due residui di cisteina probabilmente deprotonati. Gli spettri NMR registrati a pH 5.5 mostrano la perturbazione dei residui C20, C21 e H31. A questo pH, ci sono due specie che esistono in equilibrio nella soluzione: [ZnH$_2$L]$^{3+}$ e [ZnHL]$^{2+}$. Probabilmente è per questo che il segnale H31 appare perturbato negli spettri: la sua deprotonazione porta alla formazione di [ZnHL]$^{2+}$ e alla coordinazione dello Zn$^{2+}$ nella modalità {2S$^-$, N$_{im}$}, in accordo con i risultati per P1. La deprotonazione di C30 porta alla forma [ZnL]$^+$ e completa il sito di legame del

metallo, {3S⁻, N$_{im}$}, come confermato dagli spettri NMR a pH = 9.3. La forma successiva, [ZnLH$_{-1}$], è probabilmente il risultato della deprotonazione del residuo di lisina non coordinante (valore di pK 9.65, coerente con quanto osservato in precedenza). L'ultima forma del complesso, [ZnLH$_{-2}$]⁻, predominante nella soluzione sopra un pH di circa 10.60, corrisponde probabilmente alla deprotonazione della molecola d'acqua.

### 3.4 Complessi di Mn²⁺

Le costanti di stabilità dei sistemi P1:Mn²⁺ e P2:Mn²⁺ sono raccolte nella Tabella 3.4 e i grafici di speciazione in Figura 3.10.

| Peptide | Specie | Logβ | LogK | Deprotonazione |
|---------|--------|------|------|----------------|
| P1 | [MnH$_4$L]⁺ | 37.88(6) | | |
| | [MnH$_3$L] | 31.42(5) | 6.46 | His |
| | [MnH$_2$L]⁻ | 23.23(7) | 8.19 | Cys |
| | [MnHL]²⁻ | 14.46(7) | 8.77 | Cys |
| | [MnLH$_{-1}$]⁴⁻ | -6.07(4) | - | O$_{water}$, Cys |
| | | | | |
| P2 | [MnH$_5$L]⁶⁺ | 42.29(4) | | |
| | [MnH$_4$L]⁵⁺ | 38.65(2) | 3.64 | Glu |
| | [MnH$_3$L]⁴⁺ | 33.45(3) | 5.20 | His |
| | [MnHL]³⁺ | 26.12(4) | 7.33 | Cys |
| | [MnHL]²⁺ | 17.53(4) | 8.59 | Cys |
| | [MnL]⁺ | 8.20(4) | 9.33 | Cys |
| | [MnLH$_{-2}$]⁻ | -12.21(4) | - | O$_{water}$, Lys |

**Tabella 3.4**. Costanti di protonazione dei complessi P1-Mn²⁺ e P2-Mn²⁺.
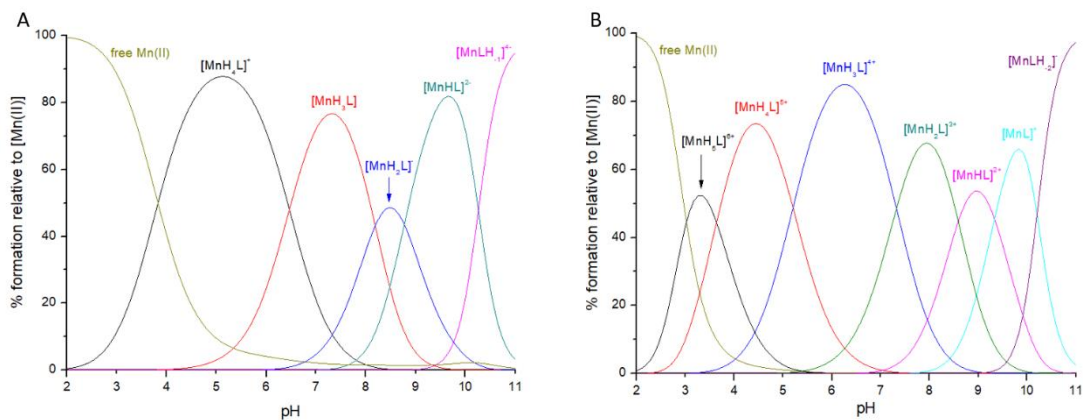
**Figura 3.10**. Grafici di speciazione per il sistema P1-Mn$^{2+}$ (a sinistra) e per il sistema P2-Mn$^{2+}$ (a destra).

Per P1, il primo complesso di Mn$^{2+}$ che si forma nella soluzione e rilevabile dalla potenziometria è [MnH$_4$L]$^+$, in cui il gruppo carbossilico C-terminale e il gruppo carbossilico della catena laterale dell'acido aspartico sono probabilmente già deprotonati [Figura 3.10]: questo è presente nella soluzione già all'inizio della titolazione e domina da pH circa 3.9 fino a 6.46. Gli spettri NMR registrati a pH 5.0 mostrano la scomparsa dei segnali relativi a D29 e a tutti i protoni di H31 [Figura 3.11].
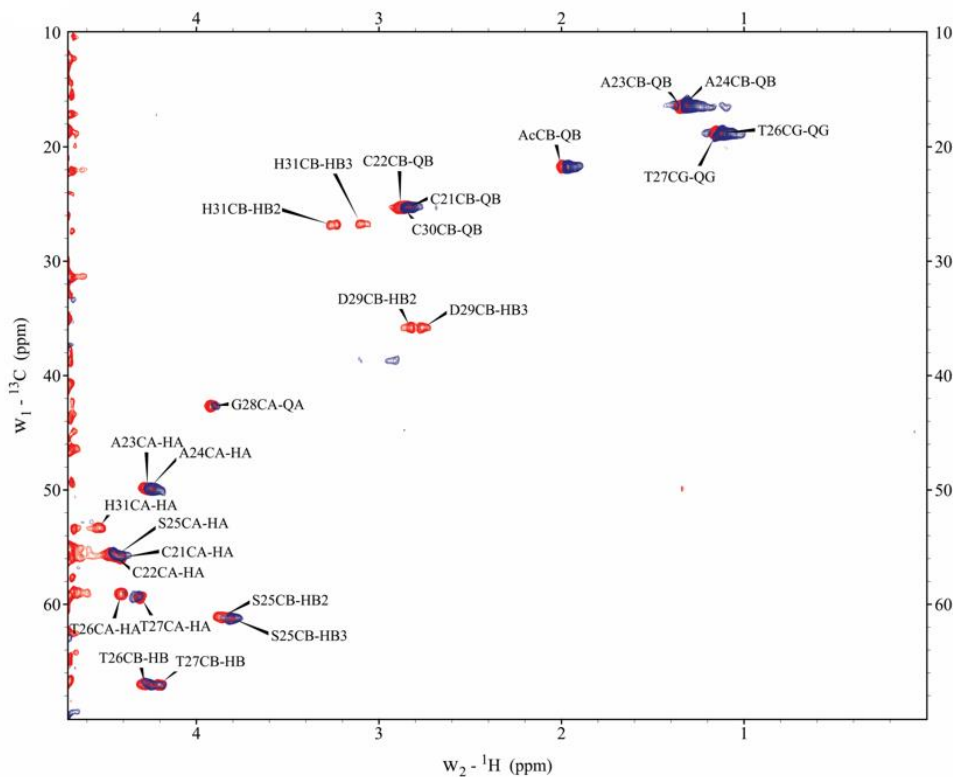
**Figura 3.11**. Paragone degli spettri $^1$H-$^{13}$C HSQC a pH 5. In rosso il peptide libero e in blu il sistema P1-Mn$^{2+}$ 1:0.02.

L'istidina è l'amminoacido C-terminale, quindi la coordinazione può avvenire sia attraverso gruppo carbossilico C-terminale che nell'azoto dell'anello imidazolico.

E' possibile che la scomparsa di tutti i segnali di H31 significhi due cose: in primo luogo, a pH = 5.0 il gruppo C-terminale deprotonato lega lo ione Mn$^{2+}$ insieme a D29 nella forma [MnH$_4$L]$^+$; in secondo luogo, la deprotonazione dell'azoto imidazolico e il legame del metallo possono già essere osservati a questo pH, poiché la forma successiva, [MnH$_3$L], che corrisponde alla deprotonazione dell'azoto imidazolico dell'istidina, inizia a formarsi a pH circa 4. La modalità di legame metallico in questa forma complessa è probabilmente {2 COO$^-$, N$_{im}$}. La deprotonazione successiva più probabile dei residui di cisteina porta alla formazione dei complessi [MnH$_2$L]$^-$ e [MnHL]$^{2-}$. La forma

[MnLH$_{-1}$]$^{4-}$ corrisponde alla deprotonazione del terzo residuo di cisteina e probabilmente di una molecola d'acqua. La forma complessa [MnL]$^{3-}$ non può essere rilevata dalla potenziometria, poiché è probabilmente solo una forma transitoria, con una concentrazione molto bassa nella soluzione. Non è del tutto chiaro se i residui di cisteina siano coinvolti nella coordinazione metallica. I valori di pK dei residui di Cys nel complesso con Mn$^{2+}$ sono 8.19 e 8.77 (il terzo valore di pK non può essere calcolato dalle titolazioni potenziometriche), mentre nel legante libero i valori erano 8.15 e 8.92 rispettivamente. L'abbassamento molto lieve del valore di pK nel complesso significa molto probabilmente che i residui di cisteina non sono coinvolti nella coordinazione del metallo. Tuttavia, gli spettri NMR registrati a pH 7.0, in cui [MnH$_2$L]$^-$ è presente nella soluzione, mostrano una diminuzione dell'intensità dei segnali sovrapposti della cisteina [Figura 3.12].
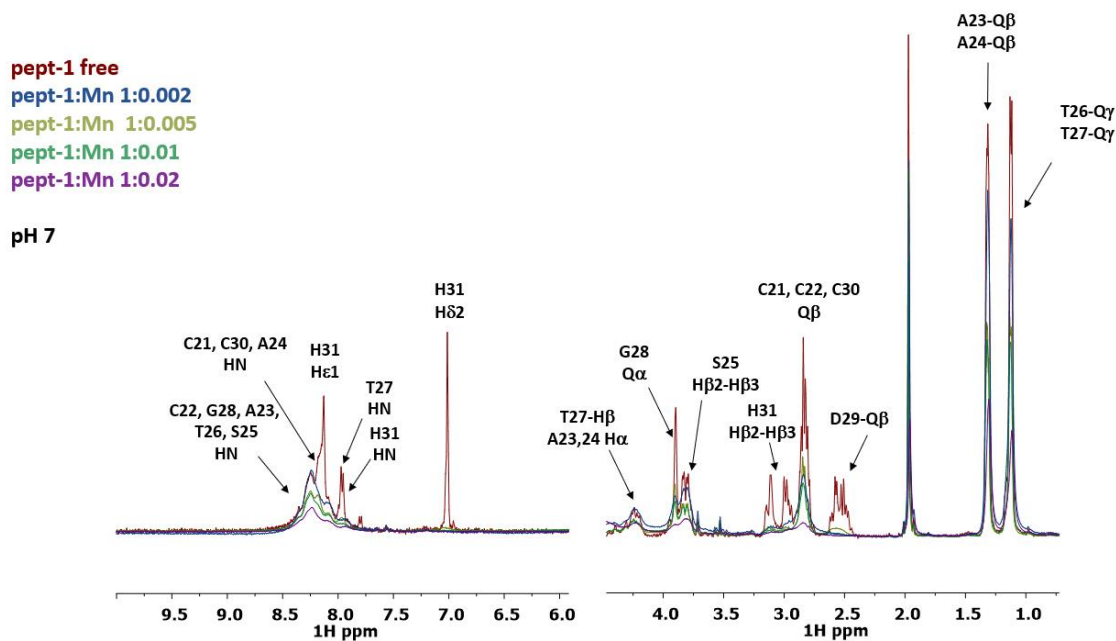


**Figura 3.12**. Titolazione $^1$H NMR del peptide P1 con aggiunte successive di Mn$^{2+}$ a pH 7.

La diminuzione è significativa e corrisponde probabilmente a più di un residuo di cisteina interessato influenzato dalla vicinanza dello ione metallico. Ciò potrebbe significare che il segnale di C30 scompare a causa della vicinanza ai residui leganti D29 e H31, e uno dei C21 o C22 lega lo ione metallico, oppure entrambi sono coinvolti nel legame con $Mn^{2+}$, mentre il C30 è orientato nel modo opposto rispetto a D29 e H31 e sperimenta solo uno scarso effetto paramagnetico. Tenendo conto di tutto ciò, la modalità di legame dello ione $Mn^{2+}$ da pH 7 in su potrebbe essere $\{2\ COO^-, N_{im}\}$, $\{2\ COO^-, N_{im}, S^-\}$ o $\{2\ COO^-, N_{im}, 2S^-\}$.

Per i complessi P2 con $Mn^{2+}$, la presenza dei residui aggiuntivi Asp (D8) e Glu (E10) rispetto a P1 ha portato al rilevamento di una forma complessa in più a pH acido: $[MnH_5L]^{6+}$, in cui il gruppo carbossilico terminale e i due residui di acido aspartico sono probabilmente deprotonati. Questa forma è presente nella soluzione fin dall'inizio della titolazione e domina in un intervallo ristretto di pH, da circa 3 a 3.64. La deprotonazione del residuo di acido glutammico porta alla formazione di $[MnH_4L]^{5+}$ con la massima concentrazione a un pH di circa 4.50. $[MnH_3L]^{4+}$ che corrisponde probabilmente alla deprotonazione dell'azoto dell'anello imidazolico dell'istidina. Questa forma coinvolge oltre l'80% degli ioni $Mn^{2+}$ nella soluzione alla massima concentrazione a pH di circa 6,3. Gli spettri NMR registrati a pH 5.5, in cui $[MnH_3L]^{4+}$ è la forma principale, indicano il legame metallico con E8, D29 e H31. La modalità di legame è probabilmente $\{2\ COO^-, N_{im}\}$ o $\{3\ COO^-, N_{im}\}$, a seconda che il gruppo carbossilico terminale dell'istidina sia coinvolto nel legame metallico o meno.

Le successive tre forme, $[MnH_2L]^{3+}$, $[MnHL]^{2+}$ e $[MnL]^+$, corrispondono molto probabilmente alla deprotonazione dei tre residui di cisteina. A pH 7.4, gli spettri NMR mostrano la scomparsa di tutti i segnali delle cisteine [Figura 3.13]. A questo punto, nella soluzione la forma principale è $[MnH_2L]^{3+}$ con un residuo di cisteina deprotonato. Tuttavia è presente anche $[MnHL]^{2+}$ contenente due residui di cisteina deprotonati. A causa dell'effetto paramagnetico del $Mn^{2+}$ sugli spettri NMR e della sovrapposizione dei segnali delle cisteine, è difficile

distinguere tra i segnali delle singole cisteine. Riteniamo che almeno uno dei residui di cisteina sia coinvolto nel legame metallico, sia interagendo direttamente con lo ione $Mn^{2+}$, sia stabilizzando il complesso. Questa interazione è probabilmente riflessa anche nelle titolazioni potenziometriche, dove la differenza tra il valore di pK del complesso e del legante libero della prima cisteina è diminuita per P2 (di 0.82), mentre per P1 il valore di pK nel complesso era superiore a quello nel legante libero. Le modalità di legame a pH superiore a 7.33 potrebbero essere {2 COO⁻, $N_{im}$, 1/2/3 S⁻} o {3 COO⁻, $N_{im}$, 1/2 S⁻}, a seconda del coinvolgimento del gruppo terminale e del numero di cisteine coinvolte. L'ultima forma rilevata è [MnLH₋₂]⁻, in cui probabilmente sono deprotonati la lisina, l'arginina o una molecola d'acqua.
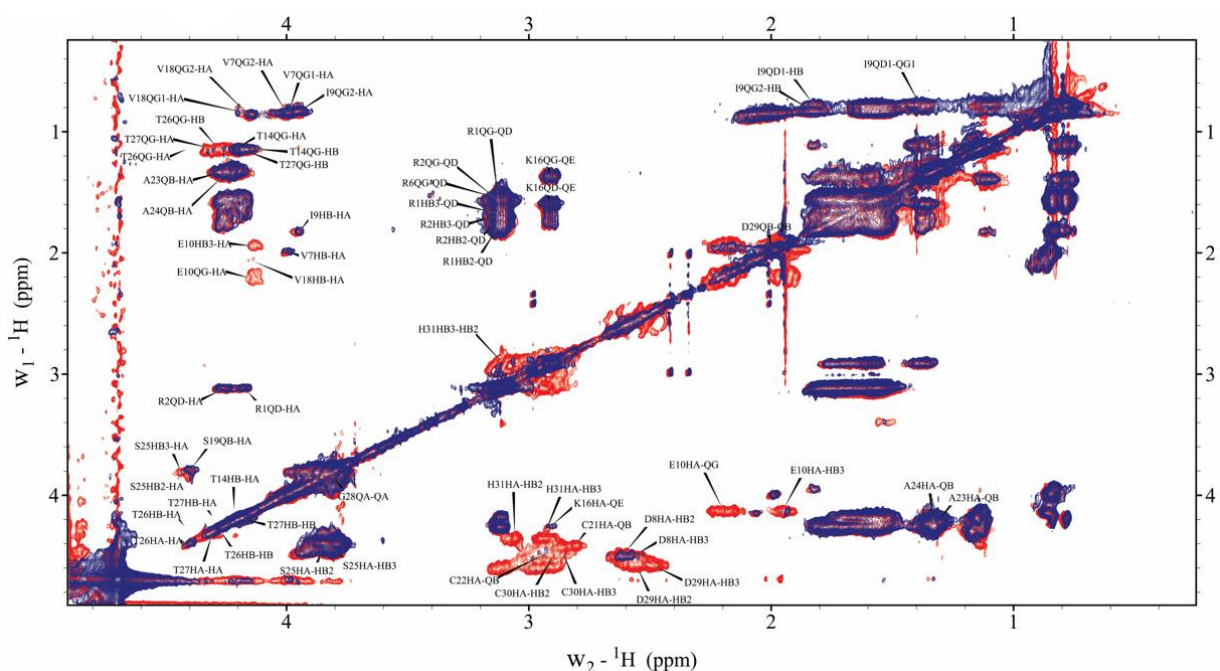


**Figura 3.13**. Regione alifatica dello spettro $^1$H-$^1$H TOCSY a pH 7.4. In rosso il peptide libero e in blu il sistema P1-$Mn^{2+}$ 1:0.02.

Gli spettri EPR registrati per i complessi di $Mn^{2+}$ per entrambi i leganti su un'ampia gamma di pH suggeriscono un metallo esacoordinato nei complessi con geometria ottaedrica. Il pattern a sei linee è caratteristico per il manganese ($I_{Mn}$ = 5/2) e gli spettri registrati assomigliano a quelli dell'esa-aquo ione di $Mn^{2+}$, il che significa che la geometria dei complessi è molto probabilmente ottaedrica, con molecole d'acqua che completano la sfera di coordinazione del metallo. Gli spettri EPR per P1 con $Mn^{2+}$ e per P2:$Mn^{2+}$ sono mostrati nella Figura 3.14. Il valore della costante di accoppiamento iperfine (A) per entrambi i complessi P1:$Mn^{2+}$ e P2:$Mn^{2+}$ a tutti i valori di pH misurati è di circa 95 G, coerente con la geometria ottaedrica dei complessi di $Mn^{2+}$.
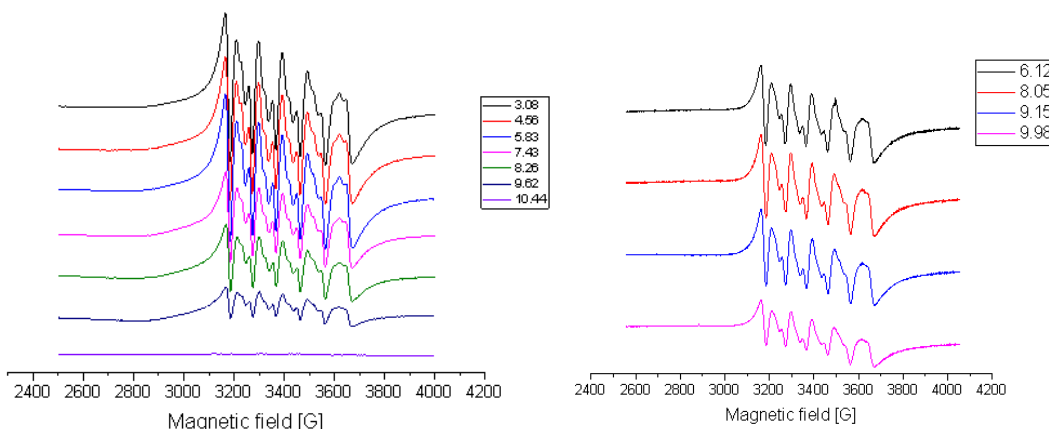


**Figura 3.14**. Spettri EPR del sistema P1-$Mn^{2+}$ (a sinistra) e del sistema P3-$Mn^{2+}$ (a destra), a diversi intervalli di pH.

Confrontando i grafici di competizione tra i leganti e lo ione metallico, si può osservare una diversa specificità per i tre ioni metallici studiati [Figura 3.15].
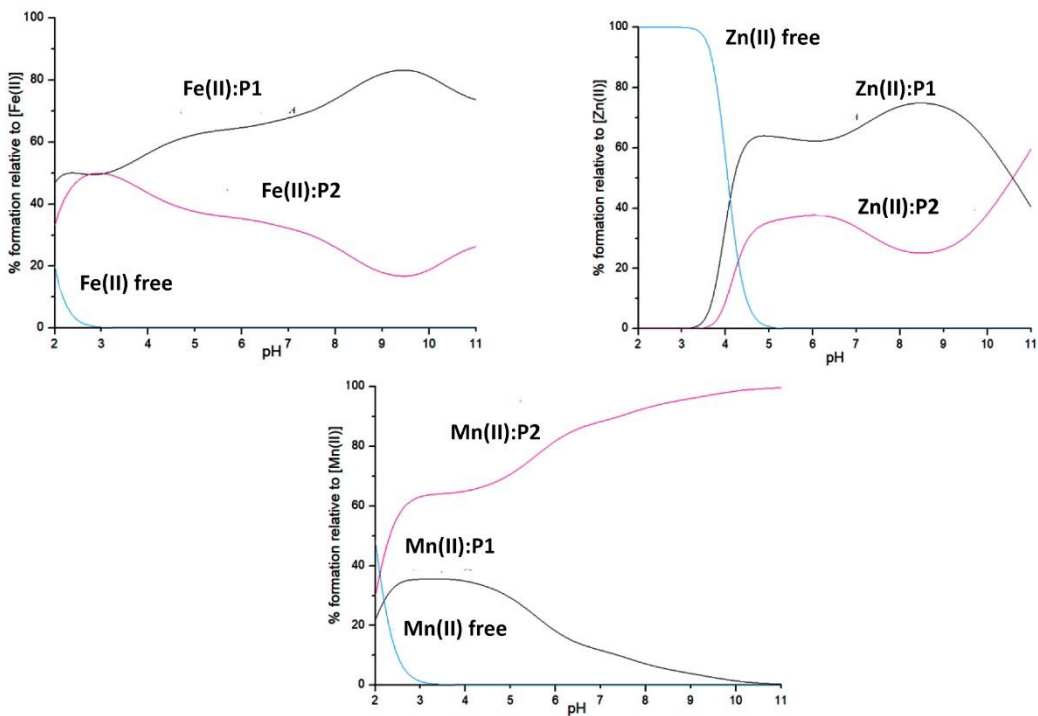
**Figura 3.15**. Grafici di competizione tra i ligandi P1 e P2 e lo ione metallico.

$Fe^{2+}$ e $Zn^{2+}$ formano complessi più forti con P1 in quasi tutto l'intervallo di pH studiato, mentre $Mn^{2+}$ forma complessi significativamente più stabili con P2, che contiene l'intera parte C-terminale citoplasmatica del FeoB di *E. coli*. Questo comportamento riflette probabilmente la differenza nell'affinità degli ioni metallici per diversi tipi di leganti: mentre $Zn^{2+}$ e $Fe^{2+}$ sono solitamente considerati acidi di Lewis *borderline* con affinità per basi *borderline* e *soft*, come i tioli, $Mn^{2+}$ nelle proteine è legato relativamente di rado ai residui di cisteina e tende a interagire maggiormente con basi più *hard*, come i leganti a base di ossigeno (ad esempio aspartato, glutammato) [69,72].

I nostri risultati sono coerenti con questo comportamento, poiché P2 (Ac-R743RARSRVDIELLATRKSVSSCCAASTTGDCH773) rispetto a P1 (Ac-C763CAASTTGDCH773) possiede due residui in più contenenti gruppi carbossilici: aspartato D8 e glutammato E10, che dalla spettroscopia NMR sembrano interagire con lo ione $Mn^{2+}$ e stabilizzare la formazione del

complesso. Il coinvolgimento dei residui di cisteina nel legame con $Mn^{2+}$ non è molto chiaro, tuttavia il loro ruolo nella formazione del complesso non sembra fondamentale come il ruolo dei leganti a base di ossigeno, vale a dire acidi aspartico e glutammico, il che si riflette nella chiara predominanza del sistema P2: $Mn^{2+}$ rispetto al sistema P1:$Mn^{2+}$ già a partire da pH 2.

Per i sistemi $Fe^{2+}$ e $Zn^{2+}$ il comportamento è contrario a quello di $Mn^{2+}$: i complessi P1 sono più stabili di quelli di P2. Ciò riflette probabilmente l'affinità più forte di $Fe^{2+}$ e $Zn^{2+}$ per gli atomi di zolfo delle cisteine, poiché l'allungamento della catena di amminoacidi in P2 non ha portato alla formazione di complessi più forti, il che significa che il sito di legame metallico primario è molto probabilmente già presente nel P1 ed è costituito da tre residui di cisteina e uno di istidina. La discrepanza della percentuale di formazione rispetto alla concentrazione dello ione metallico tra i complessi di $Fe^{2+}$ con P1 e P2 (differenza massima di circa il 66%) e $Zn^{2+}$ (differenza massima di circa il 50%) è inferiore a quella di $Mn^{2+}$ (oltre il 90% di differenza già a pH circa 8.5) e riflette probabilmente una maggiore versatilità verso diversi leganti per $Zn^{2+}$ e $Fe^{2+}$ rispetto a $Mn^{2+}$. Sebbene per $Zn^{2+}$ non abbiamo osservato specie aggiuntive per P2 rispetto a P1, abbiamo notato la presenza di una ulteriore specie per $Fe^{2+}$, in modo simile a $Mn^{2+}$, tuttavia l'influenza dell'aspartato e del glutammato è meno evidente sulla formazione del complesso $Fe^{2+}$ e probabilmente non è così importante come per $Mn^{2+}$, poiché il sistema P1:$Fe^{2+}$ ha comunque formato complessi più forti di P2:$Fe^{2+}$.


### 3.5 Conclusioni

Le nostre indagini sul trasportatore batterico FeoB, mediante l'utilizzo di tecniche come la potenziometria e la risonanza magnetica nucleare, hanno permesso di acquisire preziose informazioni riguardo alle interazioni di questa proteina con gli ioni metallici. In particolare, abbiamo focalizzato la nostra attenzione su alcuni frammenti selezionati della proteina, analizzandone la

risposta alla presenza di ioni Zn, Fe e Mn. I risultati ottenuti hanno rivelato la formazione di complessi metallo-proteici in soluzione, indicando una specifica affinità dei frammenti per tali ioni.

Attraverso i grafici di competizione tra gli ioni metallici e i singoli leganti, abbiamo potuto osservare come i complessi di $Fe^{2+}$ prevalgano per entrambi i sistemi P1 e P2 fino a un pH di circa 6.5. Successivamente, abbiamo notato un rapido aumento dei complessi di $Zn^{2+}$ che raggiungono oltre il 90% del legante libero legato a un pH di circa 7.5. È interessante sottolineare che al di sopra di pH 6.5, la stabilità dei complessi segue la serie di Irving-Williams: $Mn^{2+} < Fe^{2+} < Zn^{2+}$ [73]. Sebbene i complessi $Mn^{2+}$ non dominino mai nella soluzione, abbiamo riscontrato una discrepanza di stabilità relativamente bassa tra i complessi di $Fe^{2+}$ e $Mn^{2+}$ per il P2, indicando che il $Mn^{2+}$ forma complessi più stabili con il P2 rispetto al P1, mentre per il $Fe^{2+}$ è il contrario.

È importante sottolineare che la predominanza dei complessi di $Fe^{2+}$ di entrambi i peptidi in quasi tutto l'intervallo di pH acido, che è rilevante per la stabilità del $Fe^{2+}$, indica che la parte C-terminale citoplasmatica del FeoB potrebbe fungere da potente sito di legame per il $Fe^{2+}$, influenzando il trasporto del ferro attraverso la membrana, facilitando il trasferimento dalle proteine citoplasmatiche o agendo come sensore di $Fe^{2+}$ nel citoplasma di *E. coli*. D'altra parte, la predominanza dei complessi di $Zn^{2+}$ sopra un pH di circa 6.5 suggerisce che il frammento policisteinico C-terminale rappresenti anche un sito di legame significativo per lo $Zn^{2+}$ in condizioni basiche.

Queste scoperte aprono interessanti prospettive nella ricerca di nuove terapie antibatteriche. La capacità del trasportatore batterico FeoB di interagire con gli ioni metallici nell'ambiente sottolinea la sua potenziale rilevanza nel contesto delle infezioni batteriche. La modulazione delle interazioni tra FeoB e gli ioni metallici potrebbe rappresentare un approccio promettente per contrastare la crescita batterica indesiderata. Ulteriori studi sono sicuramente necessari per approfondire le implicazioni di queste interazioni e per determinare le condizioni ottimali per l'applicazione pratica di queste scoperte. Questa nuova

prospettiva può aprire nuove strade nella ricerca di terapie antibatteriche mirate che sfruttino l'interferenza con le interazioni metallo-proteina per inibire l'assorbimento del ferro da parte dei batteri patogeni.

I risultati di questo studio sono attualmente in fase di elaborazione finale per la stesura dell'articolo dal titolo:

**$Fe^{2+}$, $Mn^{2+}$ and $Zn^{2+}$ binding to the C- terminal region of FeoB protein: a novel insight into the coordination chemistry and specificity of the *E. coli* $Fe^{2+}$ transporter.**

Autori: B.Orzel, A.Pelucelli, M. Ostrowska, S.Potocki, H. Kozlowski, M. Peana, and E. Gumienna-Kontecka.

# Capitolo IV

## Studio dell'interazione degli ioni metallici Cu$^{2+}$ e Zn$^{2+}$ con l'interfaccia di riconoscimento di ACE2 per la proteina Spike SARS-CoV-2

### 4.1 Introduzione

L'enzima umano di conversione dell'angiotensina 2 (ACE2) riveste un ruolo fondamentale nella regolazione della pressione sanguigna. Tuttavia, di recente è diventato noto come il principale punto di ingresso nelle cellule per il virus SARS-CoV-2, responsabile della COVID-19 [39]. Questa proteina funge da recettore per il virus, permettendogli di entrare e infettare le cellule umane [39]. Il recettore ACE2 è espresso in vari tessuti, tra cui polmoni, cuore e reni, rendendolo un bersaglio cruciale per il virus per stabilire un'infezione sistemica [74].

Il recettore ACE2 appartiene alla famiglia degli enzimi noti come carbossipeptidasi, ed è una proteina transmembrana di tipo I coinvolta in diverse funzioni fisiologiche. Tra queste funzioni, regola la pressione sanguigna convertendo l'angiotensina II in angiotensina-(1-7), la quale possiede effetti vasodilatatori. Inoltre, l'ACE2 ha dimostrato di avere un effetto protettivo sul cuore e sui reni, rendendolo un potenziale target terapeutico per le malattie cardiovascolari e renali [74].

L'interazione tra la proteina *spike* del SARS-CoV-2 e il recettore ACE2 è ormai ben documentata [Figura 4.1]. La *spike* si lega al recettore ACE2 con elevata affinità, permettendo al virus di entrare nelle cellule ospiti e replicarsi [39-41]. Questa interazione provoca la perdita della funzione dell'ACE2 e l'aumento dei livelli di angiotensina II, portando a uno stato di ipertensione e stress ossidativo aumentato, che contribuisce alla gravità della COVID-19 [75]. Studi hanno

dimostrato che il numero di recettori ACE2 in determinati tessuti può influenzare la gravità della COVID-19 [75]. Ad esempio, gli individui con livelli più elevati di espressione dell'ACE2 nei polmoni sono più suscettibili a gravi problemi respiratori, mentre un'alta espressione nel cuore può portare a un maggiore rischio di complicazioni cardiovascolari. Inoltre, alcune variazioni genetiche nel gene ACE2 sono state associate a un maggiore rischio di malattia grave nei pazienti affetti da COVID-19 [75].
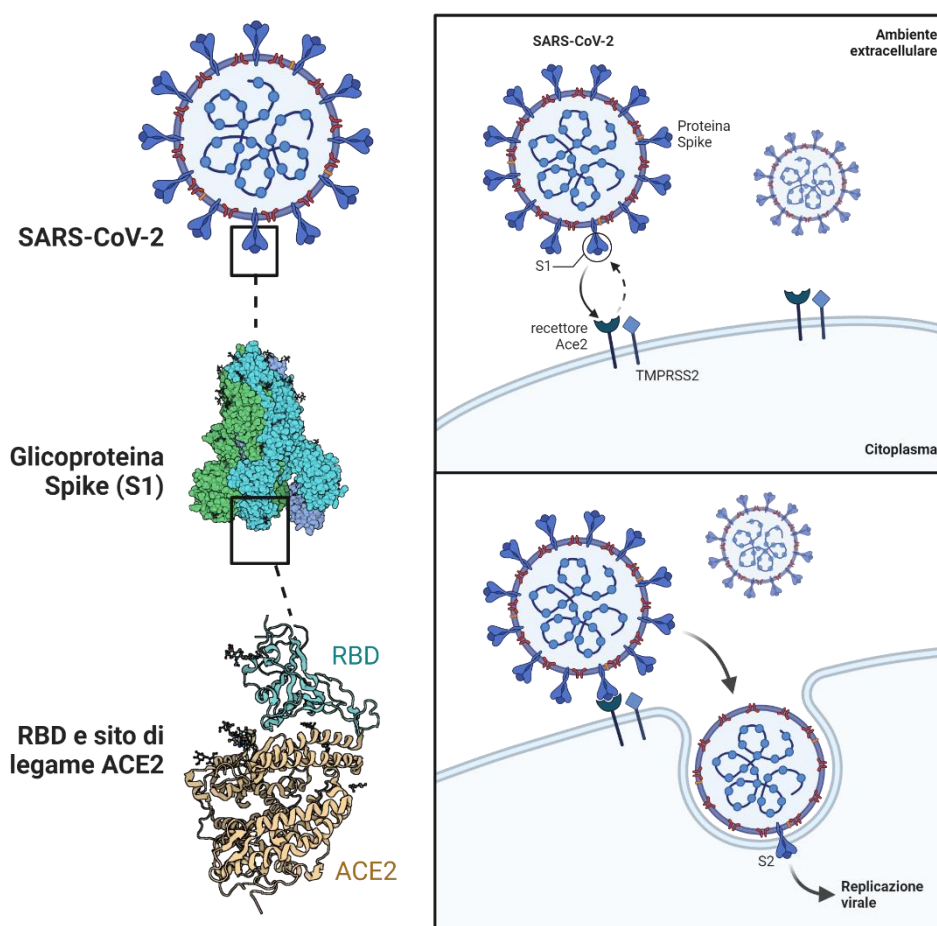


**Figura 4.1**. Meccanismo di interazione tra la glicoproteina *Spike* (S1) ed il recettore ACE2.

La specificità e l'affinità dell'interazione tra la proteina *spike* e il recettore ACE2 sono elementi cruciali per la capacità del virus SARS-CoV-2 di infettare le

cellule umane e causare la COVID-19 [37,38,76]. La proteina *spike* è una struttura trimerica composta da tre subunità identiche, che contengono due domini: il dominio N-terminale S1 e il dominio C-terminale S2. Il dominio S1 media il legame della proteina *spike* al recettore ACE2, mentre il dominio S2 è responsabile della fusione tra le membrane del virus e della cellula ospite [77].

L'interazione tra la proteina *spike* e il recettore ACE2 è specifica e guidata dall'affinità reciproca [78]. La proteina *spike* del SARS-CoV-2 si lega infatti al recettore ACE2 con un'affinità molto più elevata rispetto ad altri coronavirus [38]. Questa specificità è fondamentale affinché il virus stabilisca un'infezione sistemica e causi la malattia.

La struttura del recettore ACE2 è anch'essa essenziale per l'interazione con la proteina *spike*. Il recettore ACE2 è può assumere molteplici conformazioni, e quella preferita per il legame della proteina *spike* è stata identificata come una forma chiusa e compatta. Questa conformazione consente un'interazione ottimale tra gli amminoacidi del recettore ACE2 e la proteina *spike*, fornendo la massima affinità di legame tra le due proteine. I dettagli esatti della conformazione preferita del recettore ACE2, come la disposizione specifica degli amminoacidi e delle interazioni, sono ancora oggetto di ricerche in corso. Mutazioni nella proteina *spike* possono influenzare la sua capacità di legarsi al recettore ACE2 e ridurre l'infezione del virus [78].

Comprendere i dettagli di quest'interazione è fondamentale per lo sviluppo di terapie per prevenire e trattare la COVID-19. Ulteriori ricerche sono necessarie per comprendere appieno i meccanismi alla base dell'interazione e come contribuiscono alla gravità della malattia, anche in questo momento, quando il numero dei casi di contagio e la loro gravità sono diminuiti grazie all'intensa campagna di vaccinazioni, ma permangono ancora numerosi casi in cui l'infezione produce effetti estremamente gravi e pesanti. Inoltre, non si può escludere la comparsa di altre varianti più contagiose e letali, per cui la ricerca di un farmaco resta sempre altamente desiderabile.

Una crescente mole di prove suggerisce che la carenza di zinco sia uno dei principali determinanti del rischio e della gravità della COVID-19 [79]. Gli ioni $Zn^{2+}$ si legano a specifici residui ($H_{374}E_{402}XXH_{378}$) nel recettore e ne modulano l'attività [43], oltre a essere in grado di modificare la conformazione del recettore stesso [42]. Ciò che è particolarmente interessante nella regione dell'interfaccia di ACE2 è l'abbondanza di amminoacidi come aspartati, glutammati e l'istidina, con selettiva capacità di coordinazione verso gli ioni metallici. Per quanto riguarda l'interazione tra ACE2 e la proteina *spike* del SARS-CoV-2, si ritiene che la coordinazione degli ioni metallici possa alterare la conformazione dell'ACE2 stesso e quindi modificare la sua affinità per la proteina *spike*. In particolare, la capacità del recettore ACE2 umano di coordinare gli ioni metallici nella stessa regione in cui si lega alla proteina *spike* del SARS-CoV-2 potrebbe avere un impatto cruciale sul meccanismo di riconoscimento e interazione delle due proteine, con ripercussioni sulla loro affinità di legame che meritano di essere indagate.

In questo studio, ci siamo proposti di caratterizzare la capacità di coordinazione degli ioni $Zn^{2+}$ con frammenti di peptidi selezionati dell'interfaccia di legame dell'ACE2. In particolare, abbiamo selezionato due modelli di sequenza, P29-38 (Ac-$L_{29}$DKFNHEAED$_{38}$-NH2) e P19-42 (Ac-$S_{19}$TIEEQAKTFL29DKFNHEAED$_{38}$LFYQ$_{42}$-NH2), che comprende P29-38 e rappresenta l'intera interfaccia di legame dell'ACE2. Abbiamo studiato la loro interazione con $Zn^{2+}$ attraverso tecniche di potenziometria e risonanza magnetica nucleare (NMR).

I risultati preliminari ottenuti dai test effettuati sulla regione dell'interfaccia dell'ACE2 utilizzando MIB2, un server di predizione e modellazione dei siti di legame degli ioni metallici, sono promettenti. È stato osservato che un modello di interazione era presente, considerando diverse strutture PDB del recettore. In particolare, abbiamo potuto vedere che la maggior parte delle sequenze di coordinazione proposte dai modelli MIB2 coinvolgeva amminoacidi che

comprendono la regione 30-37, che consiste in un insieme ricco di residui di coordinazione $D_{30}$KFNHEAE$_{37}$ [Figura 4.2].
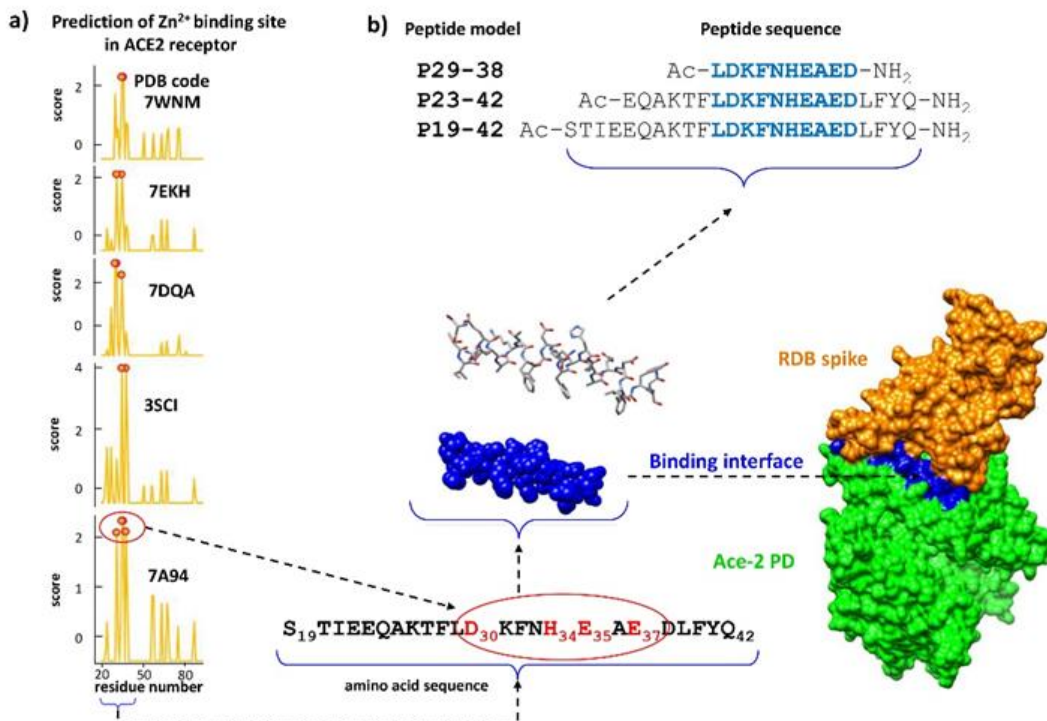


**Figura 4.2**. Previsione MIB2 dei siti di legame dello ione Zn2+ per una selezione di strutture a raggi X del recettore ACE2. I residui ricorrenti in tutte le previsioni si trovano nell'interfaccia di legame tra ACE2 e la proteina *spike*, localizzata nel frammento 30-37 aa; b) sequenza dei modelli peptidici dell'interfaccia di legame di ACE2 selezionati e analizzati in questo studio.

L'analisi di questi dati potrebbe fornire informazioni preziose sull'interazione tra ACE2 e la proteina *spike* del SARS-CoV-2 in presenza di ioni $Zn^{2+}$, contribuendo allo sviluppo di strategie terapeutiche mirate per prevenire e trattare la COVID-19.

## 4.2 Caratterizzazione in soluzione dei peptidi

Il decapeptide Ac-L$_{29}$DKFNHEAED$_{38}$-NH$_2$ (P29-38) può essere considerato un legante H$_6$L con sei costanti di protonazione nel range di pH investigato [Tabella 4.1, Figura 4.3].

**Tabella 4.1**. Costanti di protonazione del peptide libero P29-38.

| Peptide | Specie | Logβ | LogK | Deprotonazione |
|---------|--------|------|------|----------------|
| P29-38 | [H$_6$L]$^{2+}$ | 33.34(2) | 3.15 | Asp |
| | [H$_5$L]$^+$ | 30.19(2) | 3.83 | Asp |
| | [H$_4$L] | 26.36(2) | 4.38 | Glu |
| | [H$_3$L]$^-$ | 21.98(2) | 4.93 | Glu |
| | [H$_2$L]$^{2-}$ | 17.05(2) | 6.84 | His |
| | [HL]$^{3-}$ | 10.21(1) | 10.21 | Lys |
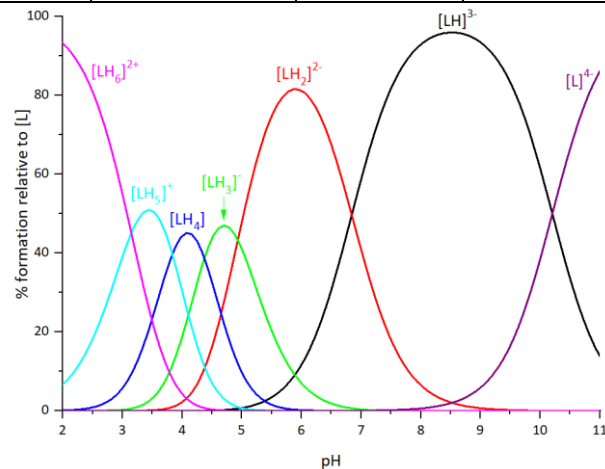


**Figura 4.3**. Grafico di speziazione per il peptide libero P29-38.

I primi due valori di pKa (3.15 e 3.83) corrispondono alla deprotonazione del gruppo carbossilico dei residui Asp30 e Asp38. I successivi due valori di pKa (4.38, 4.93) derivano invece dalla deprotonazione di Glu35 e Glu37. Un primo limite a questa analisi è stato quello di non poter distinguere tra i due residui di Asp ed i due residui di Glu tramite potenziometria. I due valori di pKa successivi (6.84 e 10.21) sono il risultato della deprotonazione delle catene

laterali di His34 e Lys31, in accordo con i valori trovati in letteratura per sistemi simili [80].

I numerosi spettri NMR registrati per il peptide libero P29-38 in un ampio range di pH confermano questi passaggi di deprotonazione. Sono state rilevate variazioni di *chemical shift* a seguito dell'aumento del pH per i nuclei di Asp e Glu a pH inferiore a 5, mentre per il residuo His sono state rilevate importanti variazioni di *chemical shift* a partire da pH 6 fino a 7.4: per quanto riguarda il residuo Lys invece, solo a partire da pH > 10 [Figura 4.4]. Purtroppo, entrambi i peptidi più lunghi, P23-42 e P19-42, si sono dimostrati molto poco solubili in acqua, ragion per cui non è stato possibile effettuare un'analisi potenziometrica. Di conseguenza, la loro capacità di coordinazione nei confronti di $Zn^{2+}$ e $Cu^{2+}$ è stata valutata solo tramite spettroscopia NMR.
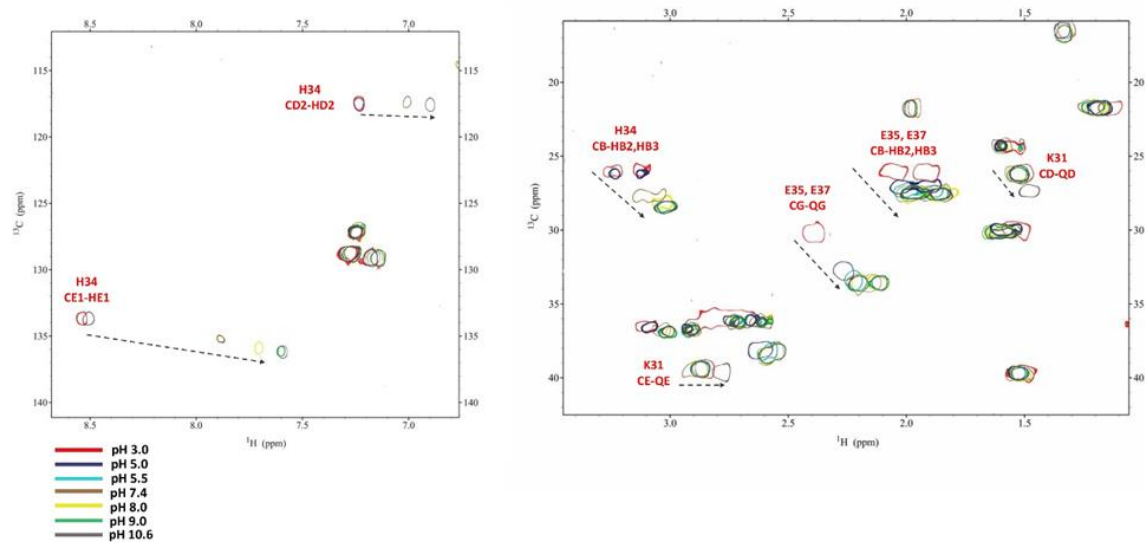


**Figura 4.4**. Confronto degli spettri HSQC $^1H$-$^{13}C$ per il peptide libero P29–38 a vari valori di pH.

## 4.3 Complessi di $Zn^{2+}$

Il peptide P29-38 forma quattro specie con $Zn^{2+}$ [Tabella 4.2, Figura 4.5].

| Specie | Logβ | LogK | Deprotonazione | Coordinazione |
|---|---|---|---|---|
| [ZnH$_2$L] | 20.34(8) | | | Asp, Asp, Glu, (Glu) |
| [ZnHL]$^-$ | 14.55(6) | 5.79 | His | (Asp), Asp, Glu, His |
| [ZnLH$_{-1}$]$^{3-}$ | -1.50(5) | 2*8.025 | H$_2$O, H$_2$O | (Asp), Asp, Glu, His |
| [ZnLH$_{-2}$]$^{4-}$ | -11.42(6) | 9.92 | Lys | (Asp), Asp, Glu, His |
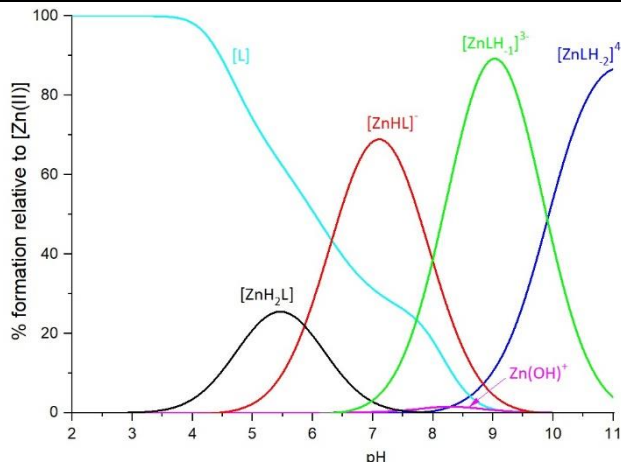


**Figura 4.5**. Grafico di speciazione per il sistema P29-38-Zn$^{2+}$.

La prima specie è [ZnH$_2$L], che inizia a pH 3.5 e raggiunge solo il 28% della concentrazione massima di Zn$^{2+}$ in soluzione a pH 5.5. A questo pH, tutti i gruppi carbossilici sono quasi completamente deprotonati, mentre i residui di His34 e Lys31 sono ancora protonati. La modalità di coordinazione proposta per Zn$^{2+}$ potrebbe coinvolgere sia i residui di aspartato Asp30 e Asp38, che uno o entrambi i residui di glutammato (Glu35 e/o Glu37). Questa specie viene però presto sostituita, a partire da pH 4.5, dalla specie [ZnHL]$^-$, che è presente in soluzione fino a pH 9.5, con un massimo a pH 7 (circa il 75% di Zn$^{2+}$ in soluzione). Il legame con Zn$^{2+}$ dovrebbe coinvolgere, per questa specie, i

residui di His34, Asp30, Asp38 e Glu37. Questa modalità di coordinazione, con His34 legata allo ione metallico, impedisce effettivamente la coordinazione di Glu35, poiché la sua catena laterale sporge verso il lato opposto del complesso. Le ultime due specie sono $[ZnLH_{-1}]^{3-}$, che inizia a formarsi da pH 6.5 fino a pH 11, con il massimo di formazione a pH 9, e $[ZnLH_{-2}]^{4-}$, che inizia a formarsi da pH 8 con un massimo a pH 11. La deprotonazione potrebbe coinvolgere due molecole d'acqua per la prima specie $[ZnLH_{-1}]^{3-}$, e il gruppo amminico di Lys31 per $[ZnLH_{-2}]^{4-}$.

La spettroscopia di risonanza magnetica nucleare è stata utilizzata per investigare il comportamento di $Zn^{2+}$ nei confronti di P29-38 in un'ampia gamma di pH come strumento di supporto ai risultati potenziometrici. È stata eseguita l'assegnazione completa dei *chemical shift* per nuclei protonici e carbonici a diversi valori di pH per il peptide libero P29-38, con l'aiuto delle tecniche complementari di spettroscopia NMR 2D $^{1}H$-$^{1}H$ TOCSY, $^{1}H$-$^{13}C$ HSQC e $^{1}H$-$^{1}H$ ROESY. Il sistema $Zn^{2+}$-P29-38 è stato analizzato a pH 5, 5.5, 6, 7.4, 8 e 9. Le Figure 24 e 25 riportano il confronto tra lo spettro TOCSY e HSQC del peptide libero e del sistema $Zn^{2+}$-P29-38 in una selezione di regioni a pH 5 e 6, rispettivamente. I segnali evidenziati in rosso si riferiscono a quelli alterati dopo l'interazione con lo ione metallico.
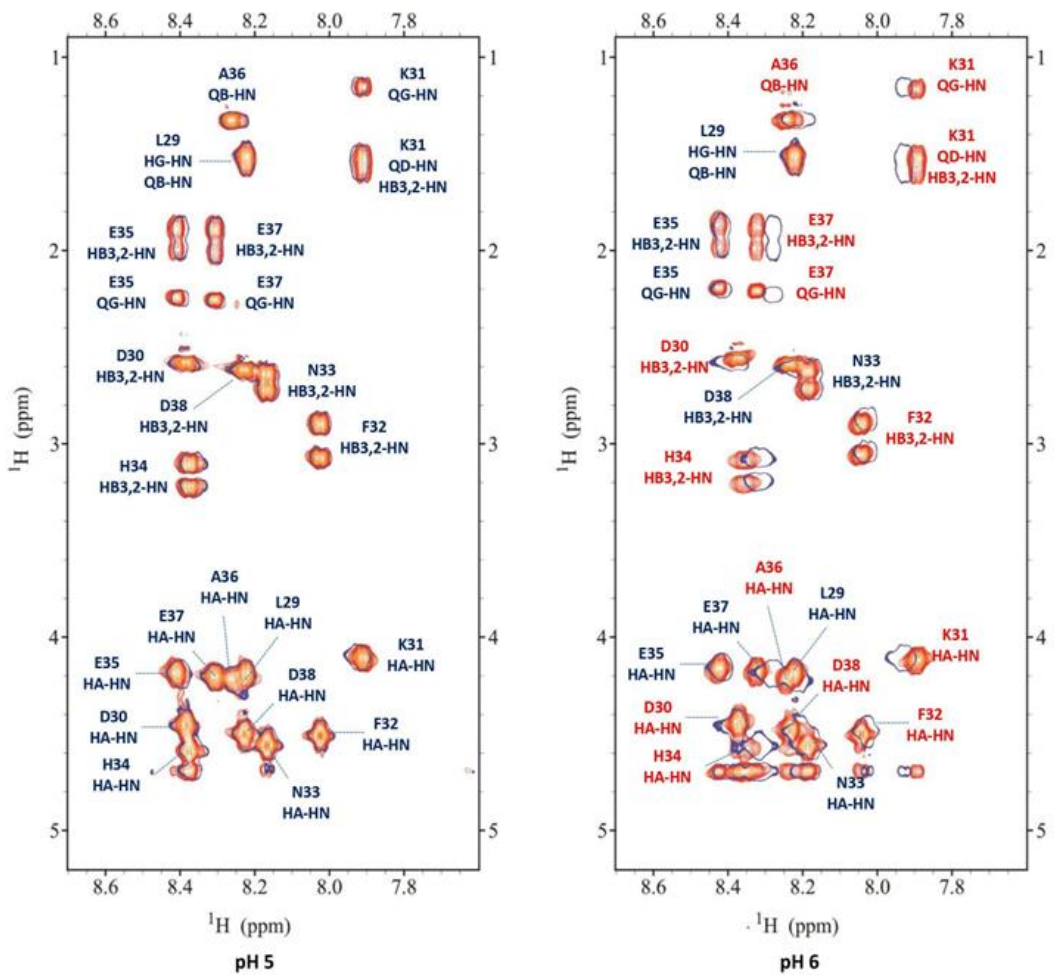
**Figura 4.6**. Sovrapposizione degli spettri $^1$H-$^1$H TOCSY per il peptide P29-38 libero (rosso) e per il sistema P29-38-Zn$^{2+}$ (blu), a pH 5 e a pH 6.
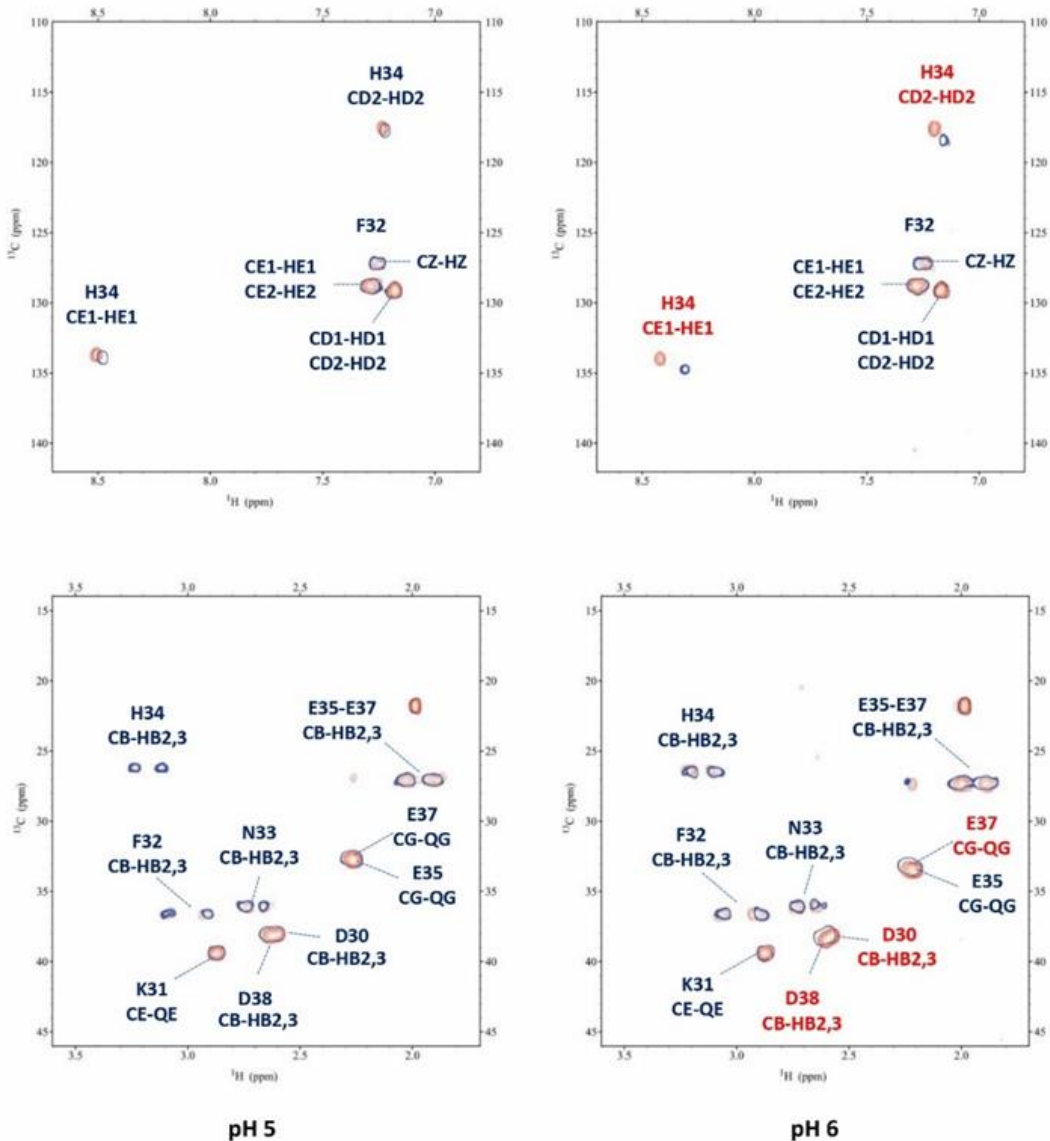
**Figura 4.7**. Sovrapposizione degli spettri $^1$H-$^{13}$C HSQC per il peptide P29-38 libero (rosso) e per il sistema P29-38-Zn$^{2+}$ (blu), a pH 5 e a pH 6.

Poiché la prima specie [ZnH$_2$L] è presente in concentrazione molto bassa, gli spettri a pH 5 mostrano poche variazioni dopo l'aggiunta di Zn$^{2+}$. Aumentando il pH fino a 6, sono osservabili diverse perturbazioni sia negli spettri TOCSY che negli spettri HSQC. Queste perturbazioni sono quasi tutte correlate ai

residui di coordinazione Asp30, Asp38 e Glu37, in accordo con le previsioni potenziometriche. Il legame dello $Zn^{2+}$ con questi residui porta anche a perturbazioni selettive su altri residui nelle vicinanze, come Lys31, Phe32 e Ala36, che vengono indirettamente influenzati dalla formazione del complesso in quanto sperimentano un diverso ambiente elettronico a seguito del successivo cambiamento conformazionale del peptide. Inoltre, i segnali di His34 sono influenzati dall'aumento del pH, in accordo con il suo coinvolgimento nel legame con il metallo in presenza della specie successiva $[ZnHL]^-$, che inizia a comparire a pH 4.5 e raggiunge la stessa concentrazione in soluzione della prima specie a pH 6. L'analisi degli spettri NMR registrati a pH 7.4 ci ha fornito informazioni complete sulla specie successiva. La Figura 4.8 riporta alcuni esempi significativi di perturbazioni selettive negli spettri $^{1}$H-$^{13}$C HSQC dei residui coinvolti nel legame con $Zn^{2+}$ [Figura 4.8a]. Inoltre, nella Figura 4.8b è riportato l'istogramma relativo alle variazioni dei *chemical shift* tra il sistema Zn-P29-38 e quello libero per i nuclei H e C. Lo schema nella Figura 4.8c fornisce un'indicazione visiva delle principali perturbazioni evidenziate attraverso l'analisi degli spettri NMR a pH 7.4, e la Figura 4.8d mostra un modello strutturale proposto per questo sistema.
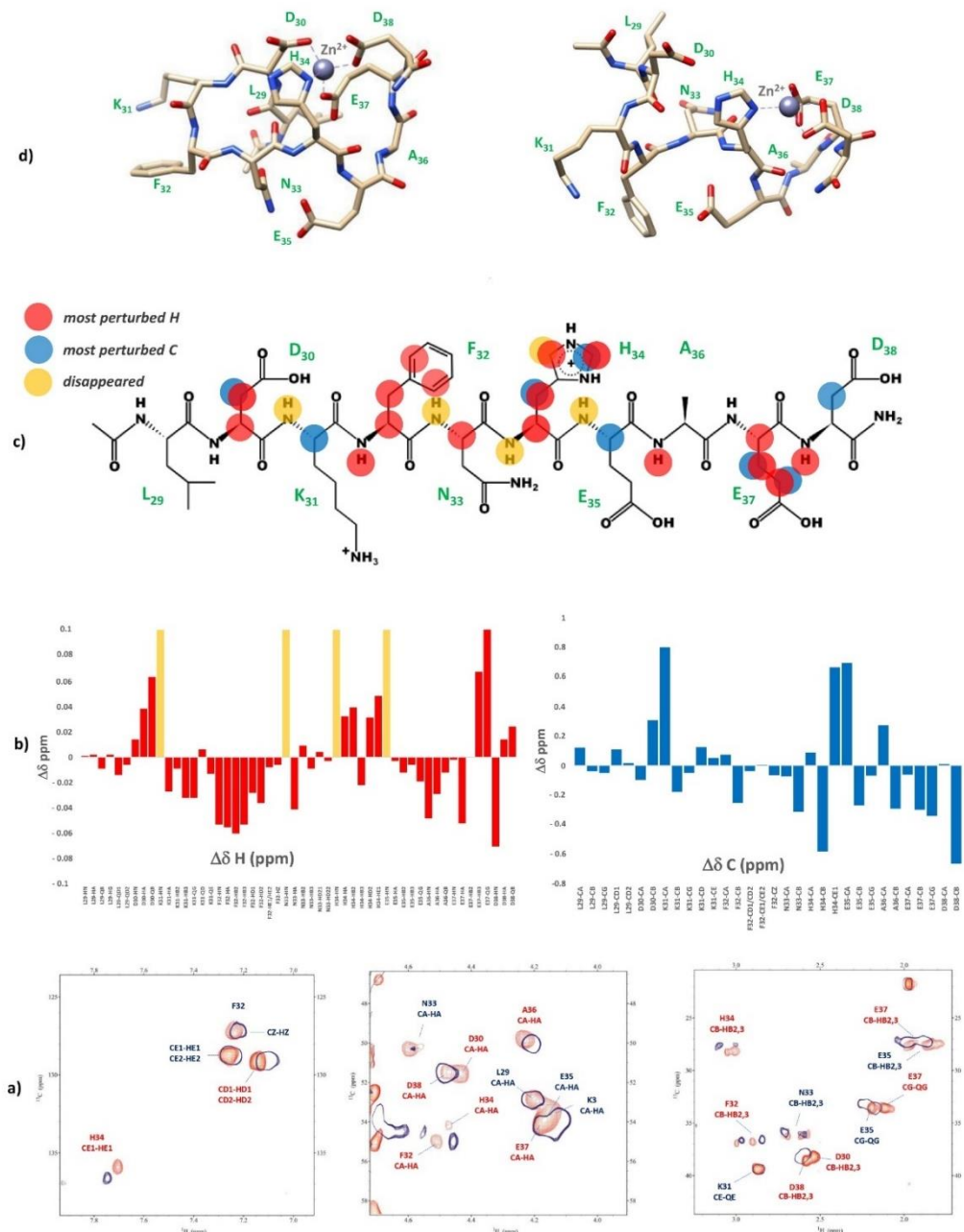
**Figura 4.8**. (a) Sovrapposizione di regioni selezionate degli spettri HSQC $^1$H-$^{13}$C per il sistema peptide libero P29-38 (arancione) e Zn$^{2+}$-P29-38 (contorni blu) a pH 7.4; (b) variazioni dei *chemical shift* $^1$H e $^{13}$C (Δδ = (sistema Zn$^{2+}$-P29-38)—(P29-38 libero)); (c) schema strutturale del peptide P29-38 su legame Zn$^{2+}$ con evidenziati i nuclei H e C maggiormente perturbati; (d) modelli strutturali della specie [ZnHL]$^{-1}$ in un modo di coordinazione {(Asp), Asp, Glu, His}.

I residui specifici sono perturbati in accordo con l'analisi potenziometrica, suggerendo una modalità di coordinazione {(Asp), Asp, Glu, His}. In particolare, le maggiori variazioni dei valori di *chemical shift* sono legate ai nuclei nella catena laterale di His34, Glu37, Asp30 e Asp38. I dati NMR confermano il legame di $Zn^{2+}$ con l'anello imidazolico dell'istidina. Le tendenze di Δδ per Glu37 (QG>HB2/3>HA) e per Asp30, Asp38 (HB2/3>HA) indicano il coinvolgimento del legame metallico attraverso i loro gruppi carbossilici. Glu35 non sembra essere coinvolto nel legame. Sono stati creati modelli strutturali per questa specie, come mostrato nella Figura 4.8d. Il sistema $Zn^{2+}$:P29-38 a pH 8 e 9 assomiglia a quello a pH 7.4, in accordo con la conclusione che la specie $[ZnH_{-1}L]^{-3}$ mantiene la stessa sfera di coordinazione di $[ZnLH]^{-}$. Nonostante la scarsa solubilità, alcune informazioni utili sulla capacità di coordinazione del peptide P23-42 verso $Zn^{2+}$ sono state valutate tramite spettroscopia NMR a pH 7. La Figura 4.9 riporta un confronto tra gli spettri 1D $^1H$ ed una selezione di spettri $^1H$-$^1H$ TOCSY a pH 7 tra il peptide libero P23-42 e il sistema legato allo zinco. Le principali perturbazioni sono state rilevate per Glu37, seguita da Asp30 e Asp38. Inoltre, alcuni residui non-coordinanti vicini hanno mostrato variazioni nei valori dei *chemical shift*, ad esempio Phe28, Lys31, Leu39 e Phe40. Sono state rilevate anche piccole variazioni per i nuclei di His34. In particolare, con l'aumento del pH, diventa evidente come i protoni dell'imidazolo dell'istidina siano sempre più spostati, in accordo con il coinvolgimento dell'anello imidazolico nel legame con il metallo in condizioni più basiche.
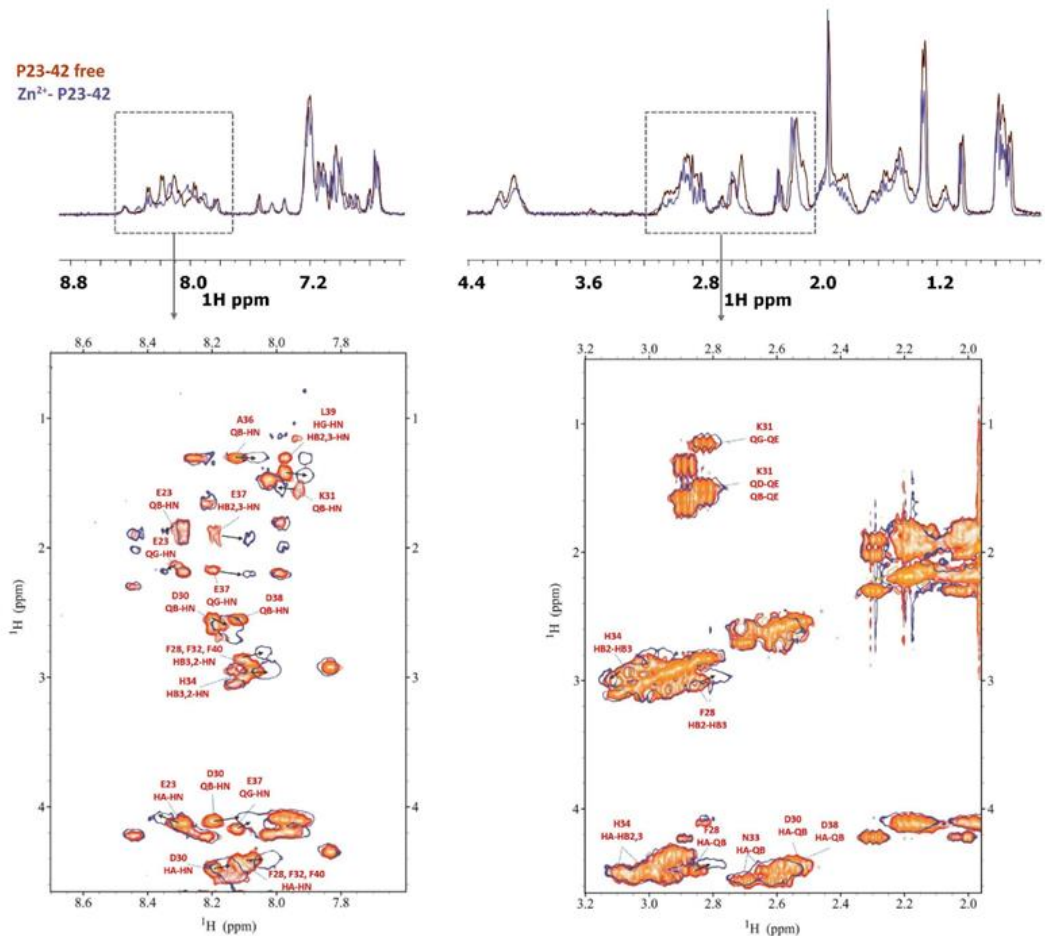
**Figura 4.9**. Sovrapposizione degli spettri 1D (in alto), e degli spettri $^1$H-$^1$H TOCSY (in basso) per il peptide P29-38 libero (rosso) e per il sistema P29-38-Zn$^{2+}$ (blu), a pH 7.

Dall'analisi NMR, il comportamento del peptide P23-42 nei confronti di Zn$^{2+}$ è simile a quello osservato per la sequenza più corta P29-38. Il sito di ancoraggio è centrato su Glu37 e Asp38 e con l'aumento del pH si verifica anche il coinvolgimento di His34. Inoltre, insieme ad Asp30, anche Glu23 potrebbe svolgere un ruolo secondario nell'interazione con il metallo, poiché i suoi nuclei sperimentano perturbazioni selettive. Il peptide P19-42 si è rivelato ancora meno solubile rispetto a P23-42, tuttavia siamo stati in grado di ottenere alcune informazioni dagli spettri NMR. Il peptide più lungo mostra, in generale, una modalità di coordinazione con Zn$^{2+}$ molto simile a quella del peptide P23-42

[Figura 4.10]. La possibilità di ottenere informazioni aggiuntive a pH basico è stata preclusa dalla precipitazione del sistema Zn-peptide per entrambi i peptidi P23-42 e P19-42.
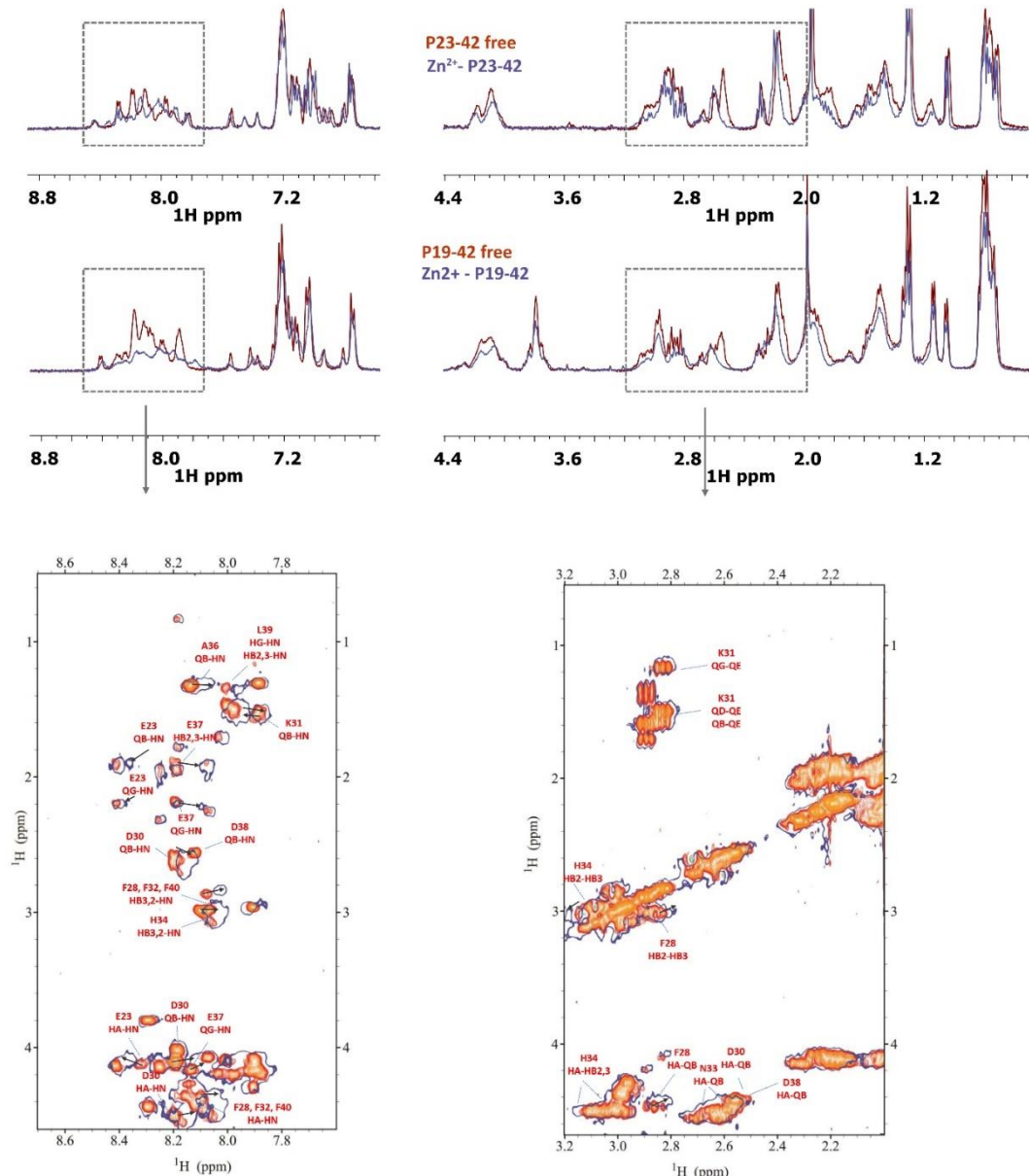


**Figura 4.10**. (sopra) Confronto degli spettri $^1$H per il sistema peptide P23–42 (arancione) e il sistema Zn$^{2+}$-P23–42 (blu) e per il sistema peptide P19–42 (arancione) e il sistema Zn$^{2+}$-P19–42 (blu) a pH 7; (in basso) selezione degli spettri $^1$H-$^1$H TOCSY per il sistema peptide P19–42 (arancione) e il sistema Zn$^{2+}$-P19–42 (blu) a pH 7.

## 4.4 Complessi di $Cu^{2+}$

Le costanti di formazione dei complessi $Cu^{2+}$-P29-38 sono riportate nella Tabella 4.3 e i relativi diagrammi di distribuzione sono mostrati nella Figura 4.11. Gli spettri UV-Vis e CD a diversi valori di pH sono invece mostrati nella Figura 4.12.

| Specie | Logβ | LogK | Deprotonazione | Coordinazione |
|---|---|---|---|---|
| $[CuH_2L]$ | 20.78(5) | | | Asp, Asp, Glu, Glu |
| $[CuHL]^-$ | 16.01(3) | 4.77 | His | Asp, Asp, (Glu), His |
| $[CuL]^{2-}$ | 3.35(3) | 2*6.33 | Ammide, Ammide | His, $2N^-_{amide}$ (Asp o Glu) |
| $[CuLH_{-1}]^{3-}$ | -4.17(4) | 7.52 | Ammide | His, $3N^-_{amide}$ |
| $[CuLH_{-2}]^{4-}$ | -13.09(5) | 8.92 | Ammide | $4N^-_{amide}$ |
| $[CuLH_{-3}]^{5-}$ | -24.29(5) | 11.20 | Lys | $4N^-_{amide}$ |

**Tabella 4.3**. Costanti di protonazione del sistema P29-38-$Cu^{2+}$.
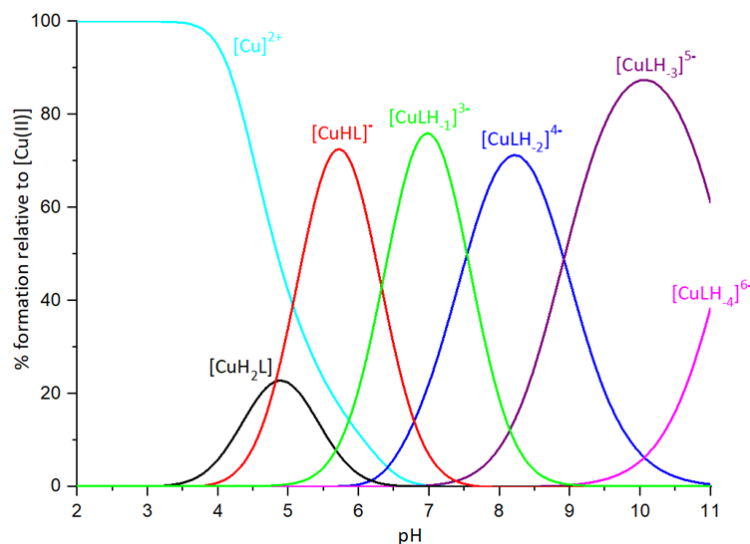


**Figura 4.11**. Grafico di speciazione per il sistema P29-38-$Cu^{2+}$.

La formazione dei complessi $Cu^{2+}$ con P29-38 inizia a un pH di circa 3.5 con la specie $[CuH_2L]$. Molto probabilmente, il metallo è legato ai gruppi carbossilici dei due residui di aspartato e dei due residui di glutammato. Questa specie ha la sua concentrazione massima a pH 4.5, ma non raggiunge neanche il 30% della quantità di ione metallico in soluzione. Di conseguenza, a causa della sua bassa abbondanza, le caratteristiche spettroscopiche di questi complessi non sono facilmente accessibili. A partire da pH 3.95 viene rilasciato un altro protone, portando alla formazione del complesso $[CuHL]^-$ che persiste fino a pH 7.5, con un massimo a pH 5.5. Questo protone deriva dalla deprotonazione dell'imidazolo di His34, che è in grado di coordinare lo ione rame a questo pH.
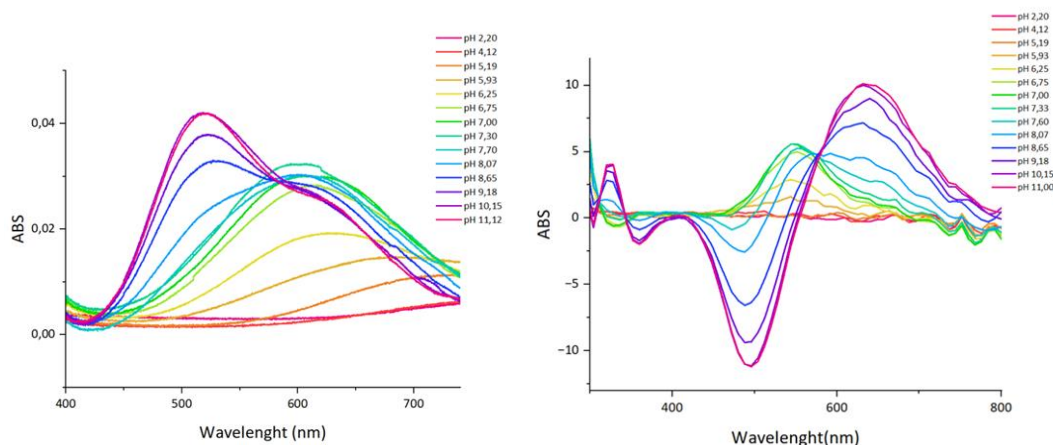


**Figura 4.12**. Spettri UV-Vis (a sinistra) e CD (a destra) per il sistema P29-38-$Cu^{2+}$.

Nello spettro UV-Vis registrato a pH 5.19, la presenza di una banda con un'assorbimento massimo a 715 nm suggerisce la presenza di un singolo atomo di azoto nella sfera di coordinazione dello ione metallico. Lo spettro UV-Vis di $[CuHL]^-$ calcolato dal software SPECFIT/32 [81] basato sugli spettri dipendenti dal pH [Figura 4.13] mostra una banda caratterizzata da λ max = 720 nm, epsilon = 50 $M^{-1}$ $cm^{-1}$ [Tabella 4.4], coerente con lo spettro sperimentale e i valori letterari per le bande di transizione 1N $\{N_{Im}\}$ $Cu^{2+}$ d-d [82,83].
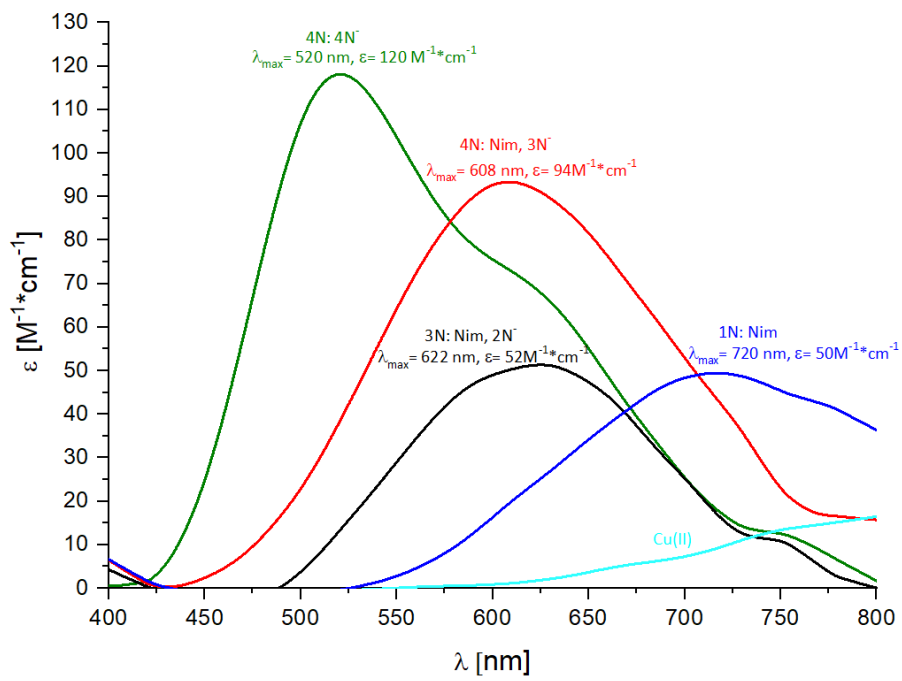
**Figura 4.13**. Bande UV-Vis calcolate per varie forme complesse di $Cu^{2+}$. Bande calcolate con il software SPECFIT/32; ciano: $Cu^{2+}$ libero, blu: $[CuHL]^-$, nero: $[CuLH_{-1}]^{3-}$, rosso: $[CuLH_{-2}]^{4-}$, verde: $[CuLH_{-3}]^{5-}$.

| Specie | Coordinazione | λ [nm] | ε [M⁻¹·cm⁻¹] |
|--------|---------------|--------|--------------|
| $[CuHL]^-$ | 1N $\{N_{Im}\}$ | 720 | 50 |
| $[CuLH_{-1}]^{3-}$ | 3N $\{N_{Im}, 2N^-\}$ | 622 | 52 |
| $[CuLH_{-2}]^{4-}$ | 4N $\{N_{Im}, 3N^-\}$ | 608 | 94 |
| $[CuLH_{-3}]^{5-}$ | 4N $\{4N^-\}$ | 520 | 120 |

**Tabella 4.4**. Parametri spettroscopici UV-Vis per il sistema P29-38-$Cu^{2+}$ calcolati con il software SPECFIT/32

Dalla spettroscopia CD è possibile rilevare l'ellitticità a partire da pH 5.19 con una banda di assorbimento positiva che appare nell'intervallo di 500-600 nm e che aumenta fino a pH 7.40, attribuibile all'interazione tra His34 (ND2) e $Cu^{2+}$, così come la presenza di bande CD caratteristiche a 235 e 340 nm [$N_{Im}$ → $Cu^{2+}$ MLCT].

A causa del carattere paramagnetico del rame, gli esperimenti di NMR per il sistema $Cu^{2+}$-peptide sono stati eseguiti mediante l'aggiunta progressiva di quantità sub-stechiometriche di ioni metallici alle soluzioni di peptide, per evitare un ampio allargamento dei segnali. Seguendo l'effetto di rilassamento selettivo sperimentato dai nuclei più vicini al $Cu^{2+}$ paramagnetico, è stato possibile localizzare nella sequenza peptidica i donatori elettronici e i cambiamenti subiti dal peptide durante l'interazione con il metallo [84,85]. La titolazione NMR di P29-38 a pH 5.5 con l'aggiunta crescente di quantità sub-stechiometriche di $Cu^{2+}$ è mostrata nella Figura 4.14. In accordo con la modalità di coordinazione proposta {Asp, Asp, (Glu), His}, l'analisi degli spettri NMR conferma il coinvolgimento dell'azoto imidazolico di His34 e dei gruppi carbossilici di Asp30, Asp38 e Glu37, poiché i loro segnali si sono selettivamente e progressivamente ridotti durante la titolazione con il $Cu^{2+}$. Il confronto di $^1H$-$^{13}C$ HSQC per il peptide P29-38 libero e per il sistema $Cu^{2+}$-P29-38 nella proporzione molare di 0.01:1 e 0.1:1 evidenzia, inoltre, tutti i residui che sono esclusi dall'effetto di rilassamento del $Cu^{2+}$, ovvero Leu29, Lys31 e Ala36, fornendo un'indicazione indiretta della loro maggior distanza dallo ione paramagnetico.
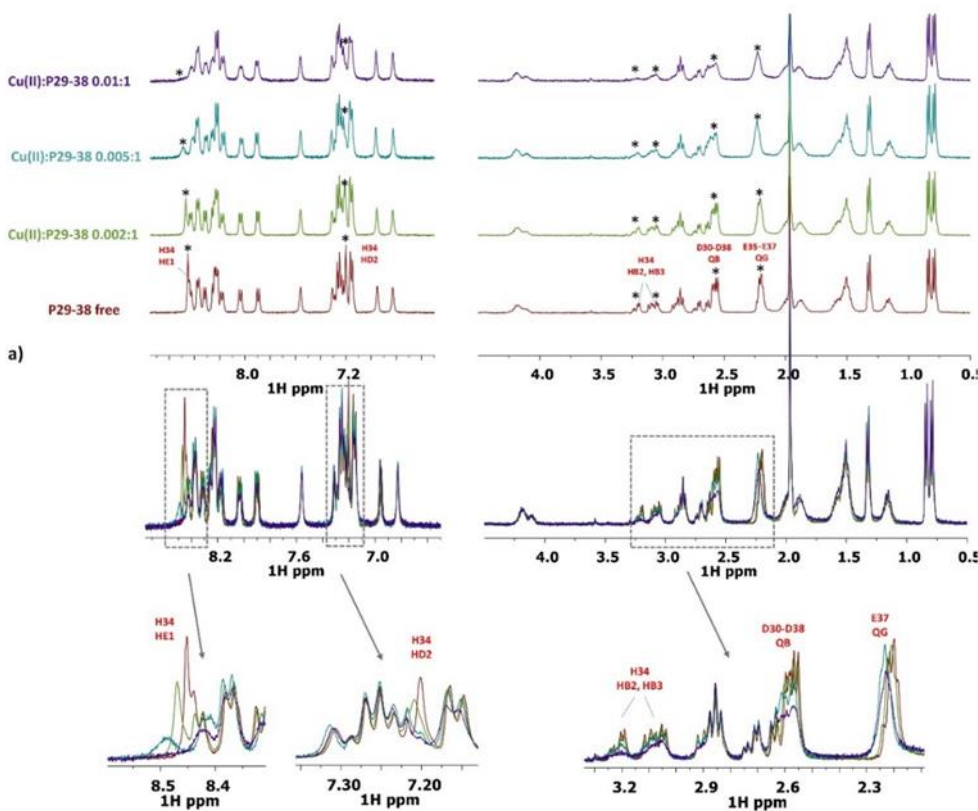
**Figura 4.14**. Confronto tra gli spettri 1D ^{1}H NMR a pH 5,5 a seguito di aggiunte crescenti di quantità sub-stechiometriche di $Cu^{2+}$.

La successiva specie $[CuLH_{-1}]^{3-}$ inizia a comparire a partire da pH 5 e deriva da due deprotonazioni consecutive che possono essere attribuite a due atomi di azoto ammidici del *backbone*. I valori medi dei pK corrispondenti di 6.33 sono compatibili con questa ipotesi. Infatti, una volta ancorato al peptide attraverso un residuo di His, $Cu^{2+}$ è in grado di spostare i protoni ammidici attraverso un effetto cooperativo che facilita la coordinazione dell'altro atomo di azoto ammidico all'aumentare del pH. A partire da pH 5.93, la banda di assorbimento UV-Vis inizia inoltre a spostarsi verso lunghezze d'onda più corte, riflettendo così la formazione di una nuova specie, $[CuLH_{-1}]^{3-}$, derivante da due deprotonazioni consecutive degli atomi di azoto ammidici del *backbone*. In questa forma, la coordinazione dello ione rame è probabilmente 3N {$N_{Im}$, 2N[-]}, λ max = 622 nm, epsilon = 52 $M^{-1}$ $cm^{-1}$ [Tabella 9]. La presenza

di [CuLH$_{-1}$]$^{3-}$ è evidenziata anche negli spettri di CD dalla formazione della banda a 540 nm (transizione d-d) e 310 nm (transizione di trasferimento di carica N$^-$ →Cu$^{2+}$), che indica il coinvolgimento delle ammidi nel coordinamento del metallo [86,87].

È stata inoltre eseguita la titolazione NMR di P29-38 con l'aggiunta crescente di quantità sub-stechiometriche di Cu$^{2+}$ a pH 7.4. La Figura 4.15 riporta i risultati di questo studio NMR.
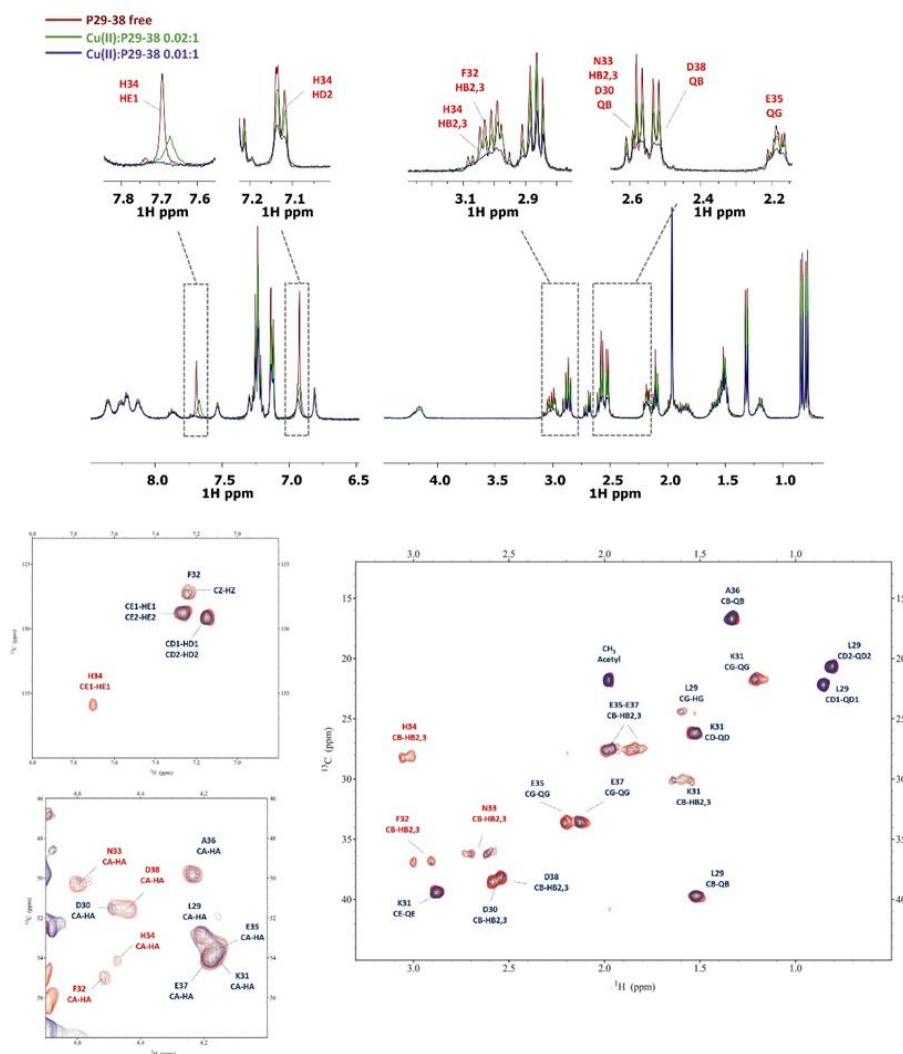


**Figura 4.15**. Confronto tra gli spettri 1D $^1$H NMR (in alto) e $^1$H $^{13}$C HSQC (in basso) a pH 7.4 a seguito di aggiunte crescenti di quantità sub-stechiometriche di Cu$^{2+}$. In rosso i segnali relativi al peptide libero, in blu i segnali relativi al sistema P29-38-Cu$^{2+}$.

Lo studio NMR eseguito a pH 7.4 ha evidenziato chiaramente il coinvolgimento di His34 nella sfera di coordinazione del $Cu^{2+}$. I protoni dell'imidazolo HD2 e HE1 hanno subito un notevole allargamento di linea insieme a HB2-HB3 nella sua catena laterale. Altri residui influenzati sono le adiacenti Asn33 e Phe32 (in particolare nei loro nuclei alfa e beta), che hanno subito la scomparsa del segnale a causa della loro vicinanza allo ione metallico paramagnetico. Dagli spettri è evidente che la partecipazione dei residui acidi nella formazione del complesso diminuisce, in accordo con il cambio della modalità di coordinazione che coinvolge gli atomi di azoto ammidici. All'aumentare del pH, un'altra ammide deprotona, con un valore di pK di 7.52. Si tratta della specie $[CuLH_{-2}]^{4-}$, caratterizzata da una coordinazione 4N $\{N_{Im}, 3N^-\}$. A causa dell'equilibrio in soluzione tra le forme di coordinazione 3N e 4N, è difficile distinguere chiaramente tra le loro bande spettroscopiche. In generale, la coordinazione $3N-Cu^{2+}$ nella forma $[CuLH_{-1}]^{3-}$ può essere chiaramente osservata a pH = 6.25, con λ max = 622 nm. A pH più elevati, fino a 7.70, la banda si sposta verso lunghezze d'onda più corte di circa 608 nm e la sua intensità aumenta, poiché la terza ammide entra nella sfera di coordinazione in $[CuLH_{-2}]^{4-}$. Le bande calcolate da SPECFIT/32 sono caratterizzate da λ max = 622 nm (epsilon = 52 $M^{-1} cm^{-1}$) e λ max = 608 nm (epsilon = 94 $M^{-1} cm^{-1}$) per le forme 3N e 4N, rispettivamente [Tabella 4.4, Figura 4.13]. Un comportamento simile è evidente anche negli spettri di CD, con l'aumento dell'intensità della banda a circa 540 nm, che aumenta fino a pH = 7.60.

La specie successiva, $[CuLH_{-3}]^{5-}$, è presente in soluzione già a partire da pH circa 7, con la sua massima concentrazione a pH circa 10. Questa forma deriva dalla deprotonazione del quarto atomo di azoto ammidico del *backbone*, con un valore di pK di 8.92. L'atomo di azoto dell'imidazolo, legato al $Cu^{2+}$ già a partire da un pH di circa 4, è probabilmente spostato dall'atomo di azoto dell'amide, risultando in una modalità di coordinazione 4N $\{4N^-\}$. Ciò può essere chiaramente visto sia nelle spettroscopie UV-Vis che nel CD. Nello spettro UV-Vis registrato a pH = 8.07, un'altra componente della banda inizia a salire a circa 520 nm, riflettendo l'equilibrio in soluzione tra le forme [CuLH-

$_2]^{4-}$ 4N {$N_{Im}$, 3N$^-$} e [CuLH$_{-3}$]$^{5-}$ 4N {4N$^-$}. Lo spettro UV-Vis calcolato per [CuLH$_{-3}$]$^{5-}$ con λ max = 520 nm (epsilon = 120 M$^{-1}$ cm$^{-1}$) [Tabella 4.4, Figura 4.13] riflette la presenza della forma 4N$^-$, in accordo con i valori riportati in letteratura [82,88]. Nello spettro di CD registrato allo stesso pH, si può osservare un cambiamento drastico rispetto agli spettri precedenti, con nuove bande a 500 nm e 650 nm che iniziano ad apparire, indicando il cambiamento nella coordinazione dello ione metallico. Infatti, tali bande di transizione d-d sono caratteristiche dei complessi quadrato planari che coinvolgono le ammidi [89]. Con l'aumento del pH fino a circa 11, l'intensità di queste bande aumenta, riflettendo l'aumento della concentrazione della forma [CuLH$_{-3}$]$^{5-}$, spostando l'equilibrio verso la modalità di coordinazione 4N$^-$. L'ultima forma complessa, [CuLH$_{-4}$]$^{6-}$, è il risultato della deprotonazione del gruppo laterale ε-amino non legante della lisina, con un valore di pK di 11.20.

Dato che a valori di pH elevati, nei sistemi Cu$^{2+}$, è stato rilevato un notevole allargamento dei segnali negli spettri NMR, che ha impedito una caratterizzazione dettagliata delle specie nella modalità di coordinazione [$N_{Im}$, 3N$^-_{amide}$], abbiamo deciso di indagare il legame del Cu$^{2+}$ al peptide P29-38 utilizzando il Ni$^{2+}$ diamagnetico. Nei peptidi che presentano un residuo di istidina a partire dalla terza posizione, il Ni$^{2+}$ forma complessi diamagnetici, a basso spin e con geometria quadrato planare a pH adeguatamente elevati. L'atomo di azoto imidazolico dell'istidina funge da sito di ancoraggio, e una volta legato a esso il Ni$^{2+}$ è in grado (come il Cu$^{2+}$) di deprotonare e legare tre ammidi aggiuntive del *backbone,* completando così la sfera di coordinazione di [$N_{Im}$, 3N$^-_{amide}$] con la formazione simultanea di tre anelli chelati fusi e la saturazione del piano di coordinazione [90,91]. Pertanto, il Ni$^{2+}$ potrebbe essere utilizzato come sonda per il Cu$^{2+}$ poiché è in grado di sostituirlo nei complessi quadrato planari, ma formando specie diamagnetiche a basso spin più facilmente indagabili mediante NMR [92,93]. La Figura 4.16 riporta la titolazione del metallo a pH 10.6, mediante l'aggiunta di quantità crescenti di ioni Ni$^{2+}$, fino a un rapporto molare Ni$^{2+}$:P29-38 di 0.8:1. La Figura 4.17 mostra gli istogrammi relativi alle variazioni dei *chemical shift* di $^1$H e $^{13}$C, lo schema

strutturale del peptide P29-38 con i nuclei H e C più perturbati e il modello strutturale proposto delle corrispondenti specie di $Ni^{2+}$.
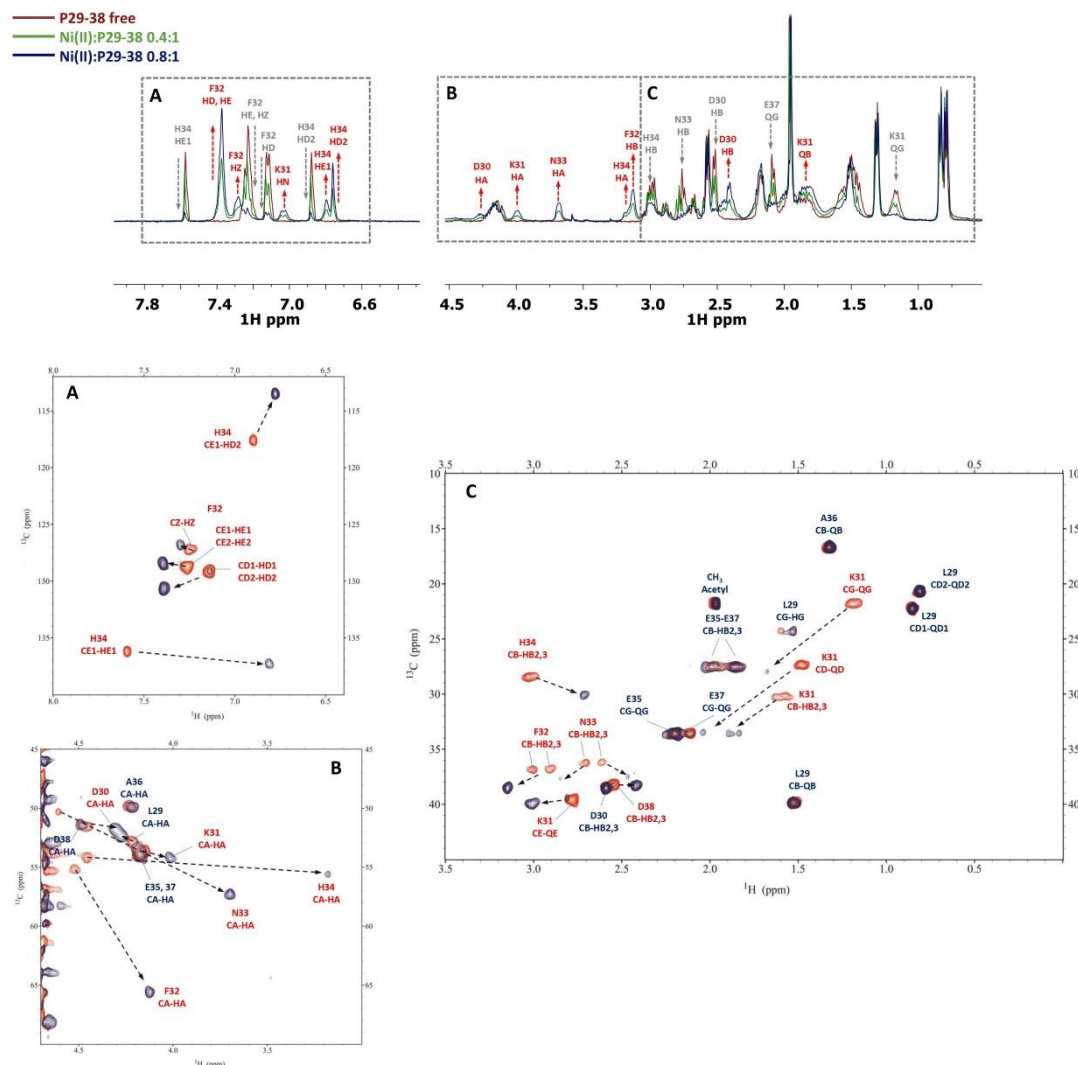


**Figura 4.16**. Confronto tra gli spettri 1D $^1$H NMR (in alto) e $^1$H $^{13}$C HSQC (in basso) a pH 10.6 a seguito di aggiunte crescenti di $Ni^{2+}$. In rosso i segnali relativi al peptide libero, in blu i segnali relativi al sistema P29-38-$Ni^{2+}$.
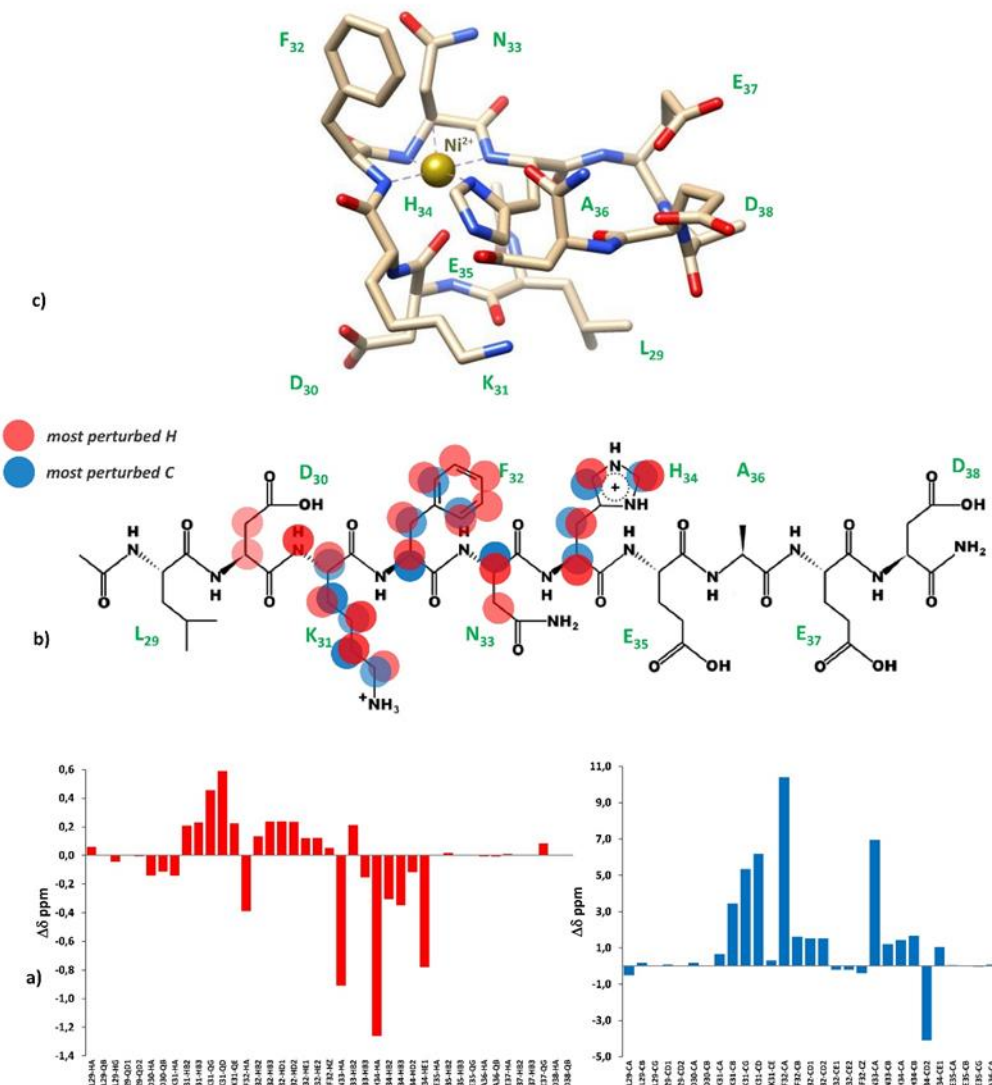
**Figura 4.17**. (a) Confronto tra le variazioni dei *chemical shift* per il sistema P29-38-Ni$^{2+}$. In rosso le variazioni relative ai nuclei H, in blu le variazioni relative ai nuclei C. (b) schema strutturale del peptide P29-38 con i nuclei H e C (evidenziati rispettivamente in rosso e blu) più perturbati dopo il legame Ni$^{2+}$; (c) Modello strutturale della specie Ni$^{2+}$ in una coordinazione del tipo [N$_{Im}$, 3N$^-_{ammide}$].

L'aggiunta di nichel al peptide ha determinato diversi cambiamenti nei segnali NMR. Lo spostamento di segnali specifici corrispondenti ai residui His34, Asn33, Phe32 e Lys31 conferma la formazione del complesso diamagnetico. Il coinvolgimento di His34 è evidente dalla graduale scomparsa delle

risonanze relative ai protoni imidazolici HD2 ed HE1, così come dei protoni alifatici HA, HB nel peptide libero. Contestualmente compare un nuovo insieme di picchi, indicando la presenza della forma legata al metallo in lenta variazione sullo spettro. Le differenze di *chemical shift* (Δδ) tra i protoni aromatici dell'imidazolo nello stato legato e libero, con un Δδ maggiore per HE1 rispetto a HD2 (Δδ HE1 = 0.783 ppm > Δδ HD2 = 0.121 ppm), forniscono una chiara evidenza del legame del metallo all'atomo di azoto imidazolico adiacente ND1.

Tutti i protoni di His34 sono schermati, indicando un aumento della densità elettronica. I cambiamenti di *chemical shift* più significativi si osservano per i residui coinvolti nella coordinazione del metallo, come His34, Asn33, Phe32 e Lys31. I protoni HA mostrano le variazioni più ampie, essendo fortemente schermati a causa dell'aumento della densità elettronica dovuta alla deprotonazione ammidica. La tendenza dei cambiamenti, con Δδ HA > Δδ HB e Δδ CA > Δδ CB, è coerente con una modalità di coordinazione che coinvolge gli atomi di azoto ammidici del *backbone* di His34, Asn33 e Phe32. I protoni HB2 e HB3 di Phe32 e Asn33 presentano diversi intorni elettronici, con un residuo spostato verso campi alti e l'altro verso campi bassi.

Questo comportamento è molto probabilmente dovuto alla posizione bloccata dei gruppi laterali di Phe32 e Asn33 sopra il complesso, che porta solo una parte del gruppo laterale a essere schermata. Sono state infatti identificate correlazioni ROE tra il protone HD fenolico di Phe32 e il protone HE1 imidazolico di His34. Sono state identificate ulteriori correlazioni ROE tra nuclei vicini e in particolare tra i protoni dei gruppi laterali di Phe32 e Asn33, che confermano la loro posizione relativa sullo stesso lato del piano di coordinazione. Allo stesso modo, i protoni dei gruppi laterali di Lys31 sono fortemente deschermati, a causa di una conformazione bloccata sul lato opposto rispetto ai gruppi laterali di Asn33 e Phe32. Una conformazione spaziale più rigida di Lys31, sotto il piano del complesso, è confermata dal fatto che durante la titolazione con $Ni^{2+}$, il protone ammidico HN di Lys31 ha

mostrato correlazioni ROE con il protone HA di Asp30, e il suo HA con i protoni HE1 e HD2 di His34. È interessante notare che questo protone HN labile riappare dopo l'aggiunta di $Ni^{2+}$ ed è probabilmente bloccato, come se fosse coinvolto in un legame idrogeno. La conformazione bloccata del *backbone* relativa alla posizione di Asp30 potrebbe spiegare, inoltre, la possibilità di una pentacoordinazione a base quadrata attraverso il carbonile di Asp30 che interagisce con il metallo in posizione assiale sotto il piano del complesso, come suggerito dal modello rappresentato in Figura 4.17c. Per verificare se il $Ni^{2+}$ fosse una buona sonda per il $Cu^{2+}$, abbiamo effettuato uno studio di competizione NMR, titolando il sistema diamagnetico $Ni^{2+}$:P29-38 (rapporto molare di 0.8:1) con una quantità crescente di $Cu^{2+}$ paramagnetico in modo sub-stoichiometrico. I segnali già spostati dovuti al legame di $Ni^{2+}$, relativi ai residui che partecipano alla complessazione del metallo, sono scomparsi selettivamente durante la titolazione, indicando che gli ioni $Cu^{2+}$ erano in grado di sostituire gli ioni $Ni^{2+}$ nello stesso sito di coordinazione. Inoltre, l'aggiunta di $Cu^{2+}$ al sistema $Ni^{2+}$:P29-38 ha fornito ulteriori indizi sul coinvolgimento del quarto atomo di azoto ammidico nella complessazione, poiché il segnale HN già citato dell'atomo di azoto amminico di Lys31 scompare a causa della sua deprotonazione e successiva coordinazione con lo ione metallico. Il coinvolgimento di Lys31 è inoltre evidenziato dalla scomparsa o dal drastico abbassamento dei segnali del suo sistema di spin, come indicazione della sua nuova posizione in prossimità dello ione paramagnetico. Un modello strutturale del complesso $Cu^{2+}$:P29-38 proposto in una sfera di coordinazione $4N^-$ ammidico è rappresentato in Figura 4.18.
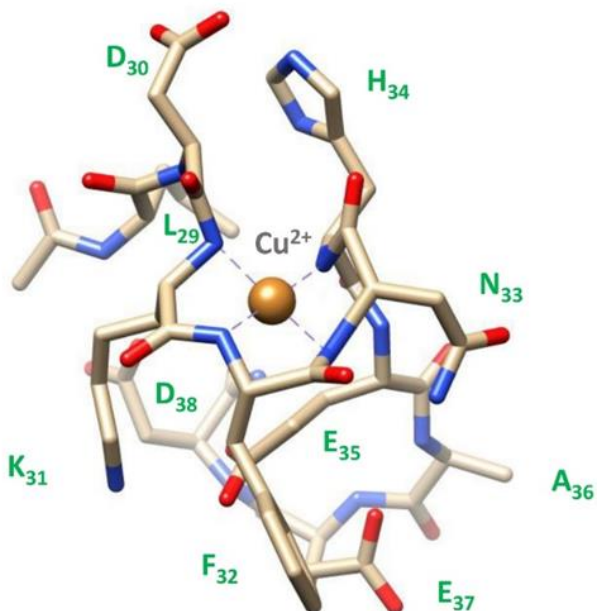
**Figura 4.18**. Modello strutturale ipotizzato per il complesso P29-38-Cu$^{2+}$ con sfera di coordinazione {4N$^{-}$}.


Lo studio NMR dei peptidi più lunghi P23-42 e P19-42 ha fornito alcune evidenze sulle preferenze di coordinazione del Cu$^{2+}$. A pH 7, sia il sistema Cu$^{2+}$-P23-42 che il sistema Cu$^{2+}$-P19-42 hanno mostrato una scomparsa selettiva dei segnali correlati a His-34, Asp-30 e Asp-38 [Figura 4.19 e 4.20], e quando il pH è stato regolato a 8, il coinvolgimento di Glu-35 e Glu-37 è apparso più evidente.
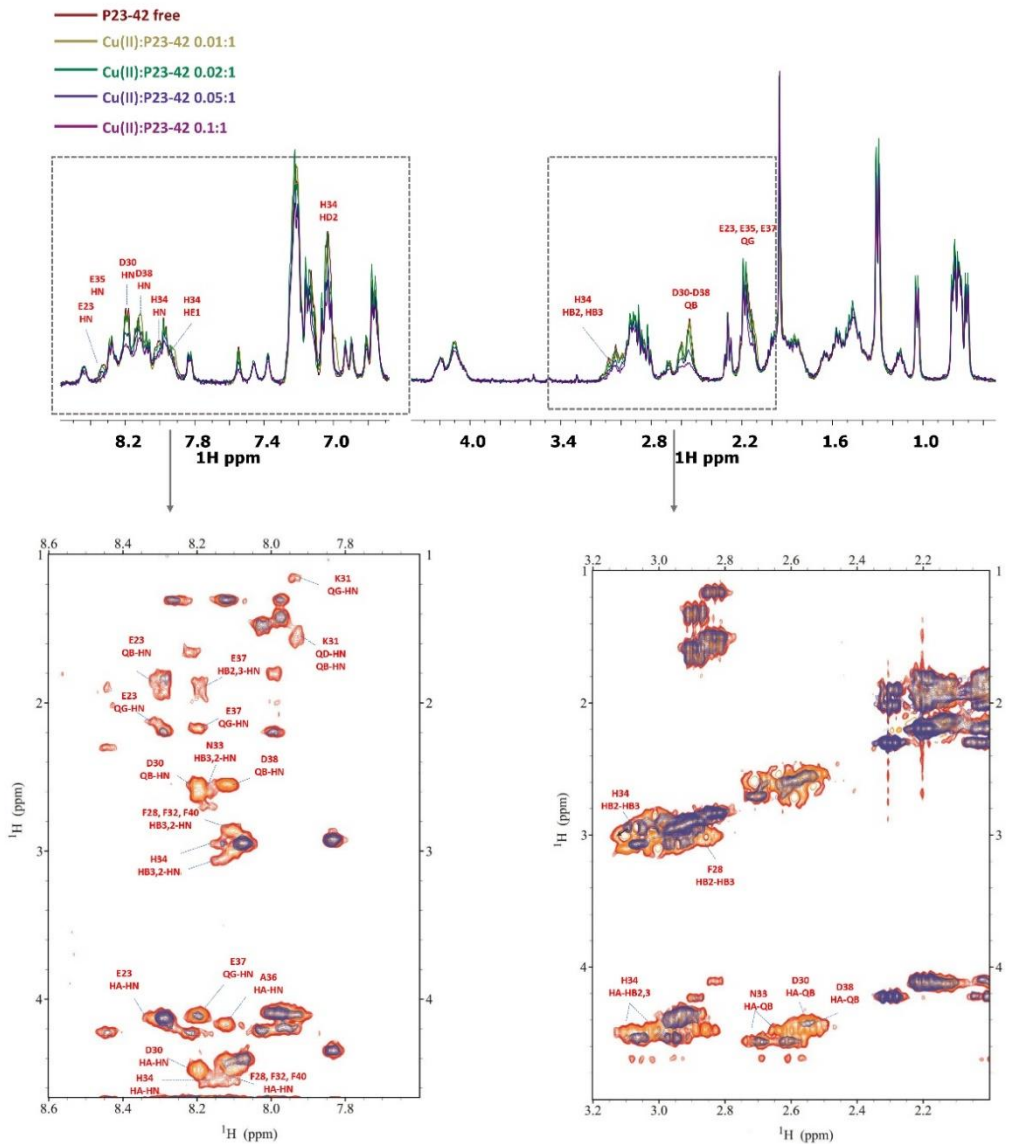
**Figura 4.19**. (sopra) Confronto degli spettri $^1$H di P23–42 con aggiunta crescente di $Cu^{2+}$ a pH 7.0; (in basso) selezione degli spettri $^1$H-$^1$H TOCSY per il sistema peptide libero P23–42 (arancione) e $Cu^{2+}$-P23–42 (blu), rapporto molare 0.1:1, a pH 7.0.
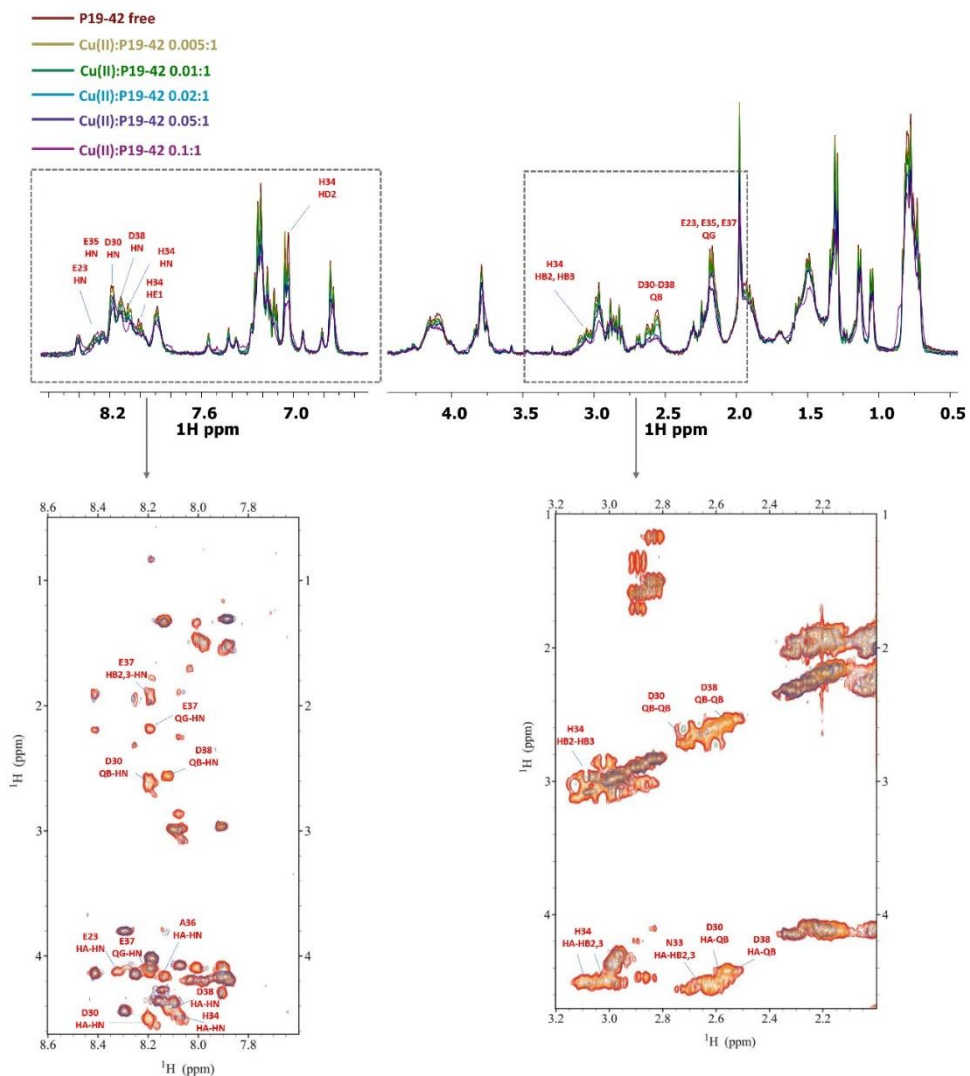
**Figura 4.20**. (sopra) Confronto degli spettri $^1H$ di P19–42 con aggiunta crescente di Cu2+ a pH 7.0; (in basso) selezione degli spettri 1H-1H TOCSY per il sistema peptide libero P19–42 (arancione) e $Cu^{2+}$-P23–42 (blu), rapporto molare 0.1:1, a pH 7.0.

A pH più elevati, l'effetto concomitante dell'allargamento di segnale e della scarsa solubilità ha impedito una migliore caratterizzazione dei sistemi $Cu^{2+}$ per entrambi i peptidi P23-42 e P19-42. Tuttavia, per ottenere ulteriori informazioni sulle specie che si formano a valori di pH elevati, abbiamo utilizzato $Ni^{2+}$ come sonda per $Cu^{2+}$ anche per il peptide più lungo P19-42. I

risultati sono stati sorprendentemente simili a quelli ottenuti per il peptide più corto P29-38. Infatti, la titolazione a pH 10.6 ha portato all'ottenimento di un sistema in cui il $Ni^{2+}$ forma un complesso planare diamagnetico che coinvolge, in modo simile al peptide P29-38, non solo gli stessi residui di coordinazione di His34 ($N_{Im}$, $N^-$), Asn33 ($N^-$), Phe32 ($N^-$) [Figura 4.21, 4.22], ma mostra anche variazioni quasi identiche per i *chemical shift* ($\Delta\delta$ ppm) tra i due sistemi [Figura 4.23].
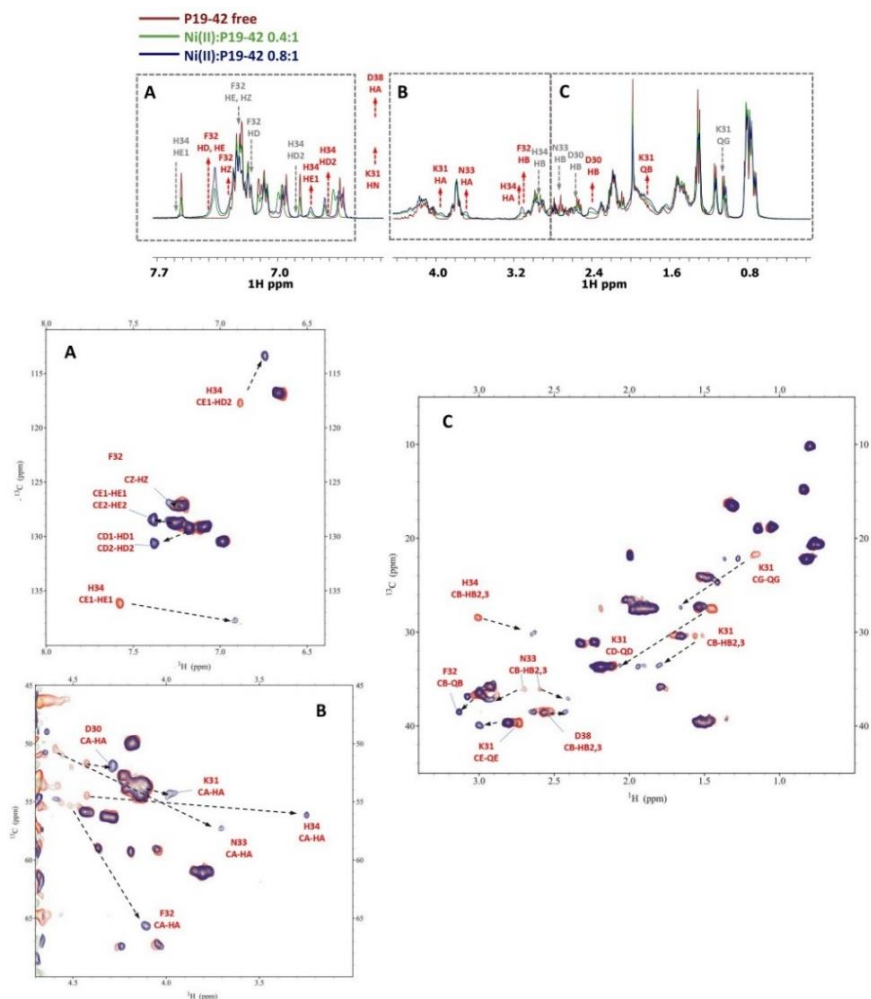


**Figura 4.21**. (sopra) Confronto degli spettri $^1$H di P19-42 con quantità crescenti di $Ni^{2+}$ a pH 10.6. Le frecce grigie indicano segnali che gradualmente diminuiscono di intensità, mentre le frecce rosse si riferiscono a nuovi segnali che compaiono gradualmente con l'aggiunta di $Ni^{2+}$; (in basso) confronto degli

spettri HSQC $^1$H-$^{13}$C di P19-42 libero (arancione) e Ni$^{2+}$-P19-42 con un rapporto molare di 0.8:1 (blu) a pH 10.6; le frecce nere indicano le nuove posizioni dei segnali NMR in seguito all'aggiunta di Ni$^{2+}$.
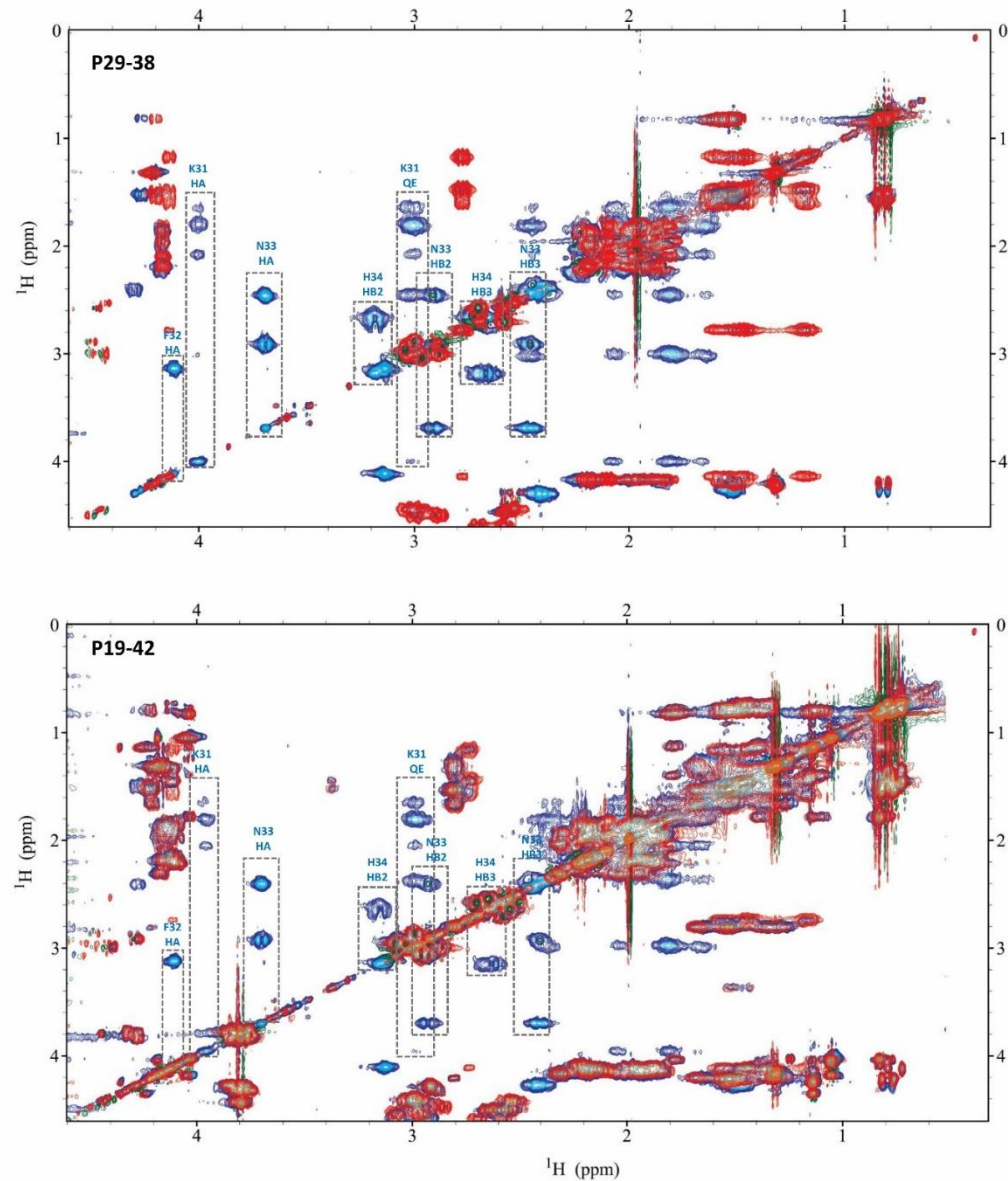


**Figura 4.22**. (in alto) Confronto degli spettri TOCSY $^1$H-$^1$H per la regione alifatica per il peptide libero P29–38 (rosso) e il sistema Ni$^{2+}$-P29–38 (blu) e (in basso) per P19–42 (rosso) e Ni$^{2+}$ -Sistema P19–42 (blu) a pH 10.6.
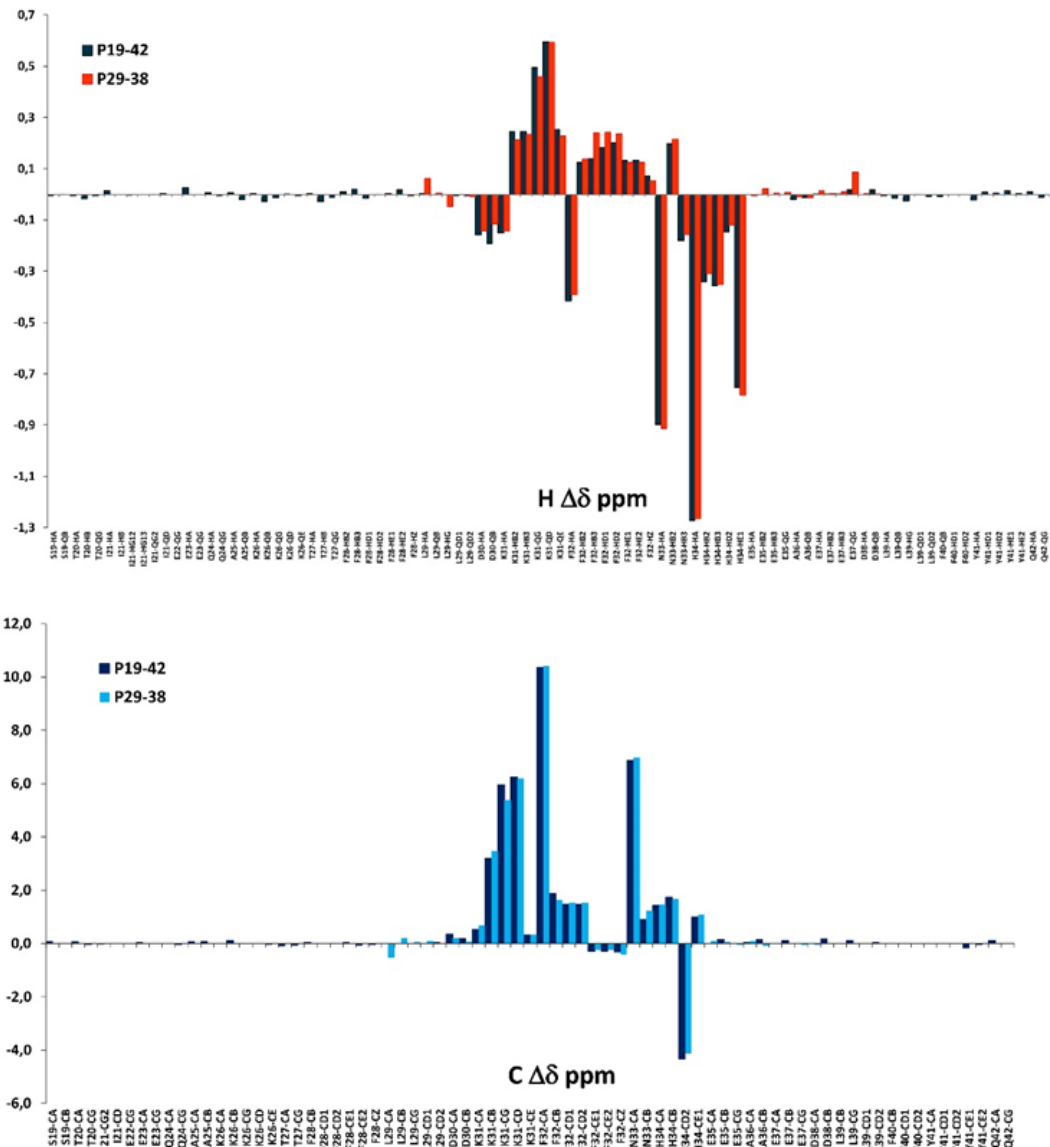
**Figura 4.23**. Confronto tra le variazioni dei *chemical shift* per i sistemi P29-38-Ni$^{2+}$ e P19-42-Ni$^{2+}$. In alto le variazioni relative ai nuclei H, in basso le variazioni relative ai nuclei C.

Come nel caso del modello più piccolo P29-38, il protone labile HN di Lys31 riappare dopo l'aggiunta di Ni$^{2+}$ e diversi ROE identificati per il sistema Ni$^{2+}$-P29-38 sono stati confermati per il sistema Ni$^{2+}$-P19-42, in particolare: Asp30HA-Lys31HN, Lys31HA-His34HD2, Lys31HA-His34HE1, Phe32HB2-

His34HD2, Asn33HB2-Phe32HD, Asn33HB3-Phe32HD, His34HE1-Phe32HD, che erano correlati con la conformazione bloccata del gruppo laterale di Phe32 e Asn33 sopra e di Lys31 sotto il piano del complesso.

Lo studio di competizione è stato condotto anche per il peptide più lungo, aggiungendo quantità crescenti di $Cu^{2+}$ al sistema $Ni^{2+}$-P19-42 a pH 10.6. Esattamente come nel caso del peptide più corto P29-38, i segnali correlati al legame con $Ni^{2+}$ e che coinvolgono His34, Asn33 e Phe32, i quali svolgono il ruolo principale nella complessazione del metallo, sono scomparsi selettivamente a seguito della sostituzione dello ione paramagnetico $Cu^{2+}$ con lo ione diamagnetico $Ni^{2+}$, in una sfera di coordinazione identica attorno all'atomo di metallo [Figura 4.24]. L'implicazione dell'azoto ammidico di Lys31 nella modalità di coordinazione $4N^-$ è evidenziata, come detto precedentemente, dalla scomparsa del suo sistema di spin HN.
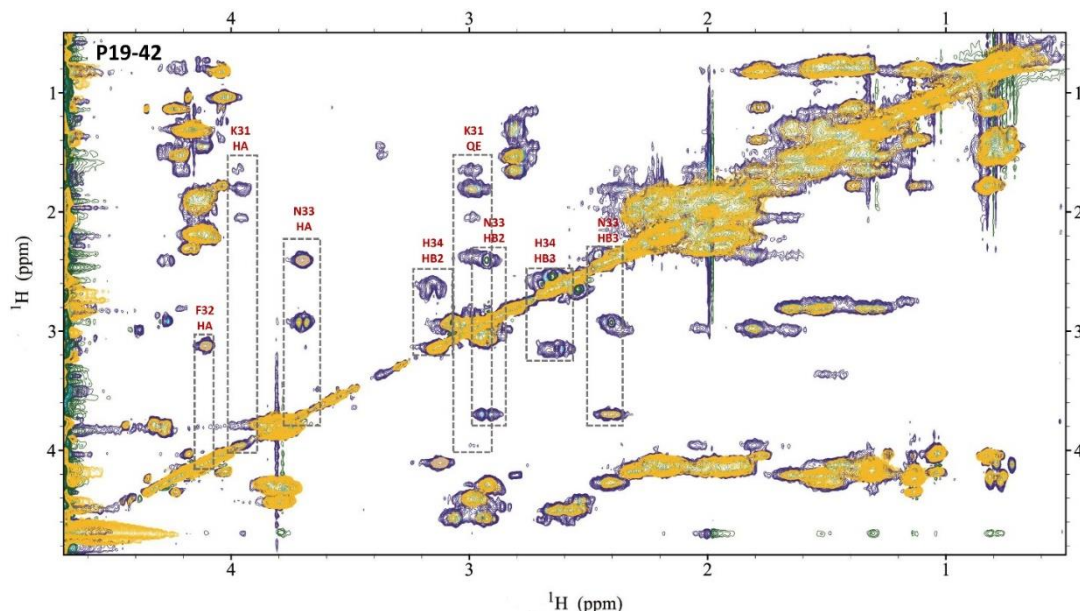


**Figura 4.24**. Confronto della regione alifatica degli spettri $^1H$-$^1H$ TOCSY per il sistema $Ni^{2+}$-P19–42 (blu) con l'aggiunta di 0.6 equivalenti di $Cu^{2+}$ (giallo), a pH 10.6.

Il grafico di competizione tra P29-38 e gli ioni $Zn^{2+}$ e $Cu^{2+}$ illustra [Figura 4.25] la formazione di complessi in una situazione ipotetica, quando quantità equimolari di tutti i reagenti vengono miscelate in soluzione.
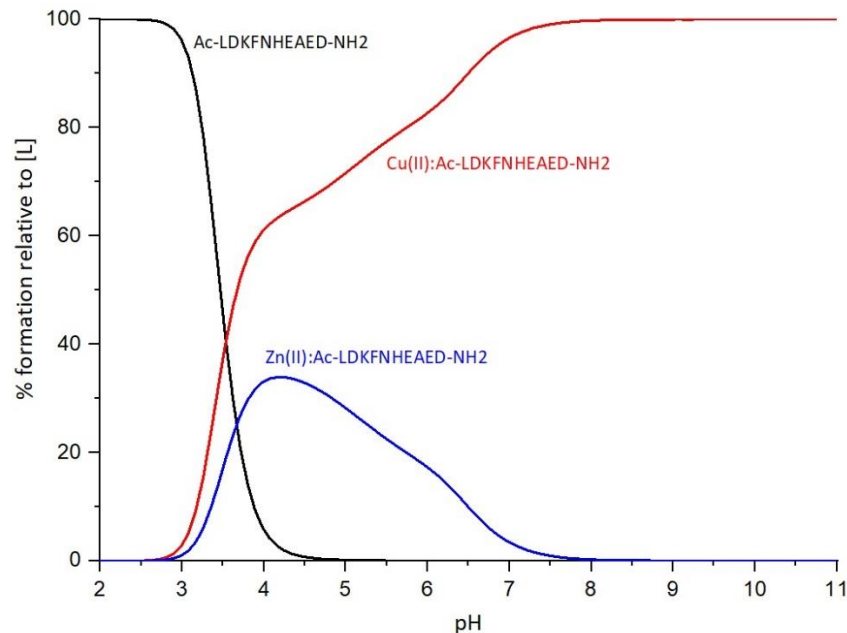


**Figura 4.25**. Grafico di competizione che mostra il comportamento dei reagenti se fossero tutti presenti in soluzione in quantità equimolari.

Fino a un pH di circa 2.8, quasi tutto il legante esiste nella forma non complessata. A partire da pH 3, l'inizio della complessazione può essere chiaramente osservato, con i complessi di rame che dominano già in queste condizioni acide, un comportamento che persiste fino a pH 11. I complessi di $Cu^{2+}$ coinvolgono rapidamente oltre il 60% delle molecole del legante a pH di circa 4. Intorno a questo pH, si raggiunge anche la concentrazione massima di complessi di $Zn^{2+}$, riflettendo l'inizio della deprotonazione e il legame dell'istidina H34 con $Zn^{2+}$. Con l'aumento del pH, la concentrazione dei complessi di $Zn^{2+}$ inizia a diminuire, con meno del 5% del ligando legato a pH 7. Al contrario, si può osservare un aumento della concentrazione dei

complessi di $Cu^{2+}$, riflettendo il coinvolgimento crescente di leganti azotati nel legame con il rame, come il residuo di istidina e i gruppi ammidici. Raggiungendo il 90% del ligando già a pH = 6.50, i complessi di $Cu^{2+}$ dominano chiaramente su quelli di $Zn^{2+}$, la cui sfera di coordinazione rimane invariata nel range di pH basico. Il comportamento osservato nel grafico di competizione di P29-38 con $Zn^{2+}$ e $Cu^{2+}$ è in accordo con la serie di Irving-Williams, secondo la quale la stabilità dei complessi di rame divalente è maggiore rispetto a quelli di zinco divalente [73]. I risultati di questo esperimento rimangono validi per una situazione ipotetica in cui si utilizzano quantità equimolari di tutti i reagenti. Nelle cellule umane, la situazione può essere completamente invertita, poiché le concentrazioni relative di rame e zinco liberi nel plasma non sono le stesse, essendo di circa $10^{-18}$-$10^{-13}$ M per il rame e intorno a $10^{-9}$ M per lo zinco [94,95].

## 4.5 Conclusioni

Lo zinco è un cofattore importante capace di stabilizzare le strutture proteiche e alterare l'affinità del substrato di varie metalloproteine. L'omeostasi dello $Zn^{2+}$ potrebbe influenzare l'espressione di ACE-2 e il legame al suo sito attivo è essenziale per la sua attività enzimatica [79]. È molto probabile che il legame dello $Zn^{2+}$ ad ACE2 possa influenzare la struttura molecolare del recettore e quindi la sua affinità di legame con il SARS-CoV-2. Allo stesso tempo, un gran numero di pazienti carenti di zinco sono risultati più inclini a sviluppare forme gravi di COVID-19 [96,97]. Il lavoro presentato qui fornisce preziose intuizioni sulla complessa chimica di coordinazione di $Zn^{2+}$ e $Cu^{2+}$ con tre frammenti peptidici del C-terminale del recettore ACE-2, una regione che svolge un ruolo cruciale nel legame con la proteina S del SARS-CoV-2. Lo studio ha utilizzato una combinazione di potenziometria, spettroscopia UV-Vis e CD, e tecniche di NMR per indagare la formazione e la modalità di coordinazione di ioni di $Zn^{2+}$ e $Cu^{2+}$ con i frammenti peptidici selezionati che imitano la regione di riconoscimento dell'interfaccia ACE2 per S. Anche la coordinazione del $Ni^{2+}$ è

stata studiata come sonda per il $Cu^{2+}$, poiché a valori di pH elevati i sistemi di $Cu^{2+}$ hanno mostrato un ampio allargamento di segnale negli spettri NMR, problema che ha impedito la caratterizzazione dettagliata delle specie nella modalità di coordinazione [$N_{Im}$, $3N^-_{amide}$]. I risultati hanno confermato le previsioni bioinformatiche ottenute da MIB2, che evidenziavano una regione altamente specifica in ACE2 per il legame dello zinco nella regione D30-Glu37. Tutti i dati sperimentali indicano che questa sequenza è in grado di legare entrambi gli ioni metallici in modo molto selettivo. Inoltre, i due peptidi più lunghi che imitano l'intero dominio mostrano lo stesso modello di coordinazione del peptide più corto, indicando che quest'ultimo è un eccellente modello per studiare le capacità di coordinazione all'interfaccia ACE2/S. Entrambi gli ioni metallici possono modificare la conformazione del peptide, che si riarrangia una volta coordinato con zinco o rame. Tali modifiche strutturali potrebbero interferire con il meccanismo di riconoscimento tra ACE2 e la proteina S, considerando anche che alcuni degli amminoacidi che partecipano o vengono perturbati dalla coordinazione del metallo svolgono un ruolo cruciale nella formazione di legami idrogeno tra le due proteine. Questi cambiamenti strutturali potrebbero diminuire l'affinità tra ACE2 e la proteina S e interferire positivamente nel meccanismo attraverso il quale il virus entra nelle cellule. Le terapie mirate ad ACE2 rappresentano una strategia generale per prevenire e trattare le infezioni da SARS-CoV-2 e le sue varianti, così come altri potenziali coronavirus che utilizzano il recettore ACE2 come via di ingresso per l'invasione virale [98]. Se fosse possibile sfruttare queste informazioni al fine di sviluppare una strategia terapeutica, questo tema potrebbe essere oggetto di nuove ricerche e aprire nuove prospettive nel trattamento di COVID-19 nei pazienti che ancora presentano sintomi gravi dopo l'infezione, o nel caso in cui emergessero nuove varianti aggressive. I risultati di questo studio sono stati pubblicati nella rivista internazionale Internation Journal of Molecular Science qui di seguito allegato.

Pelucelli, A.; Peana, M.; Orzeł, B.; Piasta, K.; Gumienna-Kontecka, E.; Medici, S.; Zoroddu, M.A. **$Zn^{2+}$ and $Cu^{2+}$ Interaction with the Recognition Interface of ACE2 for SARS-CoV-2 Spike Protein**. *International Journal of Molecular Sciences* **2023**, *24*. https://doi.org/10.3390/ijms24119202.

# Capitolo V

## Effetto dei metalli tossici sulla salute umana

### 5.1 Introduzione

Nel corso di un periodo storico particolare, segnato dalla pandemia di COVID-19, il mio percorso di dottorato è stato indubbiamente influenzato da una serie di restrizioni volte a contenere la diffusione del virus. Le normative sanitarie hanno imposto una necessaria pausa alle attività di laboratorio, inducendo una modifica sostanziale della mia metodica di ricerca. Sebbene all'inizio tale interruzione potesse sembrare un ostacolo al mio lavoro, ho deciso di sfruttare l'opportunità per focalizzarmi su una dimensione diversa dei miei argomenti di studio. Durante il lockdown ho potuto dedicare il mio tempo all'approfondimento di un tema di fondamentale importanza nel campo della chimica e della biologia: la tossicità dei metalli. La mia indagine si è concentrata sulla valutazione di come differenti metalli, sia essenziali che non essenziali, possano influenzare i sistemi biologici, dando luogo a fenomeni di tossicità a diverse dosi e in vari contesti [3]. L'analisi delle diverse forme chimiche dei metalli, delle loro capacità di legame, della solubilità e degli stati di ossidazione, ha consentito di esplorare le possibili interazioni con i bersagli cellulari e le loro implicazioni sulla salute umana [4]. Questo periodo di studio intensivo, sebbene forzato dalle circostanze, si è rivelato fruttuoso, culminando nella produzione di una serie di review scientifiche [4,24,99-101]. Questi lavori, che sono stati accolti positivamente dalla comunità accademica e pubblicati su riviste internazionali, hanno costituito un contributo significativo alla comprensione del ruolo dei metalli nel contesto biologico. In questo capitolo della mia tesi, ho pertanto deciso di riassumere i risultati di queste revisioni, allo scopo di fornire un quadro coerente e aggiornato della questione. Questo

contributo rappresenta non solo un punto di sintesi del mio lavoro durante il periodo di pandemia, ma anche un fondamentale punto di partenza per le future indagini in questo campo di ricerca.

## 5.2 Tossicità di nanoparticelle metalliche

L'esposizione umana a nanoparticelle (NP), sia naturali che derivanti da attività umane, è cresciuta notevolmente dall'epoca della Rivoluzione Industriale, con una correlazione documentata tra l'aumento dell'inquinamento da particolato e l'incidenza di malattie come il cancro e le malattie cardiovascolari e respiratorie. È chiaro che le particelle nanometriche, specialmente quelle derivanti da sorgenti naturali (come vulcani, incendi, polvere cosmica, ecc.), sono sempre state presenti nel nostro ambiente; tuttavia, dalla Rivoluzione Industriale, l'inquinamento da particolato fine, compreso quello di dimensioni nanometriche, è aumentato a causa delle emissioni industriali, del trasporto motorizzato e della crescita dell'industria nanotecnologica [102]. Studi epidemiologici mostrano una forte correlazione tra l'inquinamento da particolato atmosferico e la mortalità generale, inclusa l'incidenza di cancro e malattie cardiovascolari e respiratorie [103].

Nonostante l'evidente potenziale delle NP in vari campi tecnologici, è fondamentale un approccio scientifico ponderato per studiare i potenziali danni che possono causare. Le nostre attuali conoscenze sulla tossicologia potrebbero non essere sufficienti per affrontare la "nanotossicità", e le proprietà delle NP necessitano di un'analisi dettagliata per comprendere i loro meccanismi d'azione e sviluppare metodi di produzione sostenibili e sicuri. I dati sugli effetti delle NP sulla salute sono infatti attualmente inconcludenti, a causa delle contraddizioni tra diversi studi dovute alla varietà di fattori che influenzano la tossicità dei nanomateriali, tra cui dimensioni, forma, composizione, rivestimento, coniugazione, dispersibilità e concentrazione.

Nella review "**An updated overview on metal nanoparticles toxicity**" *Seminars in Cancer Biology*, 2021, 76, 17-26, sono stati quindi raccolti i dati esistenti relativi alle nanoparticelle metalliche e il loro utilizzo, nell'ottica di offrire una panoramica completa e ponderata sull'intera questione [100]. L' obiettivo è quello di delineare un quadro chiaro e dettagliato che possa fungere da base per comprendere le molteplici implicazioni delle nanoparticelle, dalla loro produzione alla loro interazione con i sistemi biologici. Sottolineare i vari meccanismi d'azione che queste particelle possono attivare a livello cellulare e sistemico, nonché esaminare i possibili effetti sulla salute umana a breve e lungo termine si rivela un *output* fondamentale per la ricerca scientifica. Inoltre, considerando l'importanza crescente delle nanoparticelle nel contesto industriale e tecnologico, ci si propone di discutere i metodi di produzione attualmente utilizzati, con un occhio di riguardo alla sostenibilità e alla sicurezza. L'aspirazione è quella di contribuire alla creazione di un quadro di riferimento scientifico che possa guidare lo sviluppo di strategie efficaci per la gestione e il controllo delle nanoparticelle. Questo, si spera, consentirà di massimizzare i benefici derivanti dal loro utilizzo, minimizzando contemporaneamente i possibili rischi per la salute e l'ambiente.

## 5.3 Tossicità dei metalli di transizione

I metalli essenziali svolgono un ruolo cruciale nel metabolismo cellulare umano e nelle funzioni biologiche, come la bio-mineralizzazione, il trasporto di carica e l'azione enzimatica. La carenza di questi metalli può portare a conseguenze negative per la salute, mentre un eccesso può causare tossicità [3]. Le cause della carenza di metalli essenziali includono alimentazione inadeguata, condizioni di salute specifiche, fattori genetici e scelte di vita sbagliate [104]. L'arricchimento degli alimenti e l'integrazione nutrizionale possono essere utilizzati per ripristinare il livello ottimale di ioni metallici [105,106].

I metalli non essenziali invece, ovvero quelli che non svolgono un ruolo biologico, o sono scarsamente presenti oppure, a seguito di esposizione, mostrano solo effetti dannosi. Tutti i tipi di metalli in realtà, essenziali e non, possono avere effetti tossici se l'esposizione supera un certo limite.

Nella review "**Metal Toxicity and Speciation: A Review**", *Current Medicinal Chemistry* 2021, 28, 7190-7208 [4]; quindi è stata esaminato la tossicità dei metalli non essenziali, tenendo conto delle loro specifiche caratteristiche chimiche, come le diverse forme, il carattere *hard-soft*, gli stati di ossidazione, le capacità di legame e di solubilità. Questi aspetti influenzano la loro speciazione nei sistemi biologici e, di conseguenza, i principali bersagli cellulari. I metalli tossici si dividono in due gruppi: quelli che finora hanno mostrato solo effetti negativi e quelli che non sono stati considerati essenziali per la vita a causa della loro bassa disponibilità o scarsa solubilità a pH fisiologico. Nel primo gruppo rientrano metalli come il mercurio, il piombo, il cadmio e il cromo. Alcuni di questi, come il piombo e il mercurio, sono noti contaminanti ambientali da molto tempo. Altri metalli potenzialmente tossici, come l'antimonio, il bismuto, lo zirconio, l'argento, il torio e i lantanoidi, sono generalmente insolubili in condizioni fisiologiche. Va però sottolineato che anche gli ioni metallici essenziali possono diventare tossici se presenti in dosi eccessive. In generale, i metalli tossici possono interferire con le funzioni biologiche essenziali, legandosi a biomolecole fondamentali o sostituendo i centri metallici naturali con metalli estranei. Infine, abbiamo evidenziato possibili trattamenti per l'avvelenamento da metalli basati sulla terapia chelante. Questa strategia clinica, che prevede l'uso di specifici agenti chelanti per rimuovere gli ioni metallici tossici, sembra particolarmente efficace nei casi acuti di intossicazione da metalli.

Questa review ha avuto come obiettivo quello di fornire un quadro completo sull'attuale conoscenza della tossicità dei metalli di transizione, mettendo in luce sia i benefici che i rischi associati alla loro presenza nell'organismo umano. Riconoscendo la complessità della questione, ci si proponeva di

esaminare la tossicità dei metalli di transizione da vari punti di vista. Sono stati considerati non solo i meccanismi biochimici attraverso i quali tali metalli possono esercitare effetti dannosi, ma anche le caratteristiche chimico-fisiche, come dimensioni, forma, stato di ossidazione e capacità di legame, che ne determinano la biodisponibilità e, quindi, la potenziale tossicità. La review, inoltre, ha inteso esplorare le strategie più recenti e promettenti per la prevenzione e il trattamento dell'avvelenamento da metalli. Questo include l'uso di terapie chelanti, che rappresentano attualmente l'approccio clinico più efficace in caso di intossicazione acuta, ma anche di strategie di prevenzione basate sulla regolazione dell'esposizione e sull'educazione nutrizionale. Infine, considerando l'importanza sempre crescente dei metalli di transizione in vari settori industriali e tecnologici, sono state discusse le sfide e le opportunità legate alla loro gestione sostenibile, con un occhio di riguardo ai rischi per la salute pubblica e all'impatto ambientale. In sintesi, attraverso un'analisi approfondita e multidisciplinare, in questa review ci si è proposti di fornire un contributo significativo alla comprensione del complesso tema della tossicità dei metalli di transizione, con la speranza di stimolare ulteriori ricerche e discussioni su questo argomento di grande rilevanza per la salute umana e l'ambiente.

## 5.4 Effetti dell'esposizione umana al cadmio

Scoperto nel 1817 da Friedrich Stromeyer come impurità nel carbonato di zinco, il cadmio (Cd) è un elemento naturalmente presente sulla crosta terrestre, senza funzione biologica nota negli organismi superiori, ma con una tossicità ben documentata. L'esposizione al Cd può derivare da fenomeni naturali come l'eruzione vulcanica e la combustione della biomassa, ma soprattutto da attività umane come l'utilizzo di combustibili fossili, l'estrazione di minerali metallici e le emissioni industriali. Gli esseri umani sono in parte protetti dall'esposizione al Cd grazie alla presenza di metallotioneine (MT), proteine ricche di cisteina che regolano il metabolismo dello zinco e

proteggono contro la tossicità di diversi ioni di metalli pesanti, danni al DNA e stress ossidativo [107,108]. Le MT, grazie ai numerosi gruppi sulfidrilici (-SH), possono complessare quasi tutti gli ioni Cd ingeriti in condizioni di esposizioni tollerabili. Oltre al Cd, le MT possono legare altri ioni metallici per proteggere le cellule e i tessuti dalla loro tossicità. Tuttavia, quando l'assorbimento di cadmio supera la capacità delle MT di legarlo, si verifica un accumulo soprattutto nei reni e nel fegato, con un'emivita estremamente lunga [109]. L'accumulo di Cd nei tessuti può causare stress ossidativo, danneggiare le funzioni cellulari e inibire la respirazione cellulare e la fosforilazione ossidativa. Il Cd può anche interferire con i sistemi di riparazione del DNA, che potrebbe spiegare i suoi effetti mutageni [110]. L'articolo "**Biological Effects of Human Exposure to Environmental Cadmium**", *Biomolecules* 2022, 13, prende in considerazione l'esposizione al cadmio ambientale, le sue potenziali implicazioni per la salute e le strategie per la sua bonifica ambientale e nel trattamento dell'avvelenamento nell'uomo [24].

L'obiettivo è stato quello di fornire una panoramica dell'esposizione umana al cadmio, mettendo in risalto i suoi effetti tossici, i bersagli biologici e i possibili trattamenti. I composti del cadmio, riconosciuti come cancerogeni, sono stati associati a vari tumori umani. Il cadmio induce stress ossidativo indiretto e può essere dannoso per la gravidanza. Nonostante ciò, i suoi esatti meccanismi di tossicità non sono stati completamente compresi. L'articolo sottolinea l'importanza di ulteriori ricerche, tra cui la necessità di indagare meglio il ruolo delle metallotioneine e di altre proteine nel trasporto del cadmio, l'approfondimento di un meccanismo d'azione comprovato per la carcinogenesi da cadmio e lo sviluppo di agenti chelanti più efficaci per la rimozione del cadmio dagli ambienti acquosi. L'articolo ha suscitato interesse nella comunità scientifica ed è stato selezionato come articolo copertina del Volume 13 Issue 1 della rivista scientifica Biomolecules [Figura 5.1].
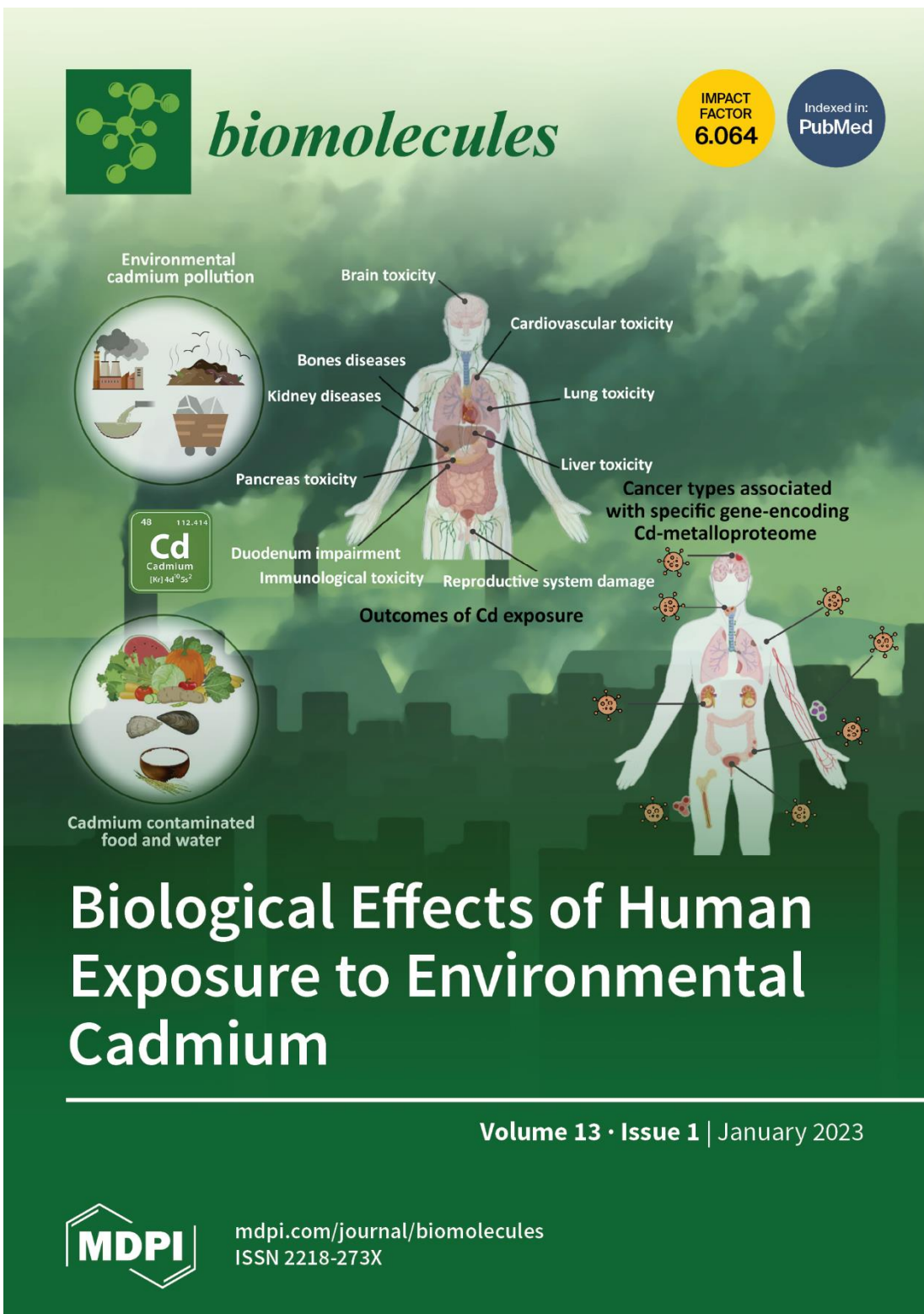
**Figura 5.1.** Cover della rivista Biomolecules per il Volume 11, fascicolo 1 del 2023.

## 5.5 Esposizione al bario e rischi per la salute

Nella review "**Environmental barium: potential exposure and health-hazards**" *Archives of Toxicology* 2021, 95, 2605-2612 [99], viene approfondito il tema della tossicità del Bario per la specie umana. Nonostante la sua presenza limitata nel cibo (tranne per le noci brasiliane) e nell'acqua potabile, il bario può accumularsi nei tessuti corporei. Anche i composti di bario possono essere tossici a seconda della loro solubilità, ma i casi di avvelenamento sono abbastanza rari. Il bario viene utilizzato in diverse applicazioni industriali ed è relativamente abbondante nella crosta terrestre. I sali di bario insolubili, come il solfato di bario, sono considerati sicuri per l'uomo e vengono utilizzati come mezzi di contrasto per gli esami radiografici. L'aumento delle preoccupazioni riguardo agli effetti dell'esposizione al bario sull'ambiente e sulla salute umana è stato causato dalla crescente consapevolezza pubblica delle numerose applicazioni di questo elemento. La presenza naturale di elevate concentrazioni di bario in suoli, piante agricole e acqua potabile ha sollevato interrogativi sulla possibile influenza dell'esposizione a lungo termine. È di vitale importanza comprendere l'entità dell'assunzione, la distribuzione e l'accumulo di bario nell'organismo umano, nonché i potenziali effetti nocivi associati. Alcune comunità potrebbero essere esposte a livelli elevati di bario, aumentando così il rischio per la salute pubblica a causa della contaminazione. Sono necessarie ulteriori ricerche per approfondire la comprensione dell'accumulo biologico del bario al fine di mitigarne gli effetti avversi in diverse situazioni di esposizione. Inoltre, è fondamentale identificare le popolazioni più vulnerabili, come bambini, donne in gravidanza e anziani, che potrebbero essere esposte a un maggiore rischio di contaminazione da bario attraverso il consumo di cibo e acqua in zone inquinate.

Quì di seguito sono riportati gli articoli integrali in formato "Review" sopra descritti e qui elencati:

- Medici, S.; Peana, M.; Pelucelli, A.; Zoroddu, M.A. An updated overview on metal nanoparticles toxicity. *Semin Cancer Biol* **2021**, *76*, 17-26. https://doi.org/10.1016/j.semcancer.2021.06.020

- Peana, M.; Pelucelli, A.; Medici, S.; Cappai, R.; Nurchi, V.M.; Zoroddu, M.A. Metal Toxicity and Speciation: A Review. *Curr Med Chem* **2021**, *28*, 7190-7208. https://doi.org/10.2174/0929867328666210324161205.

- Peana, M.; Pelucelli, A.; Chasapis, C.T.; Perlepes, S.P.; Bekiari, V.; Medici, S.; Zoroddu, M.A. Biological Effects of Human Exposure to Environmental Cadmium. *Biomolecules* **2022**, *13*. https://doi.org/10.3390/biom13010036.

- Peana, M.; Medici, S.; Dadar, M.; Zoroddu, M.A.; Pelucelli, A.; Chasapis, C.T.; Bjorklund, G. Environmental barium: potential exposure and health-hazards. *Arch Toxicol* **2021**, *95*, 2605-2612. https://doi.org/10.1007/s00204-021-03049-5.

# Bibliografia

1. Permyakov, E.A. Metal Binding Proteins. *Encyclopedia* **2021**, *1*, 261-292. https://doi.org/10.3390/encyclopedia1010024.
2. Maret, W. An Appraisal of the Field of Metallomics and the Roles of Metal Ions in Biochemistry and Cell Signaling. *Applied Sciences* **2021**, *11*. https://doi.org/10.3390/app112210846.
3. Zoroddu, M.A.; Aaseth, J.; Crisponi, G.; Medici, S.; Peana, M.; Nurchi, V.M. The essential metals for humans: a brief overview. *J Inorg Biochem* **2019**, *195*, 120-129. https://doi.org/10.1016/j.jinorgbio.2019.03.013.
4. Peana, M.; Pelucelli, A.; Medici, S.; Cappai, R.; Nurchi, V.M.; Zoroddu, M.A. Metal Toxicity and Speciation: A Review. *Curr Med Chem* **2021**, *28*, 7190-7208. https://doi.org/10.2174/0929867328666210324161205.
5. Kim, J.J.; Kim, Y.S.; Kumar, V. Heavy metal toxicity: An update of chelating therapeutic strategies. *J Trace Elem Med Biol* **2019**, *54*, 226-231. https://doi.org/10.1016/j.jtemb.2019.05.003.
6. Barnham, K.J.; Bush, A.I. Metals in Alzheimer's and Parkinson's diseases. *Curr Opin Chem Biol* **2008**, *12*, 222-228. https://doi.org/10.1016/j.cbpa.2008.02.019.
7. Kozlowski, H.; Luczkowski, M.; Remelli, M.; Valensin, D. Copper, zinc and iron in neurodegenerative diseases (Alzheimer's, Parkinson's and prion diseases). *Coordination Chemistry Reviews* **2012**, *256*, 2129-2141. https://doi.org/https://doi.org/10.1016/j.ccr.2012.03.013.
8. Kozlowski, H.; Janicka-Klos, A.; Brasun, J.; Gaggelli, E.; Valensin, D.; Valensin, G. Copper, iron, and zinc ions homeostasis and their role in neurodegenerative disorders (metal uptake, transport, distribution and regulation). *Coordination Chemistry Reviews* **2009**, *253*, 2665-2685. https://doi.org/https://doi.org/10.1016/j.ccr.2009.05.011.
9. Adlard, P.A.; Bush, A.I. Metals and Alzheimer's Disease: How Far Have We Come in the Clinic? *J Alzheimers Dis* **2018**, *62*, 1369-1379. https://doi.org/10.3233/JAD-170662.
10. Koski, L.; Ronnevi, C.; Berntsson, E.; Warmlander, S.; Roos, P.M. Metals in ALS TDP-43 Pathology. *Int J Mol Sci* **2021**, *22*. https://doi.org/10.3390/ijms222212193.
11. Boulikas, T.; Vougiouka, M. Recent clinical trials using cisplatin, carboplatin and their combination chemotherapy drugs (Review). *Oncol Rep* **2004**, *11*, 559-595. https://doi.org/10.3892/or.11.3.559.
12. Medici, S.; Peana, M.; Nurchi, V.M.; Lachowicz, J.I.; Crisponi, G.; Zoroddu, M.A. Noble metals in medicine: Latest advances. *Coordination Chemistry Reviews* **2015**, *284*, 329-350. https://doi.org/https://doi.org/10.1016/j.ccr.2014.08.002.
13. Ji, J.; Chen, G.; Zhao, J. Preparation and characterization of amino/thiol bifunctionalized magnetic nanoadsorbent and its application in rapid removal of $Pb^{2+}$ from aqueous system. *J Hazard Mater* **2019**, *368*, 255-263. https://doi.org/10.1016/j.jhazmat.2019.01.035.
14. Cantu, J.; Valle, J.; Flores, K.; Gonzalez, D.; Valdes, C.; Lopez, J.; Padilla, V.; Alcoutlabi, M.; Parsons, J. Investigation into the thermodynamics and kinetics of the binding of Cu(2+) and Pb(2+) to TiS(2) nanoparticles synthesized using a solvothermal process. *J Environ Chem Eng* **2019**, *7*. https://doi.org/10.1016/j.jece.2019.103463.

15. Crisponi, G.; Nurchi, V.M. Metal Ion Toxicity. In *Encyclopedia of Inorganic and Bioinorganic Chemistry*; 2015; pp. 1-14. https://doi.org/https://doi.org/10.1002/9781119951438.eibc0126.pub2.

16. Anthemidis, A.N.; Ioannou, K.I. Recent developments in homogeneous and dispersive liquid-liquid extraction for inorganic elements determination. A review. *Talanta* **2009**, *80*, 413-421. https://doi.org/10.1016/j.talanta.2009.09.005.

17. Fu, F.; Wang, Q. Removal of heavy metal ions from wastewaters: a review. *J Environ Manage* **2011**, *92*, 407-418. https://doi.org/10.1016/j.jenvman.2010.11.011.

18. Oliveira, V.H.B.; Rechotnek, F.; da Silva, E.P.; Marques, V.d.S.; Rubira, A.F.; Silva, R.; Lourenço, S.A.; Muniz, E.C. A sensitive electrochemical sensor for Pb2+ ions based on ZnO nanofibers functionalized by L-cysteine. *Journal of Molecular Liquids* **2020**, *309*, 113041. https://doi.org/https://doi.org/10.1016/j.molliq.2020.113041.

19. Cappai, R.; Chand, K.; Lachowicz, J.I.; Chaves, S.; Gano, L.; Crisponi, G.; Nurchi, V.M.; Peana, M.; Zoroddu, M.A.; Santos, M.A. A new tripodal-3-hydroxy-4-pyridinone for iron and aluminium sequestration: synthesis, complexation and in vivo studies. *New Journal of Chemistry* **2018**, *42*, 8050-8061. https://doi.org/10.1039/C8NJ00116B.

20. Cardiano, P.; Foti, C.; Giuffrè, O. On the interaction of N-acetylcysteine with Pb2+, Zn2+, Cd2+ and Hg2+. *Journal of Molecular Liquids* **2016**, *223*, 360-367. https://doi.org/https://doi.org/10.1016/j.molliq.2016.08.050.

21. Irto, A.; Cardiano, P.; Chand, K.; Cigala, R.M.; Crea, F.; De Stefano, C.; Gattuso, G.; Sammartano, S.; Santos, M.A. Complexation of environmentally and biologically relevant metals with bifunctional 3-hydroxy-4-pyridinones. *Journal of Molecular Liquids* **2020**, *319*, 114349. https://doi.org/https://doi.org/10.1016/j.molliq.2020.114349.

22. Irto, A.; Cardiano, P.; Chand, K.; Cigala, R.M.; Crea, F.; De Stefano, C.; Gano, L.; Gattuso, G.; Sammartano, S.; Santos, M.A. A new bis-(3-hydroxy-4-pyridinone)-DTPA-derivative: Synthesis, complexation of di-/tri-valent metal cations and in vivo M3+ sequestering ability. *Journal of Molecular Liquids* **2019**, *281*, 280-294. https://doi.org/https://doi.org/10.1016/j.molliq.2019.02.042.

23. Bjorklund, G.; Tippairote, T.; Hangan, T.; Chirumbolo, S.; Peana, M. Early-Life Lead Exposure: Risks and Neurotoxic Consequences. *Curr Med Chem* **2023**. https://doi.org/10.2174/0929867330666230409135310.

24. Peana, M.; Pelucelli, A.; Chasapis, C.T.; Perlepes, S.P.; Bekiari, V.; Medici, S.; Zoroddu, M.A. Biological Effects of Human Exposure to Environmental Cadmium. *Biomolecules* **2022**, *13*. https://doi.org/10.3390/biom13010036.

25. Agency for Toxic Substances and Disease Registry. Available online: https://www.atsdr.cdc.gov/ (accessed on may 2023).

26. Antimicrobial Resistance, C. Global burden of bacterial antimicrobial resistance in 2019: a systematic analysis. *Lancet* **2022**, *399*, 629-655. https://doi.org/10.1016/S0140-6736(21)02724-0.

27. O'Neill, J. Tackling drug-resistant infections globally: final report and recommendations. **2016**.

28. Poirel, L.; Madec, J.Y.; Lupo, A.; Schink, A.K.; Kieffer, N.; Nordmann, P.; Schwarz, S. Antimicrobial Resistance in Escherichia coli. *Microbiol Spectr* **2018**, *6*. https://doi.org/10.1128/microbiolspec.ARBA-0026-2017.

29. WHO. WHO publishes list of bacteria for which new antibiotics are urgently needed. **2017**.

30. Hennigar, S.R.; McClung, J.P. Nutritional Immunity: Starving Pathogens of Trace Minerals. *Am J Lifestyle Med* **2016**, *10*, 170-173. https://doi.org/10.1177/1559827616629117.

31. Puig, S.; Ramos-Alonso, L.; Romero, A.M.; Martinez-Pastor, M.T. The elemental role of iron in DNA synthesis and repair. *Metallomics* **2017**, *9*, 1483-1500. https://doi.org/10.1039/c7mt00116a.

32. Mikhaylina, A.; Ksibe, A.Z.; Scanlan, D.J.; Blindauer, C.A. Bacterial zinc uptake regulator proteins and their regulons. *Biochem Soc Trans* **2018**, *46*, 983-1001. https://doi.org/10.1042/BST20170228.

33. Lemos, M.L.; Balado, M. Iron uptake mechanisms as key virulence factors in bacterial fish pathogens. *J Appl Microbiol* **2020**, *129*, 104-115. https://doi.org/10.1111/jam.14595.

34. Bradley, J.M.; Svistunenko, D.A.; Wilson, M.T.; Hemmings, A.M.; Moore, G.R.; Le Brun, N.E. Bacterial iron detoxification at the molecular level. *J Biol Chem* **2020**, *295*, 17602-17623. https://doi.org/10.1074/jbc.REV120.007746.

35. Saha, R.; Saha, N.; Donofrio, R.S.; Bestervelt, L.L. Microbial siderophores: a mini review. *J Basic Microbiol* **2013**, *53*, 303-317. https://doi.org/10.1002/jobm.201100552.

36. Saha, M.; Sarkar, S.; Sarkar, B.; Sharma, B.K.; Bhattacharjee, S.; Tribedi, P. Microbial siderophores and their potential applications: a review. *Environ Sci Pollut Res Int* **2016**, *23*, 3984-3999. https://doi.org/10.1007/s11356-015-4294-0.

37. Astuti, I.; Ysrafil. Severe Acute Respiratory Syndrome Coronavirus 2 (SARS-CoV-2): An overview of viral structure and host response. *Diabetes Metab Syndr* **2020**, *14*, 407-412. https://doi.org/10.1016/j.dsx.2020.04.020.

38. Ozono, S.; Zhang, Y.; Ode, H.; Sano, K.; Tan, T.S.; Imai, K.; Miyoshi, K.; Kishigami, S.; Ueno, T.; Iwatani, Y.; et al. SARS-CoV-2 D614G spike mutation increases entry efficiency with enhanced ACE2-binding affinity. *Nat Commun* **2021**, *12*, 848. https://doi.org/10.1038/s41467-021-21118-2.

39. Beyerstedt, S.; Casaro, E.B.; Rangel, E.B. COVID-19: angiotensin-converting enzyme 2 (ACE2) expression and tissue susceptibility to SARS-CoV-2 infection. *Eur J Clin Microbiol Infect Dis* **2021**, *40*, 905-919. https://doi.org/10.1007/s10096-020-04138-6.

40. Ni, W.; Yang, X.; Yang, D.; Bao, J.; Li, R.; Xiao, Y.; Hou, C.; Wang, H.; Liu, J.; Yang, D.; et al. Role of angiotensin-converting enzyme 2 (ACE2) in COVID-19. *Crit Care* **2020**, *24*, 422. https://doi.org/10.1186/s13054-020-03120-0.

41. Perrotta, F.; Matera, M.G.; Cazzola, M.; Bianco, A. Severe respiratory SARS-CoV2 infection: Does ACE2 receptor matter? *Respir Med* **2020**, *168*, 105996. https://doi.org/10.1016/j.rmed.2020.105996.

42. Fatouros, P.R.; Roy, U.; Sur, S. Implications of SARS-CoV-2 spike protein interactions with Zn-bound form of ACE2: a computational structural study. *Biometals* **2023**, 1-10. https://doi.org/10.1007/s10534-023-00491-z.

43. Towler, P.; Staker, B.; Prasad, S.G.; Menon, S.; Tang, J.; Parsons, T.; Ryan, D.; Fisher, M.; Williams, D.; Dales, N.A.; et al. ACE2 X-ray structures reveal a large hinge-bending motion important for inhibitor binding and catalysis. *J Biol Chem* **2004**, *279*, 17996-18007. https://doi.org/10.1074/jbc.M311191200.

44. Pelucelli, A.; Peana, M.; Orzeł, B.; Piasta, K.; Gumienna-Kontecka, E.; Medici, S.; Zoroddu, M.A. Zn2+ and Cu2+ Interaction with the Recognition Interface of ACE2 for

SARS-CoV-2 Spike Protein. *International Journal of Molecular Sciences* **2023**, *24*. https://doi.org/10.3390/ijms24119202.

45. Nurchi, V.M.; de Guadalupe Jaraquemada-Pelaez, M.; Crisponi, G.; Lachowicz, J.I.; Cappai, R.; Gano, L.; Santos, M.A.; Melchior, A.; Tolazzi, M.; Peana, M.; et al. A new tripodal kojic acid derivative for iron sequestration: Synthesis, protonation, complex formation studies with Fe(3+), Al(3+), Cu(2+) and Zn(2+), and in vivo bioassays. *J Inorg Biochem* **2019**, *193*, 152-165. https://doi.org/10.1016/j.jinorgbio.2019.01.012.

46. Nurchi, V.M.; Crisponi, G.; Lachowicz, J.I.; Jaraquemada-Pelaez, M.G.; Bretti, C.; Peana, M.; Medici, S.; Zoroddu, M.A. Equilibrium studies of new bis-hydroxypyrone derivatives with Fe(3+), Al(3+), Cu(2+) and Zn(2). *J Inorg Biochem* **2018**, *189*, 103-114. https://doi.org/10.1016/j.jinorgbio.2018.09.013.

47. Nurchi, V.M.; Jaraquemada-Pelaez, M.d.G.; Lachowicz, J.I.; Zoroddu, M.A.; Peana, M.; Domínguez-Martín, A.; Choquesillo-Lazarte, D.; Remelli, M.; Szewczuk, Z.; Crisponi, G. Looking at new ligands for chelation therapy. *New Journal of Chemistry* **2018**, *42*, 8021-8034. https://doi.org/10.1039/C7NJ03947F.

48. Cappai, R.; Fantasia, A.; Barone, G.; Peana, M.F.; Pelucelli, A.; Medici, S.; Crisponi, G.; Nurchi, V.; Zoroddu, M.A. A Family of Kojic Acid Derivatives Aimed to Remediation of Pb2+ and Cd2+. *Available at SSRN 4402583* **2023**. https://doi.org/10.2139/ssrn.4402583.

49. Gans, P.; Sabatini, A.; Vacca, A. Investigation of equilibria in solution. Determination of equilibrium constants with the HYPERQUAD suite of programs. *Talanta* **1996**, *43*, 1739-1753. https://doi.org/10.1016/0039-9140(96)01958-3.

50. Alderighi, L.; Gans, P.; Ienco, A.; Peters, D.; Sabatini, A.; Vacca, A. Hyperquad simulation and speciation (HySS): a utility program for the investigation of equilibria involving soluble and partially soluble species. *Coordination Chemistry Reviews* **1999**, *184*, 311-318. https://doi.org/https://doi.org/10.1016/S0010-8545(98)00260-4.

51. Pecsok, R.L.; Meeker, R.L.; Shields, L.D. Chelates of Cadmium with Kojic Acid1. *Journal of the American Chemical Society* **1961**, *83*, 2081-2085. https://doi.org/10.1021/ja01470a012.

52. Agency for Toxic Substances and Disease Registry. Available online: https://www.atsdr.cdc.gov/csem/leadtoxicity/safety_standards.html (accessed on may 2023).

53. Agency for Toxic Substances and Disease Registry. Available online: https://www.atsdr.cdc.gov/csem/cadmium/Safety399Standards.html (accessed on may 2023).

54. World Health Organization. Guidelines for drinking-water quality: fourth edition incorporating the first addendum. Available online: https://www.who.int/publications/i/item/9789241549950 (accessed on may 2023).

55. Lau, C.K.; Krewulak, K.D.; Vogel, H.J. Bacterial ferrous iron transport: the Feo system. *FEMS Microbiol Rev* **2016**, *40*, 273-298. https://doi.org/10.1093/femsre/fuv049.

56. Ge, R.; Sun, X. Iron trafficking system in Helicobacter pylori. *Biometals* **2012**, *25*, 247-258. https://doi.org/10.1007/s10534-011-9512-8.

57. Hohle, T.H.; Franck, W.L.; Stacey, G.; O'Brian, M.R. Bacterial outer membrane channel for divalent metal ion acquisition. *Proc Natl Acad Sci U S A* **2011**, *108*, 15390-15395. https://doi.org/10.1073/pnas.1110137108.

58. Radka, C.D.; DeLucas, L.J.; Wilson, L.S.; Lawrenz, M.B.; Perry, R.D.; Aller, S.G. Crystal structure of Yersinia pestis virulence factor YfeA reveals two polyspecific metal-

binding sites. *Acta Crystallogr D Struct Biol* **2017**, *73*, 557-572. https://doi.org/10.1107/S2059798317006349.

59. Grass, G.; Franke, S.; Taudte, N.; Nies, D.H.; Kucharski, L.M.; Maguire, M.E.; Rensing, C. The metal permease ZupT from Escherichia coli is a transporter with a broad substrate spectrum. *J Bacteriol* **2005**, *187*, 1604-1611. https://doi.org/10.1128/JB.187.5.1604-1611.2005.

60. Haemig, H.A.; Moen, P.J.; Brooker, R.J. Evidence that highly conserved residues of transmembrane segment 6 of Escherichia coli MntH are important for transport activity. *Biochemistry* **2010**, *49*, 4662-4671. https://doi.org/10.1021/bi100320y.

61. Cartron, M.L.; Maddocks, S.; Gillingham, P.; Craven, C.J.; Andrews, S.C. Feo--transport of ferrous iron into bacteria. *Biometals* **2006**, *19*, 143-157. https://doi.org/10.1007/s10534-006-0003-2.

62. Sestok, A.E.; Linkous, R.O.; Smith, A.T. Toward a mechanistic understanding of Feo-mediated ferrous iron uptake. *Metallomics* **2018**, *10*, 887-898. https://doi.org/10.1039/c8mt00097b.

63. Naikare, H.; Palyada, K.; Panciera, R.; Marlow, D.; Stintzi, A. Major role for FeoB in Campylobacter jejuni ferrous iron acquisition, gut colonization, and intracellular survival. *Infect Immun* **2006**, *74*, 5433-5444. https://doi.org/10.1128/IAI.00052-06.

64. Velayudhan, J.; Hughes, N.J.; McColm, A.A.; Bagshaw, J.; Clayton, C.L.; Andrews, S.C.; Kelly, D.J. Iron acquisition and virulence in Helicobacter pylori: a major role for FeoB, a high-affinity ferrous iron transporter. *Mol Microbiol* **2000**, *37*, 274-286. https://doi.org/10.1046/j.1365-2958.2000.01987.x.

65. Lau, C.K.; Ishida, H.; Liu, Z.; Vogel, H.J. Solution structure of Escherichia coli FeoA and its potential role in bacterial ferrous iron transport. *J Bacteriol* **2013**, *195*, 46-55. https://doi.org/10.1128/JB.01121-12.

66. Severance, S.; Chakraborty, S.; Kosman, D.J. The Ftr1p iron permease in the yeast plasma membrane: orientation, topology and structure-function relationships. *Biochem J* **2004**, *380*, 487-496. https://doi.org/10.1042/BJ20031921.

67. Pearson, R.G. Hard and Soft Acids and Bases. *Journal of the American Chemical Society* **1963**, *85*, 3533-3539. https://doi.org/10.1021/ja00905a001.

68. Liang, J.; Canary, J.W. Discrimination between hard metals with soft ligand donor atoms: an on-fluorescence probe for manganese$^{2+}$. *Angew Chem Int Ed Engl* **2010**, *49*, 7710-7713. https://doi.org/10.1002/anie.201002853.

69. Andreini, C.; Cavallaro, G.; Lorenzini, S.; Rosato, A. MetalPDB: a database of metal sites in biological macromolecular structures. *Nucleic Acids Res* **2013**, *41*, D312-319. https://doi.org/10.1093/nar/gks1063.

70. Damo, S.M.; Kehl-Fie, T.E.; Sugitani, N.; Holt, M.E.; Rathi, S.; Murphy, W.J.; Zhang, Y.; Betz, C.; Hench, L.; Fritz, G.; et al. Molecular basis for manganese sequestration by calprotectin and roles in the innate immune response to invading bacterial pathogens. *Proc Natl Acad Sci U S A* **2013**, *110*, 3841-3846. https://doi.org/10.1073/pnas.1220341110.

71. Rola, A.; Potok, P.; Mos, M.; Gumienna-Kontecka, E.; Potocki, S. $Zn^{2+}$ and $Cd^{2+}$ Complexes of AMT1/MAC1 Homologous Cys/His-Rich Domains: So Similar yet So Different. *Inorg Chem* **2022**, *61*, 14333-14343. https://doi.org/10.1021/acs.inorgchem.2c02080.

72. Putignano, V.; Rosato, A.; Banci, L.; Andreini, C. MetalPDB in 2018: a database of metal sites in biological macromolecular structures. *Nucleic Acids Res* **2018**, *46*, D459-D464. https://doi.org/10.1093/nar/gkx989.

73. Irving, H.; Williams, R.J.P. 637. The stability of transition-metal complexes. *Journal of the Chemical Society (Resumed)* **1953**, 3192-3210. https://doi.org/10.1039/JR9530003192.

74. Hamming, I.; Cooper, M.E.; Haagmans, B.L.; Hooper, N.M.; Korstanje, R.; Osterhaus, A.D.; Timens, W.; Turner, A.J.; Navis, G.; van Goor, H. The emerging role of ACE2 in physiology and disease. *J Pathol* **2007**, *212*, 1-11. https://doi.org/10.1002/path.2162.

75. Verdecchia, P.; Cavallini, C.; Spanevello, A.; Angeli, F. The pivotal link between ACE2 deficiency and SARS-CoV-2 infection. *Eur J Intern Med* **2020**, *76*, 14-20. https://doi.org/10.1016/j.ejim.2020.04.037.

76. Hoffmann, M.; Kleine-Weber, H.; Pohlmann, S. A Multibasic Cleavage Site in the Spike Protein of SARS-CoV-2 Is Essential for Infection of Human Lung Cells. *Mol Cell* **2020**, *78*, 779-784 e775. https://doi.org/10.1016/j.molcel.2020.04.022.

77. Lan, J.; Ge, J.; Yu, J.; Shan, S.; Zhou, H.; Fan, S.; Zhang, Q.; Shi, X.; Wang, Q.; Zhang, L.; et al. Structure of the SARS-CoV-2 spike receptor-binding domain bound to the ACE2 receptor. *Nature* **2020**, *581*, 215-220. https://doi.org/10.1038/s41586-020-2180-5.

78. Yan, R.; Zhang, Y.; Li, Y.; Xia, L.; Guo, Y.; Zhou, Q. Structural basis for the recognition of SARS-CoV-2 by full-length human ACE2. *Science* **2020**, *367*, 1444-1448. https://doi.org/10.1126/science.abb2762.

79. Wessels, I.; Rolles, B.; Rink, L. The Potential Impact of Zinc Supplementation on COVID-19 Pathogenesis. *Front Immunol* **2020**, *11*, 1712. https://doi.org/10.3389/fimmu.2020.01712.

80. Magri, A.; Tabbi, G.; Di Natale, G.; La Mendola, D.; Pietropaolo, A.; Zoroddu, M.A.; Peana, M.; Rizzarelli, E. Zinc Interactions with a Soluble Mutated Rat Amylin to Mimic Whole Human Amylin: An Experimental and Simulation Approach to Understand Stoichiometry, Speciation and Coordination of the Metal Complexes. *Chemistry* **2020**, *26*, 13072-13084. https://doi.org/10.1002/chem.202002114.

81. Gampp, H.; Maeder, M.; Meyer, C.J.; Zuberbuhler, A.D. Calculation of equilibrium constants from multiwavelength spectroscopic data--II: SPECFIT: two user-friendly programs in basic and standard FORTRAN 77. *Talanta* **1985**, *32*, 257-264. https://doi.org/10.1016/0039-9140(85)80077-1.

82. Prenesti, E.; Daniele, P.G.; Prencipe, M.; Ostacoli, G. Spectrum–structure correlation for visible absorption spectra of copper$^{2+}$ complexes in aqueous solution. *Polyhedron* **1999**, *18*, 3233-3241. https://doi.org/https://doi.org/10.1016/S0277-5387(99)00279-X.

83. Lesiow, M.K.; Pietrzyk, P.; Bienko, A.; Kowalik-Jankowska, T. Stability of Cu$^{2+}$ complexes with FomA protein fragments containing two His residues in the peptide chain. *Metallomics* **2019**, *11*, 1518-1531. https://doi.org/10.1039/c9mt00131j.

84. Peana, M.; Gumienna-Kontecka, E.; Piras, F.; Ostrowska, M.; Piasta, K.; Krzywoszynska, K.; Medici, S.; Zoroddu, M.A. Exploring the Specificity of Rationally Designed Peptides Reconstituted from the Cell-Free Extract of Deinococcus radiodurans toward Mn$^{2+}$ and Cu$^{2+}$. *Inorg Chem* **2020**, *59*, 4661-4684. https://doi.org/10.1021/acs.inorgchem.9b03737.

85. Magri, A.; Munzone, A.; Peana, M.; Medici, S.; Zoroddu, M.A.; Hansson, O.; Satriano, C.; Rizzarelli, E.; La Mendola, D. Coordination Environment of Cu$^{2+}$ Ions Bound to N-

Terminal Peptide Fragments of Angiogenin Protein. *Int J Mol Sci* **2016**, *17*. https://doi.org/10.3390/ijms17081240.

86. Zoroddu, M.A.; Kowalik-Jankowska, T.; Medici, S.; Peana, M.; Kozlowski, H. Copper[2+] binding to Cap43 protein fragments. *Dalton Trans* **2008**, 6127-6134. https://doi.org/10.1039/b808600a.

87. Zoroddu, M.A.; Kowalik-Jankowska, T.; Kozlowski, H.; Molinari, H.; Salnikow, K.; Broday, L.; Costa, M. Interaction of Ni^{2+} and Cu^{2+} with a metal binding sequence of histone H4: AKRHRK, a model of the H4 tail. *Biochimica et Biophysica Acta (BBA) - General Subjects* **2000**, *1475*, 163-168. https://doi.org/https://doi.org/10.1016/S0304-4165(00)00066-0.

88. Kowalik-Jankowska, T.; Kadej, A.; Kuczer, M.; Czarniewska, E. Copper[2+] complexes of the Neb-colloostatin analogues containing histidine residue structure stability biological activity. *Polyhedron* **2017**, *134*, 365-375. https://doi.org/https://doi.org/10.1016/j.poly.2017.06.023.

89. Rowinska-Zyrek, M.; Wiech, A.; Wa Tly, J.; Wieczorek, R.; Witkowska, D.; Ozyhar, A.; Orlowski, M. Copper[2+]-Binding Induces a Unique Polyproline Type II Helical Structure within the Ion-Binding Segment in the Intrinsically Disordered F-Domain of Ecdysteroid Receptor from Aedes aegypti. *Inorg Chem* **2019**, *58*, 11782-11792. https://doi.org/10.1021/acs.inorgchem.9b01826.

90. Medici, S.; Peana, M.; Nurchi, V.M.; Zoroddu, M.A. The involvement of amino acid side chains in shielding the nickel coordination site: an NMR study. *Molecules* **2013**, *18*, 12396-12414. https://doi.org/10.3390/molecules181012396.

91. Peana, M.; Zdyb, K.; Medici, S.; Pelucelli, A.; Simula, G.; Gumienna-Kontecka, E.; Zoroddu, M.A. Ni[2+] interaction with a peptide model of the human TLR4 ectodomain. *J Trace Elem Med Biol* **2017**, *44*, 151-160. https://doi.org/10.1016/j.jtemb.2017.07.006.

92. Jones, C.E.; Klewpatinond, M.; Abdelraheim, S.R.; Brown, D.R.; Viles, J.H. Probing copper2+ binding to the prion protein using diamagnetic nickel2+ and 1H NMR: the unstructured N terminus facilitates the coordination of six copper2+ ions at physiological concentrations. *J Mol Biol* **2005**, *346*, 1393-1407. https://doi.org/10.1016/j.jmb.2004.12.043.

93. Peana, M.F.; Medici, S.; Ledda, A.; Nurchi, V.M.; Zoroddu, M.A. Interaction of Cu^{2+} and Ni^{2+} with Ypk9 protein fragment via NMR studies. *ScientificWorldJournal* **2014**, *2014*, 656201. https://doi.org/10.1155/2014/656201.

94. Rae, T.D.; Schmidt, P.J.; Pufahl, R.A.; Culotta, V.C.; O'Halloran, T.V. Undetectable intracellular free copper: the requirement of a copper chaperone for superoxide dismutase. *Science* **1999**, *284*, 805-808. https://doi.org/10.1126/science.284.5415.805.

95. Maret, W. Analyzing free zinc[2+] ion concentrations in cell biology with fluorescent chelating molecules. *Metallomics* **2015**, *7*, 202-211. https://doi.org/10.1039/c4mt00230j.

96. Jothimani, D.; Kailasam, E.; Danielraj, S.; Nallathambi, B.; Ramachandran, H.; Sekar, P.; Manoharan, S.; Ramani, V.; Narasimhan, G.; Kaliamoorthy, I.; et al. COVID-19: Poor outcomes in patients with zinc deficiency. *Int J Infect Dis* **2020**, *100*, 343-349. https://doi.org/10.1016/j.ijid.2020.09.014.

97. Wessels, I.; Rolles, B.; Slusarenko, A.J.; Rink, L. Zinc deficiency as a possible risk factor for increased susceptibility and severe progression of Corona Virus Disease 19. *Br J Nutr* **2022**, *127*, 214-232. https://doi.org/10.1017/S0007114521000738.

98. Oudit, G.Y.; Wang, K.; Viveiros, A.; Kellner, M.J.; Penninger, J.M. Angiotensin-converting enzyme 2-at the heart of the COVID-19 pandemic. *Cell* **2023**, *186*, 906-922. https://doi.org/10.1016/j.cell.2023.01.039.

99. Peana, M.; Medici, S.; Dadar, M.; Zoroddu, M.A.; Pelucelli, A.; Chasapis, C.T.; Bjorklund, G. Environmental barium: potential exposure and health-hazards. *Arch Toxicol* **2021**, *95*, 2605-2612. https://doi.org/10.1007/s00204-021-03049-5.

100. Medici, S.; Peana, M.; Pelucelli, A.; Zoroddu, M.A. An updated overview on metal nanoparticles toxicity. *Semin Cancer Biol* **2021**, *76*, 17-26. https://doi.org/10.1016/j.semcancer.2021.06.020.

101. Medici, S.; Peana, M.; Pelucelli, A.; Zoroddu, M.A. Rh(I) Complexes in Catalysis: A Five-Year Trend. *Molecules* **2021**, *26*. https://doi.org/10.3390/molecules26092553.

102. Hochella, M.F.; Mogk, D.W.; Ranville, J.; Allen, I.C.; Luther, G.W.; Marr, L.C.; McGrail, B.P.; Murayama, M.; Qafoku, N.P.; Rosso, K.M.; et al. Natural, incidental, and engineered nanomaterials and their impacts on the Earth system. *Science* **2019**, *363*, eaau8299. https://doi.org/10.1126/science.aau8299.

103. Chen, J.; Hoek, G. Long-term exposure to PM and all-cause and cause-specific mortality: A systematic review and meta-analysis. *Environ Int* **2020**, *143*, 105974. https://doi.org/10.1016/j.envint.2020.105974.

104. Umair, M.; Alfadhel, M. Genetic Disorders Associated with Metal Metabolism. *Cells* **2019**, *8*. https://doi.org/10.3390/cells8121598.

105. Lachowicz, J.I.; Nurchi, V.M.; Fanni, D.; Gerosa, C.; Peana, M.; Zoroddu, M.A. Nutritional iron deficiency: the role of oral iron supplementation. *Curr Med Chem* **2014**, *21*, 3775-3784. https://doi.org/10.2174/0929867321666140706143925.

106. Maret, W.; Sandstead, H.H. Zinc requirements and the risks and benefits of zinc supplementation. *J Trace Elem Med Biol* **2006**, *20*, 3-18. https://doi.org/10.1016/j.jtemb.2006.01.006.

107. Nordberg, M.; Nordberg, G.F. Metallothionein and Cadmium Toxicology-Historical Review and Commentary. *Biomolecules* **2022**, *12*. https://doi.org/10.3390/biom12030360.

108. Krężel, A.; Maret, W. The Bioinorganic Chemistry of Mammalian Metallothioneins. *Chemical Reviews* **2021**, *121*, 14594-14648. https://doi.org/10.1021/acs.chemrev.1c00371.

109. Bernhoft, R.A. Cadmium toxicity and treatment. *ScientificWorldJournal* **2013**, *2013*, 394652. https://doi.org/10.1155/2013/394652.

110. Koedrith, P.; Seo, Y.R. Advances in carcinogenic metal toxicity and potential molecular markers. *Int J Mol Sci* **2011**, *12*, 9576-9595. https://doi.org/10.3390/ijms12129576.

# An updated overview on metal nanoparticles toxicity

Serenella Medici *, Massimiliano Peana *, Alessio Pelucelli, Maria Antonietta Zoroddu

*Department of Chemistry and Pharmacy, University of Sassari, Sassari, Italy*

| ARTICLE INFO | ABSTRACT |
|---|---|
| *Keywords:*<br>Metal nanoparticles<br>Cancer<br>Nanotoxicology<br>Metal toxicity | Although thousands of different nanoparticles (NPs) have been identified and synthesized to date, well-defined, consistent guidelines to control their exposure and evaluate their potential toxicity have yet to be fully established. As potential applications of nanotechnology in numerous fields multiply, there is an increased awareness of the issue of nanomaterials' toxicity among scientists and producers managing them. An updated inventory of customer products containing NPs estimates that they currently number over 5.000; ten years ago, they were one fifth of this. More often than not, products bear no information regarding the presence of NPs in the indicated list of ingredients or components. Consumers are therefore largely unaware of the extent to which nanomaterials have entered our lives, let alone their potential risks. Moreover, the lack of certainties with regard to the safe use of NPs is curbing their applications in the biomedical field, especially in the diagnosis and treatment of cancer, where they are performing outstandingly but are not yet being exploited as much as they could. The production of radical oxygen species is a predominant mechanism leading to metal NPs-driven carcinogenesis. The release of particularly reactive metal ions capable of crossing cell membranes has also been implicated in NPs toxicity.<br><br>In this review we discuss the origin, behavior and biological toxicity of different metal NPs with the aim of rationalizing related health hazards and calling attention to toxicological concerns involved in their increasingly widespread use. |

## 1. Introduction

Nanoscience has recently been dubbed the "big science" in consideration of the importance that the applications of this new branch of science could have for everyday life. The prefix "nano" derives from the Greek word νᾶνος "nanos", which means small in stature, referring to the fact that these particles are much smaller than most of the others. In the international metric system, their size corresponds to the factor $10^{-9}$, or $1 * 10^{-9}$ meters, indicating a diameter smaller than 100 nm [1, 2]. A very large number of chemical species with different sizes, surface areas, charges and shapes can be classified as nanoparticles (NPs).

The birth of the concept of nanotechnology is commonly traced back to the intuition of the American physicist Richard Feynman. In a now famous conference held in December 1959 at the California Institute of Technology entitled "*There's plenty of room at the bottom*", he hypothesized that in the future devices could be built by directly acting on the arrangement of atoms in matter [3]. He famously referred to the possibility of physically storing the entire contents of the British Encyclopedia on the tip of a pin.

However, the term nanotechnology was coined in 1974 by University

of Tokyo researcher Norio Taniguchi to illustrate the manipulation of atoms for the production of new materials [4], and later by Eric Drexler in 1986 in his book entitled: "*Engines of creation: the coming era of nanotechnology*", where he described nanotechnology as "*a technology that will allow us to place every atom where we want it to be*" [5].

"Nanotechnology", which can be defined as "*the manipulation of matter at the scale of atoms*" gives rise to the design and construction of many new materials with features that cannot always be easily predicted from our current experience. Within the near-limitless diversity of these materials, some happen to be toxic to biological systems, others are relatively benign, and some confer health benefits.

The peculiarity of NPs is their minute size- smaller than cells and cellular organelles, an unusual property that allows them to penetrate basic biological structures.

Particles from anthropogenic activities have existed for millennia; though humans have always been exposed to nanosized inorganic particles and other naturally occurring nanomaterials deriving from many environmental phenomena on our planet (volcanic ashes, dust storms), tiny particulate pollution has greatly increased since the Industrial Revolution due to combustion-based engine transportation and the

current growth of a global nanotechnology industry [6]. Technological development has also considerably transformed the nature of particulate contamination, increasing the proportion of nanometer-sized particles and also expanding the variety of chemical composition present. According to current epidemiological studies, a strong correlation exists between particulate air pollution levels and overall population mortality, and specifically with the incidence of various cancers and cardiovascular and respiratory diseases [7].

It is known that level of exposure, nanoparticle chemistry, size, shape, agglomeration state, and electromagnetic properties, along with human factors are variables which affect the adverse effects of NPs.

Studies carried out on animal models and humans have evidenced that macrophage clearance mechanisms in the lungs remove damaging inhaled NPs less efficiently than larger particles [1,8–10]. NPs can translocate through the circulatory, lymphatic, and nervous systems to many tissues and organs, including brain and placenta (Fig. 1). Examples of toxic effects encompass tissue inflammation and altered cellular redox balance toward oxidation, which can lead to abnormal function or cell death [11].

Although many of these chemicals have interesting peculiarities for technological applications in several fields, a rational science-based approach is needed to study harm and injury caused by these materials. In fact, current knowledge of the toxicology of 'bulk' materials may not be adequate in consistently envisaging study of 'nanotoxicity'. NPs properties are needed to be studied in detail in order to understand their mechanisms of action, acquire essential information for their sustainable development and find ways to build materials that are completely harmless to humans and the environment. The human immune system, in fact, is not programmed to recognize and therefore defend itself from particles below the micron. On the other hand, nanotechnologies are an exceptional innovation in today's society as they have the advantage of modifying the properties of matter such as electronic, optical, magnetic features and response to stimuli in "smart nanomaterials". NPs can be

incorporated into many sophisticated products enhancing the performance and increasing their commercial values [12]. Nowadays, metal-, carbon-, ceramic-, polymeric- and lipid-based NPs are applied in different biological and non-biological areas including electronics, textiles, industry, healthcare, biomedicine, environment, agriculture and food [13].

Despite some unique advantages of nanomaterial, there is growing evidence that the small size of the particles and resulting large surface area may also induce undesired side effects related to, for instance, increased reactivity with cellular targets and ultimately, toxicity [14]. Several questions regarding the safety and sustainability of nanotechnology applications in consumer and industrial products remain open [15].

Since NPs are similar in size to viruses, their absorption and transport through tissues is based on non-molecular mechanisms. There is therefore concern that standard toxicological tests may not be applicable with respect to NPs, which would compromise the effectiveness of current risk assessment procedures. It is necessary to develop reliable *in vitro* and *in vivo* protocols for the systematic toxicity evaluation of any given NP based on mode of uptake (inhalation, ingestion, injection, and permeation), chemical characteristic and composition, size and shape, concentration, charge, solubility and many other characteristics. Further research is needed on their translocation inside the body and subsequent biological and toxicological effects for humans and any other living systems. The safety screening of NPs to evaluate their possible toxicity and understand the underlying mechanisms of biological interaction is a critical step needed to prevent severe future harmful effects and to design biocompatible (safe-by-design) NPs.

As awareness on the toxicity of nanomaterials grows among scientists and producers, in this review we discuss the origin, activity and biological toxicity of different metal NPs with the aim of rationalizing related health concerns.
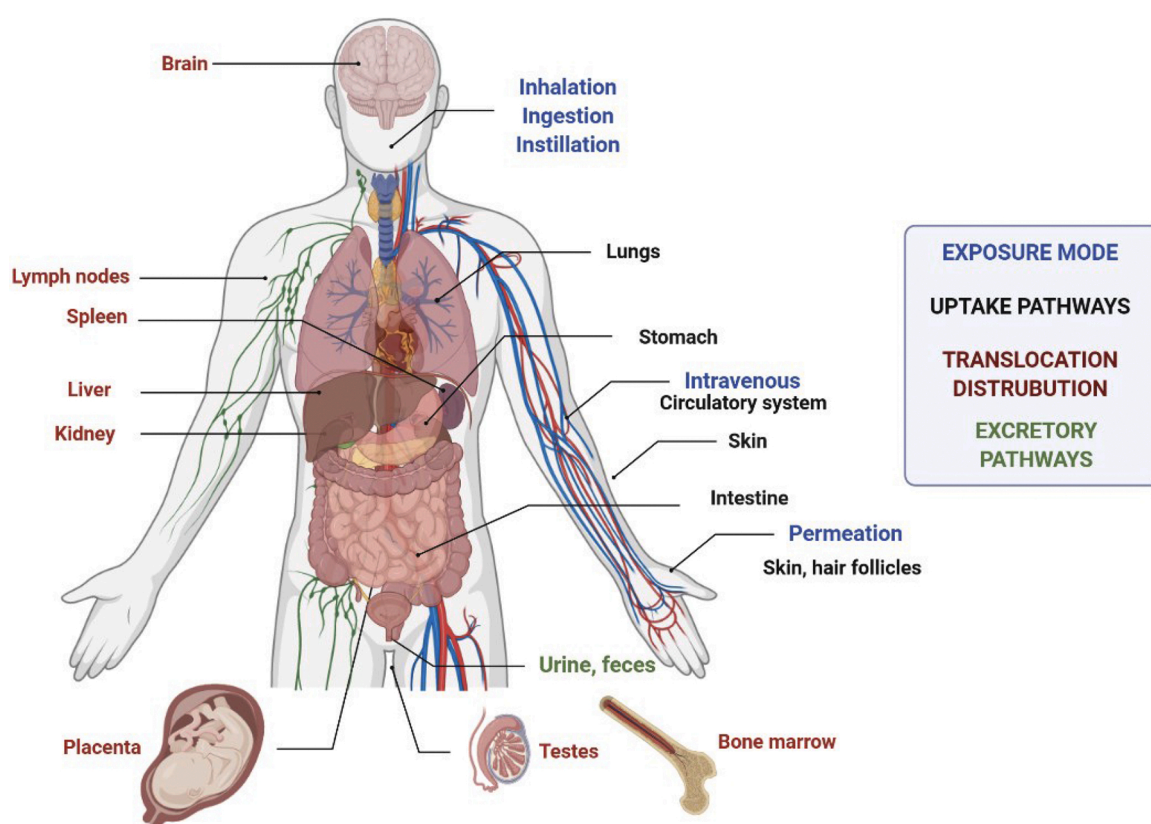


**Fig. 1.** Exposure routes, ways of uptake, translocation and distribution of NPs into human body.

## 2. Nanoparticles: origin, physicochemical properties

### 2.1. Origin

A plethora of substances with different properties and shapes can be categorized as nanomaterials.

They can be produced by natural phenomena, such as volcanic dust emissions or biological processes. But NPs can have an anthropogenic origin depending by human industrial, medical or domestic activities, high temperature processes, incineration of solid waste, combustion of fossil fuels or traffic emissions, melting and welding processes (metal particles), as well as by nanotechnology facilities, creating nanoscale products [6,16]. A complex NP mixture can also be formed at military sites as a result of high temperature bomb explosions, which create fine suspensions of particles of different types and structures [17,18]. Inorganic and metallic powders so produced are often insoluble and non-biodegradable; their small size allows them to be transported through the whole environment: water, air and soil.

### 2.2. Physicochemical parameters and properties

NPs exhibit peculiar chemical, physical, optical and biological properties, which are different from those present in materials of conventional size (bulk material).

From microscale (1.000 nm) and beyond, the properties of matter are described by classical physics whereas from Angstrom dimensions (0.1 nm) and below, physical properties are understood in terms of quantum mechanics. Consequently, the properties of NPs - which fall on the border between these two fundamental theories used to describe matter - are strictly dependent on their exact dimensions. The NPs' peculiarity comes from their nanoscale size, which determines their unique properties.

Size determines the amount of surface area, which is critical in controlling the reactivity of matter. In fact, size determines the area involved in the nanoparticle peculiar action: the smaller the particles, the greater the surface to volume ratio and, generally, the more magnified its effects. For an example, when the particle's size is around 30 nm, about 10 % of its atoms or molecules are expressed on the surface, while when the particle is sized from 10 to 3 nm, the ratio of atoms or molecules on the surface increases to 20–50 %, respectively [19]. The number of atoms or molecules on the surface determines their specific reactivity, and this is the key to understand the chemical and biological properties of a nanomaterial. The nanoscale factor appears to be responsible for the risks associated with this form of matter. Though, the increased biologic activity of NPs, due to their greater number of available specific sites of interaction and reactivity can be exploited for desirable properties (antioxidant and antibacterial activity, delivery of diagnostic probes, drugs and theranostics), this property can also lead to undesired side effects such as induction of oxidative stress, cellular dysfunction and toxicity, which are not mutually exclusive. These concerns can be summarized in this way: smaller is not always better, and nanotechnology can yield nanotoxicology. Due to their specific design, engineered NPs possess physicochemical properties that distinguish them from other natural or accidentally human-produced particulates. These properties, such as controlled size, shape, mass, chemical composition, surface charge, agglomeration and aggregation states, active surfaces and so forth, can determine their biological fate. Different combinations of physicochemical parameters, including dimensionality (1D, 2D and 3D), morphology (spherical, cubic, wires, tubes, etc.), composition (homogeneous or heterogeneous), uniformity and agglomeration state (isometric, inhomogeneous, dispersed, agglomerated) have been designed [1].

## 3. Safe or unsafe: the two faces of nanotechnology

The exponential growth of literature published on NPs is indicative of the emerging importance and relevance of research in nanotechnology. This rapidly developing field promises a plethora of potentially useful applications, but also poses many questions about possible environmental and biological risks involved in the use of NPs. A correlation between exposure and incidence of cancer of the respiratory tract (lung and nasal cancer) has been demonstrated by epidemiological studies carried out on miners and refinery workers exposed to metal particles [20,21], and tiny particles have been shown to sicken and kill workers in plants using nanotechnology [22–24]. A study by Oberdorster *et al.* showed that TiO$_2$ NPs of 20 nm, when instilled intratracheally into rats and mice, induced a much greater pulmonary neutrophil response (as the indicator of inflammation) than 250 nm TiO$_2$ NPs; with dose expressed as particle surface area the same dose response relationship was obtained for both the particles. This indicates that particle surface area seems to be a more appropriate dosimetry for comparing effects of different-sized particles provided they are of the same chemical structure (in this case anatase, TiO$_2$) [19].

The prevailing hypothesis in toxicology according to which the absorbed concentration of a substance (the dose) is directly linked to its toxicity is not valid with regard to nanotoxicology, for which a new paradigm appears to regulate the bioactivity of nanoscale materials. Mass does not seem to be the most important factor regarding biological effects respect to the number, size, active surface, shape and exposure modes of NPs.

The development of sustainable technology is critically linked to short-term and long-term safety. A meaningful example of this issue has been shown in an *in vivo* study of the potential long-term toxicity of gold NPs (AuNPs) in *Drosophila melanogaster* [25]. The results highlighted a significant genotoxic effect potentially transmissible to the descendants. The outcomes of AuNPs exposure were mutations (crooked or broken wings, compromised chests and multiplied number of eyes, modifications in body shape), decreased fertility, shortened life cycle and tissue oxidation. When these aberrant specimens were crossed with normal ones, the mutations recurred in the offspring, a sign that the toxic effects of these selected AuNPs were long-termed. Though *Drosophila melanogaster* cannot be considered a realistic human model since it is only similar in the digestive system but not in the respiratory one, this study highlighted the need to develop biocompatible nanomaterials without dangerous effects on living systems (human health and environment) and increase awareness of the risks associated with the use of nanomaterials whose safety has not been adequately assessed. The discussion on nanosafety, consequently, will focus on an evaluation of NPs' toxicology, ecotoxicology, exposure and risk assessment, mechanisms of interaction and toxicity protocols standardization.

## 4. Toxicological assessments of NPs

Several variables are needed to be considered in the critical evaluation of a selected NP in order to get reliable results thereby reducing over-emphasized toxicity or safety conclusions inherent in a non-rigorous study [26].

### 4.1. Physicochemical assessment

Delineating a physicochemical characterization of the NP under investigation is a mandatory first step often neglected in a huge amount of literature, along with the characterization of the NP's morphology, size, shape, Zeta potential, density and agglomeration or aggregation propensity. Moreover, nanomaterial characterization requires information about labelling, drug loading, release and targeting together with other eventually individual properties specific for the NPs under study [27].

Moreover, potential contamination effects (i.e. during synthesis, storage and sample preparation) or interferences with the testing media components are critical factors that could lead to potential false positive or erroneous results. The effects of the solvent (pH, temperature, ionic

strengths) and dispersion agents were not often carefully considered in early studies. Dosimetry remains a factor of uncertainty since the dose-response relation is no longer valid at the nanoscale level, as already discussed. Several methods have been described for the characterization of the physicochemical properties of manufactured nanomaterials; these techniques have also been applied to investigation of unintentionally produced NPs [28–30]. Validated protocols and standard characterization methods for NPs are a necessary requisite for inter-laboratory comparability and reproducible risk assessment [29]. Important progress has been made in terms of standardizing and validating methods for detecting NPs' intrinsic properties, such as particle shape, specific surface area, density, crystal structure, size distribution, composition and electromagnetic properties. However, characterization methods for extrinsic properties, which are medium dependent, still need to be standardized and validated. These include the NP's effective density, hydrodynamic size distribution, dustiness (a measure of dust inhalation hazard), aggregation rate, surface affinity, dissolution, ROS generation and biodurability, properties that are strictly dependent on the biological system investigated. Logically, studies conducted using simple matrices are limited in the actual evaluation of the safety or toxicity of a selected NP [31]. A number of interconnected processes such as dissolution, transformation, aggregation or disaggregation, straining, deposition or mobilization, and diffusive transport, govern the environmental fate and behavior of NPs and their subsequent spreading, accumulation, bioavailability and effects on different marine, aquatic or terrestrial biosystems [32,33]. Upon exposure to biological media, NPs, as hybrid materials, undergo various environmental changes that could govern their cellular uptake and fate [33]. This implies that the toxicity of selected NPs could be different depending on the system in which they are embedded and even on the individual organism they interact with.

For example, NPs administered into the organism once in contact with the biological environment (such as blood) will interact with its various constituents, forming a spontaneous self-assembly and stratification of different molecules on the NP's surface, that will strongly influence the NPs behavior and fate. In the case of proteins, the so-called "protein corona" will form [34].

### 4.2. Biological assessment

*In vitro* tests are particularly important for fast and low-cost toxicological evaluation of a selected NP though they are mined by several limitations. For instance, one is related to the dose required to get quantifiable biological effects, which is also strictly dependent on the dissolution, diffusion, dispersion, sedimentation and agglomeration of NPs [35]. Due to the great variability of NPs' physicochemical properties, the difference between the administered and the cellular dose can vary by several orders of magnitude when comparing different *in vitro* systems. In addition, an overdose of NPs in *in vitro* tests (and *in vivo* too), can lead to misreading of the results. Another limitation of *in vitro* essays is associated with their low translational value, as these simplified models do not necessarily predict *in vivo* effects. However, since engineered NPs are exponentially increasing on the market and because it is necessary to reduce high-cost and ethically concerning screenings involving experimental animals, *in vitro* tests are the most used methods for preliminary assessment of a nanoparticle's toxicity. These methods allow one to obtain information on the NP's ability to interfere with or activate cellular proliferation, apoptosis, necrosis, oxidative stress and DNA damage [36]. A detailed experimental protocol should be reported in order to obtain comparable and reproducible studies [37].

Several different organisms are normally considered for *in vivo* experiments. From simple organisms such as bacteria, micro crustaceans (i.e. *Daphnia magna*), microalgaes (i.e. *Chlorella vulgaris* and *Raphidocelis subcapitata*), zebrafish, fruit's fly (*Drosophila melanogaster*), worms (i.e. *Caenorhabditis elegans*) to a more complex organisms such as fishes (i.e. *Oryzias latipes)*, oysters, pigs, mice and rats. Each of these *in vivo* models is mined by advantages and limitations. Parallel to the increase in the

complexity of a selected organism, is an increase in the subsequent predictivity and translational value to humans. The chief limitations lie in progressively expensive and time-consuming tests and ever more stringent regulations and ethical constraints.

## 5. Main mechanisms of metal NPs toxicity

The main mechanisms that regulate NPs toxicity are undoubtedly associated with oxidation stress leading to inflammation, genotoxicity and major cellular organelle dysfunction (Fig. 2). Oxidative stress results from the formation of free radicals (reactive oxygen species, ROS, and reactive nitrogen species, RNS), caused by the activation of oxidative enzymatic pathways [38]. Under prolonged oxidative stress conditions, the relative unbalance or failure of the intracellular free radicals scavenging mechanism's defense capability, leads to damage in proteins, DNA and lipid components, mitochondria and endoplasmic reticulum dysfunctions and eventually to apoptosis or ferroptosis [39–42].

The principal cause of oxidative stress can be linked to some metal NPs' intrinsic characteristics, as well as their ability to generate ROS as part of cellular response to NPs invasion. For instance, ROS generation, such as superoxide anion radical ($O_2^-$), hydroxyl radical (˙OH), hydroxyl ion ($OH^-$), hydrogen peroxide ($H_2O_2$), has been implicated in the bactericidal action of metal oxide NPs [43–48]. ROS can also be generated as a result of the presence of defects in metal oxide species, such as oxygen vacancies [49,50].

Moreover, free radical intermediates can be present on the surface of the NPs, as well as in transition metal contaminants used as catalysts in case of engineered non-metal NPs. In case of functionalized NPs, the oxidative effect can also be due to redox active groups on the NPs surface [51]. Inflammation is a consequence of the body's defense system against external contaminants, including pathogen (bacterial or viral) infections. However, NPs, which have similar size of viruses, are able to trigger activation of macrophages, neutrophils and dendritic cells that will secret a number proinflammatory cytokines such as tumor necrosis factor-α (TNf-α), interleukins (IL) and growth factor-β1 (TGF-β1), leading to a cascade of immune reactions and potentially dangerous consequences such as pulmonary inflammation and fibrosis [52–55].

It is important to note that NP-related oxidative stress could be a result of particle interaction with the cell even when there is not direct production of ROS from the NPs [56,57]. The action of NPs in mitochondria may result in dysregulation of the respiratory chain and disturbance of normal cellular ROS signaling, as well as ROS generation or detoxification, thus causing indirect oxidative stress, with effects on programmed cell death [58,59].

The effects of NPs on the endoplasmic reticulum (ER) cause so-called ER stress with impairment of the protein folding processes, which can influence cell fate and development of cancer phenomena [60]. Disruption of normal cell structure and function will result in chronic key organ events and subsequent whole organism responses such as cancer, cardiovascular disease, pulmonary fibrosis, neurotoxicity and inflammation [61–63].

However, the toxicity of some nanomaterials cannot be explained by oxidative stress due to ROS production [64]. Other mechanisms involved in NP toxicity include the release of metal ions, the penetration of the cell envelope and the disruption of the cellular membrane [65, 66]. Metal ions release can occur when metal NPs are partially soluble, and this kind of toxicity has been extensively reported for engineered zinc oxide NPs (ZnO NPs) [67,68] as well as for unintentionally produced carcinogenic nickel sulfide NPs (NiS NPs) [69]. NiS NPs phagocytized by lung cells following inhalation of ultra-fine nickel containing dust are incorporated into the acidic vacuoles and subsequently dissolved in the cytoplasm. The continuous release of nickel ions will cause a selective damage in the nucleus, such as mutation, chromosomal aberrations, DNA damage, impairment of mechanism of DNA repairing and histones modifications leading to cellular transformation and carcinogenesis [70,71]. The so-called "Trojan horse" effect allows a
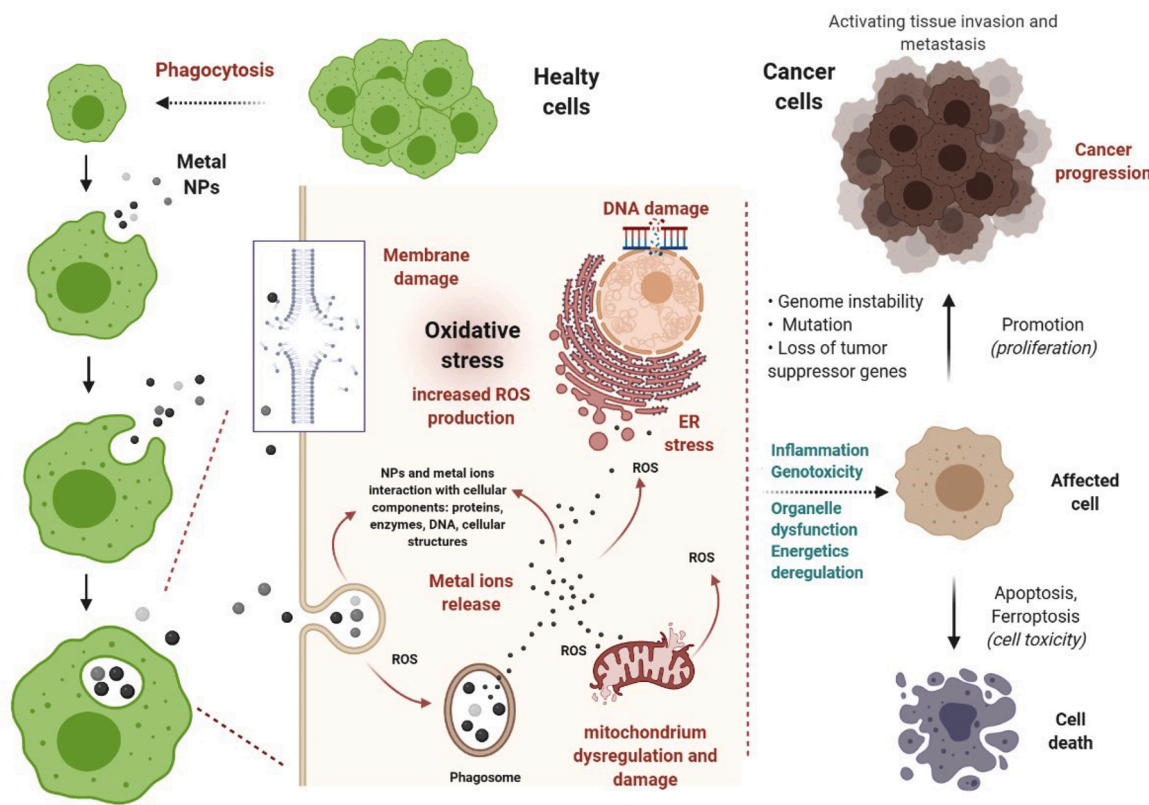
Fig. 2. Oxidative stress, inflammation and genotoxicity from phagocytosed metallic NPs leading to cell death and cancer promotion.

release of large amounts of metal ions within the cell, leading to cytotoxic consequences depending on the peculiar physicochemical properties of specific metal ions such as their redox properties. Moreover, characteristics such as oxidation state, hard-soft character and solubility, will influence the metal ion speciation in cellular environment and their interaction with biological targets [72]. In some cases, toxicity related to the release of metal ions (in particular in case of CuO NPs) can be time dependent, with initial response due to NPs themselves, and response beyond 24 h determined by the dissolved metal ions [73]. In summary, metal ions release is one of the most common recognized causes of toxicity when dealing with metal NPs that can cause genotoxic responses [74–77].

### 5.1. NPs toxicity in cancer cells

Nanotechnology finds application in cancer treatment, as a new way of therapy, which is being deeply investigate by the biomedical field. This is due to the properties of nanomaterials, as we discussed above, and to the peculiar physiology of the cancer cells. The latter show an enhanced permeability and retention effect to nanometric compounds, which tend to accumulate in the tumor sites. In this way, nanomedicine can use NPs as carriers to deliver theranostic agents into cancer cells. The microenvironment of the tumor cell shows, above other characteristics, a more acidic pH, which can be exploited to synthetize pH-sensitive smart NPs [78]. Furthermore, tumor cells overdevelop vascular tissue, therefore the synthesis of specific NPs that passively or actively target overexpressed vascular molecules, such as vascular endothelial growth factor (VEGF), integrin αvβ3 and vascular cell adhesion molecule-1 could be a way to reach the tumor microenvironment and an anticancer treatment strategy [78]. The combination of this with a lack of lymphatic drainage (typical of cancer cells) results in a prolonged retention time and improved nano-drug action in the vascular system of the tumor tissue leading to the induction of cancer cell death [79,80].

## 6. Toxicological effects of some widely used selected metal NPs

### 6.1. Zinc oxide NPs

Zinc oxide NPs (ZnO NPs) are one of the most used NPs in industry (electronics, textiles, rubber), in medicine (as antimicrobial and anti-inflammatory agents), in cosmetics, for bioimaging and drug delivery, and in other applications, including photocatalysis [81,82]. This leads to a high rate of exposure for humans, who are frequently in contact with these NPs. It has been demonstrated that they can enter the organism through different pathways, such as the respiratory and digestive tracts, as well as through dermal and parenteral routes [83]. They can thus be a threat for the human organism because of their potential to reach any organ or tissue. ZnO NPs can have potential molecular effects such as decrease in cellular viability, loss of membrane integrity or activation of cell apoptosis as demonstrated via *in vitro* and *in vivo* tests [84,85]. It is unclear how these NPs can develop their toxicity, but it has been indicated that different variables play a role in this effect. Firstly, cytotoxicity has been found to be shape- and size-dependent, as it has been noted that spherical nanoparticles sized about 40 nm exhibit higher toxicity than larger sized nanospheres; furthermore, nanorods are even more toxic than spherical ZnO NPs [86]. A second parameter which affects the potential toxic effect is the surface composition; this has been observed in relation to leukemia cells [87]. Another mechanism proposed involves the strong oxidative stress related to an over-release of zinc ions from continuous NPs dissolution in the lung of rat exposed to ZnO NPs by intratracheal instillation [88]. It has been observed that the concentration of $Zn^{2+}$ ions is significantly higher in medium exposed to ZnO NPs compared to ones exposed to Zn powder [89].

The most toxic effect of ZnO NPs in humans occurs in the respiratory system, where NPs can pass into lung tissue through alveolar epithelial cells and trigger a severe pulmonary inflammatory response [90–92]. It is possible to observe an increased secretion of IL-8 when the tissue is treated with 5 μg/mL solutions or higher. IL-8 is a chemotactic cytokine

attracting neutrophils, eosinophils, and T-lymphocytes, thus playing a role in pulmonary inflammations [93].

## 6.2. Titanium oxide NPs

Similar results were obtained for TiO$_2$ nanoparticles, which means that metal oxide NPs can play a critical role in immunological reactions causing the release of inflammatory mediators [94]. TiO$_2$ NPs are widely used as a sunscreen component, in cosmetics, as food, plastic and drug colorants, in inks and paints but also in agriculture, waste water treatment and many other areas [95]. However, TiO$_2$ NPs have also been shown to promote generation of ROS and cause oxidative stress, interfering with cell metabolism and damaging DNA [96]. TiO$_2$ and SiO$_2$ NPs, 35 nm and 70 nm in size respectively, can cause pregnancy complications when injected intravenously into pregnant mice [97]. However, a toxicological profile of TiO$_2$ NPs has not been fully defined; more studies are urgently needed in consideration of the prospects and applications TiO$_2$ can have in the medical field [98].

## 6.3. Silver NPs

Silver nanoparticles (AgNPs) are extensively used in a variety of fields, mostly because of their well-known effects as antibacterial and antiviral agents. Their usage can be direct, such as for treating infection in case of open wounds, eczema, and acne [99], or indirect, as antimicrobial agents in toothpastes, deodorants, sanitizer sprays, gels, disinfectants and soaps [100,101]. AgNPs are also used for packaging and storage of certain foods, to increase their shelf life. Although they have all these useful applications, AgNPs can easily penetrate the skin when the functional barrier is disrupted, and cause cellular damage and cytotoxicity [102]. The toxicity of silver NPs seems to be strictly related to their concentration, but it can vary for different species. Starting from simpler organisms, for Gram-positive and Gram-negative bacteria the MIC is respectively 0.9 and 0.7 µg/mL [103]. In case of organisms with higher complexity, the LC50 of AgNPs is higher, for example, the LC50s detected in the larvae and pupae stage of *Aedes aegypti* were about 3.5 and 17.7 ppm, respectively [104]. Therefore, we can hypothesize there is an inverse proportion between the toxicity of silver NPs and the complexity of the organisms being studied.

It is also important to consider that these NPs tend to agglomerate once they come into contact with biomolecules in solution. The agglomeration property drastically changes their physicochemical characteristics and, accordingly, (depending on the level of agglomeration), their toxicity [105]. Moreover, AgNPs readily ionize in aqueous solution becoming highly reactive. By increasing the dissolution of AgNPs, more Ag$^+$ ions become available to cause potential toxic effects in the environment. One of the toxic effects that could be developed by AgNPs' cellular dissolution is the interaction with NADH dehydrogenase from the respiratory chain resulting in the uncoupling of respiration from ATP synthesis [106]. These two properties (ionization and aggregation) lead to another issue: in an environmental condition with high ionic strength, both ionization and aggregation are enhanced. While an increased ionization leads to increased potential toxicity, increased aggregation has the effect of reducing toxicity. This will seem clearer by considering that the aggregation reduces the surface area for dissolution, thereby making fewer Ag$^+$ ions available on the surface.

## 6.4. Gold NPs

Gold is a metal known to be nontoxic, as it is highly unreactive and chemically inert by nature. Because of these peculiar characteristics, gold has found application in different fields, such as clinical medicine, chemistry, and industrial processes. It is widely used as a catalyst in the form of gold salts and complexes [107], or to treat rheumatoid arthritis in clinical settings [108,109]. When we go down to the nanometer scale, gold continues to exhibit unique properties, such as tunable size, easy

synthesis and modification, and diverse morphologies including spheres, rods, stars. AuNPs can thus easily adapt to many roles in the biomedical field, being widely studied as multifunctional nanoplatforms for cancer detection, diagnosis and treatment [110,111]. Therefore, they are potentially outstanding theranostics (a combination of the words "therapy" and "diagnostics"), since they are able to exert direct anti-cancer actions or can be used to deliver chemical drugs to target cancer cells upon proper derivatization, serve as bio-imaging agents for precision diagnosis and tumor localization, and behave as sensors for biomarkers and cancer cells [111–113].

Despite all these remarkable properties and possibilities of application, AuNPs are rarely translated into clinics, due to the suspect they can also be toxic to humans, at least in certain formulations or circumstances [114]. For these reasons, it is necessary to clarify once and for all their safety and the exact limits of their applications, in order to avoid any potential *in vivo* adverse effect [115].

The first and most important parameter to consider when evaluating the effects of Au NPs is the particle's size. This property determines endocytosis effectiveness, a key process deeply linked to the localization and accumulation of NPs inside the cell [116]. Particle size is usually between 1 and 200 nm, which permits cell uptake with ease: the entire process of endocytosis is mediated by nonspecific adsorption of serum proteins onto the gold's surface (formation of already cited "corona"), followed by a receptor-mediated endocytosis pathway [117]. Several studies have revealed that particle uptake is easier and more efficient when the particle's diameter is around 50 nm, while NPs of both smaller and larger diameters have more difficulties in cellular internalization [117]. Another proof of the deep link between toxicity and particle size has been presented by Pan *et al.* in their studies on NPs in the 0.8 nm–15 nm diameter range. They found that AuNPs with 1.4 nm diameters were the most cytotoxic, with IC50 value ranging from 30 mmol/L to 46 mmol/L, while other AuNPs with slightly larger diameters were 3–5 times less toxic and bigger NPs (up to 15 nm) were nontoxic [118]. In another study it was found that 45 nm AuNPs are more toxic than smaller ones, as they irreversibly damage vacuoles being released into the cytoplasm, thus disrupting many cell functions resulting in cell death [119].

By analyzing the literature reported to date about the correlation between size and toxicity of gold nanoparticles, no clear conclusion can be drawn, since the results are often in contradiction one another, as the safety of a particular AuNP seems related not only to its size, but also to its shape and, especially, its coating. Regarding the application of AuNPs for therapeutic or diagnostic purposes, this often involves functionalization of nanomaterials with biological fragments, such as peptides, ligands, or other compounds. The aim of this process is to improve the biocompatibility and achieve very specific purposes, which can be the targeted delivery of a drug or the co-delivery of a molecule to a disease site [111]. One example of this can be found in nanorod-shaped particles, since CTAB (cetyltrimethylammonium bromide) is the most used structure-directing agent in the synthesis. This creates a positively charged CTAB bilayer on the nanorods' surface, which causes of toxicity [120,121]. It has been proven that coating nanorods with PEG leads to improved biocompatibility, so it is vital to highlight the importance of the coating process and of the coating itself. Among different coating agents, PEG is considered to be the first choice to decrease toxicity, as it reduces nonspecific binding of biological molecules to surfaces and avoids macrophage recognition and phagocytosis [122]. AuNPs' toxicity can be enhanced by sodium citrate, often present on the surface of NPs since it is generally used in the chemical reduction of the metal salts, and in the stabilization of the resulting nanoparticles [123]. To circumvent capping or coating toxicity, biologically ("green") synthesized AuNPs (as well as many other metal or metal-based NPs) can be employed. This ecofriendly strategy for the preparation of NP with high biocompatibility, low toxicity and high biological activity towards either cancer or bacterial cells, exploits Au salts reduction carried out by fluids and extracts obtained from a series of natural sources, such as plants (any part),

bacteria, fungi and other microorganisms [124,125]. Often, "organic" wastes have been employed, for a "greener" preparation. Among the biomolecules naturally present in these extracts, reducing agents like alkaloids, terpenoids, phenolic compounds, proteins, enzymes, sugars, vitamins, etc. can be involved in the mechanism of AuNPs formation [126]. They often provide as well a capping for these NP, by deposition onto their surfaces, and this also allows for stabilization. Nanoparticles prepared in this way demonstrated an easier internalization in the target cells and higher cytotoxicity, being at the same time more biocompatible and less toxic to the host organism [127].

The final parameter to be considered, as previously mentioned, is the shape of the NPs, as it can influence their toxicity towards the cell. It has been observed that hexapod-like particles are less toxic than rods and cages [128]. These results are strongly linked with the uptake of AuNPs: e.g., spheres are taken up more efficiently than nanorods [129]. It has been demonstrated that spherical NPs undergo the fastest internalization, followed by cubic NPs, then rod shaped NPs and disk-like NPs. This characteristic seems to be linked to the number of faces of the NPs and to the surface charge, both properties that can lift the uptake rate up to 60 orders of magnitude, leading to an augmented toxicity rate [130]. AuNPs nanoparticles toxicity is related to the same mechanisms behind their anticancer and antibacterial activity, that are mainly linked to ROS generation and subsequent cell apoptosis [131–133].

## 7. Conclusions

Due to the remarkable properties of nanoparticles, nanotechnology is becoming ever more present in our world. Apart from industrial and technological applications, what is raising concern is the presence of NPs in consumer products increasingly available to a growing number of customers. This significantly increases human beings' exposure to substances that are new to our "environment" in terms of composition, dimension and properties. In addition to this, the short time elapsed since widespread use of nanomaterials began (less than 20 years) is not enough to ascertain long term effects on the body or to give rise to any kind of "adaptation". The lack of large epidemiological studies on this matter is surely a hurdle along the path towards full comprehension of NPs' safety or toxicity. An interesting project was proposed to keep count of new consumer products containing nanomaterials as they appear on the market. Unfortunately, the database was only updated until 2015, with an estimated 2000 products logged for that year [134]. The figures were interesting: 54 products in 2005, 1012 in 2010, 1814 from 622 different companies in 32 countries in 2013. In that year, most of these products were dedicated to health and fitness (762 products, 42 %), and NPs were also introduced as antimicrobial and antifungal agents, as well as in dietary supplements. Silver was the most used nanomaterial (435 products, 24 %) for its antibacterial properties. Another inventory is kept by the Danish government (https://nanodb. dk/en/). The database is developed via data collection and scientific assessments of the nanomaterials used in various consumer products. The NanoRiskCat categorization is also carried out. The Nanodatabase is continuously updated as new data appears on the scientific stage. At the moment, it counts more than 5000 products (5.157, exactly). It should be mentioned that most of the time customers are not even aware that what they have bought contains nanomaterials, so there is no real awareness regarding the exposure to NPs in everyday life.

Data collected in scientific studies seems contradictory, rendering much research inconclusive. This is due to the fact that too many factors are involved in NP toxicity (size, shape, composition, coating, conjugation, dispersibility, concentration, etc.), so that each and every NP has its whole other story and represents a unique case. Moreover, animal models appear to be an inadequate avenue to study NP exposure in humans not only due to ethical constraints, but also because laboratory conditions do not represent real exposure and uptake situations; results can therefore be largely overestimated or otherwise misleading. A standard method for the assessment of safety in NPs should therefore be established, in order to compare data in a significant, thorough manner. Moreover, new animal models and experiments should be designed for proper evaluation of toxicity in different simulations of exposure. This is one of the main limitations for the translation of therapeutic nanomaterials in clinical settings. These setbacks in the application of nanotechnology are a barrier to the development of new, innovative and effective treatments for a number of pathologies with terribly increasing incidence, particularly cancer.

## Transparency document

The Transparency document associated with this article can be found in the online version.

## Declaration of Competing Interest

The authors declare that there are no conflicts of interest

## References

[1] M.A. Zoroddu, S. Medici, A. Ledda, V.M. Nurchi, J.I. Lachowicz, M. Peana, Toxicity of nanoparticles, Curr. Med. Chem. 21 (33) (2014) 3837–3853, https://doi.org/10.2174/09298673216661406011162314.

[2] C.P. Poole Jr, F.J. Owens, Introduction to Nanotechnology, John Wiley & Sons, 2003.

[3] R.P. Feynman, There's Plenty of Room at the Bottom, Engineering and Science magazine, California Institute of Technology, Los Angeles, 1960.

[4] N. Taniguchi, On the basic concept of nanotechnology, Proceedings of the International Conference on Production Engineering (1974) 18–23.

[5] K.E. Drexler, Engines of Creation: The Coming Era of Nanotechnology, Anchor books, New York, NY, USA, 1986.

[6] M.F. Hochella, D.W. Mogk, J. Ranville, I.C. Allen, G.W. Luther, L.C. Marr, B. P. McGrail, M. Murayama, N.P. Qafoku, K.M. Rosso, N. Sahai, P.A. Schroeder, P. Vikesland, P. Westerhoff, Y. Yang, Natural, incidental, and engineered nanomaterials and their impacts on the Earth system, Science 363 (6434) (2019), eaau8299, https://doi.org/10.1126/science.aau8299.

[7] J. Chen, G. Hoek, Long-term exposure to PM and all-cause and cause-specific mortality: a systematic review and meta-analysis, Environ. Int. 143 (2020), 105974, https://doi.org/10.1016/j.envint.2020.105974.

[8] R. Nho, Pathological effects of nano-sized particles on the respiratory system, Nanomedicine 29 (2020), 102242, https://doi.org/10.1016/j.nano.2020.102242.

[9] E. Frohlich, S. Salar-Behzadi, Toxicological assessment of inhaled nanoparticles: role of in vivo, ex vivo, in vitro, and in silico studies, Int. J. Mol. Sci. 15 (3) (2014) 4795–4822, https://doi.org/10.3390/ijms15034795.

[10] D.E. Schraufnagel, The health effects of ultrafine particles, Exp. Mol. Med. 52 (3) (2020) 311–317, https://doi.org/10.1038/s12276-020-0403-3.

[11] G. Crisponi, V.M. Nurchi, J.I. Lachowicz, M. Peana, S. Medici, M.A. Zoroddu, Chapter 18 - Toxicity of nanoparticles: etiology and mechanisms, in: A. M. Grumezescu (Ed.), Antimicrobial Nanoarchitectonics, Elsevier, 2017, pp. 511–546, https://doi.org/10.1016/B978-0-323-52733-0.00018-5.

[12] S. Gottardo, A. Mech, J. Drbohlavova, A. Malyska, S. Bowadt, J. Riego Sintes, H. Rauscher, Towards safe and sustainable innovation in nanotechnology: state-of-play for smart nanomaterials, NanoImpact 21 (2021), 100297, https://doi.org/10.1016/j.impact.2021.100297.

[13] G. Martinez, M. Merinero, M. Perez-Aranda, E.M. Perez-Soriano, T. Ortiz, B. Begines, A. Alcudia, Environmental impact of nanoparticles' application as an emerging technology: a review, Materials (Basel) 14 (1) (2020), https://doi.org/10.3390/ma14010166.

[14] K. Grieger, J.L. Jones, S.F. Hansen, C.O. Hendren, K.A. Jensen, J. Kuzma, A. Baun, Best practices from nano-risk analysis relevant for other emerging technologies, Nat. Nanotechnol. 14 (11) (2019) 998–1001, https://doi.org/10.1038/s41565-019-0572-1.

[15] W. Najahi-Missaoui, R.D. Arnold, B.S. Cummings, Safe nanoparticles: are we there yet? Int. J. Mol. Sci. 22 (1) (2020) https://doi.org/10.3390/ijms22010385.

[16] G. Lespes, S. Faucher, V.I. Slaveykova, Natural nanoparticles, anthropogenic nanoparticles, where is the frontier? Front. Environ. Sci. 8 (71) (2020) https://doi.org/10.3389/fenvs.2020.00071.

[17] M.A. Zoroddu, S. Medici, M. Peana, V.M. Nurchi, J.I. Lachowicz, F. Laulicht-Glickc, M. Costa, Tungsten or wolfram: friend or foe? Curr. Med. Chem. 25 (1) (2018) 65–74, https://doi.org/10.2174/0929867324666170428105603.

[18] A. Faa, C. Gerosa, D. Fanni, G. Floris, P.V. Eyken, J.I. Lachowicz, V.M. Nurchi, Depleted uranium and human health, Curr. Med. Chem. 25 (1) (2018) 49–64, https://doi.org/10.2174/0929867324666170426102343.

[19] G. Oberdorster, E. Oberdorster, J. Oberdorster, Nanotoxicology: an emerging discipline evolving from studies of ultrafine particles, Environ. Health Perspect. 113 (7) (2005) 823–839, https://doi.org/10.1289/ehp.7339.

[20] Z. Zhang, S. Weichenthal, J.C. Kwong, R.T. Burnett, M. Hatzopoulou, M. Jerrett, A. van Donkelaar, L. Bai, R.V. Martin, R. Copes, H. Lu, P. Lakey, M. Shiraiwa, H. Chen, A population-based cohort study of respiratory disease and long-term

exposure to Iron and copper in fine particulate air pollution and their combined impact on reactive oxygen species generation in human lungs, Environ. Sci. Technol. 55 (6) (2021) 3807–3818, https://doi.org/10.1021/acs.est.0c05931.

[21] R.L. Prueitt, W. Li, Y.C. Chang, P. Boffetta, J.E. Goodman, Systematic review of the potential respiratory carcinogenicity of metallic nickel in humans, Crit. Rev. Toxicol. 50 (7) (2020) 605–639, https://doi.org/10.1080/10408444.2020.1803792.

[22] D. Pelclova, V. Zdimal, P. Kacer, Z. Fenclova, S. Vlckova, K. Syslova, T. Navratil, J. Schwarz, N. Zikova, H. Barosova, F. Turci, M. Komarc, T. Pelcl, J. Belacek, J. Kukutschova, S. Zakharov, Oxidative stress markers are elevated in exhaled breath condensate of workers exposed to nanoparticles during iron oxide pigment production, J. Breath Res. 10 (1) (2016), 016004, https://doi.org/10.1088/1752-7155/10/1/016004.

[23] P.T. O'Shaughnessy, Occupational health risk to nanoparticulate exposure, Environ. Sci. Process. Impacts 15 (1) (2013) 49–62, https://doi.org/10.1039/c2em30631j.

[24] V. Murashov, J. Howard, Risks to health care workers from nano-enabled medical products, J. Occup. Environ. Hyg. 12 (6) (2015), https://doi.org/10.1080/15459624.2015.1006641. D75-85.

[25] G. Vecchio, A. Galeone, V. Brunetti, G. Maiorano, L. Rizzello, S. Sabella, R. Cingolani, P.P. Pompa, Mutagenic effects of gold nanoparticles induce aberrant phenotypes in Drosophila melanogaster, Nanomedicine 8 (1) (2012) 1–7, https://doi.org/10.1016/j.nano.2011.11.001.

[26] L.J. Johnston, N. Gonzalez-Rojano, K.J. Wilkinson, B. Xing, Key challenges for evaluation of the safety of engineered nanomaterials, NanoImpact 18 (2020), 100219, https://doi.org/10.1016/j.impact.2020.100219.

[27] M. Faria, M. Bjornmalm, K.J. Thurecht, S.J. Kent, R.G. Parton, M. Kavallaris, A.P. R. Johnston, J.J. Gooding, S.R. Corrie, B.J. Boyd, P. Thordarson, A.K. Whittaker, M.M. Stevens, C.A. Prestidge, C.J.H. Porter, W.J. Parak, T.P. Davis, E.J. Crampin, F. Caruso, Minimum information reporting in bio-nano experimental literature, Nat. Nanotechnol. 13 (9) (2018) 777–785, https://doi.org/10.1038/s41565-018-0246-4.

[28] K. Rasmussen, H. Rauscher, A. Mech, J. Riego Sintes, D. Gilliland, M. Gonzalez, P. Kearns, K. Moss, M. Visser, M. Groenewold, E.A.J. Bleeker, Physico-chemical properties of manufactured nanomaterials - characterisation and relevant methods. An outlook based on the OECD Testing Programme, Regul. Toxicol. Pharmacol. 92 (2018) 8–28, https://doi.org/10.1016/j.yrtph.2017.10.019.

[29] X. Gao, G.V. Lowry, Progress towards standardized and validated characterizations for measuring physicochemical properties of manufactured nanomaterials relevant to nano health and safety risks, NanoImpact 9 (2018) 14–30, https://doi.org/10.1016/j.impact.2017.09.002.

[30] S. Mourdikoudis, R.M. Pallares, N.T.K. Thanh, Characterization techniques for nanoparticles: comparison and complementarity upon studying nanoparticle properties, Nanoscale 10 (27) (2018) 12871–12934, https://doi.org/10.1039/c8nr02278j.

[31] H.F. Krug, Nanosafety research—Are we on the right track? Angew. Chemie Int. Ed. 53 (46) (2014) 12304–12319, https://doi.org/10.1002/anie.201403367.

[32] J.R. Lead, G.E. Batley, P.J.J. Alvarez, M.-N. Croteau, R.D. Handy, M. J. McLaughlin, J.D. Judy, K. Schirmer, Nanomaterials in the environment: behavior, fate, bioavailability, and effects—An updated review, Environ. Toxicol. Chem. 37 (8) (2018) 2029–2063, https://doi.org/10.1002/etc.4147.

[33] S. Roy, Z. Liu, X. Sun, M. Gharib, H. Yan, Y. Huang, S. Megahed, M. Schnabel, D. Zhu, N. Feliu, I. Chakraborty, C. Sanchez-Cano, A.M. Alkilany, W.J. Parak, Assembly and degradation of inorganic nanoparticles in biological environments, Bioconjug. Chem. 30 (11) (2019) 2751–2762, https://doi.org/10.1021/acs.bioconjchem.9b00645.

[34] M. Hadjidemetriou, K. Kostarelos, Nanomedicine: evolution of the nanoparticle corona, Nat. Nanotechnol. 12 (4) (2017) 288–290, https://doi.org/10.1038/nnano.2017.61.

[35] N. Feliu, X. Sun, R.A. Alvarez Puebla, W.J. Parak, Quantitative particle-cell interaction: some basic physicochemical pitfalls, Langmuir 33 (27) (2017) 6639–6646, https://doi.org/10.1021/acs.langmuir.6b04629.

[36] V. Kumar, N. Sharma, S.S. Maitra, In vitro and in vivo toxicity assessment of nanoparticles, Int. Nano Lett. 7 (4) (2017) 243–256, https://doi.org/10.1007/s40089-017-0221-3.

[37] B.A. Nosek, G. Alter, G.C. Banks, D. Borsboom, S.D. Bowman, S.J. Breckler, S. Buck, C.D. Chambers, G. Chin, G. Christensen, M. Contestabile, A. Dafoe, E. Eich, J. Freese, R. Glennerster, D. Goroff, D.P. Green, B. Hesse, M. Humphreys, J. Ishiyama, D. Karlan, A. Kraut, A. Lupia, P. Mabry, T.A. Madon, N. Malhotra, E. Mayo-Wilson, M. McNutt, E. Miguel, E.L. Paluck, U. Simonsohn, C. Soderberg, B.A. Spellman, J. Turitto, G. VandenBos, S. Vazire, E.J. Wagenmakers, R. Wilson, T. Yarkoni, SCIENTIFIC STANDARDS, Promoting an open research culture, Science 348 (6242) (2015) 1422–1425, https://doi.org/10.1126/science.aab2374.

[38] S. Reuter, S.C. Gupta, M.M. Chaturvedi, B.B. Aggarwal, Oxidative stress, inflammation, and cancer: how are they linked? Free Radic. Biol. Med. 49 (11) (2010) 1603–1616, https://doi.org/10.1016/j.freeradbiomed.2010.09.006.

[39] V. Sosa, T. Moline, R. Somoza, R. Paciucci, H. Kondoh, L.L. Me, Oxidative stress and cancer: an overview, Ageing Res. Rev. 12 (1) (2013) 376–390, https://doi.org/10.1016/j.arr.2012.10.004.

[40] C. Liang, Y. Jin, Y. Li, S.C. Tjong, Interactions of zinc oxide nanostructures with mammalian cells: cytotoxic and photocatalytic toxicity, Int. J. Mol. Sci. 21 (17) (2020), https://doi.org/10.3390/ijms21176305.

[41] J. Paunovic, D. Vucevic, T. Radosavljevic, S. Mandic-Rajcevic, I. Pantic, Iron-based nanoparticles and their potential toxicity: focus on oxidative stress and apoptosis, Chem. Biol. Interact. 316 (2020), 108935, https://doi.org/10.1016/j.cbi.2019.108935.

[42] C. Zhang, Z. Liu, Y. Zhang, L. Ma, E. Song, Y. Song, "Iron free" zinc oxide nanoparticles with ion-leaking properties disrupt intracellular ROS and iron homeostasis to induce ferroptosis, Cell Death Dis. 11 (3) (2020) 183, https://doi.org/10.1038/s41419-020-2384-5.

[43] M. Maruthupandy, G. Rajivgandhi, T. Muneeswaran, J.M. Song, N. Manoharan, Biologically synthesized zinc oxide nanoparticles as nanoantibiotics against ESBLs producing gram negative bacteria, Microb. Pathog. 121 (2018) 224–231, https://doi.org/10.1016/j.micpath.2018.05.041.

[44] U. Kadiyala, E.S. Turali-Emre, J.H. Bahng, N.A. Kotov, J.S. VanEpps, Unexpected insights into antibacterial activity of zinc oxide nanoparticles against methicillin resistant Staphylococcus aureus (MRSA), Nanoscale 10 (10) (2018) 4927–4939, https://doi.org/10.1039/c7nr08499d.

[45] V.G. Reshma, S. Syama, S. Sruthi, S.C. Reshma, N.S. Remya, P.V. Mohanan, Engineered nanoparticles with antimicrobial property, Curr. Drug Metab. 18 (11) (2017) 1040–1054, https://doi.org/10.2174/1389200218666170925122201.

[46] R. Chakraborty, R.K. Sarkar, A.K. Chatterjee, U. Manju, A.P. Chattopadhyay, T. Basu, A simple, fast and cost-effective method of synthesis of cupric oxide nanoparticle with promising antibacterial potency: unraveling the biological and chemical modes of action, Biochim. Biophys. Acta 1850 (4) (2015) 845–856, https://doi.org/10.1016/j.bbagen.2015.01.015.

[47] A. Gholami, F. Mohammadi, Y. Ghasemi, N. Omidifar, A. Ebrahiminezhad, Antibacterial activity of SPIONs versus ferrous and ferric ions under aerobic and anaerobic conditions: a preliminary mechanism study, IET Nanobiotechnol. 14 (2) (2020) 155–160, https://doi.org/10.1049/iet-nbt.2019.0266.

[48] M.I. Khan, A. Mazumdar, S. Pal, S. Kumar Behera, A.J. Tamhankar, S. K. Tripathy, C. Stalsby Lundborg, A. Mishra, Biogenic Ag/CaO nanocomposites kill Staphylococcus aureus with reduced toxicity towards mammalian cells, Colloids Surf. B Biointerfaces 189 (2020), 110846, https://doi.org/10.1016/j.colsurfb.2020.110846.

[49] C. Karthikeyan, K. Varaprasad, S.K. Venugopal, S. Shakila, B.R. Venkatraman, R. Sadiku, Biocidal (bacterial and cancer cells) activities of chitosan/CuO nanomaterial, synthesized via a green process, Carbohydr. Polym. 259 (2021), 117762, https://doi.org/10.1016/j.carbpol.2021.117762.

[50] J. Gupta, D. Bahadur, Defect-mediated reactive oxygen species generation in Mg-Substituted ZnO nanoparticles: efficient nanomaterials for bacterial inhibition and cancer therapy, ACS Omega 3 (3) (2018) 2956–2965, https://doi.org/10.1021/acsomega.7b01953.

[51] J. Khalili Fard, S. Jafari, M.A. Eghbal, A review of molecular mechanisms involved in toxicity of nanoparticles, Adv. Pharm. Bull. 5 (4) (2015) 447–454, https://doi.org/10.15171/apb.2015.061.

[52] B. Sun, X. Wang, Z. Ji, R. Li, T. Xia, NLRP3 inflammasome activation induced by engineered nanomaterials, Small 9 (9-10) (2013) 1595–1607, https://doi.org/10.1002/smll.201201962.

[53] K. Donaldson, C.L. Tran, Inflammation caused by particles and fibers, Inhal. Toxicol. 14 (1) (2002) 5–27, https://doi.org/10.1080/089583701753338613.

[54] G.D. Leikauf, S.H. Kim, A.S. Jang, Mechanisms of ultrafine particle-induced respiratory health effects, Exp. Mol. Med. 52 (3) (2020) 329–337, https://doi.org/10.1038/s12276-020-0394-0.

[55] H. Zhan, X. Chang, X. Wang, M. Yang, Q. Gao, H. Liu, C. Li, S. Li, Y. Sun, LncRNA MEG3 mediates nickel oxide nanoparticles-induced pulmonary fibrosis via suppressing TGF-beta1 expression and epithelial-mesenchymal transition process, Environ. Toxicol. 36 (6) (2021) 1099–1110, https://doi.org/10.1002/tox.23109.

[56] T. Xia, M. Kovochich, J. Brant, M. Hotze, J. Sempf, T. Oberley, C. Sioutas, J.I. Yeh, M.R. Wiesner, A.E. Nel, Comparison of the abilities of ambient and manufactured nanoparticles to induce cellular toxicity according to an oxidative stress paradigm, Nano Lett. 6 (8) (2006) 1794–1807, https://doi.org/10.1021/nl061025k.

[57] M. Horie, Y. Tabei, Role of oxidative stress in nanoparticles toxicity, Free Radic. Res. (2020) 1–12, https://doi.org/10.1080/10715762.2020.1859108.

[58] A. Papp, T. Horvath, N. Igaz, M.K. Gopisetty, M. Kiricsi, D.S. Berkesi, G. Kozma, Z. Konya, I. Wilhelm, R. Patai, T.F. Polgar, T. Bellak, L. Tiszlavicz, Z. Razga, T. Vezer, Presence of titanium and toxic effects observed in rat lungs, kidneys, and central nervous system in vivo and in cultured astrocytes in vitro on exposure by titanium dioxide nanorods, Int. J. Nanomed. 15 (2020) 9939–9960, https://doi.org/10.2147/IJN.S275937.

[59] A. Gasmi, M. Peana, M. Arshad, M. Butnariu, A. Menzel, G. Bjorklund, Krebs cycle: activators, inhibitors and their roles in the modulation of carcinogenesis, Arch. Toxicol. 95 (4) (2021) 1161–1178, https://doi.org/10.1007/s00204-021-02974-9.

[60] Y. Cao, J. Long, L. Liu, T. He, L. Jiang, C. Zhao, Z. Li, A review of endoplasmic reticulum (ER) stress and nanoparticle (NP) exposure, Life Sci. 186 (2017) 33–42, https://doi.org/10.1016/j.lfs.2017.08.003.

[61] R. Thanan, S. Oikawa, Y. Hiraku, S. Ohnishi, N. Ma, S. Pinlaor, P. Yongvanit, S. Kawanishi, M. Murata, Oxidative stress and its significant roles in neurodegenerative diseases and cancer, Int. J. Mol. Sci. 16 (1) (2014) 193–217, https://doi.org/10.3390/ijms16010193.

[62] M. Murata, Inflammation and cancer, Environ. Health Prev. Med. 23 (1) (2018) 50, https://doi.org/10.1186/s12199-018-0740-1.

[63] J.D. Hayes, A.T. Dinkova-Kostova, K.D. Tew, Oxidative stress in cancer, Cancer Cell 38 (2) (2020) 167–197, https://doi.org/10.1016/j.ccell.2020.06.001.

[64] R. Landsiedel, L. Ma-Hock, A. Kroll, D. Hahn, J. Schnekenburger, K. Wiench, W. Wohlleben, Testing metal-oxide nanomaterials for human safety, Adv. Mater. 22 (24) (2010) 2601–2627, https://doi.org/10.1002/adma.200902658.

[65] K.R. Raghupathi, R.T. Koodali, A.C. Manna, Size-dependent bacterial growth inhibition and mechanism of antibacterial activity of zinc oxide nanoparticles, Langmuir 27 (7) (2011) 4020–4028, https://doi.org/10.1021/la104825u.

[66] S. Medici, M. Peana, V.M. Nurchi, M.A. Zoroddu, Medical uses of silver: history, myths, and scientific evidence, J. Med. Chem. 62 (13) (2019) 5923–5943, https://doi.org/10.1021/acs.jmedchem.8b01439.

[67] M. Heinlaan, A. Ivask, I. Blinova, H.C. Dubourguier, A. Kahru, Toxicity of nanosized and bulk ZnO, CuO and TiO2 to bacteria Vibrio fischeri and crustaceans Daphnia magna and Thamnocephalus platyurus, Chemosphere 71 (7) (2008) 1308–1316, https://doi.org/10.1016/j.chemosphere.2007.11.047.

[68] S.W. Wong, P.T. Leung, A.B. Djurisic, K.M. Leung, Toxicities of nano zinc oxide to five marine organisms: influences of aggregate size and ion solubility, Anal. Bioanal. Chem. 396 (2) (2010) 609–618, https://doi.org/10.1007/s00216-009-3249-z.

[69] H. Cangul, L. Broday, K. Salnikow, J. Sutherland, W. Peng, Q. Zhang, V. Poltaratsky, H. Yee, M.A. Zoroddu, M. Costa, Molecular mechanisms of nickel carcinogenesis, Toxicol. Lett. 127 (1) (2002) 69–75, https://doi.org/10.1016/S0378-4274(01)00485-4.

[70] Q.Y. Chen, J. Brocato, F. Laulicht, M. Costa, Mechanisms of nickel carcinogenesis, in: A. Mudipalli, J.T. Zelikoff (Eds.), Essential and Non-Essential Metals: Carcinogenesis, Prevention and Cancer Therapeutics, Springer International Publishing, Cham, 2017, pp. 181–197, https://doi.org/10.1007/978-3-319-55448-8_8.

[71] M. Peana, S. Medici, V.M. Nurchi, G. Crisponi, M.A. Zoroddu, Nickel binding sites in histone proteins: spectroscopic and structural characterization, Coord. Chem. Rev. 257 (19) (2013) 2737–2751, https://doi.org/10.1016/j.ccr.2013.02.022.

[72] M. Peana, A. Pelucelli, S. Medici, R. Cappai, V.M. Nurchi, M.A. Zoroddu, Metal toxicity and speciation: a review, Curr. Med. Chem. (2021), https://doi.org/10.2174/0929867328666210324161205.

[73] S.K. Misra, S. Nuseibeh, A. Dybowska, D. Berhanu, T.D. Tetley, E. Valsami-Jones, Comparative study using spheres, rods and spindle-shaped nanoplatelets on dispersion stability, dissolution and toxicity of CuO nanomaterials, Nanotoxicology 8 (4) (2014) 422–432, https://doi.org/10.3109/17435390.2013.796017.

[74] M. Horie, K. Fujita, H. Kato, S. Endoh, K. Nishio, L.K. Komaba, A. Nakamura, A. Miyauchi, S. Kinugasa, Y. Hagihara, E. Niki, Y. Yoshida, H. Iwahashi, Association of the physical and chemical properties and the cytotoxicity of metal oxide nanoparticles: metal ion release, adsorption ability and specific surface area, Metallomics 4 (4) (2012) 350–360, https://doi.org/10.1039/c2mt20016c.

[75] S. Sabella, R.P. Carney, V. Brunetti, M.A. Malvindi, N. Al-Juffali, G. Vecchio, S. M. Janes, O.M. Bakr, R. Cingolani, F. Stellacci, P.P. Pompa, A general mechanism for intracellular toxicity of metal-containing nanoparticles, Nanoscale 6 (12) (2014) 7052–7061, https://doi.org/10.1039/c4nr01234h.

[76] N. Golbamaki, B. Rasulev, A. Cassano, R.L. Marchese Robinson, E. Benfenati, J. Leszczynski, M.T. Cronin, Genotoxicity of metal oxide nanomaterials: review of recent data and discussion of possible mechanisms, Nanoscale 7 (6) (2015) 2154–2198, https://doi.org/10.1039/c4nr06670g.

[77] D. Wang, Z. Lin, T. Wang, Z. Yao, M. Qin, S. Zheng, W. Lu, Where does the toxicity of metal oxide nanoparticles come from: the nanoparticles, the ions, or a combination of both? J. Hazard. Mater. 308 (2016) 328–334, https://doi.org/10.1016/j.jhazmat.2016.01.066.

[78] Y. Huai, M.N. Hossen, S. Wilhelm, R. Bhattacharya, P. Mukherjee, Nanoparticle interactions with the tumor microenvironment, Bioconjug. Chem. 30 (9) (2019) 2247–2263, https://doi.org/10.1021/acs.bioconjchem.9b00448.

[79] M. Yu, J. Zheng, Clearance pathways and tumor targeting of imaging nanoparticles, ACS Nano 9 (7) (2015) 6655–6674, https://doi.org/10.1021/acsnano.5b01320.

[80] J. Fang, H. Nakamura, H. Maeda, The EPR effect: unique features of tumor blood vessels for drug delivery, factors involved, and limitations and augmentation of the effect, Adv. Drug Deliv. Rev. 63 (3) (2011) 136–151, https://doi.org/10.1016/j.addr.2010.04.009.

[81] Y. Zhang, T.R. Nayak, H. Hong, W. Cai, Biomedical applications of zinc oxide nanomaterials, Curr. Mol. Med. 13 (10) (2013) 1633–1645, https://doi.org/10.2174/1566524013666131111130058.

[82] C.Y.E. Shulin Ji, Synthesis, growth mechanism, and applications of zinc oxide nanomaterials, J. Mater. Sci. Technol. 24 (04) (2009) 457–472.

[83] R.J. Vandebriel, W.H. De Jong, A review of mammalian toxicity of ZnO nanoparticles, Nanotechnol. Sci. Appl. 5 (2012) 61–71, https://doi.org/10.2147/NSA.S23932.

[84] T. Buerki-Thurnherr, L. Xiao, L. Diener, O. Arslan, C. Hirsch, X. Maeder-Althaus, K. Grieder, B. Wampfler, S. Mathur, P. Wick, H.F. Krug, In vitro mechanistic study towards a better understanding of ZnO nanoparticle toxicity, Nanotoxicology 7 (4) (2013) 402–416, https://doi.org/10.3109/17435390.2012.666575.

[85] T.K. Hong, N. Tripathy, H.J. Son, K.T. Ha, H.S. Jeong, Y.B. Hahn, A comprehensive in vitro and in vivo study of ZnO nanoparticles toxicity, J. Mater. Chem. B 1 (23) (2013) 2985–2992, https://doi.org/10.1039/c3tb20251h.

[86] I.L. Hsiao, Y.-J. Huang, Effects of various physicochemical characteristics on the toxicities of ZnO and TiO2 nanoparticles toward human lung epithelial cells, Sci. Total Environ. 409 (7) (2011) 1219–1228, https://doi.org/10.1016/j.scitotenv.2010.12.033.

[87] D. Guo, C. Wu, H. Jiang, Q. Li, X. Wang, B. Chen, Synergistic cytotoxic effect of different sized ZnO nanoparticles and daunorubicin against leukemia cancer cells under UV irradiation, J. Photochem. Photobiol. B 93 (3) (2008) 119–126, https://doi.org/10.1016/j.jphotobiol.2008.07.009.

[88] H. Fukui, M. Horie, S. Endoh, H. Kato, K. Fujita, K. Nishio, L.K. Komaba, J. Maru, A. Miyauhi, A. Nakamura, S. Kinugasa, Y. Yoshida, Y. Hagihara, H. Iwahashi, Association of zinc ion release and oxidative stress induced by intratracheal instillation of ZnO nanoparticles to rat lung, Chem. Biol. Interact. 198 (1–3) (2012) 29–37, https://doi.org/10.1016/j.cbi.2012.04.007.

[89] S. Hackenberg, A. Scherzed, A. Technau, M. Kessler, K. Froelich, C. Ginzkey, C. Koehler, M. Burghartz, R. Hagen, N. Kleinsasser, Cytotoxic, genotoxic and pro-inflammatory effects of zinc oxide nanoparticles in human nasal mucosa cells in vitro, Toxicol. In Vitro 25 (3) (2011) 657–663, https://doi.org/10.1016/j.tiv.2011.01.003.

[90] I.S. Kim, M. Baek, S.J. Choi, Comparative cytotoxicity of Al2O3, CeO2, TiO2 and ZnO nanoparticles to human lung cells, J. Nanosci. Nanotechnol. 10 (5) (2010) 3453–3458, https://doi.org/10.1166/jnn.2010.2340.

[91] H. Liu, D. Yang, H. Yang, H. Zhang, W. Zhang, Y. Fang, Z. Lin, L. Tian, B. Lin, J. Yan, Z. Xi, Comparative study of respiratory tract immune toxicity induced by three sterilisation nanoparticles: silver, zinc oxide and titanium dioxide, J. Hazard. Mater. 248–249 (2013) 478–486, https://doi.org/10.1016/j.jhazmat.2013.01.046.

[92] Y.H. Kim, F. Fazlollahi, I.M. Kennedy, N.R. Yacobi, S.F. Hamm-Alvarez, Z. Borok, K.J. Kim, E.D. Crandall, Alveolar epithelial cell injury due to zinc oxide nanoparticle exposure, Am. J. Respir. Crit. Care Med. 182 (11) (2010) 1398–1409, https://doi.org/10.1164/rccm.201002-0185OC.

[93] N. Hadrup, F. Rahmani, N.R. Jacobsen, A.T. Saber, P. Jackson, S. Bengtson, A. Williams, H. Wallin, S. Halappanavar, U. Vogel, Acute phase response and inflammation following pulmonary exposure to low doses of zinc oxide nanoparticles in mice, Nanotoxicology 13 (9) (2019) 1275–1292, https://doi.org/10.1080/17435390.2019.1654004.

[94] Q. Chen, N. Wang, M. Zhu, J. Lu, H. Zhong, X. Xue, S. Guo, M. Li, X. Wei, Y. Tao, H. Yin, TiO2 nanoparticles cause mitochondrial dysfunction, activate inflammatory responses, and attenuate phagocytosis in macrophages: a proteomic and metabolomic insight, Redox Biol. 15 (2018) 266–276, https://doi.org/10.1016/j.redox.2017.12.011.

[95] M.S. Waghmode, A.B. Gunjal, J.A. Mulla, N.N. Patil, N.N. Nawani, Studies on the titanium dioxide nanoparticles: biosynthesis, applications and remediation, SN Appl. Sci. 1 (4) (2019) 310, https://doi.org/10.1007/s42452-019-0337-3.

[96] S. Hussain, S. Boland, A. Baeza-Squiban, R. Hamel, L.C. Thomassen, J.A. Martens, M.A. Billon-Galland, J. Fleury-Feith, F. Moisan, J.C. Pairon, F. Marano, Oxidative stress and proinflammatory effects of carbon black and titanium dioxide nanoparticles: role of particle surface area and internalized amount, Toxicology 260 (1–3) (2009) 142–149, https://doi.org/10.1016/j.tox.2009.04.001.

[97] K. Yamashita, Y. Yoshioka, K. Higashisaka, K. Mimura, Y. Morishita, M. Nozaki, T. Yoshida, T. Ogura, H. Nabeshi, K. Nagano, Y. Abe, H. Kamada, Y. Monobe, T. Imazawa, H. Aoshima, K. Shishido, Y. Kawai, T. Mayumi, S. Tsunoda, N. Itoh, T. Yoshikawa, I. Yanagihara, S. Saito, T. Tsutsumi, Silica and titanium dioxide nanoparticles cause pregnancy complications in mice, Nat. Nanotechnol. 6 (5) (2011) 321–328, https://doi.org/10.1038/nnano.2011.41.

[98] D. Ziental, B. Czarczynska-Goslinska, D.T. Mlynarczyk, A. Glowacka-Sobotta, B. Stanisz, T. Goslinski, L. Sobotta, Titanium dioxide nanoparticles: prospects and applications in medicine, Nanomaterials (Basel) 10 (2) (2020), https://doi.org/10.3390/nano10020387.

[99] F. Herzog, M.J. Clift, F. Piccapietra, R. Behra, O. Schmid, A. Petri-Fink, B. Rothen-Rutishauser, Exposure of silver-nanoparticles and silver-ions to lung cells in vitro at the air-liquid interface, Part. Fibre Toxicol. 10 (2013) 11, https://doi.org/10.1186/1743-8977-10-11.

[100] S.P. Deshmukh, S.M. Patil, S.B. Mullani, S.D. Delekar, Silver nanoparticles as an effective disinfectant: a review, Mater. Sci. Eng.: C 97 (2019) 954–965, https://doi.org/10.1016/j.msec.2018.12.102.

[101] S. Kokura, O. Handa, T. Takagi, T. Ishikawa, Y. Naito, T. Yoshikawa, Silver nanoparticles as a safe preservative for use in cosmetics, Nanomedicine 6 (4) (2010) 570–574, https://doi.org/10.1016/j.nano.2009.12.002.

[102] Z. Ferdous, A. Nemmar, Health impact of silver nanoparticles: a review of the biodistribution and toxicity following various routes of exposure, Int. J. Mol. Sci. 21 (7) (2020), https://doi.org/10.3390/ijms21072375.

[103] S. Gurunathan, J.W. Han, D.N. Kwon, J.H. Kim, Enhanced antibacterial and anti-biofilm activities of silver nanoparticles against gram-negative and gram-positive bacteria, Nanoscale Res. Lett. 9 (1) (2014) 373, https://doi.org/10.1186/1556-276X-9-373.

[104] K. Murugan, C.P. Sanoopa, P. Madhiyazhagan, D. Dinesh, J. Subramaniam, C. Panneerselvam, M. Roni, U. Suresh, M. Nicoletti, A.A. Alarfaj, M.A. Munusamy, A. Higuchi, S. Kumar, H. Perumalsamy, Y.J. Ahn, G. Benelli, Rapid biosynthesis of silver nanoparticles using Crotalaria verrucosa leaves against the dengue vector Aedes aegypti: what happens around? An analysis of dragonfly predatory behaviour after exposure at ultra-low doses, Nat. Prod. Res. 30 (7) (2016) 826–833, https://doi.org/10.1080/14786419.2015.1074230.

[105] A. Lankoff, W.J. Sandberg, A. Wegierek-Ciuk, H. Lisowska, M. Refsnes, B. Sartowska, P.E. Schwarze, S. Meczynska-Wielgosz, M. Wojewodzka, M. Kruszewski, The effect of agglomeration state of silver and titanium dioxide nanoparticles on cellular response of HepG2, A549 and THP-1 cells, Toxicol. Lett. 208 (3) (2012) 197–213, https://doi.org/10.1016/j.toxlet.2011.11.006.

[106] J. Jiravova, K.B. Tomankova, M. Harvanova, L. Malina, J. Malohlava, L. Luhova, A. Panacek, B. Manisova, H. Kolarova, The effect of silver nanoparticles and silver ions on mammalian and plant cells in vitro, Food Chem. Toxicol. 96 (2016) 50–61, https://doi.org/10.1016/j.fct.2016.07.015.

[107] I.X. Green, W. Tang, M. Neurock, J.T. Yates Jr., Spectroscopic observation of dual catalytic sites during oxidation of CO on a Au/TiO(2) catalyst, Science 333 (6043) (2011) 736–739, https://doi.org/10.1126/science.1207272.

[108] I.C. Shaw, Gold-based therapeutic agents, Chem. Rev. 99 (9) (1999) 2589–2600, https://doi.org/10.1021/cr980431o.

[109] S.J. Berners-Price, A. Filipovska, Gold compounds as therapeutic agents for human diseases, Metallomics 3 (9) (2011) 863–873, https://doi.org/10.1039/c1mt00062d.

[110] I. Venditti, Engineered gold-based nanomaterials: morphologies and functionalities in biomedical applications. A mini review, Bioengineering (Basel) 6 (2) (2019), https://doi.org/10.3390/bioengineering6020053.

[111] S. Medici, M. Peana, D. Coradduzza, M.A. Zoroddu, Gold nanoparticles and cancer: detection, diagnosis and therapy, Semin. Cancer Biol. (2021), https://doi.org/10.1016/j.semcancer.2021.06.017.

[112] D. Luo, X. Wang, C. Burda, J.P. Basilion, Recent development of gold nanoparticles as contrast agents for cancer diagnosis, Cancers (Basel) 13 (8) (2021), https://doi.org/10.3390/cancers13081825.

[113] E.C. Dreaden, A.M. Alkilany, X. Huang, C.J. Murphy, M.A. El-Sayed, The golden age: gold nanoparticles for biomedicine, Chem. Soc. Rev. 41 (7) (2012) 2740–2779, https://doi.org/10.1039/c1cs15237h.

[114] A. Sani, C. Cao, D. Cui, Toxicity of gold nanoparticles (AuNPs): a review, Biochem. Biophys. Rep. 26 (2021), 100991, https://doi.org/10.1016/j.bbrep.2021.100991.

[115] B. Fadeel, A.E. Garcia-Bennett, Better safe than sorry: understanding the toxicological properties of inorganic nanoparticles manufactured for biomedical applications, Adv. Drug Deliv. Rev. 62 (3) (2010) 362–374, https://doi.org/10.1016/j.addr.2009.11.008.

[116] C. Lopez-Chaves, J. Soto-Alvaredo, M. Montes-Bayon, J. Bettmer, J. Llopis, C. Sanchez-Gonzalez, Gold nanoparticles: distribution, bioaccumulation and toxicity. In vitro and in vivo studies, Nanomedicine 14 (1) (2018) 1–12, https://doi.org/10.1016/j.nano.2017.08.011.

[117] X. Ma, Y. Wu, S. Jin, Y. Tian, X. Zhang, Y. Zhao, L. Yu, X.J. Liang, Gold nanoparticles induce autophagosome accumulation through size-dependent nanoparticle uptake and lysosome impairment, ACS Nano 5 (11) (2011) 8629–8639, https://doi.org/10.1021/nn202155y.

[118] Y. Pan, S. Neuss, A. Leifert, M. Fischler, F. Wen, U. Simon, G. Schmid, W. Brandau, W. Jahnen-Dechent, Size-dependent cytotoxicity of gold nanoparticles, Small 3 (11) (2007) 1941–1949, https://doi.org/10.1002/smll.200700378.

[119] T. Mironava, M. Hadjiargyrou, M. Simon, V. Jurukovski, M.H. Rafailovich, Gold nanoparticles cellular toxicity and recovery: effect of size, concentration and exposure time, Nanotoxicology 4 (1) (2010) 120–137, https://doi.org/10.3109/17435390903471463.

[120] L. Wang, X. Jiang, Y. Ji, R. Bai, Y. Zhao, X. Wu, C. Chen, Surface chemistry of gold nanorods: origin of cell membrane damage and cytotoxicity, Nanoscale 5 (18) (2013) 8384–8391, https://doi.org/10.1039/c3nr01626a.

[121] Y.P. Jia, K. Shi, J.F. Liao, J.R. Peng, Y. Hao, Y. Qu, L.J. Chen, L. Liu, X. Yuan, Z. Y. Qian, X.W. Wei, Effects of cetyltrimethylammonium bromide on the toxicity of gold nanorods both in vitro and in vivo: molecular origin of cytotoxicity and inflammation, Small Methods 4 (3) (2020), 1900799, https://doi.org/10.1002/smtd.201900799.

[122] T. Niidome, M. Yamagata, Y. Okamoto, Y. Akiyama, H. Takahashi, T. Kawano, Y. Katayama, Y. Niidome, PEG-modified gold nanorods with a stealth character for in vivo applications, J. Control. Release 114 (3) (2006) 343–347, https://doi.org/10.1016/j.jconrel.2006.06.017.

[123] A. Katsumiti, I. Arostegui, M. Oron, D. Gilliland, E. Valsami-Jones, M. P. Cajaraville, Cytotoxicity of Au, ZnO and SiO(2) NPs using in vitro assays with mussel hemocytes and gill cells: relevance of size, shape and additives, Nanotoxicology 10 (2) (2016) 185–193, https://doi.org/10.3109/17435390.2015.1039092.

[124] F. Behzad, S.M. Naghib, M.A.J. kouhbanani, S.N. Tabatabaei, Y. Zare, K.Y. Rhee, An overview of the plant-mediated green synthesis of noble metal nanoparticles for antibacterial applications, J. Ind. Eng. Chem. 94 (2021) 92–104, https://doi.org/10.1016/j.jiec.2020.12.005.

[125] S.S.I. Abdalla, H. Katas, F. Azmi, M.F.M. Busra, Antibacterial and anti-biofilm biosynthesised silver and gold nanoparticles for medical applications: mechanism of action, toxicity and current status, Curr. Drug Deliv. 17 (2) (2020) 88–100, https://doi.org/10.2174/1567201817666191227094334.

[126] D. Sharma, S. Kanchi, K. Bisetty, Biogenic synthesis of nanoparticles: a review, Arab. J. Chem. 12 (8) (2019) 3576–3600, https://doi.org/10.1016/j.arabjc.2015.11.002.

[127] S.K. Vemuri, R.R. Banala, S. Mukherjee, P. Uppula, S. Gpv, A.V. Gurava Reddy, T. Malarvilli, Novel biosynthesized gold nanoparticles as anti-cancer agents against breast cancer: synthesis, biological evaluation, molecular modelling studies, Mater. Sci. Eng. C Mater. Biol. Appl. 99 (2019) 417–429, https://doi.org/10.1016/j.msec.2019.01.123.

[128] Y.-P. Jia, B.-Y. Ma, X.-W. Wei, Z.-Y. Qian, The in vitro and in vivo toxicity of gold nanoparticles, Chinese Chem. Lett. 28 (4) (2017) 691–702, https://doi.org/10.1016/j.cclet.2017.01.021.

[129] B.D. Chithrani, A.A. Ghazani, W.C. Chan, Determining the size and shape dependence of gold nanoparticle uptake into mammalian cells, Nano Lett. 6 (4) (2006) 662–668, https://doi.org/10.1021/nl0523960.

[130] S. Nangia, R. Sureshkumar, Effects of nanoparticle charge and shape anisotropy on translocation through cell membranes, Langmuir 28 (51) (2012) 17666–17671, https://doi.org/10.1021/la303449d.

[131] D. Kumar, I. Mutreja, K. Chitcholtan, P. Sykes, Cytotoxicity and cellular uptake of different sized gold nanoparticles in ovarian cancer cells, Nanotechnology 28 (47) (2017), 475101, https://doi.org/10.1088/1361-6528/aa935e.

[132] E. Kowsalya, K. MosaChristas, C.R.I. Jaquline, P. Balashanmugam, T. Devasena, Gold nanoparticles induced apoptosis via oxidative stress and mitochondrial dysfunctions in MCF-7 breast cancer cells, Appl. Organomet. Chem. 35 (1) (2021), e6071, https://doi.org/10.1002/aoc.6071.

[133] Y. Ke, M.S. Al Aboody, W. Alturaiki, S.A. Alsagaby, F.A. Alfaiz, V. P. Veeraraghavan, S. Mickymaray, Photosynthesized gold nanoparticles from Catharanthus roseus induces caspase-mediated apoptosis in cervical cancer cells (HeLa), Artif. Cells Nanomed. Biotechnol. 47 (1) (2019) 1938–1946, https://doi.org/10.1080/21691401.2019.1614017.

[134] M.E. Vance, T. Kuiken, E.P. Vejerano, S.P. McGinnis, M.F. Hochella Jr., D. Rejeski, M.S. Hull, Nanotechnology in the real world: redeveloping the nanomaterial consumer products inventory, Beilstein J. Nanotechnol. 6 (2015) 1769–1780, https://doi.org/10.3762/bjnano.6.181.

**REVIEW ARTICLE**

# Metal Toxicity and Speciation: A Review

Massimiliano Peana[1,*], Alessio Pelucelli[1], Serenella Medici[1], Rosita Cappai[2], Valeria Marina Nurchi[2] and Maria Antonietta Zoroddu[1,*]

*[1]Department of Chemistry and Pharmacy, University of Sassari, Sassari, Italy; [2]Department of Life and Environmental Sciences, University of Cagliari, Cagliari, Italy*

**Abstract:** *Background*: Essential metal ions play a specific and fundamental role in human metabolism. Their homeostasis is finely tuned, and any concentration imbalance in the form of deficiency or excess could lead to a progressive reduction and failure of normal biological function, to severe physiological and clinical outcomes, may eventually causing death. Conversely, non-essential metals are not necessary for life, and only noxious effects could arise after their exposure. Large environmental amounts of such chemicals come from both natural and anthropogenic sources, with the latter being predominant because of human activities. The dissipation of toxic metals contaminates water, air, soil, and food, causing a series of chronic and acute syndromes.

*Objective*: This review discusses the toxicity of non-essential metals considering their peculiar chemical characteristics, such as different forms, hard-soft character, oxidation states, binding capabilities, and solubility, which can influence their speciation in biological systems, and subsequently, the main cellular targets. Particular focus is given to selected toxic metals, major non-essential metals, or semimetals related to toxicity, such as mercury, lead, cadmium, chromium, nickel, and arsenic. In addition, we provide indications on the possible treatments/interventions for metal poisoning based on chelation therapy.

*Conclusion*: Toxic metal ions can exert their peculiar harmful effects in several ways. They strongly coordinate with important biological molecules on the basis of their chemical-physical characteristics (mainly HSAB properties) or replace essential metal ions from their natural locations in proteins, enzymes, or hard structures, such as bones or teeth. Metals with redox properties could be key inducers of reactive oxygen species, leading to oxidative stress and cellular damage. Therapeutic detoxification, through complexation of toxic metal ions by specific chelating agents, appears an efficacious clinical strategy, mainly in acute cases of metal intoxication.

**Keywords:** Metal speciation, metal toxicity, chelation therapy, toxic metals, metal poisoning, oxidation states.

## 1. INTRODUCTION

The fundamental role played by particular metals in the cellular metabolism of humans has long been recognized. This role is not only limited to light metals with remarkable natural abundance, such as calcium, sodium, potassium, or magnesium, but also those of high atomic weight and low abundance, such as the transition metals, iron, zinc, copper, manganese, molybdenum, and cobalt [1]. Altogether, they exert several roles ranging, in the case of calcium and magnesium, from the assembly of hard structures *via* bio-mineralization (bones, teeth, *etc.*) to structural functions in macromolecules (DNA, proteins). Sodium and potassium work mainly as charge carriers transferring information in cells and through cells and organs. Other essential metals, such as zinc, iron, and copper, play a role as enzymatic cofactors or prosthetic groups of proteins [2, 3]. Redox-active metals are able to transfer electrons and catalyze important redox reactions in enzymes [1, 4]. However, despite the demonstrated essentiality, their concentration remains an important factor since both deficiency and excess can be toxic for the normal physiological status and correct cellular activi-

*Address correspondence to these authors at the Department of Chemistry and Pharmacy, University of Sassari, Sassari, Italy; Tel: 3495263986; E-mails: peana@uniss.it, zoroddu@uniss.it

ty. Deficiency leads to a reduction of biological function, as well as irreversible and severe organ damage or death, and the excess, based on the famous Paracelsus principle "the dose makes the poison", produces serious physiological responses, abnormalities, chronic or acute intoxication and may eventually death.

Consequently, for each essential metal, there is an optimal concentration range below which metal deficiency occurs and above which toxic and lethal effects develop.

Essential metal deficiency arises due to several causes, ranging from their inadequate supply through food to specific health conditions and genetic factors [5]. Poor economic conditions, such as those experienced by people living in developing countries, generally lead to metal ions deficiency (*i.e.* iron, particularly in children and pregnant women) due to inadequate nutrition. In addition, particular health conditions (use of diuretics, or obese or post-bariatric surgery patient, *etc.*), wrong life-style choices (alcohol abuse, smoking), and incorrect diet could contribute or aggravate an existing deficiency. Genetic factors, such as the mutation of genes that encode for proteins or enzymes regulating metal ion homeostasis, are related to specific deficiencies and associated disorders (anemia for iron, Menkes's for copper, *etc.*). In addition, essential trace metals can affect the epigenome from the developing oocyte throughout life, suggesting a link between metal deficiencies and epigenetics with some specific disorders [6]. Appropriate food fortification and the use of nutritional supplementation appear the best choice to restore the optimal level of metal ions [7, 8].
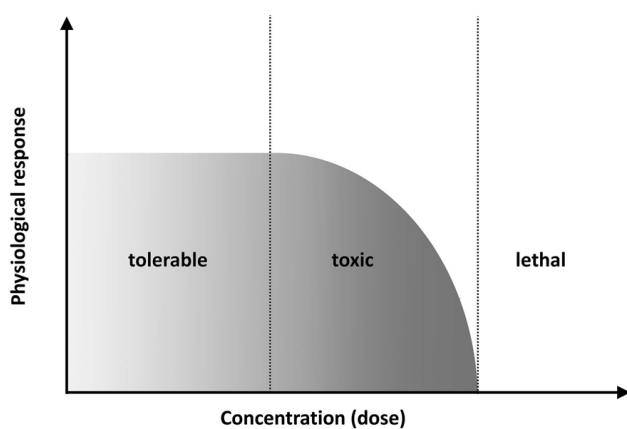


**Fig. (1).** Dose-response diagram for a non-essential element.

Non-essential metals, namely those with no biological role, can be distinguished into two groups: those not necessary for life due to their low abundance and availability and those for which only noxious effects arise after exposure. For each non-essential metal, the same toxic risks occur (Fig. **1**) beyond a tolerance limit.

However, if exposure exceeds a critical level, both essential and non-essential metals could exert toxic effects [1, 9]. This review aims to discuss the toxicity of non-essential metals considering their peculiar characteristics, such as chemical forms, speciation in biological environments, and their main cellular targets. A particular focus is given to selected toxic metals, and, in addition, indications are provided about the treatments/interventions for metal poisoning based on chelation therapy.

## 2. METALS: CHARACTERISTICS AND CLASSIFICATION

Metals are the most abundant group of chemical elements and represent about 25% of the weight of the earth's crust. Among the top ten most abundant elements on the earth's crust and in the sea, seven are metals: aluminum (8.23%), iron (5.63%), calcium (4.15%), sodium (2.36%), magnesium (2.33%), potassium (2.09%) and titanium (0.57%) [10]. In the human body, the essential metals are ten, and they can be divided into "macro-minerals," (calcium (1000 g), potassium (140 g), sodium (100 g), magnesium (30 g)), and "trace elements" (iron (5 g), zinc (2 g), copper (100 mg), manganese (16 mg), molybdenum (5 mg), and cobalt (2 mg)) [1]. These quantities correspond to the average values for a Reference Man of 70 kg. In addition, the essentiality for humans of some other metals, such as vanadium, nickel, and tin, is still under discussion [1].

In the periodic table of the elements, metals occupy different groups and periods, and, excluding the transuranics, there are 65 elements with metallic characteristics. Their properties vary continuously as they move along the periods or descend along the groups. Some of the periodic properties are: electrical and thermal conductivity, density, atomic and ionic radius, electronegativity, and oxidation numbers. In particular, with reference to electronegativity, metals are definitely electropositive elements due to their tendency to lose electrons. This trend decreases along the periods, from left to right, with the increase of the effective nuclear charge ($Z_{eff}$), while the distance and shielding remain constant, making it harder to remove electrons along the period. Conversely, this trend increases along the groups, from top to bottom, as the atomic number increases, since $Z_{eff}$ remains constant, whereas distance and shielding increase. Defined by IUPAC as

"the charge of an atom after ionic approximation of its heteronuclear bonds" [11], the oxidation state regarding metals is related to the number of electrons that they lose or appear to use when joining with another atom in compounds. Considering their low ionization energy and low electronegativity, meaning that they easily lose electrons, metals are reducing agents and easily oxidizable. The oxidation state of the group 1 metals (alkaline metals) is always +1 due to the ease of ionization of the single electron from the s valence shell to the very high second ionization energy. Group 2 (alkaline earth metals) readily loses two electrons to form cations with charge +2 and an oxidation state of +2. Most of the transition metals have multiple oxidation states, as it is relatively easy to lose one or more electrons for them, compared to group 1 or 2 elements. This is because transition metals have 5 d-orbitals partially occupied, with a variety of oxidation states depending on unstable unpaired valence electrons. The s-orbital also contributes to determining the oxidation states of transition metals. A general formula can be indicated as: highest oxidation number = number of unpaired d-electrons + 2 s-orbital electrons. However, copper and chromium do not follow this formula.

Metals react as electron-pair acceptors (Lewis acids) with donors (Lewis bases) according to the well-known scheme: A + B ⇄ A-B

The resulting species can be a pair of ions, a metal complex, a coordination compound, or an acceptor-donor complex. Based on experimental evidence, acceptors and donors were divided into hard and soft classes to explain the different characteristics of the A-B product, according to the HSAB concept (Hard and Soft Lewis Acids and Bases) [12]. It has been observed that strong acceptors prefer binding to strong donors, while weak acceptors to weak donors. This evidence is based on the different electron mobility, or polarizability, and the different electronegativity. A hard acceptor is characterized by low polarizability, low electronegativity, large positive charge density (*i.e.* high oxidation state associated with a small ion radius), however, a soft acceptors have opposite characteristics: they are big, have low charge states, and are strongly polarizable. A hard donor is characterized by low polarizability, high electronegativity, and negative charge density, and the soft donor is characterized by the opposite characteristics [13, 14].

In addition to the hard and soft groups, borderline categories should be considered. They are the intermediate between hard and soft acids and bases. Borderline acids tend to have a lower charge and somewhat larger size than hard acids, and higher charge and somewhat smaller size than soft acids. Borderline bases tend to be larger and less electronegative than hard bases, and smaller and more electronegative than soft bases. In Table **1**, metals are summarized according to their hard, soft and borderline characteristics, together with some of the most common Lewis bases.

The HSAB theory explains, under the chemical point of view, the minerals and geomaterials variety in the earth's crust and the eventual high water solubility and washout. Metals, such as magnesium ($Mg^{2+}$), calcium ($Ca^{2+}$), or aluminum ($Al^{3+}$) appear in nature as oxides, carbonates, phosphates, or sulfates. In fact, hard acids preferentially bind with hard bases, such as $O^{2-}$, $CO_3^{2-}$, $PO_4^{3-}$, $SO_4^{2-}$, whereas soft acids, such as mercury ($Hg^{2+}$), cadmium ($Cd^{2+}$), are easily found as sulfide since they have a strong affinity for soft bases, such as $S^{2-}$ ions. According to this theory, hard acids and soft bases do not form strong bonds; consequently, their minerals are easily soluble in water and are washed out without accumulating.

**Table 1. Hard and soft metals and some common Lewis bases.**

| Hard | Borderline | Soft |
|---|---|---|
| **Acids** | | |
| $Li^+$, $Na^+$, $K^+$, $Be^{2+}$, $Mg^{2+}$, $Ca^{2+}$, $Sr^{2+}$, $Sc^{3+}$, $Al^{3+}$, $Ga^{3+}$, $In^{3+}$, $Cr^{3+}$, $Co^{3+}$, $Fe^{3+}$, $As^{3+}$, $Ir^{3+}$, $La^{3+}$, $Ti^{4+}$, $Zr^{4+}$, $Th^{4+}$, $U^{4+}$, $VO^{2+}$, $UO_2^{2+}$, $BeMe_2$, $AlCl_3$, $AlMe_3$ | $Fe^{2+}$, $Co^{2+}$, $Ni^{2+}$, $Cu^{2+}$, $Zn^{2+}$, $Sn^{2+}$, $Pb^{2+}$, $Rh^{3+}$ | $Cu^+$, $Ag^+$, $Au^+$, $Hg^+$, $Cs^+$, $Tl^+$, $Hg^{2+}$, $Pd^{2+}$, $Cd^{2+}$, $Pt^{2+}$, $MoO_2^{2+}$ |
| **Bases** | | |
| $H_2O$, $OH^-$, $F^-$, $CH_3CO_2^-$, $PO_4^{3-}$, $SO_4^{2-}$, $CO_3^{2-}$, $NO_3^-$, $ClO_4^-$, $O^{2-}$, $ROH$, $RO^-$, $R_2O$, $NH_3$, $RNH_2$, $N_2H_4$ | Aniline, pyridine, $N_3^-$, $Cl^-$, $Br^-$, $NO_2^-$, $SO_3^{2-}$, $N_2$ | $S^{2-}$, $RSH$, $RS^-$, $R_2S$, $I^-$, $CN^-$, $SCN^-$, $S_2O_3^-$, $R_3P$, $R_3As$, $(RO)_3P$, $RNC$, $CO$, $C_2H_4$, $C_6H_6$, $R^-$, $H^-$ |

## 3. TOXIC ELEMENTS AND THE MAIN MECHANISM OF TOXICITY

Some metals under the form of metal ions, metal compounds, or nanoparticles (NPs) are known to have potential toxicity for humans depending both on their peculiar characteristics as well as on the degree of exposition [1, 15, 16]. They can cause acute and chronic poisoning and subsequent several health outcomes, not only in occupational settings but also in environmental high-exposure conditions, accidental intake, or suicide attempts. In addition to these circumstances, several genetic diseases are linked to metal dyshomeostasis, such as, iron overload in hereditary haemochromatosis or copper overload in Wilson's disease [17]. Altered metabolism of several transition metals has also been associated with neurodegenerative consequences and represents a potential trigger of malignant cells [18, 19]. The toxicology of a metal is strictly dependent on its chemical characteristics and kinetics of its interactions with the cell components, in the form of free ions, metal complexes, and organometallic compounds or NPs formulations. The toxic effect of metals is strictly dependent on the type of human exposure (chronic or acute), metal concentration, way of entry in the organism (inhalation, permeation, ingestion, and injection), metal speciation, and degree of health effects severity that each specific metal exerts. Generally, the pathways of metal toxicology comprise several stages, including 1) entry and absorption, 2) transport, distribution, accumulation, biotransformation, and 3) excretion.

The physico-chemical properties of metal compounds play the main role in terms of the prediction of toxicity. Their nature as organic or inorganic compounds has, in fact, important consequences on the pathways of absorption, directly affecting the solubility in hydrophilic or hydrophobic environments and, subsequently, transport, distribution, accumulation, and therefore, the resulting final effects and outcomes. In addition, for metals in NP forms, the particle size distribution, shape, charges, and dimension, together with the chemical composition, determine the potential toxicity since this is related to properties, such as solubility, degree of absorption, and deposition in the various compartments of the respiratory tract, in particular, when they are present as particulate air pollutants [15, 16]. The physical state of the metal compound, such as gaseous, dissolved, or adsorbed on solid particles, is critical for the absorption through the different tissues. The particle size is important for the absorption through the bronchial or gastrointestinal tissues; the soluble form is suitable for skin absorption, while the gaseous form is ideal for pulmonary absorption. Solubility is one of the major factors influencing the availability and absorption of metals. For instance, if the metal compound (insoluble or poorly soluble salt or in the NP formulation) is finely divided, its solubility increases. Consequently, it appears that for the purpose of a prediction or assessment of metal compounds toxicity, the intake and absorption stage is the most critical. The water solubility of metal compounds is dependent on the pH and the presence of other molecules. Consequently, solubility may vary widely in different biological fluids compared to pure water. For instance, it is known that in humans the pH of fluids varies between 2 and 6 in the stomach to pH 6.8 in the intestine and pH 7.4 in the other regions. Moreover, biological fluids are rich in the range of organic ligands, comprising amino acids, peptides, and other endogenous molecules and anions that are surely able to influence the solubility of metal compounds [20]. In addition, the oxidation states and the rate of redox conversions are the key factors governing the degree of solubility of a particular metal compound (in particular for transition metals).

Once absorbed, the metal is then transformed into the most suitable form for transport and/or accumulation; it may undergo oxidation-reduction and complexation reactions with proteins, peptides, simple amino acids, nucleic acids, *etc.*, according to their HSAB chemical characteristics, redox properties, and their speciation.

One of the mechanisms of non-essential metal ions toxicity is based on their ability (at least for some of them) to replace essential metal ions in bones, organs, or tissues. For instance, $Pb^{2+}$ can replace $Ca^{2+}$, $Mg^{2+}$, $Fe^{2+}$ (as well as $Al^{3+}$), and monovalent cations like $Na^+$, with the resulting disturbance of the normal cell metabolism [9]. Another striking example is provided by $Cd^{2+}$, able to replace $Ca^{2+}$, with a consequent alteration of the normal bone structure, leading to osteomalacia, decalcification, osteoporosis, and a series of bone deformities (*vide infra*) [21]. In addition, $Cd^{2+}$ can replace $Zn^{2+}$ present in metallothionein (MT), thus inhibiting it from acting as a cellular free radical scavenger. However, MTs, by sequestrating $Cd^{2+}$ ions, function as detoxifiers since they quench the dangerous ability of $Cd^{2+}$ to interact with other essential biomolecules [22].

Toxicity and bio-assimilability of a metal strictly depend on its chemical speciation, that is the different chemical forms under which it is distributed in a given system [23]. In fact, it is known that many essential me-

tals are found in various forms whose assimilability varies significantly. For example, for humans, the most easily absorbable form of iron is heme iron ($Fe^{2+}$), derived from hemoglobin and myoglobin of animal food sources (meat, seafood, poultry), while non-heme iron, derived from plants (vegetables, fruits, and beans) and iron-fortified foods (inorganic salts and simple organic complexes) is less easily absorbed [7, 24]. $Fe^{3+}$, which is insoluble, is the primary form of non-heme iron in food, and therefore, must be reduced to the $Fe^{2+}$ form before being transported across the enterocytes [25]. The only form of absorbable cobalt ($Co^{+}$) is the water-soluble Vitamin B12 (cobalamin) [26]. Zinc is the essential metal involved in numerous biological functions, with its binding to more than 300 enzymes and over 2000 transcriptional factors [3]. Metallic zinc is insoluble in water, and also zinc oxide, sulfide, or carbonate are almost insoluble, whereas other salts, such as acetate, nitrate, chloride, sulfate, are readily soluble in water. $Zn^{2+}$ complexes with amino acids and peptides are more assimilable than their respective inorganic forms.

Regarding the toxicity of metals, the free metal ion (aqua-ion) is generally more toxic, while metals involved in strong complexes or those associated with colloidal material are less harmful. However, mercury is an exception. In fact, methylmercury is known to have the strongest toxicity to humans [27, 28]. As a result, it is clear that not only information on the total metal concentration is required, but information on metal speciation is also needed in order to provide clear data on bioassimilability and potential toxicity.

Heavy metal exposure can cause a series of severe outcomes ranging from various types of cancers to immunodepression, inflammation, cardiovascular diseases, diabetes, neurodegenerative disorders, autoimmune disorders, and others.

Metals with redox properties have the ability to produce reactive oxygen species or nitrogen radicals species (ROS, RNS), which can react with various biological targets and components of the cell [29]. If the endogenous antioxidant defense system [superoxide dismutase (SOD), catalase (CAT), glutathione (GSH),

**Table 2. Metal ions toxicity.**

| Period | Essential Metals | Non-Essential Metals | |
|---|---|---|---|
| | Toxic in Excess | Rare or Insoluble Toxic Metal | Available Toxic Metal |
| 2 | - | - | Be |
| 3 | Na Mg | - | - |
| 4 | K Ca Cr§ Mn§ Fe Co Ni§ Cu Zn | Ti Ga | As* |
| 5 | Sn§ | Zr Nb Ru Rh | Pd Ag Cd Sb* Te* |
| 6 | - | Ba La Hf Ta W Re Os Ir | Pt Au Hg Tl Pb Bi |

§ possibly essential trace element; * semimetal.

*etc.*] is not sufficient to quench the increasing production of these radicals, a cascade of reactions will occur, inducing DNA strain-breaks, lipid peroxidation, protein modification, and other effects at the cellular level and organ levels, leading to chronic health problems, such as cardiovascular and inflammatory disease, neurodegeneration and cancer [30-32]. In addition, as already stated, redox-active and inactive metals can exert their toxic effects on cells and organs through their binding to functional groups of proteins (depending on their HSAB characteristics), or by depletion of GSH, or by replacing essential metals, leading to a dangerous interference in their homeostasis [27, 33]. This event can produce oxidative stress and new production of ROS. In Table **2**, the list of metal ions toxicity is presented along with their essentiality or non-essentiality and general availability.

## 4. CHELATION AND CHELATING AGENTS

Chelating agents in clinical practice (chelation therapy) aim to eliminate a toxic metal ion from sensitive sites in critical organs [34-36]. The crucial qualities of a chelating agent, that have been better defined through the years [37, 38], can be outlined as:

[1]  Toxicity of the chelating agent and the formed complexes.
[2]  Chemical affinity of the chelating agent for the target metal ion higher than that of the sensitive endogenous ligands.
[3]  Kinetics of exchange with endogenous ligands.
[4]  Selectivity toward the target metal ion.
[5]  Absorption and bioavailability.
[6]  Biochemical metabolism of the chelating agent once entered inside the body.
[7]  The redox potential of the formed complex.
[8]  Excretion of the formed complexes.
[9]  The chelator should not perturb the homeostasis of essential metal ions in body fluids.
[10]  It must have a low cost.
[11]  The patient must comply with the administration route.

This list of requirements might suggest that the synthesis of a chelator for a target metal ion must follow a well-defined design. Although serendipity and acumen of some researchers have been the basis of the discovery of some of the more used chelating agents, the discovery of desferrioxamine (DFO) "was a fruitful chance occurrence. The story of its discovery is most unusual because the failure of research in one direction led to the success in another" [39]; DFO is derived from ferrioxamine B (FOB), a metabolite produced by

*Streptomyces pilosus*, discovered in 1959 as an impurity in a research carried out by the pharmaceutical and chemical company Ciba on the iron-containing antibiotics ferrimycines. Although the Ciba project was discontinued in 1959, Bickel *et al* [40] produced a small amount of FOB in May 1960, and later Bickel *et al.* [41] quickly determined its structure. This molecule was thought to be a potential iron donor for iron-deficiency patients, so it was passed onto Prof. Wöhler (University of Freiburg) for the clinical trials. After toxicity studies, it was supplied to patients, who excreted it in the same unchanged quantity in urine without transferring iron to the body. Wöhler realized that the iron was bound with exceptional strength in FOB, and if iron-free FOB could be produced, it should remove iron from the body of patients with different pathologies. In the same year, Bickel *et al.* obtained DFO. Its protein targets were determined before testing it on animals to assess whether it could remove iron from hemoglobin [42]. As it removed iron only from ferritin and hemosiderin and not from hemoglobin and transferrin, clinical studies started. After promising results in animal studies, in mid-1961, Friedrich Wöhler used it to treat a patient with severe hemochromatosis, obtaining massive iron excretion in urine [43]. Later, twenty-two patients were treated successfully in the following year, after which DFO was registered in Switzerland in June 1963 and introduced into the market 2.5 years after its initial production.

In the case of copper chelating agents, we support and suggest the study of the seven attempts made to introduce new drugs; these were discovered by individual research workers and are presented in a fascinating paper by Walshe [44]. He reports inter alia his strong contribution to the treatment of Wilson's disease. This work deserves consideration for the attractive and captivating depiction of pharmacological research fifty years ago. In particular, Walshe points out that "There is, therefore, still a role for the individual researcher to make significant advances, although these are likely to remain confined to the treatment of rare diseases."

We will consider in detail some of the above-sketched requirements.

**(1)** − Chelating drugs generally present toxic side effects and should not be used if the risk is greater than the benefit. These toxic effects are of crucial concern in those diseases that require life-long treatment. Toxicity data ($LD_{50}$) in rats and mice for some chelating agents in clinical use are reported in Table **3**.

**Table 3. Toxicity data (LD$_{50}$) in rats and mice for some chelating agents in clinical use.**

| Chelating Agent | LD$_{50}$ mg/Kg | Species | Refs |
|---|---|---|---|
| Dimercaprol (BAL) | I.P. 105, S.B. 2000, I.M. 87 | rat | [45] |
| CaNa$_2$EDTA | O. 10000, I.P. 3850, I.V. 3000<br>I.P. 4500 | rat<br>mouse | [46] |
| Deferiprone (DFP) | O. 2000, I.P. 600<br>I.P. 983 | rat<br>mouse | [47] |
| Deferoxamine mesylate (DFO) | O. > 1000, I.V. 520<br>O. > 3000, I.V. 340 | rat<br>mouse | [48] |
| Unithiol (DMPS) | I.P. 1140 | rat | [49] |
| Succimer (DMSA) | O. > 5011 I.P. 500, S.B. 1725 | mouse | [50] |
| Penicillamine (D-pen) | I.P. 2080, S.B. 4020, I.V.: 2000<br>O. 720, I.P. 298, S.B. 3810, I.V. 3840 | rat<br>mouse | [51] |
| Deferasirox (Exjade) | O. 1000, I.V.150<br>O. >500 | mouse<br>rat | [45] |
| Triethylenetetramine (Trien) | I.P. 468, I.V. 350 | mouse | [46] |

**Abbreviations:** O. oral, I.P. intraperitoneal, I.M. intramuscular, I.V. intravenous, S.B. subcutaneous.
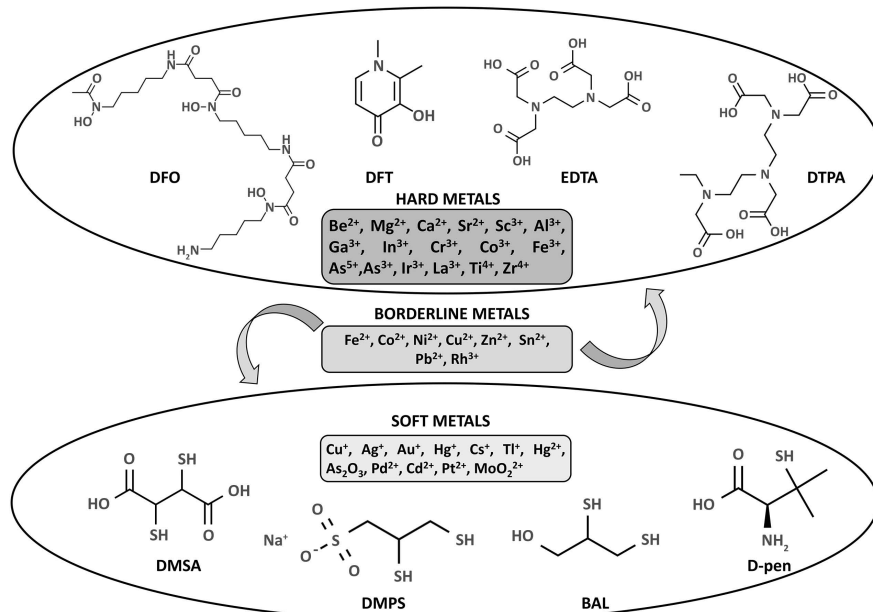


**Fig. (2).** Hard, borderline and soft metal ions (Lewis acid) and the preferable chelating agent (Lewis base) with potential higher affinity based on the HSAB theory.

As far as the toxicity of the formed complexes is concerned, some unwanted effects must be taken into account. As an example, the increase of intestinal absorption of the metal when the complex is formed in the gut or the redistribution of complexed metal ions to more dangerous sites (*e.g.*, complexation can favor the transit of the metal ion through the blood-brain barrier (BBB), entering the nervous system).

**(2)** − Chemical affinity of the chelating agent: The target metal ion (Lewis acid) and the chelat-ing agent (Lewis base) must present high affinity. Therefore, soft metal ions like Ag$^+$, Au$^+$, Cu$^+$, Hg$^{2+}$, Cd$^{2+}$, Pb$^{2+}$, and Pt$^{2+}$ should be treated with soft ligands, such as meso-2,3 dimercapto-succinic acid (DMSA), 2,3-dimercapto-1-propa-nesulfonic acid (DMPS), or D-penicillamine, while hard metal ions, such as Fe$^{3+}$, Al$^{3+}$, Cr$^{3+}$ with hard ligands, such as DFO and de-feriprone (DFP), or ethylenediaminetetraacetic acid (EDTA) and diethylenetriaminepentaacetic acid (DTPA). Both hard and soft bases can be

used for the treatment of intermediate metal ions as $Fe^{2+}$, $Ni^{2+}$, $Co^{2+}$, and $Zn^{2+}$ (Fig. **2**). High stability of the formed complexes is required both at physiological pH and at the acidic pH of urines.

When the formation of the complex between the chelating agent and target metal ion is considered *in vivo*, complex formation is a competitive reaction between proton and metal ion for the same basic sites on the ligand. Therefore, a comparison of the binding effectiveness of the chelating agent toward a metal ion cannot only be based on the stability constant, but the pM measure must be better generally used. This is defined as $-\log[M_f]$ at $[M_T] = 1\ \mu M$ and $[L_T] = 10\ \mu M$ at pH 7.4, $[M_f]$ being the concentration of free metal ion and $[M_T]$ and $[L_T]$ the total concentrations of metal and ligand, respectively. In the model for the calculation of pM, the protonation constants of the ligand and the formation constants of all formed complexes have to be taken into account. The hydroxide formation constants, instead, must not be considered, otherwise, all the ligands for which $[M_f]$ is greater (and pM lower) than that due to the hydroxide formation should result with a similar pM. The definition of pM is useful as a first insight on the chelating properties of a ligand, but a more realistic evaluation can be achieved based on the knowledge of the actual conditions of use.

**(3)** ― The toxic metal ion, either in plasma or in tissues, is generally bound to endogenous molecules, ranging from large macromolecules, such as transferrin and albumin, to small ligands, such as the citrate. The kinetic features of the exchange reaction between endogenous ligands and chelating agents mainly depend on the kinetic characteristics of the toxic metal ion, so slow reactions are predictable for metals like aluminum, chromium, and palladium.

The solubility and lipophilic features can prevent a chelating agent from reaching the intracellularly-bound target metal ion so that it can act only on the circulating toxic species. Once the circulating amount of the metal ion is chelated and excreted, a slow equilibrium between the intracellular-bound and circulating toxic metal ion is re-established. The kinetic of this equilibrium will decide the periodicity of the chelation treatment.

**(4)** ― Selectivity must be considered, *i.e.*, the ability of a chelator to form complexes with the target metal ion characterized by stability constants of several orders higher than those for the

other metal ions. In particular, the chelator should exhibit selectivity for the target metal ion in comparison to the essential ones, whose homeostasis should not be perturbed. Consequently, the relative amounts of the target and the physiological metal ions play an important role.

**(5)** ― The three key parameters like molecular size, lipophilicity, and net charge are responsible for the diffusion through biological membranes. In detail, the maximum allowed molecular weight for the absorption of a drug in the human gut is 500 g/mol [52]. Lipophilicity is evaluated by the water–octanol partition coefficient (P). Lipinski *et al.* [52] adopted a four-parameter analysis to predict membrane permeability, and their guidelines state that a limited absorption is expected when:

- The molecular weight is less than 500 g/mol;
- $\log P > 5$;
- More than 10 hydrogen bond donors are present in the molecule (as the sum of -OH and -NH groups);
- More than 10 hydrogen bond acceptors are present in the molecule (as the sum of O and N atoms).

Nowadays useful computational methods, such as the *QikProp* program or *Maestro* software [53, 54], allow the calculation with a reliable approximation of a number of the descriptors of the pharmacokinetic profile of the ligand molecule starting from its structural formula.

**(6)** ― A number of chelating agents in use are metabolized in the body to species that do not possess the chelating properties of the parent molecule. These metabolic reactions span, for example, from the glucuronidation of hydroxypyrydinones, to the acetylation of trien, or the formation of –S-S- bonds between 2,3-Dimercaptopropanol (BAL) and SH-containing ligands. When the metabolic transformation is rapid, a correct choice of the way of drug administration is of primary importance.

**(7)** ― The toxic action of a redox-active metal ion, such as $Fe^{3+}$ taken as an example, is related to the formation of ROS, which causes significant damages to tissues [55, 56].

To prevent these reactions in the organism, appropriate iron-binding proteins control the quantity of un-

bound iron. Nonetheless, iron can be mobilized from these proteins in metal imbalance conditions, taking part in redox reactions with ROS generation. In such situations, the iron redox potential can be controlled by proper chelating agents, which avoid ROS production. Siderophore molecules, with high selectivity for $Fe^{3+}$, prevent redox cycling of iron at biological conditions [57, 58]. On the contrary, when nitrogen-based ligands are used, characterized by lower redox potentials, coordinated iron is no longer protected and can be enzymatically reduced. In the case of iron complexes with the chelating agents in use, deferoxamine, deferiprone, and deferasirox, the redox potential values indicate that the ferrous oxidation state is inaccessible to biological reductants in the presence of these three chelating agents. In this way, the chelating agent exerts a protective action by preventing the metal ion from taking part in the formation of ROS when circulating in plasma before excretion.

> **(8)** ─ The same parameters illustrated for the absorption of the chelating agent into cells are also valid for the excretion of the formed metal complex. The formation of a neutral complex is of vital importance. For instance, in the case of $Fe^{3+}$ complexes, the use of a chelating agent is advisable characterized by mono charged coordinating groups (as $-CO-CO^-$ or $-CO-NO^-$ hydroxypyrydinones or hydroxamates) instead of two negatively charged groups ($-CO^--CO^-$ or $CO^--COO^-$ catechols or salicylates). The first ones lead to easily uncharged excretable complexes, and the second ones to negatively charged $[FeL_3]^{3-}$ complexes.

In the following section, some examples of toxic metals are discussed together with the indications of the currently available treatments/interventions based on chelation therapy.

## 5. TOXIC METALS

### 5.1. Mercury

Mercury is a chemical element with symbol Hg, standard atomic weight 200.59 g/mol, and atomic number 80, placed in the Group 12 of the periodic table, with electronic configuration $[Xe] \, 4f^{14} \, 5d^{10} \, 6s^2$. The oxidation states are 0, +1, +2.; it is highly soluble in polar and non-polar solvents. Mercury in water solution can reach the concentration of 0.6 μg/L at 25 °C. Mercury, of a silvery color, occurs in the liquid state (Hg) at room temperature (hence its name of quicksilver), and it can form inorganic compounds in the oxidation state

+2 ($Hg^{2+}$) and organic ones in the oxidation state +1 ($Hg^+$) [59].

The employment of mercury dates back to the Egyptian age. Ancient Greeks and Romans used Hg in ointments and cosmetics. Since the most abundant mineral of mercury is cinnabar (mercury sulfide), the mines in Almadén (Spain) dominated mercury production for over 500 years in Europe, together with other (minor) deposits in Italy and Slovenia, Perù, Mexico, and California in America, China in Asia and Algeria in Africa [60]. However, the growth of mercury production took place during the World Wars because of the consumption of explosives in the war industry for the preparation of a primary explosive, mercury(II) fulminate ($Hg(CNO)_2$) [61].

After the release of Hg containing wastes into Minamata Bay in Japan (between 1948 and 1960), and after the contamination of grain seeds with organomercury fungicides used for flour production in Iraq (in 1972), there has been great concern regarding mercury toxicity, and since then, it has been recognized that the several pathways of mercury contamination through the air, water, food, *etc.*, represent a serious health problem. Consequently, there has been a banning of different mercury application, such as dental amalgamation in China and Russia (1985 and 1990), pesticides in the USA (1993), until the Protocol on Heavy Metals (cadmium, lead, and mercury) was signed in 1998 by different countries, followed by the 2005 EU Mercury Strategy. Finally, the Minamata Convention on Mercury, a global treaty to preserve human health and the environment that includes the interdiction of new mines, the removal of existing ones, and the control measures on air emissions, was signed in 2013 [62].

The US Agency for Toxic and Disease Registry includes mercury in the list of substances that can cause the most significant problems to human health for its toxicity. Human exposure can occur by inhalation, both orally and through the skin, each one with different symptoms and consequences, as discussed below [27, 63]. From a chemical point of view, mercury toxicity mainly depends on the formation of covalent bonds with sulfur atoms of proteins and from the substitution of hydrogen atoms of proteins to form mercaptides, deactivating several essential enzymes and altering their biological functions [64, 65].

Mercury emissions from coal smoke and industrial processes are the main source of discharge and pollution. For quantification of exposure, it has been taken into account that in the presence of liquid Hg, the sur-

rounding non-ventilated air can reach 20 mg/m$^3$ of monoatomic mercury vapors. Considering that 15/20 m$^3$ of air can be inhaled daily, a full-time worker may inhale 100 - 135 mg of Hg. Due to their high liposolubility, mercury vapors are absorbed by the lungs, then enter the blood flow where they can be oxidized to Hg$^{2+}$, after which they are excreted in the urine or they cross the BBB, entering the central nervous system. Because of the large retention time, symptoms may appear after many years, such as memory loss, cerebral blindness, deafness, and palsy.

Chelation therapy can be used for the treatment of mercury intoxication [66]. On the basis of literature data from 1991 to 2015, related to the clinical treatment of mercury poisoned patients, Andersen indicated that DMPS and DMSA are more efficient than D-penicillamine and BAL in the treatment of mercury intoxication because of both oral and I.V. administration, repeated courses of chelation for long times, and low incidence of adverse effects [34]. An increasing number of human cases clearly suggests that DMPS is the optimum chelating agent in acute and chronic intoxication with inorganic mercury compounds.

## 5.2. Lead

Lead (Pb) is a bluish-grey, soft, dense metal (11.34 g/mL) in Group 14 of the periodic table of the elements with electronic configuration [Xe] 4$f^{14}$ 5$d^{10}$ 6$s^2$ 6$p^2$, standard atomic weight 207.19 g/mol. The oxidation states are 0, +2, +4. Historically, lead was employed since ancient times in plumbing, and its environmental pollution dates back to Bronze Age. Large quantities of lead, both as metal and oxide, are used in storage batteries. Lead has been utilized in ammunitions, solder and as a roofing material, in cable covering, as electrodes, shields for radiation in X-ray rooms and nuclear reactors. Lead oxide is also employed in the production of the best quality crystal glass. The organic lead (tetraethyl-lead; TEL) was in use for many decades as an anti-knock petro-fuel additive. All these uses have been drastically reduced because of the environmental alarms on lead toxicity. Although lead is one of the most useful metals, in use for more than three thousand years, it is also one of the most dangerous for humans and the environment [67].

Lead is present in the environment from natural sources, but it primarily derives from all the human uses outlined above. Occupational exposure mainly occurs in the manufacturing of lead batteries and in the production of iron, steel, and nonferrous alloys. Pain-

ters, such as Goya, suffered from inhalation and accidental ingestion of Pb$^{2+}$ from paints. Benjamin Franklin diagnosed himself as a "lead colic" because of his long exposure to lead type used in printing [62]. The general population is mainly exposed through food, drinking water, and air. Old lead-based paints, cosmetics and hair dyes, and certain non-Western cosmetics represent other important sources of exposure. Exposure to Pb$^{2+}$ can cause a variety of toxic effects that depend both on the way of exposure and the dose. The effects of lower exposures are on the nervous system; those of higher exposures produce gastrointestinal symptoms, known as lead colic. Extremely high acute exposures can lead to encephalopathy, which can be fatal, often observed in children. Exposure to high levels of lead can give rise to anemia, renal dysfunction with related high blood pressure, and an increased risk of cardiovascular diseases and stroke [67]. Lead poisoning in childhood represents a severe health problem in population groups who live in low-standard housing, and it is the most common avoidable childhood disease in the USA. Lead paints in old houses are the major source of lead exposure in childhood. Even if the exposed children do not present clinical symptoms of lead intoxication, nevertheless they are at risk of future irreversible neuropsychological diseases [68].

Lead exerts its toxicity toward different organs (*e.g.*, kidneys, bones, heart) and the nervous system, hindering numerous body processes. Lead interaction with the nervous system is the cause of behavior and learning disorders in children. Chronic toxicity can provoke renal failure, gout, anemia, and disorders of the nervous system, including brain damage in children. The effects are more serious for patients who are deficient in calcium, zinc, or iron. Pb$^{2+}$ ions affect the structure and function of bone marrow, where they exert an inhibitory action towards numerous enzymes involved in the synthesis of hemoglobin.

After absorption, lead enters the blood mostly bound to erythrocyte proteins with an average clearance half time of 35 days [69, 70], and it is distributed to soft tissues (liver, kidney, brain, and bone marrow) and bones. The body burden of lead is largely (about 95%) found in bones, with a half-life from years to decades [71]. Lead excretion occurs mainly through kidneys and in limited amounts through feces, sweat, and hair. Since lead can easily cross both BBB and placenta, the brain and the developing fetus can be largely affected by led poisoning [71, 72].

Despite the global efforts to control lead exposure, lead intoxication is still of great concern both in developed and developing countries. In chronic intoxication

(saturnism), lead is bound to thiol and carboxyl groups of various proteins, thereby hindering the normal functioning of different enzymes [73-75]. The determination of lead content in blood and protoporphyrin in erythrocytes allows ascertaining lead intoxication.

The conventional chelating agents in the treatment of acute and chronic lead intoxication were BAL, D-penicillamine, and Ca-EDTA. The introduction of DMSA, characterized by low toxicity and high efficiency, has drastically reduced the use of these ligands. DMSA is, at the moment, the first-choice chelator in low and moderate lead intoxication, being the best tolerated and the least toxic chelator for lead. Furthermore, it can be given orally or by intravenous administration [66].

### 5.3. Cadmium

Cadmium (Cd), atomic number 48 in Group 12 in the periodic table, has electronic configuration [Kr] $4d^{10} 5s^2$ and standard atomic weight 112.41 g/mol. It presents the 0, +1, and +2 oxidation states, but only $Cd^{2+}$ metal ions are stable under normal temperatures and pressures. The ionic radius 0.97 Å of $Cd^{2+}$, almost equal to that 0.99 Å of $Ca^{2+}$ and 1.02 Å of $Na^+$, explains the substitution of these two ions by $Cd^{2+}$ in their mineral forms, particularly $Ca^{2+}$ ions in bones.

The most significant properties of this metal, high electrical conductivity, great resistance to corrosion, and low melting point, determine its disparate industrial applications, ranging from metal production to anticorrosive materials, electronic components, plastic stabilizers, nickel-cadmium batteries, and paints and pigments. The uses of cadmium have been drastically reduced due to its significant environmental toxicity [76, 77]. The same as mercury and lead, it accumulates both in the body and in the environment, producing longstanding damages. The toxicity of cadmium in humans displays in a multiplicity of diseases, such as hypertension, hepatic and renal dysfunctions, reproductive effects, bone defects, and lung injuries. The International Agency for Research on Cancer (IARC) classifies cadmium as a class 1 human carcinogen, which causes tumors in the prostate, lung, kidney, and pancreas [78-80]. Acute cadmium intoxication affects mainly the liver, being hepatotoxicity the main cause of mortality [81-83]. Cadmium, after the systemic entrance, binds to metallothionein (MT) in the liver; then, the MT-Cd complex is transferred to the kidneys through the bloodstream [84]. In the kidneys, cadmium is, in part, excreted with urine and in part, accumulates with an extremely long half-life of 10 − 30 years [73]. The presence of $Cd^{2+}$ in the blood is a signal of exist-

ing exposure, while its presence in urines is an indication of chronic exposure.

Chronic weak cadmium intoxication is determined by particular situations of environmental and occupational cadmium pollution [77]. The common population is exposed by breathing cigarette smoke or eating cadmium-containing food (seafood, grains, leafy vegetables, and potatoes) [85]. The Itai-Itai disease that occurred in Japan, in the Jinzū river basin, in the fifties of the last century, is exemplificative of the dangerousness of this metal ion [86, 87]. The water of Jinzu River, highly contaminated by cadmium-rich industrial wastes, was used for rice irrigation. The surrounding population that systematically consumed this cadmium-containing rice developed the Itai-Itai disease, characterized by multiple fractures and distortion of the long bones. The amount of absorbed cadmium is greatly determined by the nutritional status, the absorption being low in people with a regular content of essential metal ions (zinc, iron, and calcium); the low body iron content determined the high incidence of Itai-Itai disease in aged women [88]. A period of 17 years had to pass from the first medical studies on humans to the setting of legal responsibilities of the mining company that discharged the cadmium by-product, polluting a river used for irrigation and drinking [89].

Suitable clinical chelation treatment is necessary to remove cadmium deposits from the liver and kidney. A variety of chelating agents have been taken into consideration [34]. The great problem in chelation therapy for cadmium toxicity is that individuals with hepatic and renal cadmium overload often suffer from minimal renal damage (reduced capacity of proximal tubular absorption with augmented urinary loss of calcium), a not-serious disease that favors, however, the development of severe renal diseases and osteomalacia.

A literature survey on the treatment of cadmium poisoning with chelating agents shows that cases of cadmium intoxication are extremely rare. The single case of clinical treatment of a patient with chronic cadmium intoxication presented by Gil *et al.* [90] suggests that GSH administration along with the chelating agent Ca-EDTA could represent a possible treatment for cadmium intoxication. The rarity of cadmium intoxication has so far prevented the establishment of a clinical schedule for cadmium chelation. Nevertheless, animal studies have demonstrated that oral chelators, EDTA, DTPA, DMSA, and DMPS, can be considered effective antidotes in cadmium poisoning.

### 5.4. Chromium

Chromium (Cr) is a brittle, hard, silver-gray metal, with the atomic number 24 in Group 6 of the periodic

table of the elements, electronic configuration [Ar] $3d^5$ $4s^2$, and standard atomic weight 51.99 g/mol. It can assume different oxidation states: -2, 0, +2, +3, +6, the most frequent being +3 and +6. Chromium is naturally found in fruits, vegetables, cheese, meat, grain, and wine. Its inorganic compounds are absorbed by humans in the intestine in a range of 0.4–3% [91].

The main uses of chromium are in chrome plating and steel production. Chromium compounds, primarily those of hexavalent chromium (chromates, dichromates, and chromium trioxide), have a diversity of applications, such as catalysts, pigments, mordants for dyeing, leather tanning, and wood preservation.

Chromium is found in all the environmental elements (air, water, and soil) and under physiological conditions and the common oxidation states are Cr(III) and Cr(VI) as a result of natural processes and human activities; Cr(VI) is present as chromate ($CrO_4^{2-}$) at pH 7. Occupational exposure is mainly related to the hexavalent compounds chromates and dichromates. The structural similarity of chromate with sulfate anion makes it possible that chromate can overcome membrane barriers and then reach the nucleus. Inside the cellular nucleus, $CrO_4^{2-}$ ions can oxidatively induce damages on genetically important compounds. Highly reactive Cr(VI) with one unpaired 3d electron can be formed and simultaneously induce the formation of radicals as RS· or OH·, which can attack DNA and affect genetic function.

The respiratory and dermal toxicity of chromium give rise to nasal irritation (at a concentration lower than < 0.01 mg/m$^3$), nasal ulcers, and perforation of the nasal septum. The oxidation state of chromium is of paramount importance in determining its toxicity, Cr(VI) being classified as a human carcinogen in Group 1 [92]. The mechanisms of chromium toxicity have been thoroughly examined in a recent review [93]. Most of the chelating agents in clinical use have been considered in experimental animal studies, while the clinical studies on chromium intoxication are relatively rare. BAL and D-penicillamine did not present positive effects, and the results on EDTA were rather contradictory. The hard chelating agents in use for the treatment of iron overload diseases, namely DFO, DFP, and deferasirox (DFX), were also proposed for the treatment of chromium poisoning, but the results on this topic are so far limited.

## 5.5. Nickel

Nickel (Ni) has the atomic number 28 in Group 10 of the periodic table of the elements, electronic configu-

ration [Ar] $3d^5 4s^2$, and atomic weight 58.69 g/mol. It presents the oxidation states 0, +2, +3. More than 70% of produced nickel is used in alloy manufacturing; the remaining is used in a variety of electrolytic processes, in batteries, welding procedures, as a catalyst, and in the glass and ceramic industry. About 43 million tons of nickel are annually released in the atmosphere as a result of anthropogenic activities, with respect to 8.5 million tons from natural sources.

The nickel content in surface water ranges from 2 to 20 µgL$^{-1}$, with the limit for nickel in drinking water being 0.07 mg L$^{-1}$ [94]. Despite some evidence that nickel may be an essential element for mammals, present in the human bloodstream at a concentration of 0.5 nM, no nickel-dependent enzyme has been so far detected in mammals [95, 96]. Nickel is extensively found both in working places and in the environment, so both occupational and environmental toxicities constitute an important health problem. Nickel toxicity is determined by the route of exposure and the solubility of its compounds [97]. Exposure to insoluble crystalline nickel compounds in working places represents a carcinogenic hazard. Workers in nickel industries exposed to concentration < 1 mg/m$^3$ of soluble nickel have no respiratory cancer risk, which is related, instead, to higher concentrations. While acute nickel poisoning is currently very rare, the most serious problem is related to the carcinogenicity of Ni$^{2+}$ compounds, classified as human carcinogens (Group 1) and as possibly carcinogenic to humans for metallic nickel (Group 2B) [98, 99]. Soluble nickel compounds are powerful skin allergens; 10 – 20% of the female and 1% of the male population present dermal sensitivity to nickel. Nickel is the most common cause of skin allergies both in exposed workers and in the general population [100, 101]. Contact hypersensitivity to nickel appears to be a result of the binding of Ni$^{2+}$ to specific histidine residues of the innate immune receptor 4 (TL-R4), which is then activated and triggers the inflammatory cytokine cascade [102, 103].

The routes of nickel uptake (gastrointestinal and skin absorption, inhalation) and its poisoning effects were thoroughly discussed by Genchi *et al.* [104]. Iatrogenic exposure, like implants and prostheses, radiographic contrast media, and intravenous or dialysis fluids, also represents a source of toxicity [105]. Cases of nickel poisoning also took place in chronic dialysis patients when nickel-polluted dialysate was used [106].

Recommended chelation therapy for nickel poisoning is sodium diethylcarbodithiolate (DDTC). DDTC

was considered useful in a huge number of human poisoning, although there is not a sufficient number of controlled human trials which support both its efficacy and lack of toxicity [107]. Disulfiram (1-(diethylthiocarbamoyldisulfanyl)-N,N-diethyl-methanethioamide), another nickel-chelating agent, was used in nickel dermatitis [108-110] and the case of nickel carbonyl poisoning [111]. However, due to its hepatotoxicity and possible redistribution of nickel to the brain, its use is controversial [110, 112]. According to Anderson, two approaches should be employed for nickel dermatitis: systemic chelation to reduce body stores and skin creams containing chelating agents to prevent the uptake of nickel into the skin [34]. A number of clinical studies pointed out the efficacy of diethyldithiocarbamate in some nickel allergic patients due to increased nickel excretion [113]. Unfortunately, as in the case of disulfiram, a fraction of patients developed hepatotoxicity [114-116]. Furthermore, the administration of diethyldithiocarbamate or disulfiram to mice caused an increase in brain nickel deposition of 700%, therefore, this chelation treatment has to be considered with care.

The clinical experience in nickel chelation is limited. Diethyldithiocarbamate (DDC) has proven to be an efficient chelating agent in nickel poisoning, and DDC and tetraethylthiuram disulfide (TTD) has been used to promote excretion of its overload in many clinical applications to lighten nickel dermatitis. In acute inorganic nickel poisoning, DDC can present deleterious effects since its administration can increase brain deposition of nickel. All the chelating agents, EDTA, D-penicillamine, DMPS, and DMSA, have been demonstrated to be efficacious chelators in animal studies [34, 117].

## 5.6. Arsenic

Arsenic (As) is the 53$^{rd}$ most abundant element in the earth's crust; it has the atomic number 33 in the Group 15 of the periodic table of the elements. Arsenic is a semimetal element with electronic configuration [Ar] $4s^2\,3d^{10}\,4p^3$, oxidation states -3, +2, +3, +5 and standard atomic weight 74.9216 g/mol. Arsenic presents various allotropes in nature, divided by colors (gray, black, yellow), but only the gray form is important for the industry. Most of the arsenic is indeed used in lead alloys (*e.g.*, car batteries and military sector), Cu compounds (*e.g.*, pigments) and semi-conductors. It is also a product of smelted mineral ores, such as Pb, Cu, and Ag. Arsenic in the atmosphere is trapped as the trioxide, $As_2O_3$. In developing countries, arsenic products are used as herbicides, pesticides, and insecticides, usually as arsenates. Arsenic production in-

creased by 25% every 10 years until 2018, when the global production was estimated at 35000 metric tons, with China (24000), Morocco (6000), Namibia (1900), and Russia (1500) as the world leaders in $As_2O_3$ production [118]. Arsenic is considered toxic for organisms because of its ability to block sulfhydryl (–SH) groups in enzymes. With this mechanism and others, arsenic has the ability to replace iodine, selenium, and phosphorus [119]. In addition, arsenic is able to block up to 200 enzymes, causing lipid peroxidation and defecting DNA synthesis and reduction [118]. The toxicity of arsenic is an important burden worldwide due to its large use in agricultural products; millions of people are exposed to this element through the food chain and herbal supplements, as well as through food processed with arsenic-contaminated water [120]. About 300 million people are exposed to arsenic-polluted aquifers, raising concerns in particular for the more sensitive population, such as pregnant women and children [121]. A safety standard arsenic limit recommended by WHO is 10 μg/l, and generally, water contains less than 1 μg As/l. In several countries, and in particular India, Bangladesh, and Vietnam, there are areas in which the arsenic level in water can reach and exceed the value of 5000 μg As/l. In the absence of an alternative water source, the tolerance limit in these regions has been increased to 50 μg As/l [118]. Several available technologies could be applied for arsenic removal from water as well as from contaminated soil. Among various techniques, which includes oxidation, coagulation-flocculation, adsorption, ion exchange, electrokinetics, the most effective appear to be electro-remediation, membrane technologies (such as ultra- micro- and nano-filtration), and phytoremediation [122]. An important source of exposure is tobacco smoke; this exposure comes from tobacco plants raised in arsenic-rich soil or treated with arsenic-rich products [123]. Arsenic toxicity can manifest in acute or chronic form. Symptoms of acute arsenic exposure include firstly a metallic taste in the mouth with a slight odor of garlic, associated with nausea, abdominal pain, vomiting, and diarrhea. These can evolve in cyanosis, convulsions, hypotension, pulmonary edema until death from heart failure, which can occur in the first few hours from the intoxication, while later on, death can occur from acute renal or liver failure [124]. Arsenic is subject to accumulation phenomena in the organism, leading to multi-systemic disease in case of chronic poisoning. Many organs are involved in arsenic chronic poisoning: heart, lungs, kidneys, liver, spleen, nervous system, gastrointestinal tract, and muscle tissue. The first deposit of arsenic in the organism occurs in keratin tissues, such as hair and nails. Then it starts concentrating in the liv-

er and kidneys, manifesting the highest levels of concentration in the body [124]. The heart damage is due to the reduced activities of antioxidant enzymes: SOD, CAT, glutathione S-transferase (GST), glutathione reductase (GR), and glutathione peroxidase (GPx) [125]. It is important to consider that arsenic can cause neuropathy and polyneuropathy, which often initiate with symptoms of irritation of the nerve trunks. When the pathology advances, ataxia, hyperpathia, and sharp pains in the extremities occurs. Therefore, there is a progressive development of movement disorders, which start with muscle weakness and end with complete paralysis [118]. Moreover, both inorganic and organic arsenic compounds can pass the human placenta in late pregnancy, indicating a potential risk for the fetus. Abnormal pregnancy outcomes have been evidenced in communities that consume water with a high concentration of As (above 50 μg/l) [126]. Despite several chelating agents are available for the treatment of acute arsenicosis, there is currently no effective and safe chelating agent for the treatment of chronic arsenic poisoning [118, 127]. Antidotes, such as BAL, DMPS, and DMSA, should be more effective due to the high affinity of arsenic towards vicinal dithiols in cellular proteins. Between these choices, DMPS (orally or intravenously) appears the most promising therapy. In severe acute cases, a combined approach based on DMPS and BAL is recommended [127]. Furthermore, the use of DMPS has shown satisfactory results in some cases of chronic arsenic poisoning.

## CONCLUSION

In this review, we discussed the toxicity of non-essential metals considering their peculiar chemical characteristics, such as different forms, hard-soft character, oxidation states, binding capabilities, and solubility, which can influence their speciation in biological systems, and subsequently, the main cellular targets. Regarding toxicity, two groups of metals can be considered: those for which only negative effects have been found so far, and those that have not been considered essential for life due to their low availability in terms of poor solubility at physiological pH or due to their very low abundance on earth. Among the metals belonging to the former group, we found the thiophilic "soft" metals, such as mercury, lead, cadmium, or the "hard" metals, such as chromium. Some of them, such as lead and mercury, are very ancient environmental contaminants; lead is the oldest known toxic metal, while mercury has been cited to describe the mortality rate of workers in mercury mines by Pliny the Elder. In addition, lead is also known to experience one of the largest anthropogenic increase in the environment.

Some of other potentially toxic metals such as Sb, Bi, Zr, Ag, Th, lanthanoides are quite insoluble under physiological conditions (pH 7), oxidizing atmosphere, together with a high chloride concentration. However even essential metal ions can be poisonous if their dose is high enough.

In general, toxic metals can tightly coordinate to important biological molecules to active sites (oxygen, nitrogen or sulfhydryl groups) or replace natural metal centers by foreign metals that have similar, although not identical, characteristics; for example, Pb or Cd for Ca in bone tissues or Cd for Zn in enzymes.

A particular focus has been given to selected toxic metals proving indications on possible treatments/interventions on metal poisoning based on chelation therapy. Therapeutic detoxification, through complexation of toxic metal ions by specific chelating agents, appears an efficacious clinical strategy mainly in acute cases of metal intoxication.

## LIST OF ABBREVIATIONS

IUPAC = The International Union of Pure and Applied Chemistry

NPs = Nanoparticles

MT = Metallothionein

SOD = Superoxide Dismutase

CAT = Catalase

GSH = Glutathione

DFO = Desferrioxamine

BBB = Blood-Brain Barrier

DFX = Deferasirox

DDTC = Diethylcarbodithiolate

TTD = Tetraethylthiuram Disulfide

## CONSENT FOR PUBLICATION

Not applicable.

## FUNDING

## CONFLICT OF INTEREST

The authors declare no conflict of interest, financial or otherwise.

## ACKNOWLEDGEMENTS

## REFERENCES

[1] Zoroddu, M.A.; Aaseth, J.; Crisponi, G.; Medici, S.; Peana, M.; Nurchi, V.M. The essential metals for humans: a brief overview. *J. Inorg. Biochem.,* **2019**, *195*, 120-129.
http://dx.doi.org/10.1016/j.jinorgbio.2019.03.013 PMID: 30939379

[2] Lontie, R. *Copper proteins and copper enzymes,* 2nd ed; CRC Press: Boca Raton, **2018**.

[3] Chasapis, C.T.; Ntoupa, P.A.; Spiliopoulou, C.A.; Stefanidou, M.E. Recent aspects of the effects of zinc on human health. *Arch. Toxicol.,* **2020**, *94*(5), 1443-1460.
http://dx.doi.org/10.1007/s00204-020-02702-9 PMID: 32394086

[4] Andreini, C.; Bertini, I.; Cavallaro, G.; Holliday, G.L.; Thornton, J.M. Metal ions in biological catalysis: from enzyme databases to general principles. *J. Biol. Inorg. Chem.,* **2008**, *13*(8), 1205-1218.
http://dx.doi.org/10.1007/s00775-008-0404-5 PMID: 18604568

[5] Umair, M.; Alfadhel, M. Genetic disorders associated with metal metabolism. *Cells,* **2019**, *8*(12), 1598.
http://dx.doi.org/10.3390/cells8121598 PMID: 31835360

[6] Wessels, I. Epigenetics and metal deficiencies. *Curr. Nutr. Rep.,* **2014**, *3*(3), 196-203.
http://dx.doi.org/10.1007/s13668-014-0091-5

[7] Lachowicz, J.I.; Nurchi, V.M.; Fanni, D.; Gerosa, C.; Peana, M.; Zoroddu, M.A. Nutritional iron deficiency: the role of oral iron supplementation. *Curr. Med. Chem.,* **2014**, *21*(33), 3775-3784.
http://dx.doi.org/10.2174/0929867321666140706143925 PMID: 25005180

[8] Maret, W.; Sandstead, H.H. Zinc requirements and the risks and benefits of zinc supplementation. *J. Trace Elem. Med. Biol.,* **2006**, *20*(1), 3-18.
http://dx.doi.org/10.1016/j.jtemb.2006.01.006 PMID: 16632171

[9] Jaishankar, M.; Tseten, T.; Anbalagan, N.; Mathew, B.B.; Beeregowda, K.N. Toxicity, mechanism and health effects of some heavy metals. *Interdiscip. Toxicol.,* **2014**, *7*(2), 60-72.
http://dx.doi.org/10.2478/intox-2014-0009 PMID: 26109881

[10] Hammond, C.R. The elements. *Handbook of chemistry and physics*; , **2000**, 81, .

[11] McNaught, A.D.; Wilkinson, A. *Compendium of chemical terminology*; Blackwell Science: Oxford, **1997**.

[12] Pearson, R.G. Hard and soft acids and bases. *J. Am. Chem. Soc.,* **1963**, *85*(22), 3533-3539.
http://dx.doi.org/10.1021/ja00905a001

[13] Jolly, W.L. *Modern inorganic chemistry*; McGraw-Hill College: New York City, **1984**.

[14] Pearson, R.G. Hard and soft acids and bases, HSAB, part 1: fundamental principles. *J. Chem. Educ.,* **1968**, *45*(9), 581.
http://dx.doi.org/10.1021/ed045p581

[15] Zoroddu, M.A.; Medici, S.; Ledda, A.; Nurchi, V.M.; Lachowicz, J.I.; Peana, M. Toxicity of nanoparticles. *Curr. Med. Chem.,* **2014**, *21*(33), 3837-3853.

http://dx.doi.org/10.2174/0929867321666140601162314 PMID: 25306903

[16] Crisponi, G.; Nurchi, V.M.; Lachowicz, J.I.; Peana, M.; Medici, S.; Zoroddu, M.A. *Antimicrobial Nanoarchitectonics*; Grumezescu, A.M., Ed.; Elsevier: Amsterdam, **2017**, pp. 511-546.
http://dx.doi.org/10.1016/B978-0-323-52733-0.00018-5

[17] Ferreira, C.R.; Gahl, W.A. Disorders of metal metabolism. *Transl. Sci. Rare Dis.,* **2017**, *2*(3-4), 101-139.
http://dx.doi.org/10.3233/TRD-170015 PMID: 29354481

[18] Bolognin, S.; Messori, L.; Zatta, P. Metal ion physiopathology in neurodegenerative disorders. *Neuromolecular Med.,* **2009**, *11*(4), 223-238.
http://dx.doi.org/10.1007/s12017-009-8102-1 PMID: 19946766

[19] Chen, Q.Y.; DesMarais, T.; Costa, M. Metals and mechanisms of carcinogenesis. *Annu. Rev. Pharmacol. Toxicol.,* **2019**, *59*, 537-554.
http://dx.doi.org/10.1146/annurev-pharmtox-010818-021031 PMID: 30625284

[20] Smith, D.R.; Nordberg, M. Chapter 2 - General Chemistry, Sampling, Analytical Methods, and Speciation. In: *Handbook on the Toxicology of Metals (Fourth Edition)*; Nordberg, G.F.; Fowler, B.A.; Nordberg, M., Eds.; Academic Press: San Diego, **2015**; Vol. 1, pp. 15-44.
http://dx.doi.org/10.1016/B978-0-444-59453-2.00002-0

[21] Kazantzis, G. Cadmium, osteoporosis and calcium metabolism. *Biometals,* **2004**, *17*(5), 493-498.
http://dx.doi.org/10.1023/B:BIOM.0000045727.76054.f3 PMID: 15688852

[22] Klaassen, C.D.; Liu, J.; Diwan, B.A. Metallothionein protection of cadmium toxicity. *Toxicol. Appl. Pharmacol.,* **2009**, *238*(3), 215-220.
http://dx.doi.org/10.1016/j.taap.2009.03.026 PMID: 19362100

[23] Templeton, D.M.; Ariese, F.; Cornelis, R.; Danielsson, L.-G.; Muntau, H.; van Leeuwen, H.P.; Lobinski, R. Guidelines for terms related to chemical speciation and fractionation of elements. Definitions, structural aspects, and methodological approaches (IUPAC Recommendations 2000). *Pure Appl. Chem.,* **2000**, *72*(8), 1453-1470.
http://dx.doi.org/10.1351/pac200072081453

[24] Ems, T.; St Lucia, K.; Huecker, M.R. M.R. In StatPearls: Treasure Island, FL, **2020**.

[25] Zhao, N.; Enns, C.A. Chapter Three - Iron Transport Machinery of Human Cells: Players and Their Interactions. In: *Current Topics in Membranes*; Argüello, J.M.; Lutsenko, S., Eds.; Academic Press: Amsterdam, **2012**; Vol. 69, pp. 67-93.
http://dx.doi.org/10.1016/B978-0-12-394390-3.00003-3

[26] Czarnek, K.; Terpiłowska, S.; Siwicki, A.K. Selected aspects of the action of cobalt ions in the human body. *Cent. Eur. J. Immunol.,* **2015**, *40*(2), 236-242.
http://dx.doi.org/10.5114/ceji.2015.52837 PMID: 26557039

[27] Bjørklund, G.; Peana, M.; Dadar, M.; Chirumbolo, S.; Aaseth, J.; Martins, N. Mercury-induced autoimmunity: drifting from micro to macro concerns on autoimmune disorders. *Clin. Immunol.,* **2020**, *213*, 108352.
http://dx.doi.org/10.1016/j.clim.2020.108352 PMID: 32032765

[28] Hong, Y.S.; Kim, Y.M.; Lee, K.E. Methylmercury exposure and health effects. *J. Prev. Med. Public Health,* **2012**, *45*(6), 353-363.
http://dx.doi.org/10.3961/jpmph.2012.45.6.353 PMID:

23230465

[29]   Jomova, K.; Valko, M. Advances in metal-induced oxidative stress and human disease. *Toxicology,* **2011**, *283*(2-3), 65-87.
http://dx.doi.org/10.1016/j.tox.2011.03.001    PMID: 21414382

[30]   Lee, J.C.; Son, Y.O.; Pratheeshkumar, P.; Shi, X. Oxidative stress and metal carcinogenesis. *Free Radic. Biol. Med.,* **2012**, *53*(4), 742-757.
http://dx.doi.org/10.1016/j.freeradbiomed.2012.06.002
PMID: 22705365

[31]   Cicero, C.E.; Mostile, G.; Vasta, R.; Rapisarda, V.; Signorelli, S.S.; Ferrante, M.; Zappia, M.; Nicoletti, A. Metals and neurodegenerative diseases. A systematic review. *Environ. Res.,* **2017**, *159*, 82-94.
http://dx.doi.org/10.1016/j.envres.2017.07.048    PMID: 28777965

[32]   Bjørklund, G.; Dadar, M.; Chirumbolo, S.; Aaseth, J.; Peana, M. Metals, autoimmunity, and neuroendocrinology: is there a connection? *Environ. Res.,* **2020**, *187*, 109541.
http://dx.doi.org/10.1016/j.envres.2020.109541    PMID: 32445945

[33]   Bjorklund, G.; Peana, M.; Maes, M.; Dadar, M.; Severin, B. The glutathione system in Parkinson's disease and its progression. *Neurosci. Biobehav. Rev.,* **2020**, *120*, 470-478.
http://dx.doi.org/10.1016/j.neubiorev.2020.10.004  PMID: 33068556

[34]   Andersen, O. Chapter 4 - Chelation Treatment During Acute and Chronic Metal Overexposures-Experimental and Clinical Studies. In: *Chelation Therapy in the Treatment of Metal Intoxication*; Aaseth, J.; Crisponi, G.; Andersen, O., Eds.; Academic Press: Boston, **2016**; pp. 85-252.
http://dx.doi.org/10.1016/B978-0-12-803072-1.00004-3

[35]   Crisponi, G.; Nurchi, V.M.; Crespo-Alonso, M.; Toso, L. Chelating agents for metal intoxication. *Curr. Med. Chem.,* **2012**, *19*(17), 2794-2815.
http://dx.doi.org/10.2174/092986712800609742    PMID: 22455585

[36]   Crisponi, G.; Nurchi, V.M.; Lachowicz, J.I.; Crespo-Alonso, M.; Zoroddu, M.A.; Peana, M. Kill or cure: misuse of chelation therapy for human diseases. *Coord. Chem. Rev.,* **2015**, *284*, 278-285.
http://dx.doi.org/10.1016/j.ccr.2014.04.023

[37]   Crisponi, G.; Nurchi, V.M.; Silvagni, R.; Faa, G. Oral iron chelators for clinical use. *Polyhedron,* **1999**, *18*(25), 3219-3226.
http://dx.doi.org/10.1016/S0277-5387(99)00277-6

[38]   Nurchi, V.M.; Crisponi, G.; Lachowicz, J.I.; Medici, S.; Peana, M.; Zoroddu, M.A. Chemical features of in use and in progress chelators for iron overload. *J. Trace Elem. Med. Biol.,* **2016**, *38*, 10-18.
http://dx.doi.org/10.1016/j.jtemb.2016.05.010    PMID: 27365273

[39]   Yawalkar, S.J. Milestones in the research and development of desferrioxamine. *Nephrol. Dial. Transplant.,* **1993**, *8*(Suppl. 1), 40-42.
http://dx.doi.org/10.1093/ndt/8.supp1.40 PMID: 8389019

[40]   Bickel, H.; Bosshardt, R.; Gäumann, E.; Reusser, P.; Vischer, E.; Voser, W.; Wettstein, A.; Zähner, H. Stoffwechselprodukte von Actinomyceten. 26. Mitteilung. Über die Isolierung und Charakterisierung der Ferrioxamine A—F, neuer Wuchsstoffe der Sideramin-Gruppe. *Helv. Chim. Acta,* **1960**, *43*(7), 2118-2128.

http://dx.doi.org/10.1002/hlca.19600430731

[41]   Bickel, H.; Hall, G.E.; Keller-Schierlein, W.; Prelog, V.; Vischer, E.; Wettstein, A. Stoffwechselprodukte von Actinomyceten. 27. Mitteilung. Über die Konstitution von Ferrioxamin B. *Helv. Chim. Acta,* **1960**, *43*(7), 2129-2138.
http://dx.doi.org/10.1002/hlca.19600430732

[42]   Bickel, H.; Keberle, H.; Vischer, E. Stoffwechselprodukte von Mikroorganismen. 43. Mitteilung. Zur Kenntnis von Desferrioxamin B. *Helv. Chim. Acta,* **1963**, *46*(4), 1385-1389.
http://dx.doi.org/10.1002/hlca.19630460433

[43]   Woehler, F. [Therapy of hemochromatosis]. *Med. Klin.,* **1962**, *57*, 1370-1376.
PMID: 14007830

[44]   Walshe, J.M. The conquest of Wilson's disease. *Brain,* **2009**, *132*(Pt 8), 2289-2295.
http://dx.doi.org/10.1093/brain/awp149 PMID: 19596747

[45]   National Center for Biotechnology Information. PubChem Compound Summary for CID 3080, Dimercaprol. Available at: https://pubchem.ncbi.nlm.nih.gov/compound/Dimercaprol (Accessed Date: October, 15, 2020).

[46]   National Center for Biotechnology Information. PubChem Compound Summary for CID 6109, Calcium disodium ethylenediaminetetraacetate. Available at: https://pubchem.ncbi.nlm.nih.gov/compound/Calcium-disodium-ethylenediaminetetraacetate (Accessed date: October 15, 2020).

[47]   National Center for Biotechnology Information. PubChem Compound Summary for CID 2972, Deferiprone. Available at: https://pubchem.ncbi.nlm.nih.gov/compound/Deferiprone (Accessed date: October 15, 2020).

[48]   National Center for Biotechnology Information. PubChem Compound Summary for CID 62881, Deferoxamine mesylate. Available at: https://pubchem.ncbi.nlm.nih.gov/compound/Deferoxamine-mesylate (Accessed date: October 15, 2020).

[49]   National Center for Biotechnology Information. PubChem Compound Summary for CID 2724039, Unithiol. Available at: https://pubchem.ncbi.nlm.nih.gov/compound/Unithiol (Accessed date: October 15, 2020).

[50]   National Center for Biotechnology Information. PubChem Compound Summary for CID 2724354, Succimer. Available at: https://pubchem.ncbi.nlm.nih.gov/compound/Succimer (Accessed date: October 15, 2020).

[51]   National Center for Biotechnology Information. PubChem Compound Summary for CID 5852, Penicillamine. Available at: https://pubchem.ncbi.nlm.nih.gov/compound/Penicillamine (Accessed date: October 15, 2020).

[52]   Lipinski, C.A.; Lombardo, F.; Dominy, B.W.; Feeney, P.J. Experimental and computational approaches to estimate solubility and permeability in drug discovery and development settings. *Adv. Drug Deliv. Rev.,* **2001**, *46*(1-3), 3-26.
http://dx.doi.org/10.1016/S0169-409X(00)00129-0 PMID: 11259830

[53]   Schrödinger LLC QikProp *Version 2.5*; New York, **2005**.

[54]   Schrodinger Inc. Maestro *version 9.3*; Portland, OR, USA, **2012**.

[55]   Chaston, T.B.; Richardson, D.R. Interactions of the pyridine-2-carboxaldehyde isonicotinoyl hydrazone class of chelators with iron and DNA: implications for toxicity in the treatment of iron overload disease. *J. Biol. Inorg. Chem.,* **2003**, *8*(4), 427-438.
http://dx.doi.org/10.1007/s00775-002-0434-3    PMID: 12761664

[56]   Macáková, K.; Mladěnka, P.; Filipský, T.; Říha, M.; Ja-

hodář, L.; Trejtnar, F.; Bovicelli, P.; Proietti Silvestri, I.; Hrdina, R.; Saso, L. Iron reduction potentiates hydroxyl radical formation only in flavonols. *Food Chem.,* **2012**, *135*(4), 2584-2592.
http://dx.doi.org/10.1016/j.foodchem.2012.06.107 PMID: 22980846

[57] Olshvang, E.; Szebesczyk, A.; Kozłowski, H.; Hadar, Y.; Gumienna-Kontecka, E.; Shanzer, A. Biomimetic ferrichrome: structural motifs for switching between narrow- and broad-spectrum activities in *P. putida* and *E. coli. Dalton Trans.,* **2015**, *44*(48), 20850-20858.
http://dx.doi.org/10.1039/C5DT02685G PMID: 26459799

[58] Hider, R.C.; Kong, X. Chemistry and biology of siderophores. *Nat. Prod. Rep.,* **2010**, *27*(5), 637-657.
http://dx.doi.org/10.1039/b906679a PMID: 20376388

[59] Bjørklund, G.; Dadar, M.; Mutter, J.; Aaseth, J. The toxicology of mercury: current research and emerging trends. *Environ. Res.,* **2017**, *159*, 545-554.
http://dx.doi.org/10.1016/j.envres.2017.08.051 PMID: 28889024

[60] Hylander, L.D.; Meili, M. 500 years of mercury production: global annual inventory by region until 2000 and associated emissions. *Sci. Total Environ.,* **2003**, *304*(1-3), 13-27.
http://dx.doi.org/10.1016/S0048-9697(02)00553-3 PMID: 12663168

[61] Akhavan, J. *The chemistry of explosives*; Royal Society of Chemistry: Cambridge, **2011**.

[62] Crisponi, G.; Nurchi, V.M. *Encyclopedia of Inorganic and Bioinorganic Chemistry*; John Wiley & Sons, L., Ed., **2015**, pp. 1-14.
http://dx.doi.org/10.1002/9781119951438.eibc0126.pub2

[63] Clarkson, T.W.; Magos, L.; Myers, G.J. The toxicology of mercury--current exposures and clinical manifestations. *N. Engl. J. Med.,* **2003**, *349*(18), 1731-1737.
http://dx.doi.org/10.1056/NEJMra022471 PMID: 14585942

[64] Guzzi, G.; La Porta, C.A.M. Molecular mechanisms triggered by mercury. *Toxicology,* **2008**, *244*(1), 1-12.
http://dx.doi.org/10.1016/j.tox.2007.11.002 PMID: 18077077

[65] Vas, J.; Monestier, M. Immunology of mercury. *Ann. N. Y. Acad. Sci.,* **2008**, *1143*(1), 240-267.
http://dx.doi.org/10.1196/annals.1443.022 PMID: 19076354

[66] Cao, Y.; Skaug, M.A.; Andersen, O.; Aaseth, J. Chelation therapy in intoxications with mercury, lead and copper. *J. Trace Elem. Med. Biol.,* **2015**, *31*, 188-192.
http://dx.doi.org/10.1016/j.jtemb.2014.04.010 PMID: 24894443

[67] Skerfving, S.; Bergdahl, I.A. *Handbook on the Toxicology of Metals (Fourth Edition)*; Nordberg, G.F.; Fowler, B.A.; Nordberg, M., Eds.; Academic Press: San Diego, **2015**, pp. 911-967.
http://dx.doi.org/10.1016/B978-0-444-59453-2.00043-3

[68] Nussbaumer-Streit, B.; Yeoh, B.; Griebler, U.; Pfadenhauer, L.M.; Busert, L.K.; Lhachimi, S.K.; Lohner, S.; Gartlehner, G. Household interventions for preventing domestic lead exposure in children. *Cochrane Database Syst. Rev.,* **2016**, *10*(10), CD006047.
http://dx.doi.org/10.1002/14651858.CD006047.pub5 PMID: 27744650

[69] Rabinowitz, M.B. Toxicokinetics of bone lead. *Environ. Health Perspect.,* **1991**, *91*, 33-37.
http://dx.doi.org/10.1289/ehp.919133 PMID: 2040248

[70] O'Flaherty, E.J. Physiologically based models for bone-seeking elements. IV. Kinetics of lead disposition in humans. *Toxicol. Appl. Pharmacol.,* **1993**, *118*(1), 16-29.
http://dx.doi.org/10.1006/taap.1993.1004 PMID: 8430422

[71] Hu, H.; Shih, R.; Rothenberg, S.; Schwartz, B.S. The epidemiology of lead toxicity in adults: measuring dose and consideration of other methodologic issues. *Environ. Health Perspect.,* **2007**, *115*(3), 455-462.
http://dx.doi.org/10.1289/ehp.9783 PMID: 17431499

[72] Hu, H. Bone lead as a new biologic marker of lead dose: recent findings and implications for public health. *Environ. Health Perspect.,* **1998**, *106*(Suppl. 4), 961-967.
http://dx.doi.org/10.1289/ehp.98106s4961 PMID: 9703479

[73] Sinicropi, M.S.; Amantea, D.; Caruso, A.; Saturnino, C. Chemical and biological properties of toxic metals and use of chelating agents for the pharmacological treatment of metal poisoning. *Arch. Toxicol.,* **2010**, *84*(7), 501-520.
http://dx.doi.org/10.1007/s00204-010-0544-6 PMID: 20386880

[74] Kern, M.; Wisniewski, M.; Cabell, L.; Audesirk, G. Inorganic lead and calcium interact positively in activation of calmodulin. *Neurotoxicology,* **2000**, *21*(3), 353-363.
PMID: 10894125

[75] Bjørklund, G.; Crisponi, G.; Nurchi, V.M.; Cappai, R.; Buha Djordjevic, A.; Aaseth, J. A review on coordination properties of thiol-containing chelating agents towards mercury, cadmium, and lead. *Molecules,* **2019**, *24*(18), 3247.
http://dx.doi.org/10.3390/molecules24183247

[76] Remelli, M.; Nurchi, V.M.; Lachowicz, J.I.; Medici, S.; Zoroddu, M.A.; Peana, M. Competition between Cd(II) and other divalent transition metal ions during complex formation with amino acids, peptides, and chelating agents. *Coord. Chem. Rev.,* **2016**, *327-328*, 55-69.
http://dx.doi.org/10.1016/j.ccr.2016.07.004

[77] Nordberg, G.F.; Nogawa, K.; Nordberg, M.; Friberg, L.T. *Handbook on the Toxicology of Metals (Third Edition)*; Nordberg, G.F.; Fowler, B.A.; Nordberg, M.; Friberg, L.T., Eds.; Academic Press: Burlington, **2007**, pp. 445-486.
http://dx.doi.org/10.1016/B978-012369413-3/50078-1

[78] International Agency for Research on Cancer. *Beryllium, cadmium, mercury, and exposures in the glass manufacturing industry*; International Agency for Research on Cancer Lyon: France, **1993**.

[79] Waalkes, M.P. Cadmium carcinogenesis. *Mutat. Res.,* **2003**, *533*(1-2), 107-120.
http://dx.doi.org/10.1016/j.mrfmmm.2003.07.011 PMID: 14643415

[80] Järup, L.; Åkesson, A. Current status of cadmium as an environmental health problem. *Toxicol. Appl. Pharmacol.,* **2009**, *238*(3), 201-208.
http://dx.doi.org/10.1016/j.taap.2009.04.020 PMID: 19409405

[81] Goering, P.L.; Klaassen, C.D. Altered subcellular distribution of cadmium following cadmium pretreatment: possible mechanism of tolerance to cadmium-induced lethality. *Toxicol. Appl. Pharmacol.,* **1983**, *70*(2), 195-203.
http://dx.doi.org/10.1016/0041-008X(83)90095-9 PMID: 6623465

[82] Sauer, J.M.; Waalkes, M.P.; Hooser, S.B.; Kuester, R.K.; McQueen, C.A.; Sipes, I.G. Suppression of Kupffer cell function prevents cadmium induced hepatocellular necrosis in the male Sprague-Dawley rat. *Toxicology,* **1997**, *121*(2), 155-164.
http://dx.doi.org/10.1016/S0300-483X(97)00062-0 PMID:

9230447

[83]     El-Ashmawy, I.M.; Youssef, S.A. The antagonistic effect of chlorpromazine on cadmium toxicity. *Toxicol. Appl. Pharmacol.,* **1999,** *161*(1), 34-39.
http://dx.doi.org/10.1006/taap.1999.8785          PMID: 10558921

[84]     Capdevila, M.; Bofill, R.; Palacios, Ò.; Atrian, S. State-of-the-art of metallothioneins at the beginning of the 21st century. *Coord. Chem. Rev.,* **2012,** *256*(1), 46-62.
http://dx.doi.org/10.1016/j.ccr.2011.07.006

[85]     Seiler, H.; Sigel, A.; Sigel, H. *Handbook on metals in clinical and analytical chemistry*; CRC Press, **1994**.

[86]     Järup, L.; Berglund, M.; Elinder, C.G.; Nordberg, G.; Vahter, M. Health effects of cadmium exposure--a review of the literature and a risk estimate. *Scand. J. Work Environ. Health,* **1998,** *24*(Suppl. 1), 1-51.
PMID: 9569444

[87]     Wang, C.; Brown, S.; Bhattacharyya, M.H. Effect of cadmium on bone calcium and 45Ca in mouse dams on a calcium-deficient diet: evidence of Itai-Itai-like syndrome. *Toxicol. Appl. Pharmacol.,* **1994,** *127*(2), 320-330.
http://dx.doi.org/10.1006/taap.1994.1168 PMID: 8048077

[88]     Kurowska, E.; Bal, W. *Advances in Molecular Toxicology*; Fishbein, J.C., Ed.; Elsevier, **2010**, Vol. 4, pp. 85-126.
http://dx.doi.org/10.1016/S1872-0854(10)04003-8

[89]     Kobayashi, J. Pollution by cadmium and the itai-itai disease in Japan. *Toxicity of heavy metals in the environment,* **1978,** 199-260.

[90]     Gil, H.-W.; Kang, E.-J.; Lee, K.-H.; Yang, J.-O.; Lee, E.-Y.; Hong, S.-Y. Effect of glutathione on the cadmium chelation of EDTA in a patient with cadmium intoxication. *Hum. Exp. Toxicol.,* **2011,** *30*(1), 79-83.
http://dx.doi.org/10.1177/0960327110369818          PMID: 20413561

[91]     Roussel, A.M.; Andriollo-Sanchez, M.; Ferry, M.; Bryden, N.A.; Anderson, R.A. Food chromium content, dietary chromium intake and related biological variables in French free-living elderly. *Br. J. Nutr.,* **2007,** *98*(2), 326-331.
http://dx.doi.org/10.1017/S000711450770168X          PMID: 17403270

[92]     Cancer, I.A.R. Chromium, nickel and welding. *IARC Monogr. Eval. Carcinog. Risks Hum.,* **1990,** *49*, 1-648.
PMID: 2232124

[93]     DesMarais, T.L.; Costa, M. Mechanisms of chromium-induced toxicity. *Curr. Opin. Toxicol.,* **2019,** *14*, 1-7.
http://dx.doi.org/10.1016/j.cotox.2019.05.003          PMID: 31511838

[94]     World Health Organization. Guidelines for drinking-water quality: incorporating first and second addenda to third edition *Recommendations*; WHO Press: Geneva, **2008**. Vol. 1

[95]     Denkhaus, E.; Salnikow, K. Nickel essentiality, toxicity, and carcinogenicity. *Crit. Rev. Oncol. Hematol.,* **2002,** *42*(1), 35-56.
http://dx.doi.org/10.1016/S1040-8428(01)00214-1 PMID: 11923067

[96]     Ragsdale, S.W. Nickel-based enzyme systems. *J. Biol. Chem.,* **2009,** *284*(28), 18571-18575.
http://dx.doi.org/10.1074/jbc.R900020200          PMID: 19363030

[97]     Cangul, H.; Broday, L.; Salnikow, K.; Sutherland, J.; Peng, W.; Zhang, Q.; Poltaratsky, V.; Yee, H.; Zoroddu, M.A.; Costa, M. Molecular mechanisms of nickel carcinogenesis. *Toxicol. Lett.,* **2002,** *127*(1-3), 69-75.
http://dx.doi.org/10.1016/S0378-4274(01)00485-4 PMID: 12052643

[98]     Collinson, S.R.; Schröder, M. Encyclopedia of Inorganic Chemistry, **2005**.
http://dx.doi.org/10.1002/0470862106.ia150

[99]     Salnikow, K.; Zhitkovich, A. Genetic and epigenetic mechanisms in metal carcinogenesis and cocarcinogenesis: nickel, arsenic, and chromium. *Chem. Res. Toxicol.,* **2008,** *21*(1), 28-44.
http://dx.doi.org/10.1021/tx700198a PMID: 17970581

[100]    Das, K.K.; Das, S.N.; Dhundasi, S.A. Nickel, its adverse health effects & oxidative stress. *Indian J. Med. Res.,* **2008,** *128*(4), 412-425.
PMID: 19106437

[101]    Gawkrodger, D.J.; Healy, J.; Howe, A.M. The prevention of nickel contact dermatitis. A review of the use of binding agents and barrier creams. *Contact Dermat.,* **1995,** *32*(5), 257-265.
http://dx.doi.org/10.1111/j.1600-0536.1995.tb00778.x
PMID: 7634778

[102]    Peana, M.; Zdyb, K.; Medici, S.; Pelucelli, A.; Simula, G.; Gumienna-Kontecka, E.; Zoroddu, M.A. Ni(II) interaction with a peptide model of the human TLR4 ectodomain. *J. Trace Elem. Med. Biol.,* **2017,** *44*, 151-160.
http://dx.doi.org/10.1016/j.jtemb.2017.07.006          PMID: 28965571

[103]    Zoroddu, M.A.; Peana, M.; Medici, S.; Potocki, S.; Kozlowski, H. Ni(II) binding to the 429-460 peptide fragment from human Toll like receptor (hTLR4): a crucial role for nickel-induced contact allergy? *Dalton Trans.,* **2014,** *43*(7), 2764-2771.
http://dx.doi.org/10.1039/C3DT52187G PMID: 24169691

[104]    Genchi, G.; Carocci, A.; Lauria, G.; Sinicropi, M.S.; Catalano, A. Nickel: human health and environmental toxicology. *Int. J. Environ. Res. Public Health,* **2020,** *17*(3), E679.
http://dx.doi.org/10.3390/ijerph17030679          PMID: 31973020

[105]    ATSDR In: *Toxicological profile for nickel; US Department of Health and Human Services*; Public Health Service: Atlanta, GA, **2005**.

[106]    Webster, J.D.; Parker, T.F.; Alfrey, A.C.; Smythe, W.R.; Kubo, H.; Neal, G.; Hull, A.R. Acute nickel intoxication by dialysis. *Ann. Intern. Med.,* **1980,** *92*(5), 631-633.
http://dx.doi.org/10.7326/0003-4819-92-5-631          PMID: 7387004

[107]    Gandhi, N.M.; Nair, C.K. Radiation protection by diethyldithiocarbamate: protection of membrane and DNA *in vitro* and *in vivo* against gamma-radiation. *J. Radiat. Res. (Tokyo),* **2004,** *45*(2), 175-180.
http://dx.doi.org/10.1269/jrr.45.175 PMID: 15304957

[108]    Christensen, J.D. Disulfiram treatment of three patients with nickel dermatitis. *Contact Dermat.,* **1982,** *8*(2), 105-108.
http://dx.doi.org/10.1111/j.1600-0536.1982.tb04154.x
PMID: 6279358

[109]    Kaaber, K.; Menné, T.; Veien, N.; Hougaard, P. Treatment of nickel dermatitis with Antabuse; a double blind study. *Contact Dermat.,* **1983,** *9*(4), 297-299.
http://dx.doi.org/10.1111/j.1600-0536.1983.tb04394.x
PMID: 6352169

[110]    Kaaber, K.; Menne, T.; Veien, N.K.; Baadsgaard, O. Some adverse effects of disulfiram in the treatment of nickel-allergic patients. *Derm. Beruf Umwelt,* **1987,** *35*(6), 209-211.
PMID: 3440439

[111]    Kurta, D.L.; Dean, B.S.; Krenzelok, E.P. Acute nickel carbonyl poisoning. *Am. J. Emerg. Med.,* **1993,** *11*(1), 64-66.

http://dx.doi.org/10.1016/0735-6757(93)90063-H PMID: 8383493

[112] Bradberry, S.M.; Vale, J.A. Therapeutic review: do diethyldithiocarbamate and disulfiram have a role in acute nickel carbonyl poisoning? *J. Toxicol. Clin. Toxicol.,* **1999**, *37*(2), 259-264.
http://dx.doi.org/10.1081/CLT-100102424 PMID: 10382560

[113] Menne, T.; Kaaber, K.; Tjell, J.C. Treatment of nickel dermatitis. (The influence of tetraethylthiuramdisulfide (Antabuse) on nickel metabolism). *Ann. Clin. Lab. Sci.,* **1980**, *10*(2), 160-164.
PMID: 7387122

[114] Menné, T.; Kaaber, K. Treatment of pompholyx due to nickel allergy with chelating agents. *Contact Dermat.,* **1978**, *4*(5), 289-290.
http://dx.doi.org/10.1111/j.1600-0536.1978.tb04560.x PMID: 217567

[115] Spruit, D.; Bongaarts, P.J.; de Jongh, G.J. Dithiocarbamate therapy for nickel dermatitis. *Contact Dermat.,* **1978**, *4*(6), 350-358.
http://dx.doi.org/10.1111/j.1600-0536.1978.tb03849.x PMID: 216526

[116] Christensen, O.B.; Kristensen, M. Treatment with disulfiram in chronic nickel hand dermatitis. *Contact Dermat.,* **1982**, *8*(1), 59-63.
http://dx.doi.org/10.1111/j.1600-0536.1982.tb04137.x PMID: 7067441

[117] Blanusa, M.; Varnai, V.M.; Piasek, M.; Kostial, K. Chelators as antidotes of metal toxicity: therapeutic and experimental aspects. *Curr. Med. Chem.,* **2005**, *12*(23), 2771-2794.
http://dx.doi.org/10.2174/092986705774462987 PMID: 16305472

[118] Bjørklund, G.; Oliinyk, P.; Lysiuk, R.; Rahaman, M.S.; Antonyak, H.; Lozynska, I.; Lenchyk, L.; Peana, M. Arsenic intoxication: general aspects and chelating agents. *Arch. Toxicol.,* **2020**, *94*(6), 1879-1897.
http://dx.doi.org/10.1007/s00204-020-02739-w PMID: 32388818

[119] Hughes, M.F.; Beck, B.D.; Chen, Y.; Lewis, A.S.; Thomas, D.J. Arsenic exposure and toxicology: a historical perspective. *Toxicol. Sci.,* **2011**, *123*(2), 305-332.
http://dx.doi.org/10.1093/toxsci/kfr184 PMID: 21750349

[120] Oberoi, S.; Barchowsky, A.; Wu, F. The global burden of disease for skin, lung, and bladder cancer caused by arsenic in food. *Cancer Epidemiol. Biomarkers Prev.,* **2014**, *23*(7), 1187-1194.
http://dx.doi.org/10.1158/1055-9965.EPI-13-1317 PMID: 24793955

[121] Naujokas, M.F.; Anderson, B.; Ahsan, H.; Aposhian, H.V.; Graziano, J.H.; Thompson, C.; Suk, W.A. The broad scope of health effects from chronic arsenic exposure: update on a worldwide public health problem. *Environ. Health Perspect.,* **2013**, *121*(3), 295-302.
http://dx.doi.org/10.1289/ehp.1205875 PMID: 23458756

[122] Singh, R.; Singh, S.; Parihar, P.; Singh, V.P.; Prasad, S.M. Arsenic contamination, consequences and remediation techniques: a review. *Ecotoxicol. Environ. Saf.,* **2015**, *112*, 247-270.
http://dx.doi.org/10.1016/j.ecoenv.2014.10.009 PMID: 25463877

[123] Ferreccio, C.; Yuan, Y.; Calle, J.; Benítez, H.; Parra, R.L.; Acevedo, J.; Smith, A.H.; Liaw, J.; Steinmaus, C. Arsenic, tobacco smoke, and occupation: associations of multiple agents with lung and bladder cancer. *Epidemiology,* **2013**, *24*(6), 898-905.
http://dx.doi.org/10.1097/EDE.0b013e31829e3e03 PMID: 24036609

[124] Fowler, B.A.; Selene, C.H.; Chou, R.J.; Jones, D.L.; Sullivan, W., Jr.; Chen, C.J. *Handbook on the Toxicology of Metals (Fourth Edition)*; Nordberg, G.F.; Fowler, B.A.; Nordberg, M., Eds.; Academic Press: San Diego, **2015**, pp. 581-624.
http://dx.doi.org/10.1016/B978-0-444-59453-2.00028-7

[125] Manna, P.; Sinha, M.; Sil, P.C. Arsenic-induced oxidative myocardial injury: protective role of arjunolic acid. *Arch. Toxicol.,* **2008**, *82*(3), 137-149.
http://dx.doi.org/10.1007/s00204-007-0272-8 PMID: 18197399

[126] Amadi, C.N.; Igweze, Z.N.; Orisakwe, O.E. Heavy metals in miscarriages and stillbirths in developing nations. *Middle East Fertil. Soc. J.,* **2017**, *22*(2), 91-100.
http://dx.doi.org/10.1016/j.mefs.2017.03.003

[127] Nurchi, V.M.; Djordjevic, A.B.; Crisponi, G.; Alexander, J.; Bjørklund, G.; Aaseth, J. Arsenic toxicity: molecular targets and therapeutic agents. *Biomolecules,* **2020**, *10*(2), 235.
http://dx.doi.org/10.3390/biom10020235 PMID: 32033229

*Review*

# Biological Effects of Human Exposure to Environmental Cadmium

**Massimiliano Peana** [1,*] **, Alessio Pelucelli** [1,*] **, Christos T. Chasapis** [2] **, Spyros P. Perlepes** [3] **, Vlasoula Bekiari** [4] **, Serenella Medici** [1] **and Maria Antonietta Zoroddu** [1]

[1] Department of Chemical, Physical, Mathematical and Natural Sciences, University of Sassari, 07100 Sassari, Italy
[2] Institute of Chemical Biology, National Hellenic Research Foundation, 11635 Athens, Greece
[3] Department of Chemistry, University of Patras, 26500 Patras, Greece
[4] School of Agricultural Science, University of Patras, 30200 Messolonghi, Greece
[*] Correspondence: peana@uniss.it (M.P.); alessiopelucelli@gmail.com (A.P.)

**Abstract:** Cadmium (Cd) is a toxic metal for the human organism and for all ecosystems. Cd is naturally found at low levels; however, higher amounts of Cd in the environment result from human activities as it spreads into the air and water in the form of micropollutants as a consequence of industrial processes, pollution, waste incineration, and electronic waste recycling. The human body has a limited ability to respond to Cd exposure since the metal does not undergo metabolic degradation into less toxic species and is only poorly excreted. The extremely long biological half-life of Cd essentially makes it a cumulative toxin; chronic exposure causes harmful effects from the metal stored in the organs. The present paper considers exposure and potential health concerns due to environmental cadmium. Exposure to Cd compounds is primarily associated with an elevated risk of lung, kidney, prostate, and pancreatic cancer. Cd has also been linked to cancers of the breast, urinary system, and bladder. The multiple mechanisms of Cd-induced carcinogenesis include oxidative stress with the inhibition of antioxidant enzymes, the promotion of lipid peroxidation, and interference with DNA repair systems. $Cd^{2+}$ can also replace essential metal ions, including redox-active ones. A total of 12 cancer types associated with specific genes coding for the Cd-metalloproteome were identified in this work. In addition, we summarize the proper treatments of Cd poisoning, based on the use of selected Cd detoxifying agents and chelators, and the potential for preventive approaches to counteract its chronic exposure.

**Keywords:** cadmium; cadmium toxicity; cadmium exposure; chronic exposure; protein targets

## 1. Introduction

Cadmium (Cd) was discovered in 1817 in Germany by Friedrich Stromeyer as an impurity in zinc carbonate ($ZnCO_3$). The name derives from the Latin word *cadmia* and the Greek word καδμεία, an older name for the common zinc (Zn) ore, calamine. Cd is naturally present in the Earth's crust, at an average concentration estimated to be between 0.1 and 0.2 parts per million (ppm) [1]. Atmospheric Cd can form as a result of natural activities, such as spontaneous biomass combustion and volcanic eruptions. Despite its natural presence on the planet, no biological function has been found for Cd in higher organisms [2], while its toxicity is well known and has been the subject of numerous studies [3]. Cd continues to occur in the environment, particularly in aerosol form, as a result of human activities, such as the burning of fossil fuels and wastes, or the process of mining metal ores and industrial emissions, representing a current threat to public health [4]. Humans are protected from chronic exposure to low Cd concentrations by the presence of metallothioneins (MTs), a family of ubiquitous small cysteine-rich proteins, the specific function of which is to regulate the metabolism of Zn. MTs play important roles in protection against ion toxicity from several heavy metals, DNA damage, and oxidative stress. Thanks to the presence of many sulfhydryl groups (–SH), MTs are able of complexing, under tolerable exposures,

almost all ingested Cd ions [2]. In the kidneys, the resulting $Cd^{2+}$-complexes are, in part, excreted with the urine. The cysteine content of MTs can be up to 30%. These residues can be arranged in motifs (e.g., Cys-x-Cys or Cys-x-x-Cys), and this aspect is fundamental for the formation of metal-binding clusters. The protective effect of MTs against metal toxicity has been largely discussed in a number of studies [5,6]. Apart from Cd, MTs can bind other metal ions, such as mercury, platinum, etc., in order to protect cells and tissues against their toxicity [7]. Mutant flies with increased quantities of MTs in their genes are able to survive on a diet rich in heavy metals, while normal flies would die from the same diet [8]. An increased expression of these proteins can be preventive against heavy metal intoxication: this expression is regulated by the metal regulatory transcription factor 1 (MTF-1).

If the amount of Cd absorbed by the human body exceeds the complexation capacity of MTs, then there will be an accumulation of the metal, mainly in the kidneys (30%) and liver (30%), with the rest dispersed throughout the other organs and having an extremely long half-life of 10–30 years [9,10]. The biological half-life of Cd in the blood has been estimated to be in the range of 75 to 128 days; however, this half-life mainly represents its deposition in the organs, not the body's clearance rate [10,11]. Cd bioaccumulation in various tissues affects cell functionality, such as proliferation and differentiation, and is responsible for oxidative stress by the generation of reactive oxygen species (ROS), despite its inability to generate free radicals directly, instead forming them via the replacement of redox-active metal ions, such as $Fe^{2+}$ and $Cu^{2+}$, from their metal-binding sites in proteins. The resulting oxidative stress will induce cellular damage and apoptosis [12]. Cd binding into the mitochondria can inhibit both cellular respiration and oxidative phosphorylation, even at low concentrations [13,14]. With these oxidative mechanisms, Cd has been shown to interfere with almost all major DNA repair systems. It is indeed able to impair nucleotide excision repair (NER), base excision repair (BER), and mismatch repair (MMR) [15]. The disturbance of DNA repair processes may explain the co-mutagenic effects in combination with other carcinogenic sources, as DNA repair systems are not only required for the repair of DNA-induced damage but also for the removal of DNA lesions due to endogenous processes and to keep replication errors low [16]. Once absorbed, the thiol groups of cysteines appear to be the critical targets of Cd ions in proteins, enzymes, and endogenous antioxidants such as glutathione (GSH, L-$\gamma$-glutamyl-L-cysteinyl-glycine). The inhibition of antioxidant defense enzymes, such as superoxide dismutase (SOD), lactate dehydrogenase (LDH), catalase (CAT), thioredoxin reductase (TrxR), and glutathione peroxidase (GPx) leads to the further dysregulation of the cellular redox state [3,12,17]. The present paper considers exposure and potential health concerns on environmental cadmium, with particular attention to its carcinogenic action. Moreover, we summarize the strategy of environmental Cd remediation and the proper treatments of Cd poisoning, based on the use of selected detoxifying agents and chelators, either alone or in combination.

## 2. The Bioinorganic Chemistry of Cadmium

Cd (electronic configuration (Kr) $4d^{10}\ 5s^2$) belongs to group 12 of the periodic table, together with zinc and mercury, but it is chemically more similar to the former than to the latter. It can be found with oxidation states 0, +1, and +2; however, only $Cd^{2+}$ ions are stable under normal conditions, as well as for Zn. Unlike mercury (Hg), which, with simple anions, form compounds having a covalent character, those of Cd have mainly ionic characteristics. $Cd^{2+}$ has an ionic radius of 0.97 Å, very similar to those of $Ca^{2+}$ (0.99 Å) and $Na^+$ (1.09 Å), facilitating their replacement in biological matrices such as bones. $Cd^{2+}$ can form coordination complexes with ligands and, particularly, with biological ones such as proteins and nucleic acids. These interactions are modulated by the innate chemical features of $Cd^{2+}$, which is a soft metal ion in the hard/soft acid-base (HSAB) classification [18,19]. The stereochemistry of $Cd^{2+}$ complexes with ligands in biological fluids is useful for understanding the biological behavior and fate of $Cd^{2+}$ ions. According to the HSAB model, $Cd^{2+}$ is a soft acid having a preference for sulfhydryl donors (soft bases), whereas hard carboxylate/carbonyl aminoacidic groups will generally prefer the borderline $Zn^{2+}$,

despite the chemical similarities between these ions [19]. The competition between $Cd^{2+}$ and other divalent cations ($Zn^{2+}$, $Mn^{2+}$, $Fe^{2+}$, $Ni^{2+}$, and $Cu^{2+}$) during complex formation with amino acids, peptides, and chelating agents has been reviewed previously [20].

$Cd^{2+}$ can have a wide range of coordination numbers (from 2 to 8), but it mostly shows the coordination numbers 4 or 6, represented, respectively, by regular tetrahedral and octahedral structures with proteins (Figure 1a,b). Depending on the protein to which Cd is bound, clusters can also be generated. MTs are a lightning example of such polynuclear complexes, as cysteine-rich regions of the proteins are able to cluster $Cd^{2+}$ (Figure 1c).
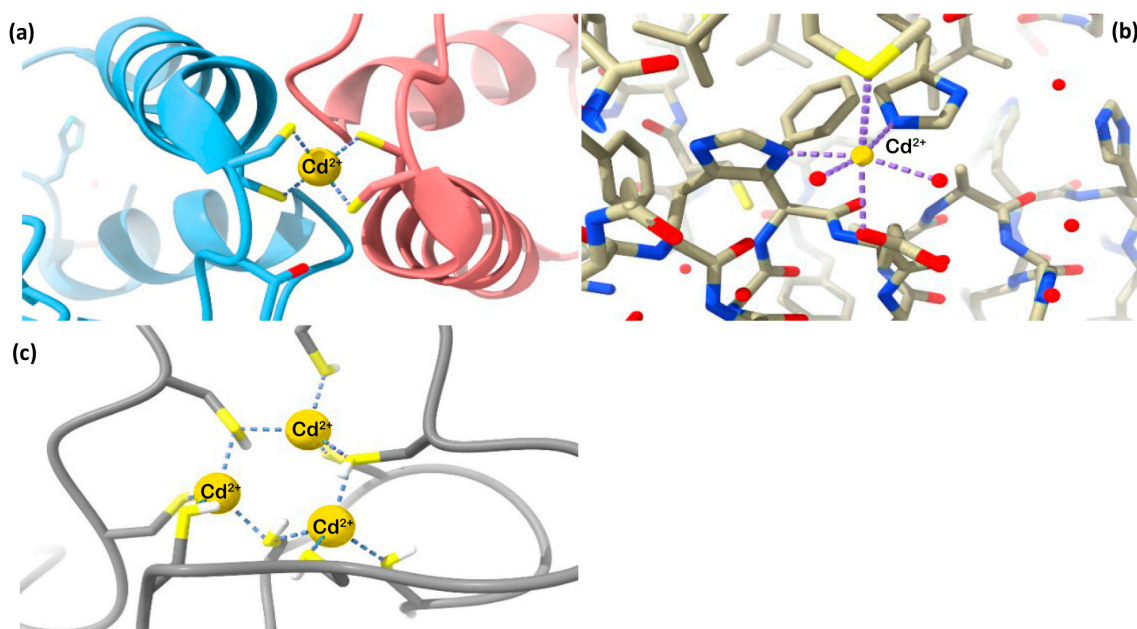


**Figure 1.** Examples of $Cd^{2+}$ coordination environment in biological systems: (**a**) regular tetrahedral $Cd^{2+}$ complexed with Hah1 metallochaperone protein (Protein Data Bank PDB 1FE0, [21]); (**b**) regular octahedral $Cd^{2+}$ complexed with cytochrome c oxidase (PDB 2EIK, [22]); (**c**) a cluster of $Cd^{2+}$ complexed with metallothionein-1 (PDB 1DFT, [23]).

The geometry distribution of $Cd^{2+}$ in the X-ray structures of those proteins deposited in the Research Collaboratory for Structural Bioinformatics Protein Data Bank (RCSB PDB https://www.rcsb.org/ accessed on 22 October 2022) in which $Cd^{2+}$ forms mononuclear complexes is shown in Figure 2 and relative data are reported in Table S1 of the Supplementary Materials. From the analysis of the solved crystal structure available in the database, it transpires that the main coordination geometries around $Cd^{2+}$ are represented by octahedral (43.0%), trigonal bipyramidal (26.7%), and tetrahedral (15.9%) forms (derived geometries were included in the count) [24].

Part of the toxicity of $Cd^{2+}$ is due to its ability to mimic other divalent ions, particularly $Zn^{2+}$ and $Ca^{2+}$, which have a similar radius and a similar valence.

A useful tool to analyze the possibilities that a metal ion has to replace another one in its natural metal coordination sites, is based on the use of a representative minimal functional site (MFS) [25]. The MFS describes the local 3D environment around the metal ion and is independent of the larger context of the protein fold in which it is embedded. In summary, MFSs do not depend on the overall macromolecular structure but instead represent a region crucial for the correct physiological function of a selected metalloprotein [25]. It is possible to extract statistical data from the analysis of MFSs (through the 3D X-ray structures of metal–proteins deposited in the Protein Data Bank), by counting how many amino acidic patterns are common to the different ligands in their coordination binding sites. It is then possible, by crossing these data with the protein selectivity for a given metal ion, to understand how probable the substitution is of the original metal ion with another

metal ion. In the case of $Cd^{2+}$, on the basis of data from Metalpdb, the database of metal sites in biological macromolecular structures (https://metalpdb.cerm.unifi.it/, accessed on 22 October 2022) [24], the analysis of the possible cadmium substitution for other metal sites yields the results shown in Figure 3 and Table S2 of the Supplementary Materials.
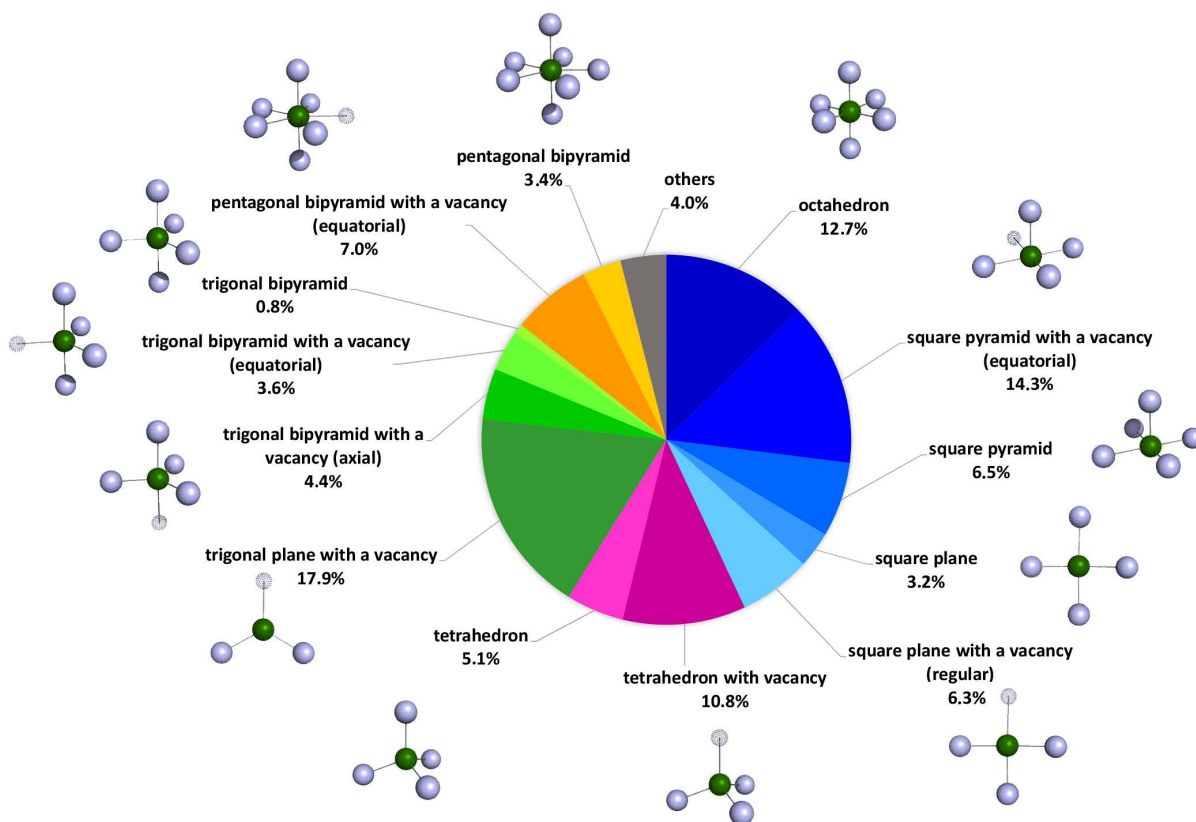


**Figure 2.** Percentage distribution of geometries for mononuclear $Cd^{2+}$ complexes in proteins, according to the Research Collaboratory for Structural Bioinformatics Protein Data Bank (RCSB PDB).
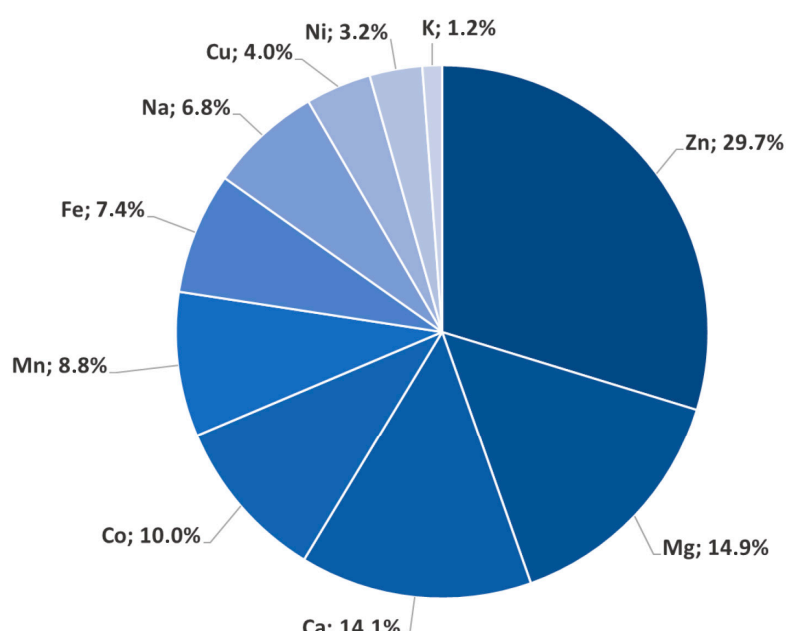


**Figure 3.** Percentage distribution of metal ions substituted by $Cd^{2+}$, according to the Research Collaboratory for Structural Bioinformatics Protein Data Bank (RCSB PDB).

Interestingly, the statistical analysis based on a total of 150,149 PDB structures showed that $Cd^{2+}$ has the probability of substituting for other metal ions in 4189 proteins (~2.8% of the total number of PDB structures). In particular, $Cd^{2+}$ has been shown to have a major affinity for the $Zn^{2+}$ binding sites (1245 proteins, 29.7%), $Ca^{2+}$ (590 proteins, 14.08%), and then $Mg^{2+}$ (610 proteins, 14.9%). While it is widely reported that $Cd^{2+}$ can substitute $Zn^{2+}$ at its metal coordination sites as well as $Ca^{2+}$, the replacement of $Mg^{2+}$ by $Cd^{2+}$ is not well known, nor has it been well studied, due to the huge variety of roles that Mg plays in the human body. It has been suggested that cadmium can interfere with the absorption of magnesium in the gastrointestinal tract, affecting its homeostasis. Conversely, several reports suggest that enhanced dietary magnesium intake can mitigate the pathogenic impact of cadmium exposure and its induced alterations in the homeostasis of zinc, copper, and magnesium itself [26,27].

## 3. Uses and Environmental Dispersion of Cadmium

After its first isolation, Cd was used for a variety of processes, firstly as a painting and plating compound (cadmium sulfide, CdS, was used as a yellowish pigment, and cadmium selenide, CdSe, was used as a red one) for about 100 years, mainly because of the particular pigment's brightness. Cadmium pigments have been used by artists since the 19th century. Because of their resistance to temperatures up to 3000 °C, these Cd-based pigments can be used for coloring hot pipes or glass; examples include red traffic lights and the lit-up stars on the Moscow Kremlin. During the last years CdS and CdSe semiconductor nanomaterials due to their photoluminescent properties have been extensively studied for their use in various environmental monitoring applications, photovoltaic cells as sensitizers, as well as bio-imaging and nanomedicine [28,29]. The majority of Cd has been used (and still is used) in battery technology, in particular, rechargeable nickel-cadmium (Ni–Cd) batteries. The invention of the rechargeable Ni–Cd battery goes back to 1899 and has played a significant role in electrical technology during the twentieth century. In 2002, the European Union put a limit on the use of Cd in electronics, repealing this action in 2016 and establishing a maximum content of Cd of 0.1%, reducing the limit on Cd MCV (maximum concentration value) in homogeneous material to 0.01% [30]. Unfortunately, only a few countries have restrictions regarding the exportation of Cd components, and even fewer have laws about its recycling. In developing countries, this is becoming a huge problem for public health, where electronic waste (e-waste) recycling activities are often conducted without all the safety measures that are needed [31,32]. Cd was a widely used component of plastics, especially PVC, where it works as a stabilizer, but now it has been completely replaced with less harmful metals and alloys, such as barium–zinc alloy. Another source of cadmium for half a century was from its use as a metrology standard from 1907 to 1960. During that period, the angstrom was defined by fixing the wavelength of the distinct, red spectral line of cadmium at 6438.4696 Å. Due to its ability to efficiently capture neutrons, the metal played a remarkable role in the development of the first nuclear reactors; cadmium-coated rods were used to control the nuclear reaction.

Large amounts of Cd are obtained as byproducts of zinc smelting, as the two metals are often naturally associated in minerals. Therefore, many of the environmental contaminations from Cd occur in areas close to the treatment and smelting plants of zinc, but also those of copper and lead. Cd is released into the environment during the disposal and incineration phases of waste containing, in particular, plastic materials, steel plated with cadmium, and nickel-cadmium batteries. Cd exposure in the workplace takes place during mining and work using Cd-containing ores [33].

## 4. Human Exposure to Cadmium

### 4.1. Ingestion

Cd tends to persist and accumulate in the soil and then enters the metabolism of plants. Its accumulation in edible plant parts, including fruits and seeds, leads to Cd's entry into the food chain [34]. This accumulation increases with the decrease in pH in

soil; consequently, acid rain has the effect of increasing Cd concentrations in plants. The foods that mainly contribute to the daily Cd intake in Western countries include cereals and bread (34%), leafy vegetables, in particular spinach, among adults (20%), potatoes (11%), legumes and nuts (7%), stem/root vegetables (6%), and fruits (5%). In terms of Eastern countries, fish and shellfish can be identified as the major Cd sources, in addition to grains and vegetables, which are represented particularly by rice [35]. A particular danger may be represented by rice grains, which account for more than half of the total Cd intake in Eastern regions of the world, at 44% in Japan [36] and 56% in China [37]. The typical dietary Cd intake has been estimated to be about 30–50 μg/day [38], but normal individuals absorb only a small portion of an orally ingested dose (1–10%) [39]. Although the health risk from dietary cadmium exposure in Eastern nations is generally low, it still remains a cause for concern for some subgroups. In fact, being disseminated across the planet, there are areas with very high levels of Cd in the soil. The crop uptake of Cd in these areas can lead to significant dietary exposures for the people living nearby. For example, in the Jinzu and Kakehashi river basins in Japan, there are areas with soil that is heavily contaminated by Cd, derived from industrial waste [40,41]. Local people who frequently consumed rice cooked with Cd-contaminated water, developed a severe kidney and bone syndrome called "Itai-Itai" disease, characterized by bone deformation and multiple fractures, especially in women [42]. The radiographs showed the presence of osteomalacia and bone decalcification, as well as osteoporosis, and a series of bone deformities due to the replacement of $Ca^{2+}$ by $Cd^{2+}$, with a consequent alteration of the normal bone structure.

It is important to note that in the US, in the late 1960s, the average Cd consumption was estimated to be around 26 μg/day/person [43], and, in the first years of the 1990s, was calculated to be around 18.9 μg/day/person [44]; now, the human Cd intake has been lowered to 4.63 μg/day/person, on average. This corresponds to a value of 75% under the tolerable limit of toxicity. The diminishing of Cd intake in the last 50 years could be attributed to the lowered activities of leaking sewage sludge into agricultural soil, because of more efficient control and environmental awareness in developed countries. These activities were mainly responsible for the transfer of Cd, adsorbed by plants, into the food chain, contributing to increasing human exposure to the metal. Some aquatic organisms can also be largely affected by Cd accumulation reaching levels above regulatory standards. While muscle tissue in fish does not represent a site of accumulation of Cd [45], in commercial oysters (*Crassostrea gigas*) from southern Korea, the mean Cd concentration of 80 samples was found to be 0.591 μg/kg, which was much higher than the mean Cd concentration in water samples, 0.0021 μg/L [46]. The acidification of seawater could increase the accumulation of Cd by most common seafood species, such as *Mytilus edulis*, *Tegillarca granosa*, and *Meretrix meretrix*, with a potential threat to seafood safety [47,48]. Several protein transporters have been identified as having a role in cadmium uptake in the intestinal tract. These include divalent metal transporter 1 (DMT1), cationic amino acid transporter 1 (CaT1), zinc transporters (ZIP4, ZIP8, ZIP14, and ZnT1), copper-transporting P-type ATPase or Menkes ATPase (ATP7A), calcium channel TRVP6, and metallothionein MT-1 and MT-2, for which the increased Cd oral concentrations resulted in relatively increased gene expression [5]. Once introduced into the blood, Cd reaches various organs, such as the kidneys and skeleton, through systemic distribution. Initially, Cd in plasma is bound with high molecular-mass proteins such as albumin, then it is found bound with proteins of the molecular size of MTs, which are believed to be responsible for transporting Cd to the kidneys [5].

### 4.2. Inhalation

Cd air levels can be hundreds of times greater in the workplace than in the general environment. For example, the Occupational Safety and Health Administration (OSHA) fixed the permissible exposure limit (PEL) of Cd fume or Cd oxide in the workplace at 0.1 mg/m$^3$, whereas concentrations of Cd in ambient air are $1 \times 10^{-6}$ mg/m$^3$ in non-industrialized ar-

eas and $4 \times 10^{-5}$ mg/m$^3$ in urban areas, respectively. Non-occupational Cd exposure from the air is not expected to pose the risk of adverse health effects. In general, Cd air levels are usually not sufficient to cause health problems among the general population. Even in those areas with high industrial emissions of Cd, its average atmospheric concentration is not higher than 35 ng Cd/m$^3$ of air. A Brazilian study showed higher blood Cd levels (~0.22 μg/L) in automotive battery-manufacturing workers than in the control group, who had a mean blood Cd level of around 0.03 μg/L. However, the mean blood Cd level in battery workers was even lower compared to the WHO standard (10 μg/L) [49]. In other words, elevated occupational exposure to Cd decreased in the last 50 years, and such a change is due to better regulations regarding Cd exposure in the workplace. Therefore, the daily deposition rate would be 0.175 ng Cd, assuming that 20 m$^3$ of air would be inhaled per day, with a deposition rate of 25% [50]. However, Cd exposure is still considered a threat in workplaces in developing countries, where safety standards are not regulated or respected. The major routes of Cd exposure occurring in the general population are from the ingestion of Cd-contaminated foods and cigarette smoking, since the tobacco plants take up Cd from polluted soil, due to its similarity to Zn [51]. Compared to non-smokers, Cd levels are four to five times higher in the blood and two to three times higher in the kidneys for tobacco smokers [52,53]. Tobacco plants accumulate every polluting metal that might be present in the neighborhood, and, in particular, arsenic (As) since some of its compounds are widely used in the production of pesticides or herbicides [54]. Since both As and Cd are classified by the IARC as belonging to Group 1 of the carcinogenic substances, Cd is believed to be linked to lung cancer in smokers, in synergism with As, as well as with other potentially toxic substances that are eventually present in tobacco leaves.

### 4.3. Permeation

There are negligible amounts of Cd absorbed through the skin; thus, it is not considered to be a critical route of exposure. However, recent research highlighted the environmental significance of photosensitive CdS and CdSe pigments and nano semiconductors, whose oxidized products (cadmium sulfate, CdSO$_4$, and cadmium selenite, CdSeO$_4$) are considerably more soluble and bioavailable and are, consequently, potentially more dangerous [55]. An in vitro study using human full-thickness skin as a model to characterize the impact of Cd exposure on skin showed that the metal penetrates only the epidermis; it was shown before that its solubility into the stratum corneum layer is a rate-limiting process [56]. Permeability is affected by the Cd concentration applied to the skin. It may also be influenced by pH and metal speciation [19]. The high concentrations of Cd in the epidermis may explain the induction of MTs, as Cd is very effective in activating their expression [56].

### 5. Effect of Human Exposure to Cadmium

### 5.1. General Effects That Are Harmful to Health

In this section, we will describe the main health adverse effects of cadmium exposure, while in the next section, the strictly carcinogenic aspects will be explored. Figure 4 illustrates the main outcomes in health effects following chronic cadmium exposure.

The organs most affected by Cd toxicity are the kidneys; as much as about 30% of body Cd is deposited in the kidney tubule region, provoking tubular damage proportionally to the quantity of Cd not bound to MTs. In one study, diabetics were more susceptible to renal tubular damage from Cd exposure than were the controls [57]. Another common disease that can be correlated to Cd exposure is osteoporosis and/or osteomalacia. Cd has a deleterious impact on bones due to its impairment of Vitamin D uptake in the kidneys. Cd also prevents the absorption of calcium at the gut level, causing general bone disease, such as the aforementioned Itai-Itai disease [58]. Cd has a remarkable role in the reproductive system, where the metal interferes in a number of ways [59]. It has been shown that Cd can alter cell adhesion in the testis, interfering with the normal migration of germ cells across the seminiferous epithelium. Furthermore, decreased testicular growth rate, plasma testosterone, and reduced sperm count and motility have been linked to Cd-induced

oxidative stress, as the result of a decrease in GPx, CAT, mitochondrial Mn–SOD, and cytosolic CuZn–SOD [60].

**Brain toxicity**
Imbalance of excitatory and inhibitory signals
Cerebral edema

**Bones diseases**
Osteomalacia
Osteoporosis
Itai-Itai disease

**Cardiovascular toxicity**
Hypertension
Myocardial infraction
Stroke

**Kidney toxicity**
Tubular damage
Impairment of vitamin D absorpion

**Lung toxicity**
Bronchitis
Obstructive lung disease
Interstitial fibrosis

**Pancreas toxicity**
Alteration of insulin release
Increase of gluconeogenesis

**Liver toxicity**
Hepatic necroinflammation

**Duonenum impairment**
Suppression of iron transport
iron-deficienct anemia

**Cancerogenicity**
Causes lung, prostate, kidney, pancreatic
and probably breast, urinary bladder and thyroid cancer

**Immunological toxicity**
Alteration of the secretion of immune cytokines
Induction of ROS production and oxidative stress
Alteration of the production of selective antibodies in immune cells

**Damage to the reproductive system**
Alteration of cell adhesion in testis
Interference with normal migration of germ cells
Decrease of plasma testosterone and testicular growth rate
Reduction of sperm count and motility

**Figure 4.** Outcomes of cadmium exposure.

Another organism district that is affected by Cd toxicity is the cardiovascular system. Cd can cause hypertension by the inhibition of the endothelial nitric oxide synthase and the suppression of acetylcholine-induced vascular relaxation [61,62]. Cd could also affect glucose metabolism by acting on a variety of different organs, such as the pancreas, liver, and adrenal gland. Studies suggest a direct effect of Cd on the pancreas, and there is evidence that Cd can alter insulin release from pancreatic β-cells while increasing the activity of all the four enzymes responsible for gluconeogenesis [63]. As has been noticed in Itai-Itai disease, Cd also seems to induce anemia, due to the suppression of erythropoietin production [64]; this mechanism, linked to the suppression of iron transport in the duodenum, may cause iron-deficient anemia [65]. Lungs are also a target organ for Cd toxicity. In chronic Cd exposure, progressive pulmonary fibrosis and impaired lung function with obstructive lung disease may occur [66,67]. Cd also induces neurological dysfunction and brain toxicity, with a complex mechanism [68,69].

Cd could be considered a weak genotoxic and mutagenic agent, due to its low affinity with DNA [70]. A number of toxicogenomic studies confirm the involvement of Cd in the mutation of the following genes: immediate early response genes (IEGs), stress response genes, transcriptional factors, and translational factors [12]. One of the mechanisms by which Cd influences gene expression involves not only the homeostasis of Ca, an element that can be directly mimicked by Cd, but also an element whose concentration inside the cell can be influenced by it [71].

### 5.2. Carcinogenicity of Cadmium

One of the major Cd-induced mechanisms of carcinogenesis is oxidative stress [12]; this is, in part, caused, as mentioned above, by changes in Ca concentrations inside the cell. Cd cannot directly produce ROS because it does not undergo Fenton-like reactions,

but, on the other hand, it can replace redox-active metal ions and can inhibit the activity of antioxidant enzymes, as well as promote lipid peroxidation [72]. The major enzymatic antioxidant is SOD, which degrades $O_2\cdot^-$, and the CAT and GSH redox system, which inactivates $H_2O_2$ and hydroperoxides. Three forms of SOD may be important: Mn-SOD (which is located in the mitochondria), Cu–Zn SOD (which resides in the cytoplasm), and extracellular SOD (which lines the blood vessels). GSH, present in high concentrations in every cell, is able to detoxify Cd in the human blood cell, and its synthesis (triggered by the transcription factor Nrf2) is enhanced after Cd exposure [73]. Cd has been shown to impair global genome nucleotide excision repair (GG-NER): it can interfere with the removal of DNA lesions in cultured mammalian cells caused by benzo[*a*]pyrene and UVC [74]. The underlying mechanism in this impairment has been identified as an interaction with the Zn-binding proteins, which show a common motif (Zn finger), where Zn is complexed to four cysteine and/or histidine residues [16,75,76]. $Cd^{2+}$ can substitute $Zn^{2+}$ in these metal binding sites, inactivating the proteins. Another process of the DNA repair pathway is base excision repair (BER), but it is different from NER. BER, in fact, is activated by a specific class of DNA repair enzymes called glycosylases. Low concentrations of Cd disturb the repair of oxidative DNA base damage, as well as DNA alkylation damage, in mammalian cells [77]. It is important to cite another mechanism that is relevant for maintaining genomic stability; the mismatch repair (MMR) is responsible for the repair of mismatched bases after DNA replication. Cells deficient in MMR usually tend to mutate often and are associated with a greater risk of developing several types of cancer. MMR also has a role in apoptosis, and it has been shown that MMR-deficient cells are about 100 times more resistant to the cytotoxicity of alkylating agents [78]. In extracts of human cells, Cd inhibited at least one step of the MMR process [79]. The underlying mechanism in this inhibition seems to be the interaction of Cd in the process of ATP binding the MMR enzymes, plus their hydrolysis, reducing their binding activity to DNA bases and interfering with their ability to recognize mismatched DNA base pairings [80,81].

Cd intoxication can also lead to cell death by apoptosis with different pathways [82,83]. The extrinsic pathway is initiated by binding the cytokine ligands, such as the Fas ligand (FasL) and the tumor necrosis factor alpha (TNF-$\alpha$), along with the death receptors, CD95/APO-1 (Fas), and the TNF receptors. Cd can alter the CD95/APO-1 (Fas)/Fas ligand (FasL) signaling pathway, especially in neuronal cells. Moreover, it can increase inflammation markers, including TNF-$\alpha$ and NF-kB, in nephrotic cells, leading to apoptosis by caspase-3 activation. On the other hand, Cd can also influence the intrinsic pathway of apoptosis, increasing the expression of the pro-apoptotic protein, Bax, and suppressing the anti-apoptotic protein, Bcl-2 [84]. In this case, a decrease in the Bcl-2/Bax ratio causes the release of cytochrome c from mitochondria and Ca from the endoplasmic reticulum (ER): this leads to the caspase cascade, with the final activation of caspase-3 and cell death. The activation of caspase-3 has a crucial role in cell death by Cd-mediated apoptosis, so it is logical to hypothesize that the inhibition of caspase-3 can prevent Cd toxicity. There are several studies in this field, claiming that certain natural substances such as taxifolin can protect from Cd apoptosis in skin cells by changing the activity of caspase-3 and -7, and other apoptotic factors [85]. Cd toxicity seems to also play a role in autophagy processes, even if this role has not been understood properly [86]. Cd shows, in fact, a different output for the cell fate in different cell lines. Cd-induced autophagy seems to promote apoptosis in skin epidermal cells [87], in mouse spleen, in neuronal cells [88], in mouse renal tubular epithelial cells, and in rat proximal tubular epithelial cells [89]. On the other hand, Cd-exposed human bronchial epithelial cells (BEAS-2BR) appeared to be autophagy-deficient, down-streaming the anti-apoptotic proteins Bcl-2 and Bcl-xl, apoptosis resistance, and possible carcinogenesis [90].

Cd alters the epigenetic signatures in the DNA of the placenta and of newborns, and some studies indicated marked sexual differences for Cd-related DNA methylation changes. Associations between early Cd exposure and DNA methylation might reflect interference with *de novo* DNA methyltransferases. In particular, the association of cadmium with the

DNA methylation of certain CpG sites within the genes of interest in organ development, glucocorticoid synthesis, and cell death has been reported [91,92].

*5.3. Cd-Metalloproteins with Relevance to Carcinogenesis*

According to a recent study, the Cd-metalloproteome might constitute up to 18.4% of the entire human proteome [93]. In the present study, we identified which genes encoding Cd-metalloproteome are genetic markers for 12 cancer types (urothelial bladder carcinoma, breast cancer, colorectal adenocarcinoma, glioblastoma, head and neck squamous cell carcinoma, kidney cancer, acute myeloid leukemia, lung adenocarcinoma, lung squamous cell carcinoma, ovarian cancer, uterine corpus endometrial carcinoma, and multiple myeloma) using the Cancer Genome Atlas (TCGA) pan-cancer repository [94]. Specifically, 12 Cd-binding proteins have been characterized as cancer-related, and their names, abundance, and tissue-specific expression in the human body are listed in Table 1. Figure 5 shows the 12 cancer types associated with each specific gene-encoding Cd-metalloproteome.

**Table 1.** Names, UniProt IDs, abundances, and tissue-specific expressions of Cd-binding proteins, annotated as genetic markers in 12 cancer types. Abundances and tissue-specific expressions were mined according to the protein abundance database PaxDB (https://pax-db.org (accessed on 21 October 2022)) and human proteome atlas database (https://www.proteinatlas.org (accessed on 21 October 2022)).

| A/A | Gene | UniProt ID | Abundance (ppm) | Protein Name | High Expression Level |
|---|---|---|---|---|---|
| 1 | *GALNT10* | Q86SR1 | 161 | Polypeptide N-acetylgalactosaminyltransferase 10 | Lung, gall bladder, kidney |
| 2 | *NOTCH4* | Q99466 | 47 | Neurogenic locus notch homolog protein 4 | Adipose, lung |
| 3 | *GZMB* | P10144 | 288 | Granzyme B | Dendritic cells |
| 4 | *BLK* | P51451 | 36 | Tyrosine-protein kinase Blk | Spleen, bone marrow |
| 5 | *AXL* | P30530 | 681 | Tyrosine-protein kinase receptor UFO | Testis, skeletal muscle |
| 6 | *TGFBR2* | P37173 | 182 | TGF-beta receptor type-2 | Adipose, breast |
| 7 | *IL2RG* | P31785 | 105 | Cytokine receptor common subunit gamma | Spleen, tonsil |
| 8 | *LCK* | P06239 | 941 | Tyrosine-protein kinase Lck | Thymus, T-cells |
| 9 | *ESR1* | P03372 | 35 | Estrogen receptor | Endometrium, cervix, uterine |
| 10 | *PRKACA* | P17612 | 697 | cAMP-dependent protein kinase catalytic subunit alpha | Cerebral cortex, testis |
| 11 | *SHC* | P29353 | 200 | SHC-transforming protein 1 | Cerebellum, thyroid gland |
| 12 | *HSP90AB1* | P08238 | 16962 | Heat shock protein HSP 90-beta | Cerebellum, adrenal gland |

Five of these proteins (tyrosine-protein kinase Blk, polypeptide N-acetylgalactosaminyltransferase 10, tyrosine-protein kinase Lck, cAMP-dependent protein kinase catalytic subunit alpha, and TGF-beta receptor type-2) are transferases. B-lymphoid tyrosine kinase (Blk) is an oncogene and a potential target for therapy with dasatinib in cutaneous T-cell lymphoma (CTCL) [95]. Gene knockdown experiments showed that Blk promoted the proliferation of malignant T-cells from CTCL patients, suggesting that Blk may function as an oncogene. Blk is also implicated in childhood acute lymphoblastic leukemia [96].

N-acetylgalactosaminyltransferase genes (GALNTs) and proteins (GalNAcTs) are involved in cancer biology. Aberrant O-glycosylation by GalNAcTs activates a wide range of proteins that carry out the interactions of sessile and motile cells affecting organogenesis and the responses to agonists, stimulating the hyperproliferation and metastization of neoplastic cells [97].
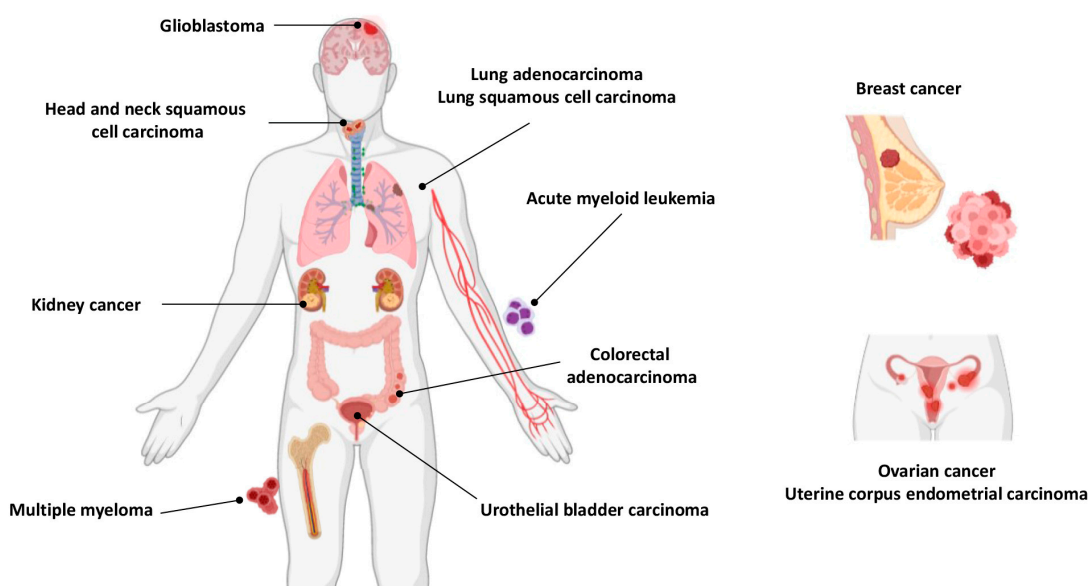
**Figure 5.** The 12 cancer types associated with specific gene-encoding Cd-metalloproteomes.

cAMP-dependent protein kinase catalytic subunit alpha is a multi-unit protein kinase that mediates the signal transduction of G-protein-coupled receptors through its activation upon cAMP binding. The cAMP/PKA signaling pathway is altered in different cancers and may be exploited for cancer therapy and/or diagnosis via cell cycle regulation and stimulated cell growth [98].

TGF-beta receptor type-2 TGF (TGFBR2) is the ligand-binding receptor for all members of the TGF-β family. TGF-beta receptor type-2 expression in cancer-associated fibroblasts regulates breast cancer cell growth and survival and is a prognostic marker in pre-menopausal breast cancer [99]. The mutational inactivation of TGFBR2 is the most common genetic event affecting the TGF-β signaling pathway and occurs in ∼20–30% of all colon cancers [100].

Among the above-mentioned 12 Cd-binding proteins, the most abundant, based on the protein abundance database PaxDB (https://pax-db.org/ (accessed on 21 October 2022)) [101], is heat shock protein HSP 90-beta, which is ranked in the top 5% of human proteins (Figure S1 in the Supplementary Materials). Heat-shock proteins are found at increased levels in many solid tumors and hematological malignancies. Their expression may, in part, account for the ability of malignant cells to maintain protein homeostasis, even in the hostile hypoxic and acidotic microenvironment of the tumor. HSP 90-beta is known as a cancer chaperone, required for the stability and function of multiple mutated, chimeric, and/or over-expressed signaling proteins that promote cancer cell growth and/or survival. It has also been implicated in many other crucial steps of carcinogenesis: the inhibition of programmed cell death and replicative senescence, the induction of tumor angiogenesis, and the activation of invasion and metastasis [102–105].

A variety of Hsp90 inhibitors have shown antitumor effects as a single agent and in combination with chemotherapy. Current Hsp90 inhibitors are categorized into several classes, based on the distinct modes of inhibition, including (i) the blockade of ATP binding, (ii) the disruption of cochaperone/Hsp90 interactions, (iii) the antagonism of client/Hsp90 associations, and (iv) interference with the post-translational modifications of Hsp90 [106].

## 6. Environmental Remediation of Cadmium

The very first prevention step regarding Cd pollution (which is actually one of the main causes of toxicity for humans) is the removal of Cd from contaminated soil and water. This task can be achieved using both physical and chemical methods: on the one hand, there are physical methods, such as adsorption, ion exchange, and reverse osmosis, while,

on the other hand, there are chemical methods, which involve precipitation, electrolysis, and solvent extraction [107]. Besides these classical methods, natural remediation from plants and other organisms has also been investigated. As an environmental pollutant, Cd, as with some other metals, is different from organic pollutants, which can be degraded by microorganisms. Microbial remediation, based on metal biosorption, is currently considered to be an efficient strategy for the detoxification of Cd from contaminated waste, water, soil, and sediments [108,109]. In the past few years, the literature has revealed an outstanding variety of microorganisms that are able to process and eliminate Cd from the environment, such as bacteria, fungi, yeasts, and different kinds of algae. In particular, bacteria such as the genera *Aeromonas*, *Bacillus*, and *Pseudomonas*, and diatom microalgae are able to efficiently accumulate Cd [110,111].

All these methods can be effective in a controlled environment, but they all need very specific conditions of climate, temperature, and humidity to be carried out in a specific ecosystem [107]. More recently, a different remediation method called "phytoremediation" has been proposed [107,112]. In the literature, it is possible to find a huge number of plant species with the peculiar skill of Cd accumulation; these plants are called Cd hyperaccumulators [113].

## 7. Detoxifying Agents and Chelating Agents for the Prevention and Treatment of Cadmium Toxicity

The toxicity of Cd has also been related to its neurotoxic effects, which develop via the changes that Cd induces in the brain enzymes. Trace elements such as Zn and selenium (Se) have been investigated as preventive agents against Cd toxicity, because of their functional role in the brain. As discussed above, $Zn^{2+}$ possesses chemical and physical characteristics that are similar to $Cd^{2+}$ and naturally compete with it for the binding sites in enzymes. Zn also induces the synthesis of the CNS-specific MT III [114], which has a high affinity for Cd and can cause detoxification by binding it. Selenium is recognized to be effective in improving antioxidant defense, immune functions, and metabolic homeostasis, with a critical role in anti-aging [115]. It plays a role in the depletion of Cd from the body by protecting it against Cd toxicity in a number of different organs, including the brain [116]. Se species combine with Cd ions, and both are excreted out of the body via the bile system. Therefore, there is less Se to form GSH peroxidase, one of the body's main antioxidants [12]. This results in the formation of greater levels of ROS and hydrogen peroxide, with relative cellular damage. Se supplementation will, therefore, be useful for increasing immunity and effectively restoring the body's antioxidant defense [115]. Se is also a cofactor of GPx, an antioxidant enzyme that can contribute to reducing Cd oxidative effects [117]. Consequently, a preventive approach to counteract chronic Cd exposure is based on the use of trace element supplements as detoxifying agents. Zn and Mg supplementation also has the potential to modulate and mitigate Cd intoxication in several organs [26,27]. In addition, several studies in animal models showed that vitamins A, C, E are able to decrease the toxic effects of Cd in the kidney, liver, spleen, blood, bones, and brain. However, further human studies are needed to clarify the role of these antioxidant vitamins in reducing Cd-induced toxicity [118].

Another strategy of prevention is action at the adsorption level, in the gastrointestinal tract. Research has indeed demonstrated that some strains of lactic acid bacteria (LAB) may be able to bind and remove heavy metals, such as Cd and lead (Pb) [119]. Moreover, probiotics such as these can have antioxidant properties for the human body, being effective against Cd-induced oxidative stress [120]. One of the most studied and convincing probiotics in this field is the *Lactobacillus plantarum* CCFM8610, which was demonstrated to have good Cd-binding ability and to be capable of protecting the liver and kidneys of mice in acute Cd intoxication [121]. This particular effect is due to the Cd sequestration at the intestinal level, reducing the bioavailability of the metal ion in tissues, and decreasing Cd-induced oxidative stress [122]. It has been demonstrated that *L. plantarum* also has a direct effect of protection against Cd-induced oxidative stress, increasing the MT protein levels in the

liver [123]. The role of N-acetyl-cysteine (NAC) has also been investigated in the past few years as a cysteine group donor with a possible key role in the biosynthesis of MTs. It has been discovered that exogenous NAC can increase the production of MTs and enhance the possibility of binding and eliminating $Cd^{2+}$ [124]. Cadmium intoxication from poisoning is extremely uncommon. The literature reported a case of Cd intoxication solved with the concomitant administration of GSH, along with the chelating agent, Ca-EDTA [125]. However, EDTA could increase the Cd levels in the kidneys, leading to renal dysfunction [126], as is the case when using dimercaprol (BAL) [127]. Penicillamine (DPA) has been found not to be efficient in Cd overdoses [128]. Meso-2,3-dimercaptosuccinic acid (succimer, DMSA) is a metal chelator not able to reach the intracellular Cd that is bound to MTs and is stored in the liver and kidneys [129]. However, a water-soluble, lipophilic chelating agent, MiADMSA, a C5-branched alkyl monoester of DMSA, can reach the stored Cd intracellularly, as well as other DMSA derivatives such as Monomethyl DMSA (MmDMSA) and Monocyclohexyl DMSA (MchDMSA) [130]. It has also been reported that a proper combination of selected chelating agents can be considered as more effective than mono-therapy [131]. This strategy considers the concomitant use of DMSA and MiADMSA, or calcium trisodium diethylene triamine pentaacetate (CaDTPA), or NAC [131].

## 8. Conclusions

In summary, this review describes the research associated with human exposure to cadmium, with an emphasis on its biological targets, toxic effects (mainly carcinogenic), and therapeutic approaches. The toxicity of $Cd^{2+}$ is, in part, due to its ability to mimic $Zn^{2+}$ and $Ca^{2+}$ in their biological roles. The presence of metallothioneins protects humans from chronic exposure to low concentrations of $Cd^{2+}$. The mechanisms of Cd-induced carcinogenesis have been related to oxidative stress with the inhibition of antioxidant enzymes, the promotion of lipid peroxidation, and interference with DNA repair systems. Strategies of prevention and treatment of Cd toxicity include the administering of trace elements, e.g., Se, as detoxifying agents, therapeutic schemes involving the use of antioxidant vitamins (A, C, E), and action at adsorption level in the gastrointestinal tract, by means of several probiotics.

Future research directions concerning the topic of this review are predicted to be: (i) an investigation of the important role of other metal-binding proteins, except the metallothioneins, and/or new receptors involved in the binding and transport of $Cd^{2+}$; (ii) advanced molecular profiling of the events associated with Cd carcinogenesis in model systems, which may allow the development of expression signatures for Cd-induced cancers; (iii) elucidation of the mechanisms for $Cd^{2+}$ clustering in the cysteine-rich regions of metallothioneins; (iv) clarification of the mechanisms that are responsible for "phytoremediation"; (v) further studies on the role played by Se in the depletion of Cd from the body; and (vi) development of selective chelating agents for $Cd^{2+}$ removal from aqueous environments via solvent extraction, an area in which our research groups are currently involved [132,133].

**Author Contributions:** Conceptualization, M.P. and A.P.; writing—original draft preparation, M.P., A.P. and C.T.C.; writing—review and editing, M.P., A.P., C.T.C., S.P.P., V.B., S.M. and M.A.Z.; visualization M.P., A.P. and C.T.C.; M.P., V.B., S.P.P., S.M. and M.A.Z. contributed to the final version of the manuscript. Revision: M.P. and S.P.P. M.P. supervised the project. All authors have read and agreed to the published version of the manuscript.

## References

1. Sharma, H.; Rawal, N.; Mathew, B.B. The characteristics, toxicity and effects of cadmium. *Int. J. Nanotechnol.* **2015**, *3*, 1–9.
2. Zoroddu, M.A.; Aaseth, J.; Crisponi, G.; Medici, S.; Peana, M.; Nurchi, V.M. The essential metals for humans: A brief overview. *J. Inorg. Biochem.* **2019**, *195*, 120–129. [CrossRef] [PubMed]
3. Maret, W.; Moulis, J.M. The bioinorganic chemistry of cadmium in the context of its toxicity. In *Metal ions in life sciences*; Springer: Berlin/Heidelberg, Germany, 2013; Volume 11, pp. 1–29.
4. Mason, R.P. *Trace Metals in Aquatic Systems*, 1st ed.; Wiley-Blackwell: Hoboken, NJ, USA, 2013.
5. Nordberg, M.; Nordberg, G.F. Metallothionein and Cadmium Toxicology-Historical Review and Commentary. *Biomolecules* **2022**, *12*, 360. [CrossRef] [PubMed]
6. Krezel, A.; Maret, W. The Bioinorganic Chemistry of Mammalian Metallothioneins. *Chem. Rev.* **2021**, *121*, 14594–14648. [CrossRef] [PubMed]
7. Klaassen, C.D.; Liu, J.; Diwan, B.A. Metallothionein protection of cadmium toxicity. *Toxicol. Appl. Pharmacol.* **2009**, *238*, 215–220. [CrossRef] [PubMed]
8. Egli, D.; Domenech, J.; Selvaraj, A.; Balamurugan, K.; Hua, H.; Capdevila, M.; Georgiev, O.; Schaffner, W.; Atrian, S. The four members of the Drosophila metallothionein family exhibit distinct yet overlapping roles in heavy metal homeostasis and detoxification. *Genes Cells* **2006**, *11*, 647–658. [CrossRef]
9. Sinicropi, M.S.; Amantea, D.; Caruso, A.; Saturnino, C. Chemical and biological properties of toxic metals and use of chelating agents for the pharmacological treatment of metal poisoning. *Arch. Toxicol.* **2010**, *84*, 501–520. [CrossRef]
10. Bernhoft, R.A. Cadmium toxicity and treatment. *Sci. World J.* **2013**, *2013*, 394652. [CrossRef]
11. Jarup, L.; Rogenfelt, A.; Elinder, C.G.; Nogawa, K.; Kjellstrom, T. Biological half-time of cadmium in the blood of workers after cessation of exposure. *Scand J. Work Environ. Health* **1983**, *9*, 327–331. [CrossRef]
12. Rani, A.; Kumar, A.; Lal, A.; Pant, M. Cellular mechanisms of cadmium-induced toxicity: A review. *Int. J. Environ. Health Res.* **2014**, *24*, 378–399. [CrossRef]
13. Branca, J.J.V.; Pacini, A.; Gulisano, M.; Taddei, N.; Fiorillo, C.; Becatti, M. Cadmium-Induced Cytotoxicity: Effects on Mitochondrial Electron Transport Chain. *Front. Cell Dev. Biol.* **2020**, *8*, 604377. [CrossRef] [PubMed]
14. Gasmi, A.; Peana, M.; Arshad, M.; Butnariu, M.; Menzel, A.; Bjørklund, G. Krebs cycle: Activators, inhibitors and their roles in the modulation of carcinogenesis. *Arch. Toxicol.* **2021**, *95*, 1161–1178. [CrossRef] [PubMed]
15. Koedrith, P.; Seo, Y.R. Advances in carcinogenic metal toxicity and potential molecular markers. *Int. J. Mol. Sci.* **2011**, *12*, 9576–9595. [CrossRef] [PubMed]
16. Beyersmann, D.; Hartwig, A. Carcinogenic metal compounds: Recent insight into molecular and cellular mechanisms. *Arch. Toxicol.* **2008**, *82*, 493. [CrossRef] [PubMed]
17. Bjørklund, G.; Zou, L.; Peana, M.; Chasapis, C.T.; Hangan, T.; Lu, J.; Maes, M. The Role of the Thioredoxin System in Brain Diseases. *Antioxidants* **2022**, *11*, 2161. [CrossRef]
18. Pearson, R.G. Chemical hardness and density functional theory. *J. Chem. Sci.* **2005**, *117*, 369–377. [CrossRef]
19. Peana, M.; Pelucelli, A.; Medici, S.; Cappai, R.; Nurchi, V.M.; Zoroddu, M.A. Metal Toxicity and Speciation: A Review. *Curr. Med. Chem.* **2021**, *28*, 7190–7208. [CrossRef]
20. Remelli, M.; Nurchi, V.M.; Lachowicz, J.I.; Medici, S.; Zoroddu, M.A.; Peana, M. Competition between Cd(II) and other divalent transition metal ions during complex formation with amino acids, peptides, and chelating agents. *Coord. Chem. Rev.* **2016**, *327-328*, 55–69. [CrossRef]
21. Wernimont, A.K.; Huffman, D.L.; Lamb, A.L.; O'Halloran, T.V.; Rosenzweig, A.C. Structural basis for copper transfer by the metallochaperone for the Menkes/Wilson disease proteins. *Nat. Struct. Biol.* **2000**, *7*, 766–771. [CrossRef]
22. Muramoto, K.; Hirata, K.; Shinzawa-Itoh, K.; Yoko-o, S.; Yamashita, E.; Aoyama, H.; Tsukihara, T.; Yoshikawa, S. A histidine residue acting as a controlling site for dioxygen reduction and proton pumping by cytochrome <em>c</em> oxidase. *Proc. Natl. Acad. Sci. USA* **2007**, *104*, 7881. [CrossRef]
23. Zangger, K.; Oz, G.; Otvos, J.D.; Armitage, I.M. Three-dimensional solution structure of mouse [Cd7]-metallothionein-1 by homonuclear and heteronuclear NMR spectroscopy. *Protein Sci.* **1999**, *8*, 2630–2638. [CrossRef] [PubMed]
24. Putignano, V.; Rosato, A.; Banci, L.; Andreini, C. MetalPDB in 2018: A database of metal sites in biological macromolecular structures. *Nucleic Acids Res.* **2018**, *46*, D459–D464. [CrossRef] [PubMed]

25. Valasatava, Y.; Rosato, A.; Cavallaro, G.; Andreini, C. MetalS(3), a database-mining tool for the identification of structurally similar metal sites. *J. Biol. Inorg. Chem.* **2014**, *19*, 937–945. [CrossRef] [PubMed]

26. Bulat, Z.; Dukic-Cosic, D.; Antonijevic, B.; Bulat, P.; Vujanovic, D.; Buha, A.; Matovic, V. Effect of magnesium supplementation on the distribution patterns of zinc, copper, and magnesium in rabbits exposed to prolonged cadmium intoxication. *Sci. World J.* **2012**, *2012*, 572514. [CrossRef]

27. Bulat, Z.P.; Djukic-Cosic, D.; Malicevic, Z.; Bulat, P.; Matovic, V. Zinc or magnesium supplementation modulates cd intoxication in blood, kidney, spleen, and bone of rabbits. *Biol. Trace Elem. Res.* **2008**, *124*, 110–117. [CrossRef]

28. Bekiari, V.; Lianos, P. High-Yield Luminescence from Cadmium Sulfide Nanoclusters Supported in a Poly(ethylene glycol) Oligomer. *Langmuir* **2000**, *16*, 3561–3563. [CrossRef]

29. Sobiech, M.; Bujak, P.; Luliński, P.; Pron, A. Semiconductor nanocrystal–polymer hybrid nanomaterials and their application in molecular imprinting. *Nanoscale* **2019**, *11*, 12030–12074. [CrossRef]

30. European Parliament. Directive (EU) 2017/2102 of the European Parliament and of the Council of 15 November 2017 amending Directive 2011/65/EU on the restriction of the use of certain hazardous substances in electrical and electronic equipment (Text with EEA relevance.). *Off. J. Eur. Union* **2017**, *L305*.

31. Xu, L.; Huo, X.; Liu, Y.; Zhang, Y.; Qin, Q.; Xu, X. Hearing loss risk and DNA methylation signatures in preschool children following lead and cadmium exposure from an electronic waste recycling area. *Chemosphere* **2020**, *246*, 125829. [CrossRef]

32. Baloch, S.; Kazi, T.G.; Baig, J.A.; Afridi, H.I.; Arain, M.B. Occupational exposure of lead and cadmium on adolescent and adult workers of battery recycling and welding workshops: Adverse impact on health. *Sci. Total. Environ.* **2020**, *720*, 137549. [CrossRef] [PubMed]

33. Hayat, M.T.; Nauman, M.; Nazir, N.; Ali, S.; Bangash, N. Chapter 7—Environmental Hazards of Cadmium: Past, Present, and Future. In *Cadmium Toxicity and Tolerance in Plants*; Hasanuzzaman, M., Prasad, M.N.V., Fujita, M., Eds.; Academic Press: Cambridge, MA, USA, 2019; pp. 163–183.

34. Chavez, E.; He, Z.L.; Stoffella, P.J.; Mylavarapu, R.S.; Li, Y.C.; Moyano, B.; Baligar, V.C. Concentration of cadmium in cacao beans and its relationship with soil cadmium in southern Ecuador. *Sci. Total. Environ.* **2015**, *533*, 205–214. [CrossRef] [PubMed]

35. Kim, K.; Melough, M.M.; Vance, T.M.; Noh, H.; Koo, S.I.; Chun, O.K. Dietary Cadmium Intake and Sources in the US. *Nutrients* **2018**, *11*. [CrossRef] [PubMed]

36. Watanabe, T.; Zhang, Z.W.; Moon, C.S.; Shimbo, S.; Nakatsuka, H.; Matsuda-Inoguchi, N.; Higashikawa, K.; Ikeda, M. Cadmium exposure of women in general populations in Japan during 1991-1997 compared with 1977-1981. *Int. Arch. Occup. Environ. Health* **2000**, *73*, 26–34. [CrossRef] [PubMed]

37. Song, Y.; Wang, Y.; Mao, W.; Sui, H.; Yong, L.; Yang, D.; Jiang, D.; Zhang, L.; Gong, Y. Dietary cadmium exposure assessment among the Chinese population. *PLoS ONE* **2017**, *12*, e0177978. [CrossRef]

38. Satarug, S.; Baker, J.R.; Urbenjapol, S.; Haswell-Elkins, M.; Reilly, P.E.; Williams, D.J.; Moore, M.R. A global perspective on cadmium pollution and toxicity in non-occupationally exposed population. *Toxicol. Lett.* **2003**, *137*, 65–83. [CrossRef]

39. Horiguchi, H.; Oguma, E.; Sasaki, S.; Miyamoto, K.; Ikeda, Y.; Machida, M.; Kayama, F. Dietary exposure to cadmium at close to the current provisional tolerable weekly intake does not affect renal function among female Japanese farmers. *Environ. Res.* **2004**, *95*, 20–31. [CrossRef]

40. Nogawa, K.; Suwazono, Y.; Nishijo, M.; Sakurai, M.; Ishizaki, M.; Morikawa, Y.; Watanabe, Y.; Kido, T.; Nakagawa, H. Increase of lifetime cadmium intake dose-dependently increased all cause of mortality in female inhabitants of the cadmium-polluted Jinzu River basin, Toyama, Japan. *Environ. Res.* **2018**, *164*, 379–384. [CrossRef]

41. Nishijo, M.; Nogawa, K.; Suwazono, Y.; Kido, T.; Sakurai, M.; Nakagawa, H. Lifetime Cadmium Exposure and Mortality for Renal Diseases in Residents of the Cadmium-Polluted Kakehashi River Basin in Japan. *Toxics* **2020**, *8*. [CrossRef]

42. Uetani, M.; Kobayashi, E.; Suwazono, Y.; Kido, T.; Nogawa, K. Cadmium exposure aggravates mortality more in women than in men. *Int. J. Environ. Health Res.* **2006**, *16*, 273–279. [CrossRef]

43. Duggan, R.E.; Lipscomb, G.Q. Dietary intake of pesticide chicals in the United States (II), June 1966—April 1968. *Pestic. Monit. J.* **1969**, *2*, 153–162.

44. Choudhury, H.; Harvey, T.; Thayer, W.C.; Lockwood, T.F.; Stiteler, W.M.; Goodrum, P.E.; Hassett, J.M.; Diamond, G.L. Urinary cadmium elimination as a biomarker of exposure for evaluating a cadmium dietary exposure–biokinetics model. *J. Toxicol. Environ. Health A* **2001**, *63*, 321–350. [CrossRef] [PubMed]

45. Mahjoub, M.; Fadlaoui, S.; El Maadoudi, M.; Smiri, Y. Mercury, Lead, and Cadmium in the Muscles of Five Fish Species from the Mechraa-Hammadi Dam in Morocco and Health Risks for Their Consumers. *J. Toxicol.* **2021**, *2021*, 8865869. [CrossRef] [PubMed]

46. Mok, J.S.; Yoo, H.D.; Kim, P.H.; Yoon, H.D.; Park, Y.C.; Lee, T.S.; Kwon, J.Y.; Son, K.T.; Lee, H.J.; Ha, K.S.; et al. Bioaccumulation of heavy metals in oysters from the southern coast of Korea: Assessment of potential risk to human health. *Bull. Environ. Contam. Toxicol.* **2015**, *94*, 749–755. [CrossRef] [PubMed]

47. Mok, J.S.; Kwon, J.Y.; Son, K.T.; Choi, W.S.; Shim, K.B.; Lee, T.S.; Kim, J.H. Distribution of heavy metals in muscles and internal organs of Korean cephalopods and crustaceans: Risk assessment for human health. *J. Food Prot.* **2014**, *77*, 2168–2175. [CrossRef] [PubMed]

48. Shi, W.; Zhao, X.; Han, Y.; Che, Z.; Chai, X.; Liu, G. Ocean acidification increases cadmium accumulation in marine bivalves: A potential threat to seafood safety. *Sci. Rep.* **2016**, *6*, 20197. [CrossRef] [PubMed]

49. Conterato, G.M.; Bulcao, R.P.; Sobieski, R.; Moro, A.M.; Charao, M.F.; de Freitas, F.A.; de Almeida, F.L.; Moreira, A.P.; Roehrs, M.; Tonello, R.; et al. Blood thioredoxin reductase activity, oxidative stress and hematological parameters in painters and battery workers: Relationship with lead and cadmium levels in blood. *J. Appl. Toxicol.* **2013**, *33*, 142–150. [CrossRef]

50. Oberdorster, G. Airborne cadmium and carcinogenesis of the respiratory tract. *Scand J. Work Environ. Health* **1986**, *12*, 523–537. [CrossRef]

51. Mannino, D.M.; Holguin, F.; Greves, H.M.; Savage-Brown, A.; Stock, A.L.; Jones, R.L. Urinary cadmium levels predict lower lung function in current and former smokers: Data from the Third National Health and Nutrition Examination Survey. *Thorax* **2004**, *59*, 194–198. [CrossRef]

52. Satarug, S.; Moore, M.R. Adverse health effects of chronic exposure to low-level cadmium in foodstuffs and cigarette smoke. *Environ. Health Perspect* **2004**, *112*, 1099–1103. [CrossRef]

53. Barregard, L.; Fabricius-Lagging, E.; Lundh, T.; Molne, J.; Wallin, M.; Olausson, M.; Modigh, C.; Sallsten, G. Cadmium, mercury, and lead in kidney cortex of living kidney donors: Impact of different exposure sources. *Environ. Res.* **2010**, *110*, 47–54. [CrossRef]

54. Bjørklund, G.; Oliinyk, P.; Lysiuk, R.; Rahaman, M.S.; Antonyak, H.; Lozynska, I.; Lenchyk, L.; Peana, M. Arsenic intoxication: General aspects and chelating agents. *Arch. Toxicol.* **2020**, *94*, 1879–1897. [CrossRef] [PubMed]

55. Liu, H.; Gao, H.; Long, M.; Fu, H.; Alvarez, P.J.J.; Li, Q.; Zheng, S.; Qu, X.; Zhu, D. Sunlight Promotes Fast Release of Hazardous Cadmium from Widely-Used Commercial Cadmium Pigment. *Environ. Sci. Technol.* **2017**, *51*, 6877–6886. [CrossRef] [PubMed]

56. Chavatte, L.; Juan, M.; Mounicou, S.; Leblanc Noblesse, E.; Pays, K.; Nizard, C.; Bulteau, A.L. Elemental and molecular imaging of human full thickness skin after exposure to heavy metals. *Metallomics* **2020**, *12*, 1555–1562. [CrossRef] [PubMed]

57. Akesson, A.; Lundh, T.; Vahter, M.; Bjellerup, P.; Lidfeldt, J.; Nerbrand, C.; Samsioe, G.; Stromberg, U.; Skerfving, S. Tubular and glomerular kidney effects in Swedish women with low environmental cadmium exposure. *Environ. Health Perspect* **2005**, *113*, 1627–1631. [CrossRef]

58. Kjellstrom, T. Mechanism and epidemiology of bone effects of cadmium. *IARC Sci. Publ.* **1992**, 301–310.

59. Pizent, A.; Tariba, B.; Zivkovic, T. Reproductive toxicity of metals in men. *Arh. Hig. Rada Toksikol.* **2012**, *63* (Suppl. 1), 35–46. [CrossRef]

60. Thompson, J.; Bannigan, J. Cadmium: Toxic effects on the reproductive system and the embryo. *Reprod. Toxicol.* **2008**, *25*, 304–315. [CrossRef]

61. Eum, K.D.; Lee, M.S.; Paek, D. Cadmium in blood and hypertension. *Sci. Total Environ.* **2008**, *407*, 147–153. [CrossRef]

62. Gallagher, C.M.; Meliker, J.R. Blood and urine cadmium, blood pressure, and hypertension: A systematic review and meta-analysis. *Environ. Health Perspect* **2010**, *118*, 1676–1684. [CrossRef]

63. Edwards, J.R.; Prozialeck, W.C. Cadmium, diabetes and chronic kidney disease. *Toxicol. Appl. Pharmacol.* **2009**, *238*, 289–293. [CrossRef]

64. Horiguchi, H.; Teranishi, H.; Niiya, K.; Aoshima, K.; Katoh, T.; Sakuragawa, N.; Kasuya, M. Hypoproduction of erythropoietin contributes to anemia in chronic cadmium intoxication: Clinical study on Itai-itai disease in Japan. *Arch. Toxicol.* **1994**, *68*, 632–636. [CrossRef] [PubMed]

65. Fujiwara, Y.; Lee, J.Y.; Banno, H.; Imai, S.; Tokumoto, M.; Hasegawa, T.; Seko, Y.; Nagase, H.; Satoh, M. Cadmium induces iron deficiency anemia through the suppression of iron transport in the duodenum. *Toxicol. Lett.* **2020**, *332*, 130–139. [CrossRef] [PubMed]

66. Li, F.J.; Surolia, R.; Singh, P.; Dsouza, K.G.; Stephens, C.T.; Wang, Z.; Liu, R.M.; Bae, S.; Kim, Y.I.; Athar, M.; et al. Fibrinogen mediates cadmium-induced macrophage activation and serves as a predictor of cadmium exposure in chronic obstructive pulmonary disease. *Am. J. Physiol. Lung Cell Mol. Physiol.* **2022**, *322*, L593–L606. [CrossRef] [PubMed]

67. Li, F.J.; Surolia, R.; Li, H.; Wang, Z.; Liu, G.; Liu, R.M.; Mirov, S.B.; Athar, M.; Thannickal, V.J.; Antony, V.B. Low-dose cadmium exposure induces peribronchiolar fibrosis through site-specific phosphorylation of vimentin. *Am. J. Physiol. Lung Cell Mol. Physiol.* **2017**, *313*, L80–L91. [CrossRef]

68. Rinaldi, M.; Micali, A.; Marini, H.; Adamo, E.B.; Puzzolo, D.; Pisani, A.; Trichilo, V.; Altavilla, D.; Squadrito, F.; Minutoli, L. Cadmium, Organ Toxicity and Therapeutic Approaches: A Review on Brain, Kidney and Testis Damage. *Curr. Med. Chem.* **2017**, *24*, 3879–3893. [CrossRef]

69. Branca, J.J.V.; Morucci, G.; Pacini, A. Cadmium-induced neurotoxicity: Still much ado. *Neural. Regen. Res.* **2018**, *13*, 1879–1882. [CrossRef]

70. Filipic, M.; Fatur, T.; Vudrag, M. Molecular mechanisms of cadmium induced mutagenicity. *Hum. Exp. Toxicol.* **2006**, *25*, 67–77. [CrossRef]

71. Joseph, P.; Muchnok, T.K.; Klishis, M.L.; Roberts, J.R.; Antonini, J.M.; Whong, W.-Z.; Ong, T.-m. Cadmium-Induced Cell Transformation and Tumorigenesis Are Associated with Transcriptional Activation of c-fos, c-jun, and c-myc Proto-Oncogenes: Role of Cellular Calcium and Reactive Oxygen Species. *Toxicol. Sci.* **2001**, *61*, 295–303. [CrossRef]

72. Liu, J.; Qu, W.; Kadiiska, M.B. Role of oxidative stress in cadmium toxicity and carcinogenesis. *Toxicol. Appl. Pharmacol.* **2009**, *238*, 209–214. [CrossRef]

73. Ogasawara, Y.; Takeda, Y.; Takayama, H.; Nishimoto, S.; Ichikawa, K.; Ueki, M.; Suzuki, T.; Ishii, K. Significance of the rapid increase in GSH levels in the protective response to cadmium exposure through phosphorylated Nrf2 signaling in Jurkat T-cells. *Free Radic. Biol. Med.* **2014**, *69*, 58–66. [CrossRef]

74. Schwerdtle, T.; Ebert, F.; Thuy, C.; Richter, C.; Mullenders, L.H.F.; Hartwig, A. Genotoxicity of Soluble and Particulate Cadmium Compounds: Impact on Oxidative DNA Damage and Nucleotide Excision Repair. *Chem. Res. Toxicol.* **2010**, *23*, 432–442. [CrossRef] [PubMed]

75. Birkou, M.; Chasapis, C.T.; Marousis, K.D.; Loutsidou, A.K.; Bentrop, D.; Lelli, M.; Herrmann, T.; Carthy, J.M.; Episkopou, V.; Spyroulias, G.A. A Residue Specific Insight into the Arkadia E3 Ubiquitin Ligase Activity and Conformational Plasticity. *J. Mol. Biol.* **2017**, *429*, 2373–2386. [CrossRef] [PubMed]

76. Chasapis, C.T.; Kandias, N.G.; Episkopou, V.; Bentrop, D.; Spyroulias, G.A. NMR-based insights into the conformational and interaction properties of Arkadia RING-H2 E3 Ub ligase. *Proteins Struct. Funct. Bioinform.* **2012**, *80*, 1484–1489. [CrossRef] [PubMed]

77. Fatur, T.; Lah, T.T.; Filipic, M. Cadmium inhibits repair of UV-, methyl methanesulfonate- and N-methyl-N-nitrosourea-induced DNA damage in Chinese hamster ovary cells. *Mutat. Res.* **2003**, *529*, 109–116. [CrossRef] [PubMed]

78. Hsieh, P.; Yamane, K. DNA mismatch repair: Molecular mechanism, cancer, and ageing. *Mech. Ageing Dev.* **2008**, *129*, 391–407. [CrossRef]

79. Jin, Y.H.; Clark, A.B.; Slebos, R.J.C.; Al-Refai, H.; Taylor, J.A.; Kunkel, T.A.; Resnick, M.A.; Gordenin, D.A. Cadmium is a mutagen that acts by inhibiting mismatch repair. *Nat. Genet.* **2003**, *34*, 326–329. [CrossRef]

80. Wieland, M.; Levin, M.K.; Hingorani, K.S.; Biro, F.N.; Hingorani, M.M. Mechanism of Cadmium-Mediated Inhibition of Msh2-Msh6 Function in DNA Mismatch Repair. *Biochemistry* **2009**, *48*, 9492–9502. [CrossRef]

81. Lützen, A.; Liberti, S.E.; Rasmussen, L.J. Cadmium inhibits human DNA mismatch repair in vivo. *Biochem. Biophys. Res. Commun.* **2004**, *321*, 21–25. [CrossRef]

82. Wang, S.; Ren, X.; Hu, X.; Zhou, L.; Zhang, C.; Zhang, M. Cadmium-induced apoptosis through reactive oxygen species-mediated mitochondrial oxidative stress and the JNK signaling pathway in TM3 cells, a model of mouse Leydig cells. *Toxicol. Appl. Pharmacol.* **2019**, *368*, 37–48. [CrossRef]

83. Yuan, Y.; Zhang, Y.; Zhao, S.; Chen, J.; Yang, J.; Wang, T.; Zou, H.; Wang, Y.; Gu, J.; Liu, X.; et al. Cadmium-induced apoptosis in neuronal cells is mediated by Fas/FasL-mediated mitochondrial apoptotic signaling pathway. *Sci. Rep.* **2018**, *8*, 8837. [CrossRef]

84. Ghajari, H.; Hosseini, S.A.; Farsi, S. The Effect of Endurance Training Along with Cadmium Consumption on Bcl-2 and Bax Gene Expressions in Heart Tissue of Rats. *Ann. Mil. Health Sci. Res.* **2019**, *17*, e86795. [CrossRef]

85. Moon, S.H.; Lee, C.M.; Nam, M.J. Cytoprotective effects of taxifolin against cadmium-induced apoptosis in human keratinocytes. *Hum. Exp. Toxicol.* **2019**, *38*, 992–1003. [CrossRef]

86. Gu, J.; Wang, Y.; Liu, Y.; Shi, M.; Yin, L.; Hou, Y.; Zhou, Y.; Chu Wong, C.K.; Chen, D.; Guo, Z.; et al. Inhibition of Autophagy Alleviates Cadmium-Induced Mouse Spleen and Human B Cells Apoptosis. *Toxicol. Sci.* **2019**, *170*, 109–122. [CrossRef] [PubMed]

87. Chiarelli, R.; Roccheri, M.C. Heavy Metals and Metalloids as Autophagy Inducing Agents: Focus on Cadmium and Arsenic. *Cells* **2012**, *1*. [CrossRef]

88. Zhang, H.; Dong, X.; Zhao, R.; Zhang, R.; Xu, C.; Wang, X.; Liu, C.; Hu, X.; Huang, S.; Chen, L. Cadmium results in accumulation of autophagosomes-dependent apoptosis through activating Akt-impaired autophagic flux in neuronal cells. *Cell. Signal.* **2019**, *55*, 26–39. [CrossRef]

89. Luo, T.; Zhang, H.; Yu, Q.; Liu, G.; Long, M.; Zhang, K.; Liu, W.; Song, R.; Bian, J.; Gu, J.; et al. ERK1/2 MAPK promotes autophagy to suppress ER stress-mediated apoptosis induced by cadmium in rat proximal tubular cells. *Toxicol. Vitr.* **2018**, *52*, 60–69. [CrossRef]

90. Wang, Y.; Mandal, A.K.; Son, Y.-O.K.; Pratheeshkumar, P.; Wise, J.T.F.; Wang, L.; Zhang, Z.; Shi, X.; Chen, Z. Roles of ROS, Nrf2, and autophagy in cadmium-carcinogenesis and its prevention by sulforaphane. *Toxicol. Appl. Pharmacol.* **2018**, *353*, 23–30. [CrossRef] [PubMed]

91. Vilahur, N.; Vahter, M.; Broberg, K. The Epigenetic Effects of Prenatal Cadmium Exposure. *Curr. Environ. Health Rep.* **2015**, *2*, 195–203. [CrossRef] [PubMed]

92. Wang, B.; Li, Y.; Shao, C.; Tan, Y.; Cai, L. Cadmium and its epigenetic effects. *Curr. Med. Chem.* **2012**, *19*, 2611–2620. [CrossRef]

93. Chasapis, C.T. Shared gene-network signatures between the human heavy metal proteome and neurological disorders and cancer types. *Metallomics* **2018**, *10*, 1678–1686. [CrossRef]

94. Weinstein, J.N.; Collisson, E.A.; Mills, G.B.; Shaw, K.R.; Ozenberger, B.A.; Ellrott, K.; Shmulevich, I.; Sander, C.; Stuart, J.M. The Cancer Genome Atlas Pan-Cancer analysis project. *Nat. Genet.* **2013**, *45*, 1113–1120. [CrossRef] [PubMed]

95. Petersen, D.L.; Krejsgaard, T.; Berthelsen, J.; Fredholm, S.; Willerslev-Olsen, A.; Sibbesen, N.A.; Bonefeld, C.M.; Andersen, M.H.; Francavilla, C.; Olsen, J.V.; et al. B-lymphoid tyrosine kinase (Blk) is an oncogene and a potential target for therapy with dasatinib in cutaneous T-cell lymphoma (CTCL). *Leukemia* **2014**, *28*, 2109–2112. [CrossRef] [PubMed]

96. Montero-Ruiz, O.; Alcantara-Ortigoza, M.A.; Betancourt, M.; Juarez-Velazquez, R.; Gonzalez-Marquez, H.; Perez-Vera, P. Expression of RUNX1 isoforms and its target gene BLK in childhood acute lymphoblastic leukemia. *Leuk Res.* **2012**, *36*, 1105–1111. [CrossRef] [PubMed]

97. Hussain, M.R.; Hoessli, D.C.; Fang, M. N-acetylgalactosaminyltransferases in cancer. *Oncotarget* **2016**, *7*, 54067–54081. [CrossRef] [PubMed]

98. Sapio, L.; Di Maiolo, F.; Illiano, M.; Esposito, A.; Chiosi, E.; Spina, A.; Naviglio, S. Targeting protein kinase A in cancer therapy: An update. *Excli. J.* **2014**, *13*, 843–855.

99. Busch, S.; Acar, A.; Magnusson, Y.; Gregersson, P.; Rydén, L.; Landberg, G. TGF-beta receptor type-2 expression in cancer-associated fibroblasts regulates breast cancer cell growth and survival and is a prognostic marker in pre-menopausal breast cancer. *Oncogene* **2015**, *34*, 27–38. [CrossRef]

100. Biswas, S.; Chytil, A.; Washington, K.; Romero-Gallo, J.; Gorska, A.E.; Wirth, P.S.; Gautam, S.; Moses, H.L.; Grady, W.M. Transforming growth factor beta receptor type II inactivation promotes the establishment and progression of colon cancer. *Cancer Res.* **2004**, *64*, 4687–4692. [CrossRef]

101. Wang, M.; Herrmann, C.J.; Simonovic, M.; Szklarczyk, D.; von Mering, C. Version 4.0 of PaxDb: Protein abundance data, integrated across model organisms, tissues, and cell-lines. *PROTEOMICS* **2015**, *15*, 3163–3168. [CrossRef]

102. Den, R.B.; Lu, B. Heat shock protein 90 inhibition: Rationale and clinical potential. *Ther. Adv. Med. Oncol.* **2012**, *4*, 211–218. [CrossRef]

103. Moser, C.; Lang, S.A.; Stoeltzing, O. Heat-shock Protein 90 (Hsp90) as a Molecular Target for Therapy of Gastrointestinal Cancer. *Anticancer Res.* **2009**, *29*, 2031.

104. Mahalingam, D.; Swords, R.; Carew, J.S.; Nawrocki, S.T.; Bhalla, K.; Giles, F.J. Targeting HSP90 for cancer therapy. *Br. J. Cancer* **2009**, *100*, 1523–1529. [CrossRef]

105. Neckers, L. Heat shock protein 90: The cancer chaperone. *J. Biosci.* **2007**, *32*, 517–530. [CrossRef]

106. Li, Y.; Zhang, T.; Schwartz, S.J.; Sun, D. New developments in Hsp90 inhibitors as anti-cancer therapeutics: Mechanisms, clinical perspective and more potential. *Drug Resist. Updat.* **2009**, *12*, 17–27. [CrossRef] [PubMed]

107. Mahajan, P.; Kaushal, J. Role of Phytoremediation in Reducing Cadmium Toxicity in Soil and Water. *J. Toxicol.* **2018**, *2018*, 4864365. [CrossRef] [PubMed]

108. Chellaiah, E.R. Cadmium (heavy metals) bioremediation by Pseudomonas aeruginosa: A minireview. *Appl. Water Sci.* **2018**, *8*, 154. [CrossRef]

109. Kumar, A.; Subrahmanyam, G.; Mondal, R.; Cabral-Pinto, M.M.S.; Shabnam, A.A.; Jigyasu, D.K.; Malyan, S.K.; Fagodiya, R.K.; Khan, S.A.; Yu, Z.G. Bio-remediation approaches for alleviation of cadmium contamination in natural resources. *Chemosphere* **2021**, *268*, 128855. [CrossRef]

110. Fakhar, A.; Gul, B.; Gurmani, A.R.; Khan, S.M.; Ali, S.; Sultan, T.; Chaudhary, H.J.; Rafique, M.; Rizwan, M. Heavy metal remediation and resistance mechanism of Aeromonas, Bacillus, and Pseudomonas: A review. *Crit. Rev. Environ. Sci. Technol.* **2022**, *52*, 1868–1914. [CrossRef]

111. Chasapis, C.T.; Peana, M.; Bekiari, V. Structural Identification of Metalloproteomes in Marine Diatoms, an Efficient Algae Model in Toxic Metals Bioremediation. *Molecules* **2022**, *27*. [CrossRef]

112. Shah, V.; Daverey, A. Phytoremediation: A multidisciplinary approach to clean up heavy metal contaminated soil. *Environ. Technol. Innov.* **2020**, *18*, 100774. [CrossRef]

113. Raza, A.; Habib, M.; Kakavand, S.N.; Zahid, Z.; Zahra, N.; Sharif, R.; Hasanuzzaman, M. Phytoremediation of Cadmium: Physiological, Biochemical, and Molecular Mechanisms. *Biology (Basel)* **2020**, *9*. [CrossRef]

114. Hidalgo, J.; Aschner, M.; Zatta, P.; Vasak, M. Roles of the metallothionein family of proteins in the central nervous system. *Brain Res. Bull.* **2001**, *55*, 133–145. [CrossRef] [PubMed]

115. Bjørklund, G.; Shanaida, M.; Lysiuk, R.; Antonyak, H.; Klishch, I.; Shanaida, V.; Peana, M. Selenium: An Antioxidant with a Critical Role in Anti-Aging. *Molecules* **2022**, *27*. [CrossRef] [PubMed]

116. Cardoso, B.R.; Roberts, B.R.; Bush, A.I.; Hare, D.J. Selenium, selenoproteins and neurodegenerative diseases. *Metallomics* **2015**, *7*, 1213–1228. [CrossRef]

117. Liu, M.C.; Xu, Y.; Chen, Y.M.; Li, J.; Zhao, F.; Zheng, G.; Jing, J.F.; Ke, T.; Chen, J.Y.; Luo, W.J. The effect of sodium selenite on lead induced cognitive dysfunction. *Neurotoxicology* **2013**, *36*, 82–88. [CrossRef]

118. Sitek, A.; Kozlowska, L. The role of well-known antioxidant vitamins in the prevention of cadmium-induced toxicity. *Int. J. Occup. Med. Environ. Health* **2022**, *35*, 367–392. [CrossRef] [PubMed]

119. Halttunen, T.; Collado, M.C.; El-Nezami, H.; Meriluoto, J.; Salminen, S. Combining strains of lactic acid bacteria may reduce their toxin and heavy metal removal efficiency from aqueous solution. *Lett. Appl. Microbiol.* **2008**, *46*, 160–165. [CrossRef]

120. Forsyth, C.B.; Farhadi, A.; Jakate, S.M.; Tang, Y.; Shaikh, M.; Keshavarzian, A. Lactobacillus GG treatment ameliorates alcohol-induced intestinal oxidative stress, gut leakiness, and liver injury in a rat model of alcoholic steatohepatitis. *Alcohol* **2009**, *43*, 163–172. [CrossRef] [PubMed]

121. Zhai, Q.; Wang, G.; Zhao, J.; Liu, X.; Tian, F.; Zhang, H.; Chen, W. Protective effects of Lactobacillus plantarum CCFM8610 against acute cadmium toxicity in mice. *Appl. Environ. Microbiol.* **2013**, *79*, 1508–1515. [CrossRef] [PubMed]

122. Zhu, J.; Yu, L.; Shen, X.; Tian, F.; Zhao, J.; Zhang, H.; Chen, W.; Zhai, Q. Protective Effects of Lactobacillus plantarum CCFM8610 against Acute Toxicity Caused by Different Food-Derived Forms of Cadmium in Mice. *Int. J. Mol. Sci.* **2021**, *22*. [CrossRef]

123. Zhai, Q.; Wang, G.; Zhao, J.; Liu, X.; Narbad, A.; Chen, Y.Q.; Zhang, H.; Tian, F.; Chen, W. Protective effects of Lactobacillus plantarum CCFM8610 against chronic cadmium toxicity in mice indicate routes of protection besides intestinal sequestration. *Appl. Environ. Microbiol.* **2014**, *80*, 4063–4071. [CrossRef]

124. Deng, X.; Xia, Y.; Hu, W.; Zhang, H.; Shen, Z. Cadmium-induced oxidative damage and protective effects of N-acetyl-L-cysteine against cadmium toxicity in *Solanum nigrum* L. *J. Hazard. Mater* **2010**, *180*, 722–729. [CrossRef] [PubMed]

125. Gil, H.W.; Kang, E.J.; Lee, K.H.; Yang, J.O.; Lee, E.Y.; Hong, S.Y. Effect of glutathione on the cadmium chelation of EDTA in a patient with cadmium intoxication. *Hum. Exp. Toxicol.* **2011**, *30*, 79–83. [CrossRef]

126. Wu, X.; Su, S.; Zhai, R.; Chen, K.; Jin, T.; Huang, B.; Zhou, Y.; Ge, X.; Wei, G.; Liao, R. Lack of reversal effect of EDTA treatment on cadmium induced renal dysfunction: A fourteen-year follow-up. *Biometals* **2004**, *17*, 435–441. [CrossRef] [PubMed]

127. Gonick, H.C. Nephrotoxicity of cadmium & lead. *Indian J. Med. Res.* **2008**, *128*, 335–352.

128. Jalilehvand, F.; Leung, B.O.; Mah, V. Cadmium(II) complex formation with cysteine and penicillamine. *Inorg. Chem.* **2009**, *48*, 5758–5771. [CrossRef]

129. Patrick, L. Toxic metals and antioxidants: Part II. The role of antioxidants in arsenic and cadmium toxicity. *Altern. Med. Rev. A J. Clin. Ther.* **2003**, *8*, 106–128.

130. Flora, S.J.; Pachauri, V. Chelation in metal intoxication. *Int. J. Environ. Res. Public Health* **2010**, *7*, 2745–2788. [CrossRef]

131. Rafati Rahimzadeh, M.; Kazemi, S.; Moghadamnia, A.A. Cadmium toxicity and treatment: An update. *Caspian J. Intern. Med.* **2017**, *8*, 135–145. [CrossRef]

132. Routzomani, A.; Lada, Z.G.; Angelidou, V.; C, P.R.; Psycharis, V.; Konidaris, K.F.; Chasapis, C.T.; Perlepes, S.P. Confirming the Molecular Basis of the Solvent Extraction of Cadmium(II) Using 2-Pyridyl Oximes through a Synthetic Inorganic Chemistry Approach and a Proposal for More Efficient Extractants. *Molecules* **2022**, *27*. [CrossRef]

133. Mazarakioti, E.C.; Beobide, A.S.; Angelidou, V.; Efthymiou, C.G.; Terzis, A.; Psycharis, V.; Voyiatzis, G.A.; Perlepes, S.P. Modeling the Solvent Extraction of Cadmium(II) from Aqueous Chloride Solutions by 2-pyridyl Ketoximes: A Coordination Chemistry Approach. *Molecules* **2019**, *24*. [CrossRef]

**REVIEW ARTICLE**

# Environmental barium: potential exposure and health-hazards

Massimiliano Peana[1] · Serenella Medici[1] · Maryam Dadar[2] · Maria Antonietta Zoroddu[1] ·
Alessio Pelucelli[1] · Christos T. Chasapis[3,4] · Geir Bjørklund[5]

## Abstract

The relatively widespread presence of environmental barium is raising a growing public awareness as it can lead to different health conditions. Its presence in humans may produce several effects, especially among those chronically exposed from low to moderate doses. Barium accumulation can mainly occur by exposure in the workplace or from drinking contaminated water. However, this element is also assumed with the diet, mainly from plant foods. The average amount of barium intake worldwide and its geographical variation is little known due to the lack of research attention. Barium was never considered as an essential nutrient for humans, although it is undoubtedly naturally abundant enough and distinctive in its chemical properties that it might well have some biochemical function, e.g., for regulatory purposes, both in animals and plants. The information on the potential health effects of barium exposure is primarily based on animal studies and reported as comprising kidney diseases, neurological, cardiovascular, mental, and metabolic disorders. The present paper considers exposure and potential health concerns on environmental barium, giving evidence to information that can be used in future epidemiological and experimental studies.

**Keywords** Barium · Drinking water · Environmental exposure

## Introduction

Barium is an alkaline earth metal whose natural abundance places it as the 14th most common element on the Earth's crust at around 500 ppm, more abundant than zinc. Due to its high chemical reactivity, it is never found as a free element, but in the form of salts as sulfates and carbonates.

✉ Serenella Medici
  sere@uniss.it

✉ Geir Bjørklund
  bjorklund@conem.org

1 Department of Chemistry and Pharmacy, University of Sassari, via Vienna 2, 07100 Sassari, Italy

2 Razi Vaccine and Serum Research Institute, Agricultural Research, Education and Extension Organization (AREEO), Karaj, Iran

3 NMR Center, Instrumental Analysis Laboratory, School of Natural Sciences, University of Patras, Patras, Greece

4 School of Agricultural Science, University of Patras, Messolonghi, Greece

5 Council for Nutritional and Environmental Medicine, Toften 24, 8610 Mo i Rana, Norway

Barium does not have a recognized biological role in humans (Zoroddu et al. 2019). However, it appears to be essential for some organisms' proper growth, such as desmid green alga *Closterium moniliferum* containing vesicles with barium sulfate in the crystalline form as barite (Krejci et al. 2011). Human uptake is linked to absorption mainly through food, and drinking water to a lesser extent. It has been evaluated that food, in general, contains less than 3 mg/100 g, except for Brazilian nuts (150–300 mg/100 g), while the content in drinking water is variable, depending on the geographical area, but it mainly lies in the order of tens of micrograms per liter (Poddalgoda et al. 2017). Bread alone contributes to the daily intake of dietary barium with a 20%. Average barium levels in body tissues are estimated to be around 20 mg (Emsley 1998). Biomonitoring reports have been performed on barium concentration in urines of exposed mice to establish the potential health consequences in humans (Poddalgoda et al. 2017).

The toxicity of barium compounds for both acute and chronic exposure (vide infra) is well documented and is dependent on their solubility. Nevertheless, reported cases of barium poisoning remain rather limited, with around 40 acute intoxications involving less than 250 people during

the past seven decades, as surveyed in 2014 (Bhoelan et al. 2014).

Barium is employed in many industrial applications (Chałupnik et al. 2019; Dallas and Williams 2001). Barium salts (nitrate and sulfate), are used in many productions, such as plastics, ceramics, adhesives, in drilling fluids for oils and gas wells, as a green coloring in fireworks by burning barium nitrate and chlorate, as a white pigment in paints or to preserve old frescoes. Barium-containing hair dyes are used in some countries (Khalili et al. 2016; Platzek 2010; Pragst et al. 2017), and barium sulfate ($BaSO_4$) is permitted by the Cosmetic Directive of the European Union and may be utilized as a colorant in cosmetics and personal care products. Moreover, the study of new materials for medical, industrial, and technological applications led to the development of nanoparticles based on $BaSO_4$ (Konduru et al. 2014; Webster et al. 2013) or barium composites (Genchi et al. 2016; Marino et al. 2019), thus increasing the possibility of environmental contamination (Crisponi et al. 2017; Zoroddu et al. 2014). However, it should be unlikely that the total contribution from unnatural sources of barium, such as cosmetics or local industry, can be significant enough to explain the high concentrations of this element found in the hair of the population during various screenings. It is much more probable, for partly hypothetical, but nevertheless, plausible reasons that have been explained above, that most of it come either from the diet or drinking water, or a combination of the two.

The importance of evaluating risk connected to barium exposure or poisoning increases as the use of barium for industrial purposes grows steadily. Here we would like to give an overview of the different routes of exposure for humans and how they can affect health.

## Barium chemistry

Barium (Ba), whose name derives from the Greek *barys*, s, i.e., "heavy", belongs to group IIA, alkaline earth metals, of the Periodic Table ($Z = 56$; atomic mass 137.34 uma). It is silvery-white in aspect, soft, and easily oxidized by oxygen in air and water. For this reason, it cannot be found in nature as the native element, but only under the form of a divalent cation, $Ba^{2+}$, mainly contained in sulfates (barite or baryte, $BaSO_4$) and carbonates (witherite, $BaCO_3$). Other barium salts as acetate, chloride, sulfide, nitrate, or compounds such as barium hydroxide are obtained from barite, and they show a wide range of solubility in water. However, since their natural occurrence is uncommon, there is no particular concern about the contamination of drinking water by natural sources, while barium pollution deriving from anthropogenic activities and its diffusion in the environment is rather alarming.

## Barium in soils and plants

### Barium in soil

The average crustal abundance of barium is estimated to be around 425 ppm (Nan et al. 2018), being the 14th element in order of abundance on the Earth crust, so it is not a very scarce metal in ordinary rocks, compared for instance to manganese, which is only a little more than twice as abundant as barium. However, chemical fertilizers rich in potassium ($K^+$) and/or ammonium ($NH_4^+$) ions may mobilize $Ba^{2+}$ ions that clay minerals in the soil had previously adsorbed because of competition between $K^+$ or $NH_4^+$ and $Ba^{2+}$ to the same binding sites on the negatively charged basal surfaces of clay minerals (Fig. 1).

However, $Ba^{2+}$ is also strongly adsorbed by clay minerals (Atun and Bascetin 2003) since it has an ionic radius not much different from $K^+$ (Killops and Killops 2005; Misra 2012), and therefore fits sterically well into the same positions where $K^+$ ions are bound. Simultaneously, the electrostatic attraction force to the negatively charged surface of the clay mineral crystal is twice as high for $Ba^{2+}$ as for $K^+$, thus helping the process.

According to Krauskopf (1982), the ionic radius for $Ba^{2+}$ hexacoordinated to six negatively charged oxygen atoms (octahedral coordination) is 1.34 Å, while it is 1.33 Å for $K^+$, 1.47 Å for rubidium ($Rb^+$), 1.67 Å for cesium ($Cs^+$), 0.97 Å for $Na^+$, 0.68 Å for $Li^+$, 1.12 Å for $Sr^{2+}$, 0.99 Å for $Ca^{2+}$, 0.66 Å for $Mg^{2+}$, 1.20 Å for $Pb^{2+}$, 0.97 Å for $Cd^{2+}$ and 0.74 Å for $Zn^{2+}$ (Krauskopf 1982). $Rb^+$, because of its larger ionic radius, will bind even more strongly than $K^+$ to the surface of clay minerals, which makes it a useful indicator element (by measuring the Rb/K ratio in soils or plants) for studying natural soil-forming processes or their anthropogenic disturbance, e.g., because of pollution (acid rain), as it has been done in Norway, where it was found that the Rb/K ratio in forest trees was higher in districts that had been especially severely affected by acid rain deposition (Løbersli 1991), most likely because it is not leached by the acid rain away from its position at the surface of the clay mineral equally as easily as it happens with $K^+$. For understanding the processes that may have led to barium enrichment in soils, it would probably be useful to measure concentrations of both rubidium and potassium in soils and plants at the same time as barium is measured, and strontium and calcium concentrations as well.

The Ba/Sr and Pb/Sr concentration ratios of the soil also depend, of course, on the nature of the source rocks, since the average Ba/Sr and Pb/Sr concentration ratios are much higher for granitic rocks (with 600 ppm Ba, 285 ppm Sr and 20 ppm Pb) than for basalts (with 250 ppm Ba, 465 ppm Sr and 5 ppm Pb) (Krauskopf 1982; Misra 2012).
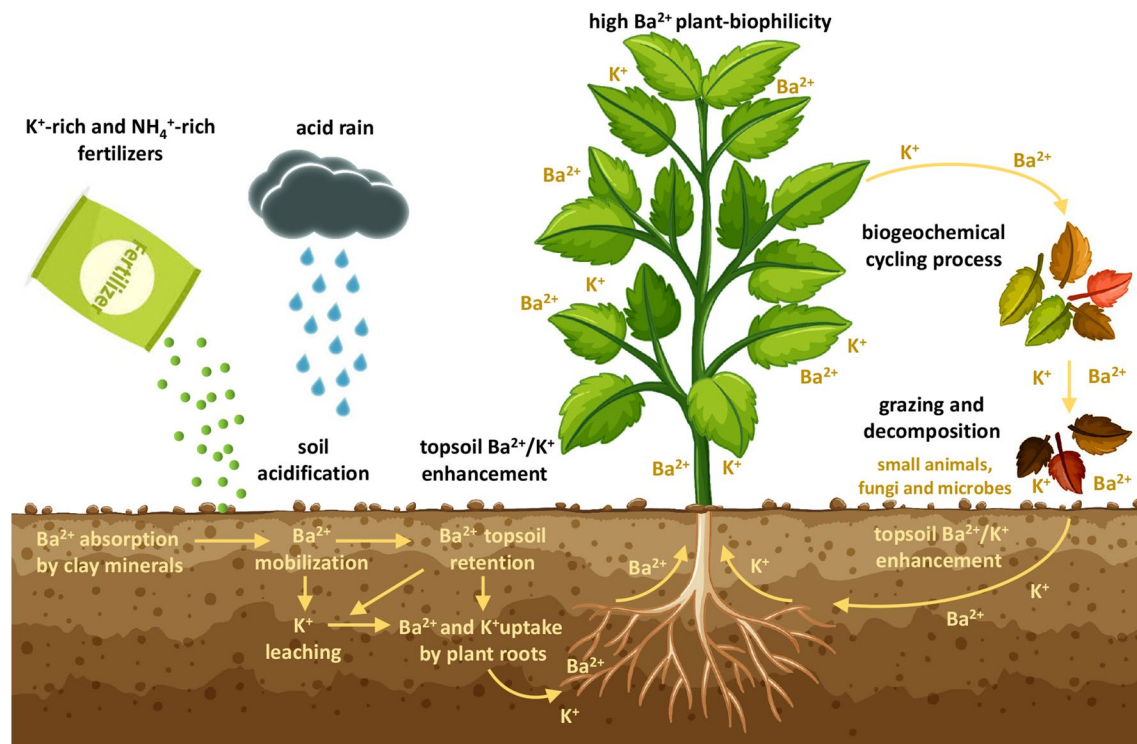
**Fig. 1** Barium absorption and mobilization in soil and barium uptake by plants in a biogeochemical cycling process

Soil acidification because of fertilizer application will cause reduction of the negative charge on the surface of clay minerals and partly release all cations tightly bound to their surface, such as $K^+$, $NH_4^+$, and $Ba^{2+}$, but also cations such as $Mg^{2+}$ (which to a great measure is incorporated into the primary structure of clay minerals rather than only being bound at their surface), $Zn^{2+}$ and $Cu^{2+}$ (Blume et al. 2016; Bohn et al. 2011; Marschner 2012).

It might also be speculated that $Ba^{2+}$ that has been adsorbed on clay minerals perhaps could be preferentially retained, compared to $K^+$, in the topsoil during the natural development of soil profiles either because of easier leaching of $K^+$, compared to $Ba^{2+}$, or because of lower uptake of $K^+$ compared to $Ba^{2+}$ in plant roots, which will lead to more up-concentration of $Ba^{2+}$ than of $K^+$ at the top of the soil profile, similarly as what happens with all plant-biophilic elements that are not too readily leachable in the topsoil (Gökmenoğlu 1991) (Fig. 1). This might lead to gradual enhancement of the topsoil's Ba/K concentration ratio until more $K^+$ and $NH_4^+$ are added in the form of fertilizers and mobilize much of the previously accumulated $Ba^{2+}$. Between these two different possible mechanisms for enhancing the $Ba^{2+}/K^+$ concentration ratio in the topsoil, preferential leaching of $K^+$, since $Ba^{2+}$ with its double positive charge might be more strongly bound to the clay minerals than $K^+$, would appear to be the most plausible one (Fig. 1).

## Barium uptake by plants

Barium in plants should most likely almost entirely come from natural sources since it is not an element found at high concentrations in phosphorites or in any other of the raw materials used in the production of commercial fertilizers. Its concentration in seawater, from which primary phosphorites originally deposited, is low, only 0.03 ppm (Moore 1997; Pyle et al. 2017), since it is limited by the high concentration of sulfate ions in the marine environment, which contains around 885 ppm sulfur (Boon and Jones 2016; Hsieh and Henderson 2017), and the low-solubility product of $BaSO_4$. Moreover, there is no local enhancement of the seawater sulfate concentration at sites of phosphorite deposition, which would have been needed to precipitate barium from seawater in the form of barite crystals.

Studies of the elemental composition of plants have shown that barium is a strong plant-biophilic element, as illustrated by comparing the Ba/Zn concentration ratios in apple and tomato leaves with the estimated average Ba/Zn abundance ratio for the continental crust. In one study, apple leaves were found to contain 49 ppm of barium and 12.5 ppm of zinc, while tomato leaves contained 63 ppm of barium and 30.9 ppm of zinc (Padilla and Anderson 2002). As previously reminded, the continental crust is estimated to contain 425 ppm of barium and 70 ppm of zinc (Krauskopf 1982), making barium somewhat less, but not much less

plant-biophilic than zinc. Barium must, therefore, be taken up by active transport in the plant roots, either because it follows some of the other plant nutrient elements (using the same membrane transport system(s) in the root cells or mycorrhiza) or because it might perhaps function as a plant nutrient itself. However, $Ba^{2+}$ is apparently not taken up by plant roots in preference to $K^+$, judging from admittedly minimal data (Fig. 1).

Even if it should be correct that root uptake of $Ba^{2+}$ in plants is somewhat poorer than $K^+$, plants will nevertheless transport both elements upwards to their leaves (or to the needles if conifers) from deeper layers of the soil—with the vertical extent of this transport depending on the average and maximum depth of the plant roots. There will thus be a local biogeochemical cycling process for both elements, where transport by water flow through the xylem from the roots up to the leaves or needles (where water evaporates, leaving silicon and other dissolved plant nutrient behind) is followed by grazing and decomposition of plant litter by small animals, fungi and microbes in the soil, leading to the release of both elements to the topsoil (mainly with feces and urines). This release process will finally be followed by the removal of both elements by leaching processes and subsequent transport downwards through the soil profile until they are once more taken up by the plant roots and transported upwards again to the aerial parts of the plants, thus making the whole cycle repeat itself (Fig. 1).

If the quotient between the rate constants for removal of $Ba^{2+}$ and $K^+$ from topsoil by vertical leaching is smaller than the corresponding quotient between the rate constants for uptake of both elements in the plant roots, the cyclic process described above must lead to progressive enhancement of the Ba/K concentration ratio of the topsoil (compared to deeper parts of the soil profile) until finally a steady state is reached, so that the Ba/K concentration ratio in the topsoil does not increase anymore. It may be expected, though, that the effectiveness of this mechanism of enrichment of $Ba^{2+}$ in the topsoil by a biogeochemical cycling process combined with some kind of partial chromatographic separation of different elements may strongly depend on the depth of the root system of the plants—with sort of a long "chromatographic column" making the process of element fractionation more efficient than a short one. So the process will probably be much more effective in such forests, where the trees have deeper roots than in open grasslands. However, the chromatographic separation process must be expected to be even less effective in such farmlands that are used for cereal or other food crop production and therefore are plowed every year than it is in permanent grasslands that are never utilized for the production of cereals or other annual food plants and therefore never plowed.

Barium is chemically very similar to radium (Ra), which belongs to the same group in the Periodic System. In an environment with much soluble uranium (U) in the soil, it must be expected that radium from radioactive decay of uranium will be taken up by plant roots at substantial levels, similarly as barium does, and much better than uranium itself; there is no reason to expect that radium will be a substantially less plant-biophile than barium. If the bioavailability of barium for uptake in the plant roots is high, the same must also be expected for radium in the soil. The observation supports this assumption since Brazil nuts (seeds of the tree *Bertholletia excelsa*) contain not only much barium, but also much radium (Armelin et al. 2019; Parekh et al. 2008; Turner et al. 1958). The accumulation of radium (and barium) is not due to the high concentration of uranium in the soil where the tree grows but rather to the very extensive and effective root system of the tree.

## Agricultural plants and barium uptake

It might be speculated that barium accumulation in the topsoils might have happened in many places before most of the land was cleared for agriculture, for example, in Southern Asia, i.e., when forests still covered much of the land. Considering both the climate—with a long, dry winter monsoon season—and the nature of local soils (with a high content of sand or coarse silt particles that were deposited by rivers from Himalaya soon after they had come down to the plain in front of the mountains, but with enough clay minerals in the soil because of subsequent chemical weathering that it may have functioned as a giant chromatographic column), it is a reasonable speculation that tree species with deep roots may have dominated the natural forests of the area before farming took over, similarly as for the pine forests growing on sand plains in several valleys in Southern Norway. This type of forest may presumably have provided almost optimal conditions for the accumulation of $Ba^{2+}$ to high concentrations (and with high Ba/K concentration ratios) in the topsoils. It is not entirely implausible that a similar chromatographic process in the soil might also be part of the explanation for the high barium concentrations that have been found in Brazil nuts (Gonçalves et al. 2009; Lemire et al. 2010; Parekh et al. 2008).

However, it is possible that barium, except for the rather particular and peculiar problem of high concentrations in Brazil nuts, may have received much less research attention worldwide, compared to several other plant-biophilic elements, because it has been thought neither to be essential for the plants nor toxic, while the potential value of studying concentration ratios such as Ba/K and Rb/K in soils and plants as indicators of environmental change (because of acid rain, deforestation leading to enhanced soil erosion, anthropogenic fires or commercial fertilizer application on arable lands) may have been overlooked. Its potential value as an indicator element helps study

processes happening in forest soils because acid rain seems to have been more or less ignored in polluted areas in Europe, and it is not clear how much barium may be deposited from acid rain because of the barium content in coal.

As for plant food grown on soils containing high barium levels, both from natural and industrial origins, different indications come from studies carried out in distinct parts of the world. For instance, research conducted in the areas around the world's largest barium mine in Dahebian, Tian-zhu, Guizhou Province, southwestern China, considered the total concentrations and phytoavailability of barium in samples of paddy soils and paired samples of rice grown in the same places. All the soils were heavily contaminated, with barium concentrations ranging from about 520 to 65 mg/kg, which was reflected in the equally high levels in rice (up to 3.5 mg/kg). Nevertheless, a parallel study on risk assessment showed that the population had low exposure to barium deriving from rice than the other routes of exposure present in the highly contaminated mining area (Lu et al. 2019).

Plants can be seriously affected by high concentrations of toxic metals like barium, which can activate undesirable modifications in their metabolic activity. Plants respond to its presence with the production of reactive oxygen species (ROS). This oxidative stress is counteracted by developing a dual cellular system composed of enzymatic and non-enzymatic species able to transform ROS and their side-products into stable innocuous molecules. This occurrence was studied in two brassica species exposed to increasing barium concentrations, up to 500 μM. Their response was evaluated by examining a series of parameters such as plant morphology and development, antioxidant enzymatic activities in the leaves, and production of secondary metabolites. Both species were able to survive to the highest levels of barium. Nevertheless, the stress caused by exposure to the toxic metal activated the antioxidant paths, which were evidenced by changes in the leaves activity of catalase, ascorbate peroxidase, and guaiacol peroxidase (Bouslimi et al. 2021).

Comparable results were found in the investigation on the effects of high levels of barium on Tanzania guinea grass (de Souza Cardoso and Monteiro 2021), which were able to induce phytotoxicity by acting on several mechanisms related to growth and nutritional status and lead to the weakening of the adult plants and death of basal sprouts. Sulfur supplements seem to reduce barium phytotoxicity by acting positively on the superoxide dismutase and guaiacol peroxidase activities and proline metabolism (de Souza Cardoso and Monteiro 2021), but also via the precipitation of insoluble $BaSO_4$, thus sequestering the toxic metal in the plant (de Souza Cardoso and Monteiro 2021). These results evidence that plants can survive in areas with massive barium pollution, but their viability may be affected. In this case, the use of sulfur-rich soil conditioners may be beneficial for heavily exposed plants.

## Barium toxicity

Highly insoluble barium salts, such as $BaSO_4$, are considered non or slightly toxic for the human organism, while soluble species are often considered harmful. Barium sulfate is used as a routine contrast agent in the X-ray medical diagnosis of colorectal and upper gastrointestinal disturbances since it remains essentially unabsorbed and is thus innoxious to humans. On the other hand, ingestion of soluble barium salts induces dangerous cell processes like hypokalemic paralysis, resulting in respiratory and cardiac arrest (vide infra) (Oskarsson 2015). In this respect, a singular case of suicide has been reported by swallowing high doses of soluble barium acetate (Fenu et al. 2021).

Food ingestion of barium, particularly as carbonate, is the most frequent cause of barium poisoning. Barium carbonate is easily dissolved in the stomach's acidic environment, which makes it a strong poison. In the past, barium carbonate was therefore used as a rodenticide. Contamination with barium may also occur by inhalation and skin contact (Krishna et al. 2020), especially in the workplace.

Acute poisoning may cause several symptoms, such as gastrointestinal (gastric pain, nausea, vomiting, and diarrhea), metabolic (hypokalemia, leading in turn to ventricular tachycardia, hypertension and/or hypotension, muscle weakness, and paralysis), cardiovascular (changes in heart rhythm and increased or decreased blood pressure), musculoskeletal (numbness, muscle weakness, and paralysis), and neurological (tremors, seizures, and mydriasis) effects (Moffett et al. 2007) (Fig. 2).

On the other hand, chronic exposure can be dangerous, especially for children and young people, since it can affect their health during a long lifespan. However, unlike other heavy metals, barium seems to be a non-carcinogenic species, and the Department of Health and Human Services and the International Agency for Research on Cancer have not assessed this point yet. Moreover, the conclusions drawn by US EPA are that barium is not likely to be carcinogenic to humans following oral exposure, and its carcinogenic potential cannot be determined following inhalation, as stated in 2007. Nevertheless, recent studies may indicate the contrary. Human nontumorigenic HaCaT keratinocytes exposed to barium showed an ability to promote anchorage-independent growth and invasion, together with the transforming activity of various other nontumorigenic cells (Kato et al. 2020). More studies are needed to clarify this aspect since the evidence on barium carcinogenicity is rather limited.

Barium does not lead to bioaccumulation in human tissues, but if insoluble compounds are inhaled, their levels
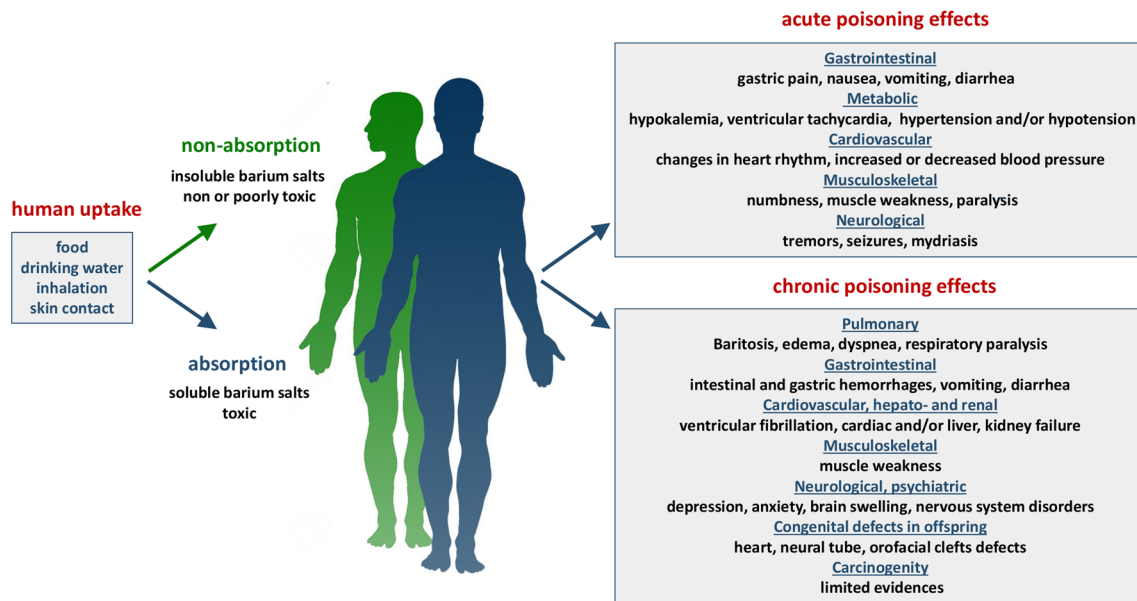
**Fig. 2** Barium uptake and health hazards from acute and chronic exposure

can build up in the lungs to cause a benign condition known as "Baritosis".

Consumption of drinking water containing barium levels much above the Environmental Protection Agency (EPA) drinking water guidelines for relatively short periods can cause gastrointestinal disturbances and muscle weakness (which is consistent with a hypothesis that barium might be an essential nutrient mainly functioning as an intracellular signal substance, i.e., as a second messenger). Moreover, barium attacks the potassium inward rectifier channels (IRCs) of the KCNJx gene family. It can efficiently bind the potassium selectivity filter region, thus blocking the relative conducting pore. IRCs take part in several of the human organism's physiological processes, and these are strongly affected by barium that is highly expressed in all muscle tissues (Bhoelan et al. 2014).

Toxic concentrations of barium were found in workers and the rest of the population living in the oil fields of Thar Jath, South Sudan, due to heavy contamination of the groundwater and surface basins caused by the massive use of $BaSO_4$ in the drilling mud, together with galena (PbS). This affected not only humans but also livestock, causing their death. Samples of hair were taken from volunteers living at a different distance from the oil plant. As expected, barium concentrations increased as the distance decreased (Pragst et al. 2017). Pollution of industrial sites should thus be carefully controlled and avoided as much as possible since barium compounds can easily reach the water tables and surface basins, and if there is no decontamination plant to treat the drinking water, a serious threat is posed to the health of the population. Moreover, trees and plants can mobilize

insoluble barium salts (vide supra), leading to increased barium levels in humans from plant food consumption.

Ingesting high doses of barium for a long time can damage the kidneys and is associated with cardiovascular malfunction (Dallas and Williams 2001). However, there is most likely a good safety margin between even the highest natural barium intake and the threshold for toxic effects.

An important aspect of barium contamination is emerging from different studies correlated with congenital defects in newborn children. For instance, a strong correlation was found between prenatal exposure (measured by barium levels in the hair of pregnant women) and increased risk for heart defects (Zhang et al. 2018), neural tube defects (Wang et al. 2020), and orofacial clefts (Lv et al. 2021; Pi et al. 2019) in their offspring. Thus, special care should be devoted to the decontamination of water consumed by fertile and pregnant women.

Another risk factor was found for older women since barium seems to increase depression (Lv et al. 2021). Interestingly, this association was not found in men.

## Health impacts of barium from environmental exposure

Barium exposure can be divided into chronic (more than one year), intermediate (15–364 days), and acute (< 14 days). Intermediate exposure types were studied for inhalation and oral routes in animals, while chronic exposures were investigated predominantly for the oral route (Kravchenko et al. 2014). However, in humans,

chronic exposures were better studied for oral and inhalation routes, while intermediate exposures were only examined for the oral route. Highly detailed studies of barium exposure and the toxic impacts on human health have been requested, although it is difficult to translate the effects in animals to human models. Most barium exposure in humans occurs by inhalation or ingestion (Gould et al. 1973; McNeill and Isoardi 2019; Siddiqui 2017). The most important toxic effects include pulmonary edema, intestinal and gastric hemorrhages, cardiac and/or renal failure, and respiratory paralysis (Krishna et al. 2020; McNeill and Isoardi 2019; Poddalgoda et al. 2017) (Fig. 2). Furthermore, highly soluble $BaCl_2$, as a human toxin, causes cardiac arrhythmias, vomiting, diarrhea, liver and kidney failure, anxiety, disorders of the nervous system (i.e., tremors), dyspnea, and—in severe cases—ventricular fibrillation, paralysis, and brain swelling (Bohn et al. 2011; Krauskopf 1982; McNeill and Isoardi 2019). However, as previously mentioned, barium poisoning is rather uncommon.

## Concluding remarks

Increased concerns about the potential effects of environmental barium exposure on human health have been induced by a growing increase in public awareness of the vast gamut of barium applications. The presence of naturally high barium concentrations in many soils, agricultural plants, and drinking water led to scientific analyses that tried to highlight the potential effects of exposure to this element. Awareness of environmental intake, distribution, and aggravation of barium in the human organism and its potentially toxic effects is essential because several communities are exposed to high barium levels resulting in an elevated risk for public health from barium contamination. Future investigation is hotly demanded to improve an understanding of barium bioaccumulation to restrict its potential health effects in different exposure situations. Further, it is also critical to recognize potentially vulnerable populations such as children, pregnant women, and the elderly at higher risk of barium exposure from food and drinking water in polluted areas.

## Declarations

**Conflict of interest** The authors declare that they have no conflict of interest. The authors declare that they have no known competing financial interests or personal relationships that could have influenced the work reported in this paper.

## References

Armelin MJA, Maihara VA, Cozzolino SM, Silva PS, Saiki M (2019) Concentrations of Se, Ba, Zn and Mn in Brazil nuts. Braz J Radiat Sci. https://doi.org/10.15392/bjrs.v7i2A.701

Atun G, Bascetin E (2003) Adsorption of barium on kaolinite, illite and montmorillonite at various ionic strengths. Radiochim Acta 91(4):223–228

Bhoelan BS, Stevering CH, van der Boog ATJ, van der Heyden MAG (2014) Barium toxicity and the role of the potassium inward rectifier current. Clin Toxicol (Phila) 52(6):584–593. https://doi.org/10.3109/15563650.2014.923903

Blume H-P, Brümmer GW, Horn R, Kandeler E, Kögel-Knabner I, Kretzschmar R, Stahr K, Wilke B-M (2016) Scheffer/schachtschabel: lehrbuch der bodenkunde. Springer-Verlag

Bohn HL, McNeal BL, O'Connor GA (2011) Soil chemistry: chemical units. Wiley

Boon M, Jones F (2016) Barium sulfate crystallization from synthetic seawater. Cryst Growth Des 16(8):4646–4657. https://doi.org/10.1021/acs.cgd.6b00729

Bouslimi H, Ferreira R, Dridi N, Brito P, Martins-Dias S, Caçador I, Sleimi N (2021) Effects of barium stress in brassica juncea and cakile maritima: the indicator role of some antioxidant enzymes and secondary metabolites. Phyton-Int J Exp Bot. https://doi.org/10.32604/phyton.2020.011752

Chałupnik S, Wysocka M, Chmielewska I, Samolej K (2019) Radium removal from mine waters with the application of barium chloride and zeolite: comparison of efficiency. J Sustain Min 18(4):174–181. https://doi.org/10.1016/j.jsm.2019.07.002

Crisponi G, Nurchi VM, Lachowicz JI, Peana M, Medici S, Zoroddu MA (2017) Chapter 18—toxicity of nanoparticles: etiology and mechanisms. In: Grumezescu AM (ed) Antimicrobial nanoarchitectonics. Elsevier, pp 511–546

Dallas CE, Williams PL (2001) Barium: rationale for a new oral reference dose. J Toxicol Environ Health B Crit Rev 4(4):395–429. https://doi.org/10.1080/109374001753146216

de Souza Cardoso AA, Monteiro FA (2021) Sulfur supply reduces barium toxicity in Tanzania guinea grass (Panicum maximum) by inducing antioxidant enzymes and proline metabolism. Ecotoxicol Environ Saf 208:111643. https://doi.org/10.1016/j.ecoenv.2020.111643

Emsley J (1998) The elements. Clarendon Press, Oxford (**Oxford University Press, New York**)

Fenu EM, Brower JO, O'Neill TE (2021) Suicide by an unusual compound: a case of barium acetate toxicity. Am J Forensic Med Pathol. https://doi.org/10.1097/PAF.0000000000000663

Genchi GG, Marino A, Rocca A, Mattoli V, Ciofani G (2016) Barium titanate nanoparticles: promising multitasking vectors in nanomedicine. Nanotechnology 27(23):232001. https://doi.org/10.1088/0957-4484/27/23/232001

Gökmenoğlu Z (1991) Sorption behaviour of Ba++, Co++ and Zn++ ions on alumina, kaolinite and magnesite. Bilkent University

Gonçalves AM, Fernandes KG, Ramos LA, Cavalheiro ÉT, Nóbrega JA (2009) Determination and fractionation of barium in Brazil nuts. J Braz Chem Soc 20(4):760–769. https://doi.org/10.1590/S0103-50532009000400020

Gould DB, Sorrell MR, Lupariello AD (1973) Barium sulfide poisoning: some factors contributing to survival. Arch Intern Med 132(6):891–894. https://doi.org/10.1001/archinte.132.6.891

Hsieh Y-T, Henderson GM (2017) Barium stable isotopes in the global ocean: tracer of Ba inputs and utilization. Earth Planet Sci Lett 473:269–278. https://doi.org/10.1016/j.epsl.2017.06.024

Kato M, Ohgami N, Ohnuma S, Hashimoto K, Tazaki A, Xu H, Kondo-Ida L, Yuan T et al (2020) Multidisciplinary approach to assess the toxicities of arsenic and barium in drinking water.

Environ Health Prev Med 25(1):16–16. https://doi.org/10.1186/s12199-020-00855-8

Khalili F, Mahvi A, Nasseri S, Yunesian M, Djahed B, Yaseri M (2016) Risk assessment of non-carcinogenic heavy metals (barium, cadmium, and lead) in hair color in markets of Tehran. Iranian Journal of Health and Environment 9(1):27–40

Killops S, Killops V (2005) Introduction to organic geochemistry, vol 5. Wiley

Konduru N, Keller J, Ma-Hock L, Groters S, Landsiedel R, Donaghey TC, Brain JD, Wohlleben W et al (2014) Biokinetics and effects of barium sulfate nanoparticles. Part Fibre Toxicol 11:55. https://doi.org/10.1186/s12989-014-0055-3

Krauskopf K (1982) Introduction to geochemistry, 2nd edn. McGraw-Hill Book Company, Auckland, Singapore

Kravchenko J, Darrah TH, Miller RK, Lyerly HK, Vengosh A (2014) A review of the health impacts of barium from natural and anthropogenic exposure. Environ Geochem Health 36(4):797–814. https://doi.org/10.1007/s10653-014-9622-7

Krejci MR, Wasserman B, Finney L, McNulty I, Legnini D, Vogt S, Joester D (2011) Selectivity in biomineralization of barium and strontium. J Struct Biol 176(2):192–202. https://doi.org/10.1016/j.jsb.2011.08.006

Krishna S, Jaiswal A, Sujata GM, Sharma DK, Ali Z (2020) Barium poisoning with analytical aspects and its management. Int J Adv Res Med Chem 2(1):20–27

Lemire M, Fillion M, Barbosa F Jr, Guimarães JRD, Mergler D (2010) Elevated levels of selenium in the typical diet of Amazonian riverside populations. Sci Total Environ 408(19):4076–4084. https://doi.org/10.1016/j.scitotenv.2010.05.022

Løbersli EM (1991) Soil acidification and metal uptake in plants. PhD. thesis, University of Trondheim, Norway

Lu Q, Xu X, Liang L, Xu Z, Shang L, Guo J, Xiao D, Qiu G (2019) Barium concentration, phytoavailability, and risk assessment in soil-rice systems from an active barium mining region. Appl Geochem 106:142–148. https://doi.org/10.1016/j.apgeochem.2019.05.010

Lv J, Li Y-l, Ren W-q, Li R, Chen J-r, Bao C, Du Z-p, Feng S et al (2021) Increased depression risk for elderly women with high blood levels of strontium and barium. Environ Chem Lett. https://doi.org/10.1007/s10311-020-01146-y

Marino A, Almici E, Migliorin S, Tapeinos C, Battaglini M, Cappello V, Marchetti M, de Vito G et al (2019) Piezoelectric barium titanate nanostimulators for the treatment of glioblastoma multiforme. J Colloid Interface Sci 538:449–461. https://doi.org/10.1016/j.jcis.2018.12.014

Marschner H (2012) Marschner's mineral nutrition of higher plants, vol 89. Academic press

McNeill IR, Isoardi KZ (2019) Barium poisoning: an uncommon cause of severe hypokalemia. Toxicol Commun 3(1):88–90. https://doi.org/10.1080/24734306.2019.1691340

Misra KC (2012) Introduction to geochemistry: principles and applications. John Wiley & Sons

Moffett D, Smith C, Stevens Y, Ingerman L, Swarts S, Chappell L (2007) Toxicological profile for barium and barium compounds. Agency for toxic substances and disease registry. US Department of Health and Human Services, Atlanta, Georgia

Moore WS (1997) High fluxes of radium and barium from the mouth of the Ganges-Brahmaputra River during low river discharge suggest a large groundwater source. Earth Planet Sci Lett 150(1–2):141–150. https://doi.org/10.1016/S0012-821X(97)00083-6

Nan X-Y, Yu H-M, Rudnick RL, Gaschnig RM, Xu J, Li W-Y, Zhang Q, Jin Z-D et al (2018) Barium isotopic composition of the upper continental crust. Geochim Cosmochim Acta 233:33–49. https://doi.org/10.1016/j.gca.2018.05.004

Oskarsson A (2015) Chapter 29—barium. In: Nordberg GF, Fowler BA, Nordberg M (eds) Handbook on the toxicology of metals, 4th edn. Academic Press, San Diego, pp 625–634

Padilla KL, Anderson KA (2002) Trace element concentration in tree-rings biomonitoring centuries of environmental change. Chemosphere 49(6):575–585. https://doi.org/10.1016/s0045-6535(02)00402-2

Parekh P, Khan A, Torres M, Kitto M (2008) Concentrations of selenium, barium, and radium in Brazil nuts. J Food Compost Anal 21(4):332–335. https://doi.org/10.1016/j.jfca.2007.12.001

Pi X, Jin L, Li Z, Liu J, Zhang Y, Wang L, Ren A (2019) Association between concentrations of barium and aluminum in placental tissues and risk for orofacial clefts. Sci Total Environ 652:406–412. https://doi.org/10.1016/j.scitotenv.2018.10.262

Platzek T (2010) Risk from exposure to arylamines from consumer products and hair dyes. Front Biosci (Elite Ed) 2:1169–1183

Poddalgoda D, Macey K, Assad H, Krishnan K (2017) Development of biomonitoring equivalents for barium in urine and plasma for interpreting human biomonitoring data. Regul Toxicol Pharmacol 86:303–311. https://doi.org/10.1016/j.yrtph.2017.03.022

Pragst F, Stieglitz K, Runge H, Runow K-D, Quig D, Osborne R, Runge C, Ariki J (2017) High concentrations of lead and barium in hair of the rural population caused by water pollution in the Thar Jath oilfields in South Sudan. Forensic Sci Int 274:99–106. https://doi.org/10.1016/j.forsciint.2016.12.022

Pyle K, Hendry K, Sherrell R, Meredith M, Venables H, Lagerström M, Morte-Rodenas A (2017) Coastal barium cycling at the West Antarctic Peninsula. Deep Sea Res Part II Top Stud Oceanogr 139:120–131. https://doi.org/10.1016/j.dsr2.2016.11.010

Siddiqui B (2017) Symptoms mimicking those of hypokalemic periodic paralysis induced by soluble barium poisoning. Fed Pract 34(7):42

Turner R, Radley J, Mayneord W (1958) The naturally occurring alfa-ray activity of foods. Health Phys 1(3):268–275. https://doi.org/10.1097/00004032-195807000-00002

Wang C, Pi X, Chen Y, Wang D, Yin S, Jin L, Li Z, Ren A et al (2020) Prenatal exposure to barium and the occurrence of neural tube defects in offspring. Sci Total Environ 764:144245. https://doi.org/10.1016/j.scitotenv.2020.144245

Webster TJ, Stout AI, GE, Yang, (2013) Nano-BaSO4: a novel anti-microbial additive to pellethane. Int J Nanomedicine. https://doi.org/10.2147/ijn.s40300

Zhang N, Liu Z, Tian X, Chen M, Deng Y, Guo Y, Li N, Yu P et al (2018) Barium exposure increases the risk of congenital heart defects occurrence in offspring. Clin Toxicol (Phila) 56(2):132–139. https://doi.org/10.1080/15563650.2017.1343479

Zoroddu MA, Medici S, Ledda A, Nurchi VM, Lachowicz JI, Peana M (2014) Toxicity of nanoparticles. Curr Med Chem 21(33):3837–3853. https://doi.org/10.2174/092986732166614060116231a

Zoroddu MA, Aaseth J, Crisponi G, Medici S, Peana M, Nurchi VM (2019) The essential metals for humans: a brief overview. J Inorg Biochem 195:120–129. https://doi.org/10.1016/j.jinorgbio.2019.03.013

# Bibliografia

1. Permyakov, E.A. Metal Binding Proteins. *Encyclopedia* **2021**, *1*, 261-292. https://doi.org/10.3390/encyclopedia1010024.
2. Maret, W. An Appraisal of the Field of Metallomics and the Roles of Metal Ions in Biochemistry and Cell Signaling. *Applied Sciences* **2021**, *11*. https://doi.org/10.3390/app112210846.
3. Zoroddu, M.A.; Aaseth, J.; Crisponi, G.; Medici, S.; Peana, M.; Nurchi, V.M. The essential metals for humans: a brief overview. *J Inorg Biochem* **2019**, *195*, 120-129. https://doi.org/10.1016/j.jinorgbio.2019.03.013.
4. Peana, M.; Pelucelli, A.; Medici, S.; Cappai, R.; Nurchi, V.M.; Zoroddu, M.A. Metal Toxicity and Speciation: A Review. *Curr Med Chem* **2021**, *28*, 7190-7208. https://doi.org/10.2174/0929867328666210324161205.
5. Kim, J.J.; Kim, Y.S.; Kumar, V. Heavy metal toxicity: An update of chelating therapeutic strategies. *J Trace Elem Med Biol* **2019**, *54*, 226-231. https://doi.org/10.1016/j.jtemb.2019.05.003.
6. Barnham, K.J.; Bush, A.I. Metals in Alzheimer's and Parkinson's diseases. *Curr Opin Chem Biol* **2008**, *12*, 222-228. https://doi.org/10.1016/j.cbpa.2008.02.019.
7. Kozlowski, H.; Luczkowski, M.; Remelli, M.; Valensin, D. Copper, zinc and iron in neurodegenerative diseases (Alzheimer's, Parkinson's and prion diseases). *Coordination Chemistry Reviews* **2012**, *256*, 2129-2141. https://doi.org/https://doi.org/10.1016/j.ccr.2012.03.013.
8. Kozlowski, H.; Janicka-Klos, A.; Brasun, J.; Gaggelli, E.; Valensin, D.; Valensin, G. Copper, iron, and zinc ions homeostasis and their role in neurodegenerative disorders (metal uptake, transport, distribution and regulation). *Coordination Chemistry Reviews* **2009**, *253*, 2665-2685. https://doi.org/https://doi.org/10.1016/j.ccr.2009.05.011.
9. Adlard, P.A.; Bush, A.I. Metals and Alzheimer's Disease: How Far Have We Come in the Clinic? *J Alzheimers Dis* **2018**, *62*, 1369-1379. https://doi.org/10.3233/JAD-170662.
10. Koski, L.; Ronnevi, C.; Berntsson, E.; Warmlander, S.; Roos, P.M. Metals in ALS TDP-43 Pathology. *Int J Mol Sci* **2021**, *22*. https://doi.org/10.3390/ijms222212193.
11. Boulikas, T.; Vougiouka, M. Recent clinical trials using cisplatin, carboplatin and their combination chemotherapy drugs (Review). *Oncol Rep* **2004**, *11*, 559-595. https://doi.org/10.3892/or.11.3.559.
12. Medici, S.; Peana, M.; Nurchi, V.M.; Lachowicz, J.I.; Crisponi, G.; Zoroddu, M.A. Noble metals in medicine: Latest advances. *Coordination Chemistry Reviews* **2015**, *284*, 329-350. https://doi.org/https://doi.org/10.1016/j.ccr.2014.08.002.
13. Ji, J.; Chen, G.; Zhao, J. Preparation and characterization of amino/thiol bifunctionalized magnetic nanoadsorbent and its application in rapid removal of Pb (II) from aqueous system. *J Hazard Mater* **2019**, *368*, 255-263. https://doi.org/10.1016/j.jhazmat.2019.01.035.
14. Cantu, J.; Valle, J.; Flores, K.; Gonzalez, D.; Valdes, C.; Lopez, J.; Padilla, V.; Alcoutlabi, M.; Parsons, J. Investigation into the thermodynamics and kinetics of the binding of Cu(2+) and Pb(2+) to TiS(2) nanoparticles synthesized using a solvothermal process. *J Environ Chem Eng* **2019**, *7*. https://doi.org/10.1016/j.jece.2019.103463.

15. Crisponi, G.; Nurchi, V.M. Metal Ion Toxicity. In *Encyclopedia of Inorganic and Bioinorganic Chemistry*; 2015; pp. 1-14. https://doi.org/https://doi.org/10.1002/9781119951438.eibc0126.pub2.

16. Anthemidis, A.N.; Ioannou, K.I. Recent developments in homogeneous and dispersive liquid-liquid extraction for inorganic elements determination. A review. *Talanta* **2009**, *80*, 413-421. https://doi.org/10.1016/j.talanta.2009.09.005.

17. Fu, F.; Wang, Q. Removal of heavy metal ions from wastewaters: a review. *J Environ Manage* **2011**, *92*, 407-418. https://doi.org/10.1016/j.jenvman.2010.11.011.

18. Oliveira, V.H.B.; Rechotnek, F.; da Silva, E.P.; Marques, V.d.S.; Rubira, A.F.; Silva, R.; Lourenço, S.A.; Muniz, E.C. A sensitive electrochemical sensor for Pb2+ ions based on ZnO nanofibers functionalized by L-cysteine. *Journal of Molecular Liquids* **2020**, *309*, 113041. https://doi.org/https://doi.org/10.1016/j.molliq.2020.113041.

19. Cappai, R.; Chand, K.; Lachowicz, J.I.; Chaves, S.; Gano, L.; Crisponi, G.; Nurchi, V.M.; Peana, M.; Zoroddu, M.A.; Santos, M.A. A new tripodal-3-hydroxy-4-pyridinone for iron and aluminium sequestration: synthesis, complexation and in vivo studies. *New Journal of Chemistry* **2018**, *42*, 8050-8061. https://doi.org/10.1039/C8NJ00116B.

20. Cardiano, P.; Foti, C.; Giuffrè, O. On the interaction of N-acetylcysteine with Pb2+, Zn2+, Cd2+ and Hg2+. *Journal of Molecular Liquids* **2016**, *223*, 360-367. https://doi.org/https://doi.org/10.1016/j.molliq.2016.08.050.

21. Irto, A.; Cardiano, P.; Chand, K.; Cigala, R.M.; Crea, F.; De Stefano, C.; Gattuso, G.; Sammartano, S.; Santos, M.A. Complexation of environmentally and biologically relevant metals with bifunctional 3-hydroxy-4-pyridinones. *Journal of Molecular Liquids* **2020**, *319*, 114349. https://doi.org/https://doi.org/10.1016/j.molliq.2020.114349.

22. Irto, A.; Cardiano, P.; Chand, K.; Cigala, R.M.; Crea, F.; De Stefano, C.; Gano, L.; Gattuso, G.; Sammartano, S.; Santos, M.A. A new bis-(3-hydroxy-4-pyridinone)-DTPA-derivative: Synthesis, complexation of di-/tri-valent metal cations and in vivo M3+ sequestering ability. *Journal of Molecular Liquids* **2019**, *281*, 280-294. https://doi.org/https://doi.org/10.1016/j.molliq.2019.02.042.

23. Bjorklund, G.; Tippairote, T.; Hangan, T.; Chirumbolo, S.; Peana, M. Early-Life Lead Exposure: Risks and Neurotoxic Consequences. *Curr Med Chem* **2023**. https://doi.org/10.2174/0929867330666230409135310.

24. Peana, M.; Pelucelli, A.; Chasapis, C.T.; Perlepes, S.P.; Bekiari, V.; Medici, S.; Zoroddu, M.A. Biological Effects of Human Exposure to Environmental Cadmium. *Biomolecules* **2022**, *13*. https://doi.org/10.3390/biom13010036.

25. Agency for Toxic Substances and Disease Registry. Available online: https://www.atsdr.cdc.gov/ (accessed on may 2023).

26. Antimicrobial Resistance, C. Global burden of bacterial antimicrobial resistance in 2019: a systematic analysis. *Lancet* **2022**, *399*, 629-655. https://doi.org/10.1016/S0140-6736(21)02724-0.

27. O'Neill, J. Tackling drug-resistant infections globally: final report and recommendations. **2016**.

28. Poirel, L.; Madec, J.Y.; Lupo, A.; Schink, A.K.; Kieffer, N.; Nordmann, P.; Schwarz, S. Antimicrobial Resistance in Escherichia coli. *Microbiol Spectr* **2018**, *6*. https://doi.org/10.1128/microbiolspec.ARBA-0026-2017.

29. WHO. WHO publishes list of bacteria for which new antibiotics are urgently needed. **2017**.

30. Hennigar, S.R.; McClung, J.P. Nutritional Immunity: Starving Pathogens of Trace Minerals. *Am J Lifestyle Med* **2016**, *10*, 170-173. https://doi.org/10.1177/1559827616629117.

31. Puig, S.; Ramos-Alonso, L.; Romero, A.M.; Martinez-Pastor, M.T. The elemental role of iron in DNA synthesis and repair. *Metallomics* **2017**, *9*, 1483-1500. https://doi.org/10.1039/c7mt00116a.

32. Mikhaylina, A.; Ksibe, A.Z.; Scanlan, D.J.; Blindauer, C.A. Bacterial zinc uptake regulator proteins and their regulons. *Biochem Soc Trans* **2018**, *46*, 983-1001. https://doi.org/10.1042/BST20170228.

33. Lemos, M.L.; Balado, M. Iron uptake mechanisms as key virulence factors in bacterial fish pathogens. *J Appl Microbiol* **2020**, *129*, 104-115. https://doi.org/10.1111/jam.14595.

34. Bradley, J.M.; Svistunenko, D.A.; Wilson, M.T.; Hemmings, A.M.; Moore, G.R.; Le Brun, N.E. Bacterial iron detoxification at the molecular level. *J Biol Chem* **2020**, *295*, 17602-17623. https://doi.org/10.1074/jbc.REV120.007746.

35. Saha, R.; Saha, N.; Donofrio, R.S.; Bestervelt, L.L. Microbial siderophores: a mini review. *J Basic Microbiol* **2013**, *53*, 303-317. https://doi.org/10.1002/jobm.201100552.

36. Saha, M.; Sarkar, S.; Sarkar, B.; Sharma, B.K.; Bhattacharjee, S.; Tribedi, P. Microbial siderophores and their potential applications: a review. *Environ Sci Pollut Res Int* **2016**, *23*, 3984-3999. https://doi.org/10.1007/s11356-015-4294-0.

37. Astuti, I.; Ysrafil. Severe Acute Respiratory Syndrome Coronavirus 2 (SARS-CoV-2): An overview of viral structure and host response. *Diabetes Metab Syndr* **2020**, *14*, 407-412. https://doi.org/10.1016/j.dsx.2020.04.020.

38. Ozono, S.; Zhang, Y.; Ode, H.; Sano, K.; Tan, T.S.; Imai, K.; Miyoshi, K.; Kishigami, S.; Ueno, T.; Iwatani, Y.; et al. SARS-CoV-2 D614G spike mutation increases entry efficiency with enhanced ACE2-binding affinity. *Nat Commun* **2021**, *12*, 848. https://doi.org/10.1038/s41467-021-21118-2.

39. Beyerstedt, S.; Casaro, E.B.; Rangel, E.B. COVID-19: angiotensin-converting enzyme 2 (ACE2) expression and tissue susceptibility to SARS-CoV-2 infection. *Eur J Clin Microbiol Infect Dis* **2021**, *40*, 905-919. https://doi.org/10.1007/s10096-020-04138-6.

40. Ni, W.; Yang, X.; Yang, D.; Bao, J.; Li, R.; Xiao, Y.; Hou, C.; Wang, H.; Liu, J.; Yang, D.; et al. Role of angiotensin-converting enzyme 2 (ACE2) in COVID-19. *Crit Care* **2020**, *24*, 422. https://doi.org/10.1186/s13054-020-03120-0.

41. Perrotta, F.; Matera, M.G.; Cazzola, M.; Bianco, A. Severe respiratory SARS-CoV2 infection: Does ACE2 receptor matter? *Respir Med* **2020**, *168*, 105996. https://doi.org/10.1016/j.rmed.2020.105996.

42. Fatouros, P.R.; Roy, U.; Sur, S. Implications of SARS-CoV-2 spike protein interactions with Zn-bound form of ACE2: a computational structural study. *Biometals* **2023**, 1-10. https://doi.org/10.1007/s10534-023-00491-z.

43. Towler, P.; Staker, B.; Prasad, S.G.; Menon, S.; Tang, J.; Parsons, T.; Ryan, D.; Fisher, M.; Williams, D.; Dales, N.A.; et al. ACE2 X-ray structures reveal a large hinge-bending motion important for inhibitor binding and catalysis. *J Biol Chem* **2004**, *279*, 17996-18007. https://doi.org/10.1074/jbc.M311191200.

44. Pelucelli, A.; Peana, M.; Orzeł, B.; Piasta, K.; Gumienna-Kontecka, E.; Medici, S.; Zoroddu, M.A. Zn2+ and Cu2+ Interaction with the Recognition Interface of ACE2 for

SARS-CoV-2 Spike Protein. *International Journal of Molecular Sciences* **2023**, *24*. https://doi.org/10.3390/ijms24119202.

45. Nurchi, V.M.; de Guadalupe Jaraquemada-Pelaez, M.; Crisponi, G.; Lachowicz, J.I.; Cappai, R.; Gano, L.; Santos, M.A.; Melchior, A.; Tolazzi, M.; Peana, M.; et al. A new tripodal kojic acid derivative for iron sequestration: Synthesis, protonation, complex formation studies with Fe(3+), Al(3+), Cu(2+) and Zn(2+), and in vivo bioassays. *J Inorg Biochem* **2019**, *193*, 152-165. https://doi.org/10.1016/j.jinorgbio.2019.01.012.

46. Nurchi, V.M.; Crisponi, G.; Lachowicz, J.I.; Jaraquemada-Pelaez, M.G.; Bretti, C.; Peana, M.; Medici, S.; Zoroddu, M.A. Equilibrium studies of new bis-hydroxypyrone derivatives with Fe(3+), Al(3+), Cu(2+) and Zn(2). *J Inorg Biochem* **2018**, *189*, 103-114. https://doi.org/10.1016/j.jinorgbio.2018.09.013.

47. Nurchi, V.M.; Jaraquemada-Pelaez, M.d.G.; Lachowicz, J.I.; Zoroddu, M.A.; Peana, M.; Domínguez-Martín, A.; Choquesillo-Lazarte, D.; Remelli, M.; Szewczuk, Z.; Crisponi, G. Looking at new ligands for chelation therapy. *New Journal of Chemistry* **2018**, *42*, 8021-8034. https://doi.org/10.1039/C7NJ03947F.

48. Cappai, R.; Fantasia, A.; Barone, G.; Peana, M.F.; Pelucelli, A.; Medici, S.; Crisponi, G.; Nurchi, V.; Zoroddu, M.A. A Family of Kojic Acid Derivatives Aimed to Remediation of Pb2+ and Cd2+. *Available at SSRN 4402583* **2023**. https://doi.org/10.2139/ssrn.4402583.

49. Gans, P.; Sabatini, A.; Vacca, A. Investigation of equilibria in solution. Determination of equilibrium constants with the HYPERQUAD suite of programs. *Talanta* **1996**, *43*, 1739-1753. https://doi.org/10.1016/0039-9140(96)01958-3.

50. Alderighi, L.; Gans, P.; Ienco, A.; Peters, D.; Sabatini, A.; Vacca, A. Hyperquad simulation and speciation (HySS): a utility program for the investigation of equilibria involving soluble and partially soluble species. *Coordination Chemistry Reviews* **1999**, *184*, 311-318. https://doi.org/https://doi.org/10.1016/S0010-8545(98)00260-4.

51. Pecsok, R.L.; Meeker, R.L.; Shields, L.D. Chelates of Cadmium with Kojic Acid1. *Journal of the American Chemical Society* **1961**, *83*, 2081-2085. https://doi.org/10.1021/ja01470a012.

52. Agency for Toxic Substances and Disease Registry. Available online: https://www.atsdr.cdc.gov/csem/leadtoxicity/safety_standards.html (accessed on may 2023).

53. Agency for Toxic Substances and Disease Registry. Available online: https://www.atsdr.cdc.gov/csem/cadmium/Safety399Standards.html (accessed on may 2023).

54. World Health Organization. Guidelines for drinking-water quality: fourth edition incorporating the first addendum. Available online: https://www.who.int/publications/i/item/9789241549950 (accessed on may 2023).

55. Lau, C.K.; Krewulak, K.D.; Vogel, H.J. Bacterial ferrous iron transport: the Feo system. *FEMS Microbiol Rev* **2016**, *40*, 273-298. https://doi.org/10.1093/femsre/fuv049.

56. Ge, R.; Sun, X. Iron trafficking system in Helicobacter pylori. *Biometals* **2012**, *25*, 247-258. https://doi.org/10.1007/s10534-011-9512-8.

57. Hohle, T.H.; Franck, W.L.; Stacey, G.; O'Brian, M.R. Bacterial outer membrane channel for divalent metal ion acquisition. *Proc Natl Acad Sci U S A* **2011**, *108*, 15390-15395. https://doi.org/10.1073/pnas.1110137108.

58. Radka, C.D.; DeLucas, L.J.; Wilson, L.S.; Lawrenz, M.B.; Perry, R.D.; Aller, S.G. Crystal structure of Yersinia pestis virulence factor YfeA reveals two polyspecific metal-

binding sites. *Acta Crystallogr D Struct Biol* **2017**, *73*, 557-572. https://doi.org/10.1107/S2059798317006349.

59. Grass, G.; Franke, S.; Taudte, N.; Nies, D.H.; Kucharski, L.M.; Maguire, M.E.; Rensing, C. The metal permease ZupT from Escherichia coli is a transporter with a broad substrate spectrum. *J Bacteriol* **2005**, *187*, 1604-1611. https://doi.org/10.1128/JB.187.5.1604-1611.2005.

60. Haemig, H.A.; Moen, P.J.; Brooker, R.J. Evidence that highly conserved residues of transmembrane segment 6 of Escherichia coli MntH are important for transport activity. *Biochemistry* **2010**, *49*, 4662-4671. https://doi.org/10.1021/bi100320y.

61. Cartron, M.L.; Maddocks, S.; Gillingham, P.; Craven, C.J.; Andrews, S.C. Feo--transport of ferrous iron into bacteria. *Biometals* **2006**, *19*, 143-157. https://doi.org/10.1007/s10534-006-0003-2.

62. Sestok, A.E.; Linkous, R.O.; Smith, A.T. Toward a mechanistic understanding of Feo-mediated ferrous iron uptake. *Metallomics* **2018**, *10*, 887-898. https://doi.org/10.1039/c8mt00097b.

63. Naikare, H.; Palyada, K.; Panciera, R.; Marlow, D.; Stintzi, A. Major role for FeoB in Campylobacter jejuni ferrous iron acquisition, gut colonization, and intracellular survival. *Infect Immun* **2006**, *74*, 5433-5444. https://doi.org/10.1128/IAI.00052-06.

64. Velayudhan, J.; Hughes, N.J.; McColm, A.A.; Bagshaw, J.; Clayton, C.L.; Andrews, S.C.; Kelly, D.J. Iron acquisition and virulence in Helicobacter pylori: a major role for FeoB, a high-affinity ferrous iron transporter. *Mol Microbiol* **2000**, *37*, 274-286. https://doi.org/10.1046/j.1365-2958.2000.01987.x.

65. Lau, C.K.; Ishida, H.; Liu, Z.; Vogel, H.J. Solution structure of Escherichia coli FeoA and its potential role in bacterial ferrous iron transport. *J Bacteriol* **2013**, *195*, 46-55. https://doi.org/10.1128/JB.01121-12.

66. Severance, S.; Chakraborty, S.; Kosman, D.J. The Ftr1p iron permease in the yeast plasma membrane: orientation, topology and structure-function relationships. *Biochem J* **2004**, *380*, 487-496. https://doi.org/10.1042/BJ20031921.

67. Pearson, R.G. Hard and Soft Acids and Bases. *Journal of the American Chemical Society* **1963**, *85*, 3533-3539. https://doi.org/10.1021/ja00905a001.

68. Liang, J.; Canary, J.W. Discrimination between hard metals with soft ligand donor atoms: an on-fluorescence probe for manganese(II). *Angew Chem Int Ed Engl* **2010**, *49*, 7710-7713. https://doi.org/10.1002/anie.201002853.

69. Andreini, C.; Cavallaro, G.; Lorenzini, S.; Rosato, A. MetalPDB: a database of metal sites in biological macromolecular structures. *Nucleic Acids Res* **2013**, *41*, D312-319. https://doi.org/10.1093/nar/gks1063.

70. Damo, S.M.; Kehl-Fie, T.E.; Sugitani, N.; Holt, M.E.; Rathi, S.; Murphy, W.J.; Zhang, Y.; Betz, C.; Hench, L.; Fritz, G.; et al. Molecular basis for manganese sequestration by calprotectin and roles in the innate immune response to invading bacterial pathogens. *Proc Natl Acad Sci U S A* **2013**, *110*, 3841-3846. https://doi.org/10.1073/pnas.1220341110.

71. Rola, A.; Potok, P.; Mos, M.; Gumienna-Kontecka, E.; Potocki, S. Zn(II) and Cd(II) Complexes of AMT1/MAC1 Homologous Cys/His-Rich Domains: So Similar yet So Different. *Inorg Chem* **2022**, *61*, 14333-14343. https://doi.org/10.1021/acs.inorgchem.2c02080.

72. Putignano, V.; Rosato, A.; Banci, L.; Andreini, C. MetalPDB in 2018: a database of metal sites in biological macromolecular structures. *Nucleic Acids Res* **2018**, *46*, D459-D464. https://doi.org/10.1093/nar/gkx989.

73. Irving, H.; Williams, R.J.P. 637. The stability of transition-metal complexes. *Journal of the Chemical Society (Resumed)* **1953**, 3192-3210. https://doi.org/10.1039/JR9530003192.

74. Hamming, I.; Cooper, M.E.; Haagmans, B.L.; Hooper, N.M.; Korstanje, R.; Osterhaus, A.D.; Timens, W.; Turner, A.J.; Navis, G.; van Goor, H. The emerging role of ACE2 in physiology and disease. *J Pathol* **2007**, *212*, 1-11. https://doi.org/10.1002/path.2162.

75. Verdecchia, P.; Cavallini, C.; Spanevello, A.; Angeli, F. The pivotal link between ACE2 deficiency and SARS-CoV-2 infection. *Eur J Intern Med* **2020**, *76*, 14-20. https://doi.org/10.1016/j.ejim.2020.04.037.

76. Hoffmann, M.; Kleine-Weber, H.; Pohlmann, S. A Multibasic Cleavage Site in the Spike Protein of SARS-CoV-2 Is Essential for Infection of Human Lung Cells. *Mol Cell* **2020**, *78*, 779-784 e775. https://doi.org/10.1016/j.molcel.2020.04.022.

77. Lan, J.; Ge, J.; Yu, J.; Shan, S.; Zhou, H.; Fan, S.; Zhang, Q.; Shi, X.; Wang, Q.; Zhang, L.; et al. Structure of the SARS-CoV-2 spike receptor-binding domain bound to the ACE2 receptor. *Nature* **2020**, *581*, 215-220. https://doi.org/10.1038/s41586-020-2180-5.

78. Yan, R.; Zhang, Y.; Li, Y.; Xia, L.; Guo, Y.; Zhou, Q. Structural basis for the recognition of SARS-CoV-2 by full-length human ACE2. *Science* **2020**, *367*, 1444-1448. https://doi.org/10.1126/science.abb2762.

79. Wessels, I.; Rolles, B.; Rink, L. The Potential Impact of Zinc Supplementation on COVID-19 Pathogenesis. *Front Immunol* **2020**, *11*, 1712. https://doi.org/10.3389/fimmu.2020.01712.

80. Magri, A.; Tabbi, G.; Di Natale, G.; La Mendola, D.; Pietropaolo, A.; Zoroddu, M.A.; Peana, M.; Rizzarelli, E. Zinc Interactions with a Soluble Mutated Rat Amylin to Mimic Whole Human Amylin: An Experimental and Simulation Approach to Understand Stoichiometry, Speciation and Coordination of the Metal Complexes. *Chemistry* **2020**, *26*, 13072-13084. https://doi.org/10.1002/chem.202002114.

81. Gampp, H.; Maeder, M.; Meyer, C.J.; Zuberbuhler, A.D. Calculation of equilibrium constants from multiwavelength spectroscopic data--II: SPECFIT: two user-friendly programs in basic and standard FORTRAN 77. *Talanta* **1985**, *32*, 257-264. https://doi.org/10.1016/0039-9140(85)80077-1.

82. Prenesti, E.; Daniele, P.G.; Prencipe, M.; Ostacoli, G. Spectrum–structure correlation for visible absorption spectra of copper(II) complexes in aqueous solution. *Polyhedron* **1999**, *18*, 3233-3241. https://doi.org/https://doi.org/10.1016/S0277-5387(99)00279-X.

83. Lesiow, M.K.; Pietrzyk, P.; Bienko, A.; Kowalik-Jankowska, T. Stability of Cu(ii) complexes with FomA protein fragments containing two His residues in the peptide chain. *Metallomics* **2019**, *11*, 1518-1531. https://doi.org/10.1039/c9mt00131j.

84. Peana, M.; Gumienna-Kontecka, E.; Piras, F.; Ostrowska, M.; Piasta, K.; Krzywoszynska, K.; Medici, S.; Zoroddu, M.A. Exploring the Specificity of Rationally Designed Peptides Reconstituted from the Cell-Free Extract of Deinococcus radiodurans toward Mn(II) and Cu(II). *Inorg Chem* **2020**, *59*, 4661-4684. https://doi.org/10.1021/acs.inorgchem.9b03737.

85. Magri, A.; Munzone, A.; Peana, M.; Medici, S.; Zoroddu, M.A.; Hansson, O.; Satriano, C.; Rizzarelli, E.; La Mendola, D. Coordination Environment of Cu(II) Ions Bound to N-

Terminal Peptide Fragments of Angiogenin Protein. *Int J Mol Sci* **2016**, *17*. https://doi.org/10.3390/ijms17081240.

86. Zoroddu, M.A.; Kowalik-Jankowska, T.; Medici, S.; Peana, M.; Kozlowski, H. Copper(II) binding to Cap43 protein fragments. *Dalton Trans* **2008**, 6127-6134. https://doi.org/10.1039/b808600a.

87. Zoroddu, M.A.; Kowalik-Jankowska, T.; Kozlowski, H.; Molinari, H.; Salnikow, K.; Broday, L.; Costa, M. Interaction of Ni(II) and Cu(II) with a metal binding sequence of histone H4: AKRHRK, a model of the H4 tail. *Biochimica et Biophysica Acta (BBA) - General Subjects* **2000**, *1475*, 163-168. https://doi.org/https://doi.org/10.1016/S0304-4165(00)00066-0.

88. Kowalik-Jankowska, T.; Kadej, A.; Kuczer, M.; Czarniewska, E. Copper(II) complexes of the Neb-colloostatin analogues containing histidine residue structure stability biological activity. *Polyhedron* **2017**, *134*, 365-375. https://doi.org/https://doi.org/10.1016/j.poly.2017.06.023.

89. Rowinska-Zyrek, M.; Wiech, A.; Wa Tly, J.; Wieczorek, R.; Witkowska, D.; Ozyhar, A.; Orlowski, M. Copper(II)-Binding Induces a Unique Polyproline Type II Helical Structure within the Ion-Binding Segment in the Intrinsically Disordered F-Domain of Ecdysteroid Receptor from Aedes aegypti. *Inorg Chem* **2019**, *58*, 11782-11792. https://doi.org/10.1021/acs.inorgchem.9b01826.

90. Medici, S.; Peana, M.; Nurchi, V.M.; Zoroddu, M.A. The involvement of amino acid side chains in shielding the nickel coordination site: an NMR study. *Molecules* **2013**, *18*, 12396-12414. https://doi.org/10.3390/molecules181012396.

91. Peana, M.; Zdyb, K.; Medici, S.; Pelucelli, A.; Simula, G.; Gumienna-Kontecka, E.; Zoroddu, M.A. Ni(II) interaction with a peptide model of the human TLR4 ectodomain. *J Trace Elem Med Biol* **2017**, *44*, 151-160. https://doi.org/10.1016/j.jtemb.2017.07.006.

92. Jones, C.E.; Klewpatinond, M.; Abdelraheim, S.R.; Brown, D.R.; Viles, J.H. Probing copper2+ binding to the prion protein using diamagnetic nickel2+ and 1H NMR: the unstructured N terminus facilitates the coordination of six copper2+ ions at physiological concentrations. *J Mol Biol* **2005**, *346*, 1393-1407. https://doi.org/10.1016/j.jmb.2004.12.043.

93. Peana, M.F.; Medici, S.; Ledda, A.; Nurchi, V.M.; Zoroddu, M.A. Interaction of Cu(II) and Ni(II) with Ypk9 protein fragment via NMR studies. *ScientificWorldJournal* **2014**, *2014*, 656201. https://doi.org/10.1155/2014/656201.

94. Rae, T.D.; Schmidt, P.J.; Pufahl, R.A.; Culotta, V.C.; O'Halloran, T.V. Undetectable intracellular free copper: the requirement of a copper chaperone for superoxide dismutase. *Science* **1999**, *284*, 805-808. https://doi.org/10.1126/science.284.5415.805.

95. Maret, W. Analyzing free zinc(II) ion concentrations in cell biology with fluorescent chelating molecules. *Metallomics* **2015**, *7*, 202-211. https://doi.org/10.1039/c4mt00230j.

96. Jothimani, D.; Kailasam, E.; Danielraj, S.; Nallathambi, B.; Ramachandran, H.; Sekar, P.; Manoharan, S.; Ramani, V.; Narasimhan, G.; Kaliamoorthy, I.; et al. COVID-19: Poor outcomes in patients with zinc deficiency. *Int J Infect Dis* **2020**, *100*, 343-349. https://doi.org/10.1016/j.ijid.2020.09.014.

97. Wessels, I.; Rolles, B.; Slusarenko, A.J.; Rink, L. Zinc deficiency as a possible risk factor for increased susceptibility and severe progression of Corona Virus Disease 19. *Br J Nutr* **2022**, *127*, 214-232. https://doi.org/10.1017/S0007114521000738.

98. Oudit, G.Y.; Wang, K.; Viveiros, A.; Kellner, M.J.; Penninger, J.M. Angiotensin-converting enzyme 2-at the heart of the COVID-19 pandemic. *Cell* **2023**, *186*, 906-922. https://doi.org/10.1016/j.cell.2023.01.039.

99. Peana, M.; Medici, S.; Dadar, M.; Zoroddu, M.A.; Pelucelli, A.; Chasapis, C.T.; Bjorklund, G. Environmental barium: potential exposure and health-hazards. *Arch Toxicol* **2021**, *95*, 2605-2612. https://doi.org/10.1007/s00204-021-03049-5.

100. Medici, S.; Peana, M.; Pelucelli, A.; Zoroddu, M.A. An updated overview on metal nanoparticles toxicity. *Semin Cancer Biol* **2021**, *76*, 17-26. https://doi.org/10.1016/j.semcancer.2021.06.020.

101. Medici, S.; Peana, M.; Pelucelli, A.; Zoroddu, M.A. Rh(I) Complexes in Catalysis: A Five-Year Trend. *Molecules* **2021**, *26*. https://doi.org/10.3390/molecules26092553.

102. Hochella, M.F.; Mogk, D.W.; Ranville, J.; Allen, I.C.; Luther, G.W.; Marr, L.C.; McGrail, B.P.; Murayama, M.; Qafoku, N.P.; Rosso, K.M.; et al. Natural, incidental, and engineered nanomaterials and their impacts on the Earth system. *Science* **2019**, *363*, eaau8299. https://doi.org/10.1126/science.aau8299.

103. Chen, J.; Hoek, G. Long-term exposure to PM and all-cause and cause-specific mortality: A systematic review and meta-analysis. *Environ Int* **2020**, *143*, 105974. https://doi.org/10.1016/j.envint.2020.105974.

104. Umair, M.; Alfadhel, M. Genetic Disorders Associated with Metal Metabolism. *Cells* **2019**, *8*. https://doi.org/10.3390/cells8121598.

105. Lachowicz, J.I.; Nurchi, V.M.; Fanni, D.; Gerosa, C.; Peana, M.; Zoroddu, M.A. Nutritional iron deficiency: the role of oral iron supplementation. *Curr Med Chem* **2014**, *21*, 3775-3784. https://doi.org/10.2174/0929867321666140706143925.

106. Maret, W.; Sandstead, H.H. Zinc requirements and the risks and benefits of zinc supplementation. *J Trace Elem Med Biol* **2006**, *20*, 3-18. https://doi.org/10.1016/j.jtemb.2006.01.006.

107. Nordberg, M.; Nordberg, G.F. Metallothionein and Cadmium Toxicology-Historical Review and Commentary. *Biomolecules* **2022**, *12*. https://doi.org/10.3390/biom12030360.

108. Krężel, A.; Maret, W. The Bioinorganic Chemistry of Mammalian Metallothioneins. *Chemical Reviews* **2021**, *121*, 14594-14648. https://doi.org/10.1021/acs.chemrev.1c00371.

109. Bernhoft, R.A. Cadmium toxicity and treatment. *ScientificWorldJournal* **2013**, *2013*, 394652. https://doi.org/10.1155/2013/394652.

110. Koedrith, P.; Seo, Y.R. Advances in carcinogenic metal toxicity and potential molecular markers. *Int J Mol Sci* **2011**, *12*, 9576-9595. https://doi.org/10.3390/ijms12129576.